*Scale-up in Chemical Engineering*. Marko Zlokarnik

ISBNs: 3-527-30266-2 (Hardback); 3-527-60056-6 (Electronic)

*Marko Zlokarnik*

**Scale-Up in Chemical Engineering**

*Scale-up in Chemical Engineering*. Marko Zlokarnik

ISBNs: 3-527-30266-2 (Hardback); 3-527-60056-6 (Electronic)

*Marko Zlokarnik*

# Scale-Up in Chemical Engineering

WILEY-VCH

*Scale-up in Chemical Engineering*. Marko Zlokarnik

ISBNs: 3-527-30266-2 (Hardback); 3-527-60056-6 (Electronic)

***Prof. Dr. Marko Zlokarnik***
Grillparzerstraße 58
8010 Graz
Austria
e-mail: zloka@mail.nextra.at



**Library of Congress Card No. applied for.**
A catalogue record for this book is available from the British Library

**Die Deutsche Bibliothek –**
**CIP Cataloguing-in-Publication-Data**
A catalogue record for this publication is available from Die Deutsche Bibliothek



Printed in the Federal Republic of Germany
Printed on acid-free paper.

**Typesetting** Kühn & Weyh, Satz und Medien, Freiburg
**Printing** betz-druck GmbH, Darmstadt
**Bookbinding** J. Schäffer GmbH & Co. KG, Grünstadt

**ISBN** 3-527-30266-2

*Scale-up in Chemical Engineering*. Marko Zlokarnik

ISBNs: 3-527-30266-2 (Hardback); 3-527-60056-6 (Electronic)

This book is dedicated to my friend and teacher
**Dr. phil. Dr.-Ing. h. c. Juri Pawlowski**

*Scale-up in Chemical Engineering*. Marko Zlokarnik


ISBNs: 3-527-30266-2 (Hardback); 3-527-60056-6 (Electronic)

# Contents

*Scale-up in Chemical Engineering.* Marko Zlokarnik


ISBNs: 3-527-30266-2 (Hardback); 3-527-60056-6 (Electronic)

## Preface

In this day and age, chemical engineers are faced with many research and design problems which are so complicated that they cannot be solved with numerical mathematics. In this context, one only has to think of processes involving fluids with temperature-dependent physical properties or non-Newtonian flow behavior. Fluid mechanics in heterogeneous material systems exhibiting coalescence phenomena or foaming also demonstrates this problem. The scaling up of equipment needed for dealing with such material systems often presents serious hurdles which can be frequently overcome only with the aid of partial similarity.

In general, the university graduate has not at all been adequately trained to deal with such problems. On the one hand, treatises on dimensional analysis, the theory of similarity and scale-up methods included in common, "run of the mill" textbooks on chemical engineering are out of date. In addition, they are only seldomly written in such a manner that would popularize these methods. On the other hand, there is no motivation for this type of research at universities since, as a rule, they are not confronted with scale-up tasks and are therefore not equipped with the necessary apparatus on the bench-scale.

All of these points give the totally wrong impression that the methods referred to are – at most – of only marginal importance in practical chemical engineering, because otherwise they would have been dealt with in greater depth at the university level!

The aim of this book is to remedy this deficiency. It presents dimensional analysis – this being the only secure foundation of the scale-up – in such a way that it can be immediately and easily understood, even without a mathematical background.

Due to the increasing importance of biotechnology, which employs non-Newtonian fluids by far more frequently than chemical industry does, variable physical properties (e.g. temperature dependence, shear-dependence of viscosity) are treated in detail. It must be kept in mind that in scaling up such processes, apart from the geometrical and process-related similarity, the material similarity also has to be considered.

The theoretical foundations of dimensional analysis and of scale-up are presented and discussed in the first half of this book. This theoretical framework is demonstrated by twenty examples, all of which deal with interesting engineering problems taken from current practice.

The second half of this book deals with the integral dimensional-analytical treatment of problems taken from the areas of mechanical, thermal and chemical process engineering. In this respect, the term "integral" is used to indicate that, in the treatment of each problem, dimensional analysis was applied from the very beginning and that, as a consequence, the performance and evaluation of tests were always in accordance with its predictions.

A thorough consideration of this approach not only provides the reader with a practical guideline for their own use; it also shows the unexpectedly large advantage offered by these methods.

The interested reader, intending to solve a concrete problem but is not familiar with the dimensional-analytical methodology, does not need to read this book from cover to cover in order to solve the respective task in this manner. It is sufficient to read the first seven chapters (ca. 50 pages), these dealing with the dimensional analysis and the generation of dimensionless numbers. Subsequently, the reader can scrutinize the examples given in the second part of this book and choose that one example which helps find a solution to the problem under consideration. In doing so, the task at hand can be solved in the dimensional-analytical way. Only the practical treatment of such problems facilitates understanding for the benefit and efficiency of these methods.

In the course of the past 35 years where I have been investigating dimensional-analytical working methods from the practical point of view, my friend and colleague, Dr. *Juri Pawlowski*, has been an invaluable teacher and adviser. I am indebted to him for innumerable suggestions and tips as well as for his comments on this manuscript. I would like to express my gratitude to him at this point.

In closing, my sincere thanks also go to my former employer, the company BAYER AG, Leverkusen/Germany. In the "Engineering Department Applied Physics" I could devote my whole professional life to process engineering research and development. This company always permitted me to spend a considerable amount of time to basic research in the field of chemical engineering in addition to my company duties and corporate research.

# Symbols

**Latin symbols**

| | |
|---|---|
| a | volume-related phase boundary surface $a \equiv A/V$ |
| *a* | thermal diffusivity; $a \equiv k/(\rho C_p)$ |
| A | area, surface |
| c, $\Delta c$ | concentration, concentration difference |
| **c** | velocity of sound in a vacuum |
| $C_p$ | heat capacity, mass-related |
| $c_s$ | saturation concentration |
| d | characteristic diameter |
| $d_b$ | bubble diameter, usually formulated as "*Sauter* mean diameter" $d_{32}$ |
| $d_{32}$ | *Sauter* mean diameter of gas bubbles and drops, respectively |
| $d_p$ | particle diameter |
| D | vessel diameter, pipe diameter |
| *D* | diffusivity |
| $D_{eff}$ | effective axial dispersion coefficient |
| E | energy |
| | enhancement factor in chemisorption; eq. (14.50) |
| | activation energy in chemical reactions |
| | efficiency factor of the absorption process (Section 10.3.2) |
| *f* | functional dependence |
| F | force |
| *F* | degree of humidity |
| g | acceleration due to gravity |
| G | mass flow |
| **G** | gravitational constant |
| h | heat transfer coefficient |
| H | height |
| | base dimension of the amount of heat |
| **J** | *Joule's* mechanical heat equivalent |
| k | reaction rate constant |
| | thermal conductivity |
| | proportionality constant (Section 8.5) |
| **k** | *Boltzmann* constant |

| | |
|---|---|
| $k_G$ | gas-side mass transfer coefficient |
| $k_L$ | liquid-side mass transfer coefficient |
| $k_La$ | volume-related liquid-side mass transfer coefficient |
| $k_F$ | flotation rate constant |
| K | consistency index (Section 8.5) |
| l | characteristic length |
| L | base dimension of length |
| m | mass |
| m | flow index (Section 8.5) |
| mol | amount of substance |
| M | base dimension of mass |
| n | stirrer speed |
| N | base dimension of amount of substance |
| | number of stages |
| $N_x$ | normal stress (x = 1 or 2); eq. (8.68, 8.69) |
| p, $\Delta p$ | pressure, pressure drop |
| P | power, power of stirrer |
| q | volume throughput |
| Q | heat flow |
| r | rank of the dimensional matrix |
| | reaction rate |
| R | heat of reaction |
| **R** | universal gas constant |
| S | cross-sectional area ($\propto D^2$) |
| $S_i$ | coalescence parameters (in i numbers) |
| t | running time |
| T | base dimension of time |
| *T* | temperature |
| ***T*** | absolute temperature |
| u | tip speed ($u = \pi nd$) |
| | parameter in standard representation (Chapter 8) |
| U | over-all heat transfer coefficient (Example 23) |
| v | velocity, superficial velocity |
| V | volume |
| w | parameter in standard representation (Chapter 8) |
| z | number |

**Greek symbols**

| | |
|---|---|
| $\alpha$ | angle |
| $\beta$ | temperature coefficient of density, eq. (8.14) |
| | specific breakage energy (Example 30) |
| $\gamma$ | deformation |
| $\gamma_0$ | temperature coefficient of viscosity, eq. (8.5) |
| | shear rate, eq. (8.54) |
| $\Delta$ | difference |

| | |
|---|---|
| $\delta$ | thickness of film, layer, wall |
| $\varepsilon$ | gas hold-up in the liquid |
| $\varepsilon$ | mass-related power, $\varepsilon \equiv P/\rho V$ |
| $\zeta$ | friction factor in pipe flow; eq. (3.8) |
| $\Theta$ | base dimension of temperature |
| | contact angle |
| | time constant (Chapter 8) |
| $\theta$ | duration of time |
| $\Lambda$ | macro-scale of turbulence |
| $\lambda$ | relaxation time (Section 8.5) |
| | *Kolmogorov*'s micro-scale of turbulence (Section 10.1) |
| $\mu$ | dynamic viscosity |
| | electrophoretic mobility (Example 40) |
| $\mu$ | scale factor, $\mu \equiv l_T/l_M$ |
| $\nu$ | kinematic viscosity |
| $\rho$ | density |
| $\rho C_p$ | heat capacity, volume-related |
| $\sigma$ | surface tension, phase boundary tension |
| $\sigma_z$ | tensile strength (Example 30) |
| $\tau$ | mean residence time, $\tau = V/q$ |
| | shear stress, eq. (8.54) |
| $\tau_0$ | yield stress |
| $\varphi$ | portion (volume, mass) |
| $\psi$ | numerical value (Chapter 8.2) |
| $\phi$ | degree of fill |

**Indices**

| | |
|---|---|
| c | continuous phase |
| d | dispersed phase |
| e | end value |
| F | flock |
| G | gas (gaseous) |
| L | liquid |
| min | minimum |
| M | model-scale |
| 0 | start condition |
| p | particle |
| s | saturation value |
| | height of the layer |
| S | solid, foam |
| t | condition at time t |
| T | technological-scale, full-scale |
| w | wall |

*Scale-up in Chemical Engineering*. Marko Zlokarnik


ISBNs: 3-527-30266-2 (Hardback); 3-527-60056-6 (Electronic)

# 1 Introduction

A chemical engineer is generally concerned with the industrial implementation of processes in which the chemical or microbiological conversion of material takes place in conjunction with the transfer of mass, heat, and momentum. These processes are *scale-dependent*, i.e. they behave differently on a small scale (in laboratories or pilot plants) and a large scale (in production). Also included are heterogeneous chemical reactions and most unit operations. Understandably, chemical engineers have always wanted to find ways of simulating these processes *in models* in order to gain knowledge which will then assist them in designing new industrial plants. Occasionally, they are faced with the same problem for another reason: an industrial facility already exists but does not function properly, if at all, and suitable measurements have to be carried out in order to discover the cause of these difficulties as well as provide a solution.

Irrespective of whether the model involved represents a "scale-up" or a "scale-down", certain important questions will always apply:

- How small can the model be? Is one model sufficient or should tests be carried out with models of different sizes?
- When must or when can physical properties differ? When must the measurements be carried out on the model with the original system of materials?
- Which rules govern the adaptation of the process parameters in the model measurements to those of the full-scale plant?
- Is it possible to achieve complete similarity between the processes in the model and those in its full-scale counterpart? If not: how should one proceed?

These questions touch on the theoretical fundamentals of models, these being based on dimensional analysis. Although they have been used in the field of fluid dynamics and heat transfer for more than a century – cars, aircraft, vessels and heat exchangers were scaled up according to these principles – these methods have gained only a modest acceptance in chemical engineering. The reasons for this have already been explained in the preface.

The importance of dimensional-analytical methodology for current applications in this field can be best exemplified by practical examples. Therefore, the main emphasis of this book lies on the integral treatment of chemical engineering problems by dimensional analysis.

From the area of *mechanical* process engineering, stirring in homogeneous and in gassed fluids as well as the mixing of particulate matter are treated. Furthermore, atomization of liquids with nozzles, production of liquid/liquid dispersions (emulsions) in emulsifiers and the grinding of solids in stirred ball mills is dealt with. As peculiarities, scale-up procedures are presented for the flotation cells for waste water purification, for the separation of aerosols in dust separators by means of inertial forces as well for the temporal course of spin drying in centrifugal filters.

From the area of *thermal* process engineering, the mass and heat transfer in stirred vessels and in bubble columns is treated. In the case of mass transfer in the gas/liquid system, coalescence phenomena are also dealt with in detail. The problem of simultaneous mass and heat transfer is discussed in association with film drying and in continuous electrophoresis.

In dealing with *chemical* process engineering, conducting chemical reactions in a tubular reactor and in a packed bed reactor (solid-catalyzed reactions) is discussed. In consecutive-competitive reactions between two liquid partners, a maximum possible selectivity is only achievable in a tubular reactor under the condition that backmixing of educts and products is completely prevented. The scale-up for such a process is presented. Finally, the dimensional-analytical framework is presented for the reaction rate of a fast chemical reaction in the gas/liquid system, which is to a certain degree limited by mass transfer.

Last but not least, in the final chapter it is demonstrated with a few examples that different types of motions in the *living world* can also be described by dimensional analysis. In this manner the validity range of the pertinent dimensionless numbers can be given. The processes of motion in Nature are subjected to the same physical framework conditions (restrictions) as the technological world.

*Scale-up in Chemical Engineering.* Marko Zlokarnik


ISBNs: 3-527-30266-2 (Hardback); 3-527-60056-6 (Electronic)

# 2
# Dimensional Analysis

## 2.1
## The Fundamental Principle

Dimensional analysis is based upon the recognition that a mathematical formulation of a chemical or physical technological problem can be of general validity only if it is *dimensionally homogenous*, i.e. if it is valid in any system of dimensions.

## 2.2
## What is a Dimension?

A dimension is a purely *qualitative* description of a sensory perception of a physical entity or natural appearance. Length can be experienced as height, depth and breadth. Mass presents itself as a light or heavy body and time as a short moment or a long period. The dimension of length is Length (L), the dimension of a mass is Mass (M), and so on.

Each physical concept can be associated with a type of quantity and this, in turn, can be assigned to a dimension. It can happen that different quantities display the same dimension. *Example:* Diffusivity ($D$), thermal diffusivity ($a$) and kinematic viscosity ($\nu$) all have the same dimension $[L^2\,T^{-1}]$.

## 2.3
## What is a Physical Quantity?

In contrast to a dimension, a physical quantity represents a *quantitative* description of a physical quality:

$$\text{physical quantity} = \text{numerical value} \times \text{measuring unit}$$

*Example:* A mass of 5 kg: m = 5 kg. The measuring unit of length can be a meter, a foot, a cubit, a yardstick, a nautical mile, a light year, and so on. Measuring units of energy are, for example, Joule, cal, eV. (It is therefore necessary to establish the measuring units in an appropriate measuring system.)

## 2.4 Base and Derived Quantities, Dimensional Constants

A distinction is made between base or primary quantities and the secondary quantities which are derived from them (derived quantities). Base quantities are based on standards and are quantified by comparison with them. According to the Système International d' Unités (SI), mass is classified as a primary quantity instead of force, which was used some forty years ago.

Secondary quantities are derived from primary ones according to physical laws, e.g. velocity = length/time: [v] = L/T. Its coherent measuring unit is m/s. Coherence of the measuring units means that the secondary quantities have to have only such measuring units which correspond with *per definitionem* fixed primary ones and therefore present themselves as power products of themselves. Giving the velocity in mph (miles per hour) would contradict this.

If a secondary quantity has been established by a physical law, it can happen that it contradicts another one.

### Example a

According to Newton's 2nd law of motion, the force, F, is expressed as a product of mass, m, and acceleration, a: $F = m\ a$, having the dimension of $[M\ L\ T^{-2}]$. According to Newton's law of gravitation, force is defined by $F \propto m_1\ m_2/r^2$, thus leading to completely another dimension $[M^2\ L^{-2}]$. To remedy this, the gravitational constant **G** – a dimensional constant – had to be introduced to ensure the dimensional homogeneity of the latter equation:
$F = \mathbf{G}\ m_1\ m_2/r^2$.

$$\mathbf{G}\ [M^{-1}\ L^3\ T^{-2}] = 6.673 \times 10^{-11}\ m^3/(kg\ s^2)$$

### Example b

A similar example is the introduction of the universal gas constant, **R**, which ensures that in the perfect gas equation of state $p\ V = n\ \mathbf{R}\ T$ the already fixed secondary unit for work
$W = p\ V\ [M\ L^2\ T^{-2}]$ is not offended.

$$\mathbf{R}\ [M\ L^2\ T^{-2}\ N^{-1}\ \Theta^{-1}] = 8.313\ J/(mol\ K)$$

Another class of derived quantities is represented by the coefficients in transfer equations for momentum, mass and heat. They were also established by the respective physical laws – therefore they are often called "defined quantities" – and can only be determined via measurement of their constituents.

In chemical process engineering it frequently happens that new secondary quantities have to be introduced. The dimensions and the coherent measuring units of them can easily be fixed. *Example*: volume-related liquid-side mass transfer coefficient $k_La\ [T^{-1}]$.

## 2.5 Dimensional Systems

A dimensional system consists of all the primary and secondary dimensions and corresponding measuring units. The currently used "Système International d'unités (SI) is based on seven base dimensions. They are presented in **Table 1** together with their corresponding base units.

**Table 2** refers to some very frequently used secondary measuring units which have been named after famous researchers.

**Table 1** Base quantities, their dimensions and units according to SI

| *Base quantity* | *Base dimension* | *SI base unit* | |
|---|---|---|---|
| length | L | m | meter |
| mass | M | kg | kilogram |
| time | T | s | second |
| thermodynamic temperature | Θ | K | kelvin |
| amount of substance | N | mol | mole |
| electric current | I | A | ampere |
| luminous intensity | J | cd | candela |

**Table 2** Important secondary measuring units in mechanical engineering, named after famous researchers

| *Sec. quantity* | *Dimension* | *Measuring unit* | *Name* |
|---|---|---|---|
| force | $M\,L\,T^{-2}$ | $kg\,m\,s^{-2} \equiv N$ | Newton |
| pressure | $M\,L^{-1}\,T^{-2}$ | $kg\,m^{-1}\,s^{-2} \equiv Pa$ | Pascal |
| energy | $M\,L^{2}\,T^{-2}$ | $kg\,m^{2}\,s^{-2} \equiv J$ | Joule |
| power | $M\,L^{2}\,T^{-3}$ | $kg\,m^{2}\,s^{-3} \equiv W$ | Watt |

**Table 3** Commonly used secondary quantities and their respective dimensions according to the currently used SI units in mechanical and thermal problems

| *Physical entity* | *Dimension* |
|---|---|
| area | $L^2$ |
| volume | $L^3$ |
| angular velocity, shear rate, frequency | $T^{-1}$ |
| velocity | $L\,T^{-1}$ |
| acceleration | $L\,T^{-2}$ |
| kinematic viscosity, diffusivity, thermal diffusivity | $L^2\,T^{-1}$ |
| density | $M\,L^{-3}$ |
| surface tension | $M\,T^{-2}$ |
| dynamic viscosity | $M\,L^{-1}\,T^{-1}$ |
| momentum | $M\,L\,T^{-1}$ |
| force | $M\,L\,T^{-2}$ |
| pressure, tension | $M\,L^{-1}\,T^{-2}$ |
| angular momentum | $M\,L^2\,T^{-1}$ |
| mechanical energy, work, torque | $M\,L^2\,T^{-2}$ |
| power | $M\,L^2\,T^{-3}$ |
| specific heat | $L^2\,T^{-2}\,\Theta^{-1}$ |
| heat conductivity | $M\,L\,T^{-3}\,\Theta^{-1}$ |
| heat transfer coefficient | $M\,T^{-3}\,\Theta^{-1}$ |

If, in the formulation of a problem, only the base dimensions [M, L, T] occur in the dimensions of the involved quantities, then it is a mechanical problem. If [Θ] occurs, then it is a thermal problem and if [N] occurs it is a chemical problem.

In a chemical reaction the molecules (or the atoms) of the reaction partners react with each other and not their masses. Their number (amount) results from the mass of the respective substance according to its molecular mass. One mole (SI unit: mole) of a chemically pure compound consists of $N_A = 6.022 \times 10^{23}$ entities (molecules, atoms). The information about the amount of substance is obtained by dividing the mass of the chemically pure substance by its molecular mass. To put it even more precisely: In the reaction between gaseous hydrogen and chlorine one mole of hydrogen reacts with one mole of chlorine according to the equation

$$H_2 + Cl_2 = 2\,HCl$$

and two moles of hydrochloric acid are produced. Consequently, it is completely insignificant that with respect to the masses 2 g of $H_2$ reacted with 71 g of $Cl_2$ to produce 73 g of HCl.

## 2.6 Dimensional Homogeneity of a Physical Content

It has already been emphasized that a physical relationship can be of general validity only if it is formulated *dimensionally homogeneously*, i.e. if it is valid with any system of dimensions (section 2.1). The aim of dimensional analysis is to check whether the physical content under consideration can be formulated in a dimensionally homogeneous manner or not. The procedure necessary to accomplish this consists of two parts:

a) Initially, all physical parameters necessary to describe the problem are listed. This so-called "relevance list" of the problem consists of the quantity in question (as a rule only one) and all the parameters which influence it. The target quantity is the only dependent variable and the influencing parameters should be primarily independent of each other. Example: Out of material properties $\mu$, $\nu$ and $\rho$ only two should be chosen, because they are linked together by the definition equation: $\nu \equiv \mu/\rho$.
b) In the second step, the dimensional homogeneity of the physical content is checked by transferring it into a dimensionless form. This is the foundation of the so-called pi theorem (see section 2.7). The dimensional homogeneity comes to the dimensionless formulation of the physical content in question.

**Note:** A dimensionless expression is dimensionally homogeneous!

This point will be made clear by three examples.

**Example 1**: What determines the period of oscillation of a pendulum?

We first draw a sketch depicting a pendulum and write down all the quantities which could be involved in this question [1]. It may be assumed that the period of oscillation of a pendulum depends on the length and mass of the pendulum, the gravitational acceleration and the amplitude of the swing:

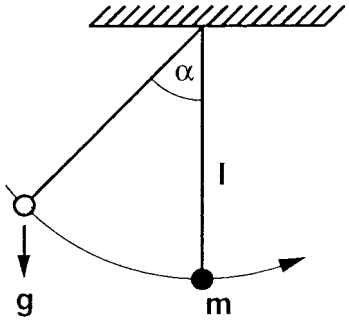


| *physical quantity* | *Symbol* | *Dimension* |
|---|---|---|
| Period of oscillation | $\theta$ | T |
| Length of pendulum | l | L |
| Mass of pendulum | m | M |
| Gravitational acceleration | g | $LT^{-2}$ |
| Amplitude (angle) | $\alpha$ | – |

Our aim is to establish θ as a function of l, m, g and α :

$$\theta = f(l, m, g, \alpha) \tag{2.1}$$

Can this dependency be dimensionally homogeneous? **No!** The first thing that now becomes clear is that the base dimension of mass [M] only occurs in the mass m itself. Changing its measuring unit, e.g. from kilograms to pounds, would change the numerical value of the function. This is unacceptable. Either our list should include a further variable containing M, or mass is not a relevant variable. If we assume – by simplification*) – the latter, the above relationship is reduced to:

$$\theta = f(l, g, \alpha) \tag{2.2}$$

Both l and g contain the base dimension of length. When combined as a ratio l/g they become dimensionless with respect to L and are therefore independent of changes in the base dimension of length:

$$\theta = f\ (l/g, \alpha) \tag{2.3}$$

On the left-hand side of the equation we have the dimension T and on the right $T^2$. To remedy this, we will have to write $\sqrt{l/g}$. This expression will keep its dimension [T] only if it remains unchanged, therefore we have to put it as a constant in front of the function *f*. Because α is dimensionless anyway, the final result of the dimensional analysis reads:

$$\theta = \sqrt{l/g}\ f(\alpha) \ \rightarrow\ \theta\ \sqrt{g/l} = f(\alpha) \tag{2.4}$$

The dependency between four dimensional quantities, containing two base dimensions (L and T) in their dimensions, is reduced to a 4 – 2 = 2 parametric relationship between dimensionless expressions ("numbers")!

This equation is the only statement that dimensional analysis can offer in this case. It is not capable of producing information on the form of *f*. The integration of Newton's equation of motion for small amplitudes leads to $f(\alpha) = 2\pi$; the period of oscillation is then independent of α. The relationship can now be expressed as:

$$\theta\ \sqrt{g/l} = 2\pi \tag{2.5}$$

The left-hand side of the expression is a *dimensionless* number, its numerical value being 2π.

*) In case of a real pendulum the density and viscosity of air should also be introduced into the relevance list. Both contain mass in their dimensions. However, this would unnecessarily complicate the problem at this step. Therefore we will consider a physical pendulum with a point mass in a vacuum.

The elegant solution of this example should not tempt the reader to believe that dimensional analysis can solve every problem solely by a theoretical consideration. To treat this example by dimensional analysis, the acceleration due to gravity ($g = 9.81\ m\ s^{-2}$) had to be known, this being calculated from the gravitational law. *Sir Isaak Newton* derived it from *Kepler*'s laws of planet movements. *Bridgman*'s ([1], p.12) comment on this situation is particularly appropriate:

*"The problem cannot be solved by the philosopher in his armchair, but the knowledge involved was gathered only by someone at some time soiling his hands with direct contact".*

**Example 2**: Dripping of a liquid from a capillary

The simplest method to produce droplets is to drip a liquid slowly out of a capillary under the influence of gravity. Due to the low shear rate, the viscosity of the liquid will, as a rule, have no influence. In this case the target quantity, particle diameter (here: droplet diameter) $d_p$, will depend only on the wetted capillary diameter d, the surface tension σ and the weight gρ of the dripping liquid:

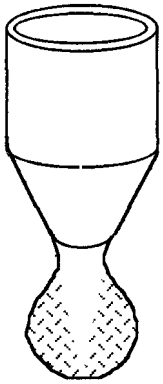

| *physical quantity* | *symbol* | *dimension* |
|---|---|---|
| droplet diameter | dp | L |
| capillary diameter | d | L |
| surface tension | σ | $M\ T^{-2}$ |
| weight of the liquid | gρ | $M\ L^{-2}\ T^{-2}$ |

Anticipating $d_p/d$ as the "target dimensionless number", the remaining three quantities (d, σ, gρ) can only produce one additional dimensionless number.

By the quotient $\sigma/g\rho$ $[L^2]$ two base dimensions [M, T] are eliminated at once, so that by the division of this expression by $d^2$ the dimensionless number

$$\frac{g\rho\, d^2}{\sigma} \equiv Bd \tag{2.6}$$

is formed, which is named Bond number Bd. The above dimensional relationship is, therefore, reduced to the functional dependence

$$d_p/d = f(Bd) \tag{2.7}$$

Eq. (2.7) represents the dimensionless formulated dependence of the correlation between the dimensional quantities in the above table. If the function *f* is determined with measurements, then one speaks of the *process equation*. This reads here as [2]:

$$d_p/d = 1.6\ Bd^{-1/3} \tag{2.8}$$

The essence of the scale-up will be demonstrated with a slightly more compilicated example:

**Example 3**: Correlation between the meat size and roasting time

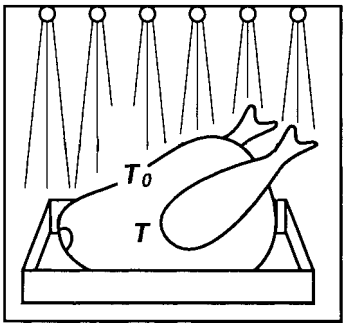


Firstly, we have to recall the physical situation and, in order to facilitate understanding, we should draw a sketch. At high oven temperatures heat is transferred from the heating elements to the meat surface by both radiation and heat convection. From there it is transferred solely by unsteady-state heat conduction which surely represents the rate limiting step of the heating process.

The higher the thermal conductivity, k, of the body, the faster the heat spreads out. The higher its volume-related heat capacity, $\rho C_p$, the slower the heat transfer. Therefore, the unsteady-state heat conduction is characterized by only one material property, the thermal diffusivity, $a \equiv k/\rho C_p$, of the body.

Roasting is an endothermic process. The meat is ready when a certain temperature distribution ($T$) is reached within it. The target quantity is the time duration, $\theta$, necessary to achieve this temperature field.

After these considerations we are able to precisely draw up the relevance list:

| *physical quantity* | *symbol* | *dimension* |
|---|---|---|
| roasting time | $\theta$ | T |
| meat surface | A | $L^2$ |
| thermal diffusivity | $a$ | $L^2\,T^{-1}$ |
| surface temperature | $T_0$ | $\Theta$ |
| temperature distribution | $T$ | $\Theta$ |

The base dimension of temperature, $\Theta$, appears only in two quantities. They can therefore be contained in only one dimensionless quantity:

$$\Pi_1 \equiv T/T_0 \quad \text{or} \quad (T_0 - T)/T_0 \tag{2.9}$$

The residual three quantities form one additional dimensionless number:

$$\Pi_2 \equiv a\theta/A \equiv \text{Fo} \tag{2.10}$$

In the theory of heat transfer, $\Pi_2$ is known as the Fourier number, Fo. Now, the roasting process is presented in a two-dimensional framework:

$$T/T_0 = f(\text{Fo}) \tag{2.11}$$

In this example, five dimensional quantities produce two dimensionless numbers. This was to be expected because their dimensions contain three base dimensions: $5 - 3 = 2$.

The question concerning the correlation between the roasting time and the meat size can now be easily answered, even without explicitly knowing the function *f*. To reach the same temperature distribution $T/T_0$ or $(T_0 - T)/T_0$ in differently sized bodies, the dimensionless number $\mathrm{Fo} \equiv a\theta/\mathrm{A}$ must display the same (= idem, identical) numerical value. Because thermal diffusivity *a* remains unaltered in the meat of same species ($a$ = idem), this leads to

$$T/T_0 = \text{idem} \rightarrow \mathrm{Fo} \equiv a\theta/\mathrm{A} = \text{idem} \rightarrow \mathrm{q}/\mathrm{A} = \text{idem} \rightarrow \theta \propto \mathrm{A} \tag{2.12}$$

This statement is obviously useless as a scale-up rule because meat is bought according to weight and not to surface. One can easily remedy this. In bodies, the following correlation between mass, m, surface, A, and volume, V, exists:

$$\mathrm{m} = \rho \mathrm{V} \propto \rho \mathrm{L}^3 \propto \rho \mathrm{A}^{3/2} \qquad (\mathrm{A} \propto \mathrm{L}^2)$$

Therefore, from $\rho$ = idem it follows

$$\mathrm{A} \propto \mathrm{m}^{2/3} \qquad \text{and thus} \qquad \theta \propto \mathrm{A} \propto \mathrm{m}^{2/3}$$

From this correlation we obtain the scale-up rule

$$\theta_2/\theta_1 \propto (\mathrm{m}_2/\mathrm{m}_1)^{2/3} \tag{2.13}$$

This is the scale-up criterion for the roasting time of meat of the same kind ($a$, $\rho$ = idem). It states that in doubling the mass of meat, the cooking time will increase by $2^{2/3} = 1.58$.

*G.B. West* [3] refers to "inferior" cookbooks which simply say something like "20 minutes per pound", implying a linear relationship with weight. However, there exist "superior" cookbooks, such as the "Better Homes and Gardens Cookbook" (Des Moines Meredith Corp. 1962), which recognize the nonlinear nature of this relationship. The graphical representation of measurements given in this book confirms the relationship

$$\theta \propto \mathrm{m}^{0.6}$$

which is very close to the theoretical evaluation giving $\theta \propto \mathrm{m}^{2/3} = \mathrm{m}^{0.67}$.

These three transparent and easy to understand examples clearly show how dimensional analysis deals with specific problems and what conclusions it allows. Now, it should be easier to understand *Lord Rayleigh's* sarcastic comment with which he began his short essay on "The Principle of Similitude" [4]:

*"I have often been impressed by the scanty attention paid even by original workers in physics to the great principle of similitude. It happens not infrequently that results in the form of "laws" are put forward as novelties on the basis of elaborate experiments, which might have been predicted a priori after a few minutes' consideration".*

From the above examples we can also learn that the transformation of a physical content from a dimensional into a dimensionless form is automatically accompanied by an essential *compression* of the statement: The set of the dimensionless numbers is smaller than the set of the quantities contained in them, but it describes the problem equally comprehensively. (In the third example the dependency between 5 dimensional parameters is reduced to a dependency between only 2 demensionsless numbers!) This is the proof of the so-called pi theorem (pi after $\Pi$, the sign used for products), which is formulated in the next Section:

## 2.7 The pi Theorem

- Every physical relationship between n physical quantities can be reduced to a relationship between $m = n - r$ mutually independent dimensionless groups, whereby r stands for the rank of the dimensional matrix, made up of the physical quantities in question and generally equal to (or in some few cases smaller than) the number of the base quantities contained in their secondary dimensions.

For mathematical proofs see e.g. *Pawlowski* [5] und *Görtler* [6].

The pi theorem is often associated with the name of *E. Buckingham*, because he introduced this term in 1914. However, the proof of this theorem was already accomplished in the course of a mathematical analysis of partial differential equations by *A. Federmann* in 1911. (See [6], section 4.6: Historical remarks concerning the pi theorem.)

The first important advantage of using dimensional analysis exists in the essential **compression of the statement**. The second important advantage of its use is related to the **safeguarding of a secure scale-up**. This will be convincingly shown in the next two examples.

*Scale-up in Chemical Engineering.* Marko Zlokarnik
Copyright © 2002 Wiley-VCH Verlag GmbH & Co. KGaA
ISBNs: 3-527-30266-2 (Hardback); 3-527-60056-6 (Electronic)


# 3
# Generation of Pi-sets by Matrix Transformation

As a rule, more than two dimensionless numbers are necessary to describe a physico-technological problem; they cannot be produced as shown in the first three examples. The classical method to approach this problem involved a solution of a system of linear algebraic equations. They were formed separately for each of the base dimensions by exponents with which they appeared in the physical quantities. *J. Pawlowski* [5] replaced this relatively awkward and involved method by a simple and transparent matrix transformation ("equivalence transformation") which will be presented in detail in the next example.

**Example 4**: The pressure drop of a homogeneous fluid in a straight, smooth pipe (ignoring the inlet effects)

Here, the relevance list consists of the following elements:

| | |
|---|---|
| target quantity: | pressure drop, $\Delta p$ |
| geometric parameters: | diameter, d, and length, l, of the pipe |
| material parameters: | density, $\rho$, and kinematic viscosity, $\nu$, of the fluid |
| process related parameter: | volume-related throughput, q |

$$\{\Delta p;\ d,\ l;\ \rho,\ \nu;\ q\} \tag{3.1}$$

With the dimensions of these quantities a dimensional matrix is formed. Their columns are assigned to the individual physical quantities and the rows to the exponents with which the base dimensions appear in the respective dimensions of these quantities (example: $\Delta p$ $[M^1\ L^{-1}\ T^{-2}]$). This dimensional matrix is subdivided into a quadratic core matrix and a residual matrix, whereby the rank r of the matrix (here r = 3) in most cases corresponds to the number of the base dimensions appearing in the dimensions of the physical quantities.

| | $\Delta p$ | $q$ | $d$ | $l$ | $\rho$ | $\nu$ |
|---|---|---|---|---|---|---|
| mass M | 1 | 0 | 0 | 0 | 1 | 0 |
| length L | –1 | 3 | 1 | 1 | –3 | 2 |
| time T | –2 | –1 | 0 | 0 | 0 | –1 |
| | core matrix | | | residual matrix | | |

The nature of the steps which have to be carried out now makes this dimensional matrix less than ideal because it is necessary to know that each of the individual elements of the residual matrix will appear in only one of the dimensionless numbers, while the elements of the core matrix may appear as "fillers" in the denominators of all of them. The residual matrix should therefore be loaded with essential variables such as the target quantity and the most important physical properties and process-related parameters. Variables with an, as yet, uncertain influence on the process must also be included in this group. If, later, these variables are found to be irrelevant, only the dimensionless number concerned will have to be deleted while leaving the others unaltered.

Since the core matrix has to be transformed into a unity matrix (zero-free main diagonal, otherwise zeros) the "fillers" should be arranged in such a way as to facilitate a minimum of linear transformations.

The following reorganization of the above dimensional matrix fulfills both of these aims:

| | ρ | ***d*** | ν | Δ***p*** | ***q*** | ***l*** |
|---|---|---|---|---|---|---|
| mass M | 1 | 0 | 0 | 1 | 0 | 0 |
| length L | –3 | 1 | 2 | –1 | 3 | 1 |
| time T | 0 | 0 | –1 | –2 | –1 | 0 |
| | core matrix | | | residual matrix | | |

Now, with the first linear transformation of the rows the so-called Gaußian algorithm is carried out (zero-free main diagonal, beneath it zeros). It determines the rank of the matrix. The rank r = 3 is confirmed.

| | ρ | ***d*** | ν | Δ***p*** | ***q*** | ***l*** |
|---|---|---|---|---|---|---|
| $Z_1 = M$ | 1 | 0 | 0 | 1 | 0 | 0 |
| $Z_2 = 3M + L$ | 0 | 1 | 2 | 2 | 3 | 1 |
| $Z_3 = -T$ | 0 | 0 | 1 | 2 | 1 | 0 |
| | core matrix | | | residual matrix | | |

However, in this procedure, it could happen that a zero-free diagonal does not arise. Before concluding that the rank of the matrix is in fact r < 3, one should examine whether another arrangement of the core matrix makes a zero-free main diagonal possible.

Now, only one further linear transformation of the rows is necessary to transform the core matrix into a unity matrix, see the matrix below.

When generating dimensionless numbers, each element of the residual matrix forms the numerator of a fraction while its denominator consists of the fillers from the unity matrix with the exponents indicated in the residual matrix, see eq. (3.2).

| | ρ | ***d*** | ν | Δ***p*** | ***q*** | ***l*** |
|---|---|---|---|---|---|---|
| $Z'_1 = Z_1$ | **1** | 0 | 0 | 1 | 0 | 0 |
| $Z'_2 = Z_2 - 2\,Z_3$ | 0 | **1** | 0 | –2 | 1 | 1 |
| $Z'_3 = Z_3$ | 0 | 0 | **1** | 2 | 1 | 0 |
| | unity matrix | | | residual matrix | | |

$$\Pi_1 \equiv \frac{\Delta p}{\rho^1 d^{-2} \nu^2} = \frac{\Delta p\, d^2}{\rho\, \nu^2} \quad \Pi_2 \equiv \frac{q}{\rho^0 d^1 \nu^1} = \frac{q}{d\, \nu} \quad \Pi_3 \equiv \frac{l}{\rho^0 d^1 \nu^0} = \frac{l}{d} \tag{3.2}$$

The dimensionless number $\Pi_1$ does not usually occur as a target number for Δp. It has the disadvantage that it contains the essential physical property, kinematic viscosity ν, which is already contained in the process number (which is where it belongs). This disadvantage can easily be overcome by appropriately combining the dimensionless numbers $\Pi_1$ and $\Pi_2$. This results in the well-known Euler number

$$Eu \equiv \Pi_1\, \Pi_2^{-2} \equiv \frac{\Delta p\, d^4}{\rho\, q^2} \tag{3.3}$$

which is often combined with $\Pi_3 \equiv L/d$ to obtain an *intensively formulated target number*. This takes into account that in sufficiently long pipes the effects of the inlet can certainly be ignored and the proportionality $\Delta p \propto l$ exists. This combination of dimensionless numbers is called the friction factor in pipe flow ζ:

$$\zeta \equiv Eu\; d/l \equiv \Pi_1\, \Pi_2^{-2}\, \Pi_3^{-1} \equiv \frac{\Delta p\, d^4}{\rho\, q^2} \frac{d}{l} \tag{3.4}$$

- **Note:** The pi-theorem only stipulates the number of the dimensionless numbers and not their form. Their form is laid down by the user, because it must suit the physics of the process and be suitable for the evaluation and presentation of the experimental data.
  The structure of the dimensionless numbers depends on the variables contained in the core matrix. The Euler number, obtained by combining $\Pi_1$ and $\Pi_2$ in the example above, would have been obtained automatically if ν and q had been exchanged in the core matrix.
- **Note:** All Π sets obtained from one and the same relevance list are equivalent to each other and can be mutually transformed at pleasure!

The dimensionless number $\Pi_2$ is, in fact, the well-known Reynolds number, Re, even though it appears in another form here. Now, we will explain the structure that a dimensionless number must have in order to be called a Reynolds number. (This example is equally valid for all other named dimensionless groups.) The Reynolds number is defined as being any dimensionless number combining a *characteristic* velocity, v, and a *characteristic* measurement of length, l, with the kinematic viscosity of the fluid, $\nu \equiv \mu/\rho$. The following dimensionless numbers are equally capable of meeting these requirements:

$$\mathrm{Re} \equiv \frac{v l \rho}{\mu} = \frac{v l}{\nu} \;\hat{=}\; \frac{q}{D\nu} \;\hat{=}\; n\, d\, \frac{d}{\nu} = \frac{n\, d^2}{\nu} \tag{3.5}$$

Here, v is interpreted as being either a superficial velocity, $v = q/S \propto q/D^2$, or the tip speed of the stirrer, $u \propto n\, d$; n is stirrer speed, d is stirrer diameter.
This method of compiling a complete set of dimensionless numbers makes it clear that the numbers formed in this way cannot contain numerical values or any other constant. These appear in dimensionless groups only when they are established and interpreted as ratios on the basis of known physical interrelations. Examples:

$$\begin{aligned} &\mathrm{Re} \equiv \pi\, n\, d^2/\nu && \text{where } \pi\, n\, d \text{ is the tip speed and} \\ &\mathrm{Eu} \equiv \Delta p/(v^2\, \rho/2) && \text{where } v^2\, \rho/2 \text{ is the kinetic energy.} \end{aligned} \tag{3.6}$$

Since such expressions are of the same value as the analytically derived ones, it is always necessary to present the definition!

In the above-mentioned case of the pressure drop of the volume flow in a straight pipe, this method of compiling a complete set of dimensionless numbers produces the relationship

$$f(\mathrm{Eu}\; d/l,\; \mathrm{Re}) = 0 \;\rightarrow\; f(\zeta,\; \mathrm{Re}) = 0 \quad \text{with} \quad \zeta \equiv \mathrm{Eu}\; d/l \tag{3.7}$$

The information contained in this relationship is the maximum that dimensional analysis can offer on the basis of a relevance list, which we assumed to be complete. Dimensional analysis cannot provide any information about the form of the function *f*, i.e., the sort of pi-relationship involved. This information can only be obtained experimentally or by some additional theoretical considerations.

In their famous study *Stanton and Pannell* [7] evaluated the process equation of this problem $f$ (Eu d/l, Re) = 0 by measurements. **Fig. 1** shows the result of their work which impressively demonstrates the significance of the Reynolds number for pipe flow. The remark of *B. Eck* [8] hits the nail on the head:

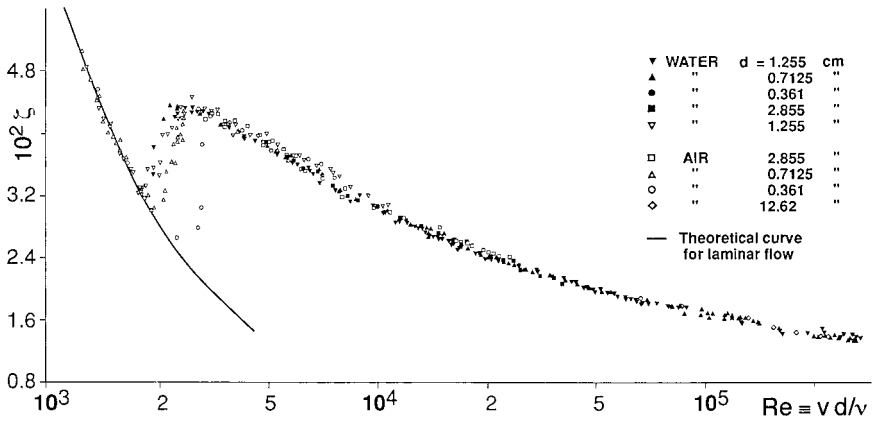


**Fig. 1** Pressure drop characteristic of a straight, smooth pipe; after [7].

*"If one represented – as it was once usual – ζ as a function of the velocity* v*, one would obtain not a curve, but a galaxy. Here, the Reynold's law must strike even a beginner with an elemental force".*

ζ is the "friction factor", which is defined here (according to physical interrelation) as follows:

$$\zeta \equiv \frac{\Delta p}{(\rho/2)v^2}\,\frac{d}{l} = 2(\pi/4)^2\,\frac{\Delta p\; d^4}{\rho\; q^2}\,\frac{d}{l} = 1.24\ \mathrm{Eu}\ d/l \tag{3.8}$$

The drawn-in curve is valid for the laminar flow range (Re < 2300) and corresponds to the analytical expression ("process equation")

$$\zeta = 64\ \mathrm{Re}^{-1} \quad \text{resp.} \quad \zeta\,\mathrm{Re} = 64 \tag{3.9}$$

This connection could have been clearly demonstrated had the authors chosen to present their test results in a double-logarithmical plot; this would have produced a straight line with a slope of –1 in this range of Re! ζRe can be viewed as a new dimensionless number that does not include the fluid density, ρ:

$$\zeta\mathrm{Re} \equiv \frac{2\Delta p}{\rho v^2}\,\frac{d}{l}\,\frac{vd\rho}{\mu} = \frac{2\Delta p d^2}{v\mu l} = 64 \tag{3.10}$$

It is only with the pi-relationship that the relevance to the problem and the operational range of individual variables becomes clear. Only now are we able to clearly distinguish between the laminar and the turbulent range. (The scattering of the measuring points around Re ≈ 2300 makes it clear that in smooth pipes the turbulence is often delayed.)

This example also shows that the pi-set compiled on the basis of the relevance list does no more than define the maximum pi-space, which may well shrink at the insight gained by measurements.

In the transition range ($\mathrm{Re} = 2.3 \times 10^3 - 1.0 \times 10^6$) the following process equations are valid:

$$\begin{aligned} &\zeta = 0.3164\ \mathrm{Re}^{-0.25} && \mathrm{Re} \le 8 \times 10^4 && \text{(Blasius)} \\ &\zeta = 0.0054 + 0.396\ \mathrm{Re}^{-0.3} && \mathrm{Re} \le 1.5 \times 10^6 && \text{(Hermann)} \end{aligned} \tag{3.11}$$

In the turbulent flow range, which appears in industrially rough (≈ smooth) pipes at $\mathrm{Re} > 10^6$, the following applies:

$$\zeta = \mathrm{const} \tag{3.12}$$

With respect to the dependence Δp(v) the following holds:

| | | |
|---|---|---|
| laminar range | ($\zeta \propto \mathrm{Re}^{-1}$) | $\Delta p \propto v$ |
| transition range | ($\zeta \propto \mathrm{Re}^{-0.3}$) | $\Delta p \propto v^{1.7}$ |
| turbulent range | (ζ = const) | $\Delta p \propto v^2$ |

Later on, *Nikuradse* [9] examined these correlations for artificially roughened pipes (by sticking sand particles onto the inner wall surface) and represented them in a pi-space extended by the geometrical number $d_p/d$. He and later researchers, for example [10], were primarily interested in the transition range of the Re number, where the wall roughness is of the same order of magnitude as the wall boundary layer.

Before the experimental data of Fig. 1 will be discussed in detail with respect to the scale-up, two important conclusions can be derived from the facts presented so far:

1. The fact that the analytical presentations of the pi-relationships encountered in engineering literature often take the shape of power products does not stem from certain laws inherent to dimensional analysis. It can be simply explained by the engineer's preference for depicting test results in double-logarithmic plots. Curve sections which can be approximated as straight lines are then analytically expressed as power products. Where this proves less than easy, the engineer will often be satisfied with the curves alone, cf. Fig 1.
2. The "benefits" of dimensional analysis are often discussed. The above example provides a welcome opportunity to make the following comments. The five-parametrical dimensional relationship
   $\{\Delta p/l; d; \rho, \nu, q\}$

can be represented by means of dimensional analysis as $\zeta(Re)$ and plotted as a *single* curve (Fig. 1). If we wanted to represent this relationship in a dimensional way and avoid creating a "galaxy" at the same time [8], we would need 25 diagrams with 5 curves in each! If we had assumed that only 5 measurements per curve were sufficient, the graphic representation of this problem still would have required 625 measurements. The enormous savings in time and energy made possible by the application of dimensional analysis are consequently easy to appreciate. These significant advantages have already been pointed out by *Langhaar* [11].

*Scale-up in Chemical Engineering.* Marko Zlokarnik
Copyright © 2002 Wiley-VCH Verlag GmbH & Co. KGaA
ISBNs: 3-527-30266-2 (Hardback); 3-527-60056-6 (Electronic)


# 4
# Scale-Invariance of the Pi-space – the Foundation of the Scale-up

It has already been pointed out that using dimensional analysis to handle a physical problem and, consequently, to present it in the framework of a complete set of dimensionless numbers, is the only sure way of producing a simple and reliable scale-up from the small-scale model to the full-scale technological plant. The theory of models states that:

- Two processes may be considered completely similar if they take place in a similar geometrical space and if all the dimensionless numbers necessary to describe them have the same numerical value ($\Pi_i$ = idem).

This statement is supported by the results shown in Fig. 1. The researchers carried out their measurements in smooth pipes with diameters d = 0.36 – 12.63 cm, thereby changing the scale in the range of 1 : 35. Furthermore, the physical properties of the fluid tested (water or air) varied widely. Nevertheless, the relationship $\zeta(Re)$ did not display this change: Every numerical value of Re still corresponded to a specific numerical value of $\zeta$! **The pi-space is scale-independent, it is scale invariant!** The pi-relationship presented is therefore valid not only for the examined laboratory devices but also for any other geometrically similar arrangement:

- Every point in a pi-framework, determined by the pi-relationship, corresponds to an infinite number of possible implementations.

This aspect is of special importance with respect to change in the linear dimension, because it is the foundation of a reliable scale-up.

With these facts the distinction between the pi-space and the original x-space is particularly clear. In a x-space $f(x_i) = 0$, which is constituted of dimensional quantities in the representation

$$x_1 = f(x_2) \quad x_j = \text{const},$$

each point of the $(x_1, x_2)$-space corresponds to solely one realization.

This characteristic of pi-representation represents the basis of the concept of similarity based on dimensional analysis: Processes which are described by the same pi-relationship are considered similar to each other if they correspond to the same point in the pi-framework. From the standpoint of dimensional analysis it is there-

fore completely insignificant whether the dimensionless numbers in question can be interpreted as ratios of forces, flows and so on. The question concerning the equality of these proportions is completely irrelevant.

Two realizations of the same physical interrelation are considered similar (*complete* similarity), when m – 1 dimensionless numbers of the m-dimensional pi-space have the same numerical value (pi = idem), because the m-th pi-number will then automatically also have the same numerical value.

To exercise the scale-up procedure already on this simple example of Fig. 1, let us imagine a pipeline in which a certain fluid (natural gas or crude oil) with a certain volume-related throughput, q, should be conveyed. Our aim is to find the pressure drop, $\Delta p$, of the fluid flow in the pipeline in order to design pumps and compressors.

We start by building a geometrically similar small-scale model of the technical pipeline. We already know the physical properties of the fluid, its throughput as well as the dimensions of the industrial plant (index $_T$) and therefore we also have the numerical value for $Re_T$ in operation. The same numerical value can be kept constant in the test apparatus (index $_M$) by the correct choice of conveying device and model fluid:

$$Re = idem \rightarrow Re_T = Re_M \rightarrow \left(\frac{v\,l}{\nu}\right)_T = \left(\frac{v\,l}{\nu}\right)_M \tag{4.1}$$

According to our knowledge of the pertinent pi-space (Fig. 1), Re = idem implies Eu = idem. The numerical value of the Euler number $Eu_M$, measured in the model-scale at the given $Re_M$ value, therefore corresponds to that of the full-scale plant. This then allows us to determine the numerical value of $\Delta p_T$ in the industrial plant from the numerical value of $Eu_M$ in the model and the given operational parameters:

$$Eu = idem \rightarrow Eu_T = Eu_M \rightarrow \left(\frac{\Delta p}{\rho\, v^2}\right)_T = \left(\frac{\Delta p}{\rho\, v^2}\right)_M \tag{4.2}$$

Of course, the concept of complete similarity does not guarantee that a process will be the same in the model as in the full-scale version in *every* respect; it is only the same with respect to particular aspect under examination, which has been described by the appropriate pi- relationship. In order to demonstrate this fact with the help of the above example, it should be remembered that the flow conditions in two smooth pipes of different scales should be considered similar when Re = idem and, according to the pressure drop characteristics, will therefore have the same numerical value of $\zeta \equiv Eu\ d/l$. However, this does not mean that heat transfer conditions prevalent in the two pipes are the same. For that to be the case, the relevant pi-relationship, $Nu = f(Re, Pr)$, requires that both the Reynolds number and the Prandtl number have the same numerical value (temperature-independent physical properties of the medium being supposed).

The more comprehensive the similarity demanded between the model ($_M$) and the full-scale device ($_T$) and the greater the

$$\textbf{scale-up factor}\ \mu \equiv l_T/l_M \qquad (l - \text{any characteristic length}) \tag{4.3}$$

the harder it is to perform the scale-up. This undertaking could even fail completely if a model material system with the appropriate physical properties cannot be obtained. A further difficulty is that a scale-up involving large changes of scale may cause changes to the pi-space. An example here is the case of forced non-isothermal flow, in which progression in scale results in free convection and consequently the Grashof number, $Gr \equiv \beta\ \Delta T\ l^3\ g/\nu^2$, becomes relevant to the problem. As an opposite example, it should be mentioned that with progression of the scaling down the pipe diameter, surface phenomena will sometimes come into play (e.g. the capillarity effect). In this case, a further pi-number appears which contains the surface tension σ (Weber number, We; Bond number, Bd).

The following example has been chosen because it impressively demonstrates the scale-invariance of the pi-space. Besides this, in the matrix transformation we will encounter a reduction of the rank r of the matrix. This will enable us to understand why, in the definition of the pi-theorem (section 2.7), it was pointed out that the rank of the matrix does *not always* equals the number of base dimensions contained in the dimensions of the respective physical quantities.

**Example 5**: Heat transfer from a heated wire to an air stream

This example, taken from [12], belongs to the field of heat transfer by convection. Here the heat transfer coefficient, h, represents the target quantity. This quantity can be determined only via the general heat transfer equation

$$Q = h\ A\ \Delta T \tag{4.4}$$

Electrically heated wires and pipes with the diameter, d, are mounted horizontally and are cooled by an air stream. The relevance list reads:

| | |
|---|---|
| target quantity: | heat transfer coefficient, h |
| geometric parameters: | diameter, d, of the wire or pipe |
| material parameter: | density, ρ, and kin. viscosity, ν ; heat conductivity, k; volume-related heat capacity, $\rho C_p$, of the gas |
| process-related parameters: | flow velocity, v, of the gas |

$$\{h;\ d;\ \rho,\ \nu,\ k,\ \rho C_p;\ v\} \tag{4.5}$$

A conveniently constructed dimensional matrix (for dimensions see Table 3) contains a core matrix which is transformed in three steps into the unity matrix. It just so happens that in the last linear transformation the 1. row and the ρ-columns eliminate. This represents a **reduction of the rank, r, of the matrix**.

| | | ρ | ***d*** | ***ν*** | ***k*** | ***h*** | $\rho C_p$ | ν |
|---|---|---|---|---|---|---|---|---|
| mass | M | 1 | 0 | 0 | 1 | 1 | 1 | 0 |
| length | L | –3 | 1 | 1 | 1 | 0 | –1 | 2 |
| time | T | 0 | 0 | –1 | –3 | –3 | –2 | –1 |
| temperature | Θ | 0 | 0 | 0 | –1 | –1 | –1 | 0 |
| M | | 1 | 0 | 0 | 1 | 1 | 1 | 0 |
| 3 M + L | | 0 | 1 | 1 | 4 | 3 | 2 | 2 |
| T | | 0 | 0 | –1 | –3 | –3 | –2 | –1 |
| Θ | | 0 | 0 | 0 | –1 | –1 | –1 | 0 |
| M | | 1 | 0 | 0 | 1 | 1 | 1 | 0 |
| 3 M + L + T | | 0 | 1 | 0 | 1 | 0 | 0 | 1 |
| –T | | 0 | 0 | 1 | 3 | 3 | 2 | 1 |
| Θ | | 0 | 0 | 0 | –1 | –1 | –1 | 0 |
| M + Θ | | | | | | | | |
| 3 M + L – T + Θ | | | **1** | 0 | 0 | –1 | –1 | 1 |
| –T + 3 Θ | | | 0 | **1** | 0 | 0 | –1 | 1 |
| –Θ | | | 0 | 0 | **1** | 1 | 1 | 0 |

This does not mean that the gas density, ρ, is irrelevant, but that it has been just fully taken into account by the kinematic viscosity $\nu = \mu/\rho$. If we would have taken the dynamic viscosity, μ, instead of the kinematic one, ν, this elimination would not have occurred, because μ [M $L^{-1}$ $T^{-1}$] contains mass in its dimensions. However, the result would have been the same: In both cases 7 – 4 = 6 – 3 = 3 pi-numbers result. These are

$$\Pi_1 \equiv \frac{h\ d}{k} \equiv \mathrm{Nu} - \text{Nusselt number} \tag{4.6}$$

$$\Pi_2 \equiv \frac{\rho C_p\ d\ v}{k} \rightarrow\ \Pi_2\ \Pi_3 \equiv \frac{\rho C_p\ \nu}{k} = \frac{\mu\, C_p}{k} \equiv \mathrm{Pr} - \text{Prandtl number} \tag{4.7}$$

$$\Pi_3 \equiv \frac{\nu}{d\,v} \equiv \mathrm{Re}^{-1} - \text{Reynolds number} \tag{4.8}$$

The functional dependence

$$\mathrm{Nu} = f(\mathrm{Pr}, \mathrm{Re}) \tag{4.9}$$

is reduced when working with air to

$$\mathrm{Nu} = f(\mathrm{Re}). \tag{4.10}$$

This is because the Pr number here is largely temperature independent and therefore has a constant numerical value: $\mathrm{Pr} \approx 0.70 = \text{const}$.

Functional dependence $\mathrm{Nu} = f(\mathrm{Re})$ is represented in **Fig. 2**. These measurements were performed with wires of d = 0.0189–1.00 mm and pipes of d = 2.99–150.0 mm.

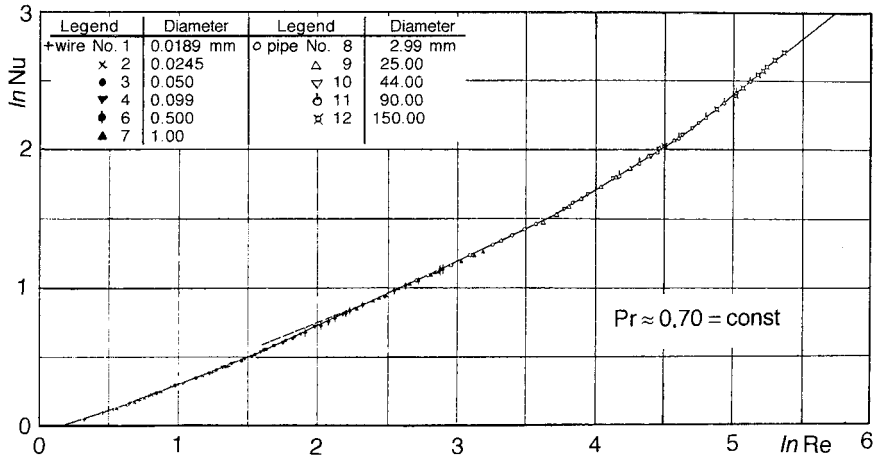


**Fig. 2** Heat transfer characteristic of wires and pipes streamed crossways by the air flow; from [12]

This corresponded to a scale-range of $\mu = 1 : 8.000$. Therefore, with the result in Fig. 2, the scale-invariance is particularly impressively proved.

The process equations in this pi-space read [13]:

$$Nu = 0.43 + 0.48\ Re^{0.5} \qquad 1 < Re < 4 \times 10^3 \tag{4.11}$$

$$Nu \propto Re^{0.8} \qquad Re > 2 \times 10^5 \tag{4.12}$$

*U. Grigull* [14] pointed out that the correspondence $h \propto v^{0.5}$ means the predominance of the laminar boundary layer, whereas $h \propto v^{0.8}$ refers to the prevailing of the turbulent boundary layer.

*Scale-up in Chemical Engineering.* Marko Zlokarnik


ISBNs: 3-527-30266-2 (Hardback); 3-527-60056-6 (Electronic)

# 5
# Important Tips Concerning the Compilation of the Problem Relevance List

## 5.1
## Treatment of Universal Physical Constants

The relevance list must also include universal physical constants such as the universal gas constant, **R**, the speed of light in a vacuum, **c**, or even the acceleration of a gravitational field (on Earth the acceleration due to gravity, g), if these constants influence the process concerned. The fact that a relevant physical quantity is a constant can never be a reason not to include it in the relevance list! By failing to consider the relevance of gravitational acceleration, the chemical engineer may find he has made a serious mistake!

Failing to consider gravitational acceleration when dealing with problems of process engineering is clearly not new. *Lord Rayleigh* [4] complained bitterly saying:

*"I refer to the manner in which gravity is treated. When the question under consideration depends essentially upon gravity, the symbol of gravity (g) makes no appearance, but when gravity does not enter the question at all, g obtrudes itself conspicuously".*

This is all the more surprising in view of the fact that the relevance of this quantity is easy enough to recognize if one asks the following question:

- Would the process function differently if it took place on the moon instead of on Earth?

If the answer to this question is affirmative, g is a relevant variable.

In fluid dynamics g is often effective in connection with $\rho$ or with $\Delta\rho$ as weight or as a weight difference.

## 5.2
## Introduction of Intermediate Quantities

Relevance lists of some problems contain a whole host of parameters. This makes the elaboration of the process characteristic a difficult endeavor. In some cases a closer look at a problem (or previous experience) facilitates a reduction of the num-

ber of physical quantities in the relevance list. This is the case when some relevant variables affect the process by way of a so-called *intermediate quantity*. Assuming that this intermediate quantity can be measured experimentally, it should be included in the problem relevance list, if this facilitates the removal of more than one quantity from the list. If, e.g., the target quantity, y, depends on five parameters

$$y = f_1\,(x_1, x_2, x_3, x_4, x_5),$$

and three of which can be replaced by an intermediate quantity z

$$z = f_2\,(x_2, x_3, x_4),$$

then the introduction of z reduces the functional dependence by two parameters to

$$y = f_3\,(x_1, z, x_5).$$

In the following, a few examples regarding this are mentioned.

A universally known intermediate quantity is the flow velocity, v, in pipes or the so-called superficial gas velocity, $v_G$, in stirring vessels at gassing or in bubble columns:

$$v = \frac{\text{volume throughput } q}{\text{cross-sectional area } S} \propto \frac{q}{D^2} \qquad S = \pi D^2/4$$

Its introduction into the relevance list replaces two quantities: throughput, q, and diameter, D.

A settling process (sedimentation) depends on the parameters of the disperse phase. They can be substituted by the sedimentation velocity $v_s$:

$$v_s = f\,(d_p, g\Delta\rho, \varphi_p, \mu)$$

($d_p$ – mean particle diameter, $g\Delta\rho$ – weight difference, $\varphi_p$ – volume portion of the solid phase, $\mu$ – dynamic density of the liquid.)

In some cases, e.g. in the flotation process, Example 7, it is possible to replace a great many influencing parameters by only one or two intermediate quantities. Then, it is legitimate to speak of intermediate quantities as of "lumped parameters".

A tableting process depends on the physical parameters, as e.g. mean particle diameter $d_p$, bulk density (porosity), flow behaviour (lubricating ability) of the powder, which depends also on humidity. These physical properties can be replaced by the lumped parameter powder compressibility $\kappa$ [136].

The importance of introducing intermediate quantities will now be demonstrated by two elegant examples.

**Example 6**: Homogenization of liquid mixtures with different densities and viscosities

The mixing time, $\theta$, needed for a complete homogenization of two Newtonian liquids, one resting at the start in a layer on top of the other, is normally determined by a decolorization method. For a given stirrer, installed in a vessel of known geometry, and for a material system *without* density and viscosity differences, the mixing time depends on the stirrer diameter, d, (as the characteristic geometric parameter in stirring); density, $\rho$, dynamic viscosity, $\mu$, stirrer speed, n:

$$\{\theta; d; \rho, \mu; n\} \tag{5.1}$$

This 5-parametric dimensional space leads to the 2-parametric mixing time characteristic:

$$n\theta = f(\mathrm{Re}) \quad \text{where} \quad \mathrm{Re} \equiv n\, d^2\rho/\mu = n\, d^2/\nu \tag{5.2}$$

For a material system *with* density and viscosity differences, the 5-parametric relevance list, eq. (5.1), has to be extended by the physical properties of the second mixing component, by the volume ratio of both phases, $\varphi = V_2/V_1$, and – inevitably – by the weight difference, $g\Delta\rho$, due to the prevailing density differences, to a 9-parametric dimensional space [15]:

$$\{\theta; d; \rho_1, \mu_1, \rho_2, \mu_2, \varphi; g\Delta\rho, n\} \tag{5.3}$$

This leads to a mixing time characteristic consisting of six pi-numbers:

$$n\theta = f(\mathrm{Re}, \mathrm{Ar}, \rho_2/\rho_1, \mu_2/\mu_1, \varphi) \tag{5.4}$$

Herein $\mathrm{Re} \equiv n\, d^2/\nu_1$ – Reynolds number and $\mathrm{Ar} \equiv g\Delta\rho\, d^3/(\rho_1\, \nu_1^2)$ – Archimedes number.

In a meticulous visual observation of this mixing process (the slow disappearance of the schlieren as a result of the balancing of the density differences) one will note that the coarse macro-mixing is quickly completed as compared with the micro-mixing which takes very long time. Certainly, this long-lasting process takes place in a material system, the physical properties of which already correspond to the homogeneous mixture:

$$\mu^* = f(\mu_1, \mu_2, \varphi) \quad \text{and} \quad \rho^* = f(\rho_1, \rho_2, \varphi) \tag{5.5}$$

By the introduction of the intermediate quantities $\mu^*$ and $\rho^*$ the relevance list (5.3) is reduced by three parameters:

$$\{\theta; d; \rho^*, \mu^*; g\Delta\rho, n\} \tag{5.6}$$

Now, the mixing time characteristic consists of only three pi-numbers:

$$n\theta = f(Re^*, Ar^*) \tag{5.7}$$

(The pi-numbers Re* and Ar* have to be formed by ρ* and μ*.)

In this pi-space, the process equation has been evaluated for the cross-beam stirrer, whereby the scale was altered by μ = 1 : 2 and the process parameters were widely varied [15]. The process equation found reads

$$\sqrt{n\theta} = 51.6\ Re^{*-1}\ (Ar^{*1/3} + 3) \qquad 10^1 < Re^* < 10^5;\ 10^2 < Ar^* < 10^{11} \tag{5.8}$$

This means that the mixing time increases in this flow range by $(\Delta\rho/\rho^*)^{2/3}$. An increase of $\Delta\rho/\rho^*$ by a decade, e.g. from $10^{-2}$ to $10^{-1}$, would lengthen the mixing time by a factor of 4.6.

This example clearly shows the advantage of introducing intermediate quantities in complicated problems. These findings will be also confirmed by the next example.

**Example 7**: Dissolved air flotation process

In a flotation process, tiny gas bubbles adhere to the naturally hydrophobic or artificially hydrophobised surface of solid particles making them float to the liquid surface, from where they can be removed as foam. For the removal and concentration of activated sludge in the biological waste water purification process, both dissolved air and degasifying flotation [16] can be used. In both cases, a gas mixture (air or $CO_2 + N_2$) is first dissolved in the respective liquid under higher pressure and is released, after decompression, in the form of tiny gas bubbles. The devices for this procedure consist of either longitudinally streamed through basins or of flotation cells, **Fig. 3 a**. To enable a vertical flow through the flotation cell, the cell is spatially separated into a flotation chamber and an annular space. In the latter, the liquid flows slowly downwards and the residual flocks rise upwards. In this way a complete removal of the particles is achieved.

Flotation is a depletion process which obeys a time law of the 1st order and is described by the flotation rate constant, $k_F$. The target quantity, "solids discharge A", corresponds to the chemical conversion, X, in 1st order reactions:

$$A \equiv X \equiv (c_0 - c)/c_0 = 1 - c/c_0 = 1 - \exp(-k_F\, t) \tag{5.9}$$

Now we will examine the flotation process taking place in the flotation cell (s. Fig. 3 a) of a given geometry (characteristic linear measurement of length being the cell diameter D).

The problem here consists in listing the material parameters because, in activated sludge, they fluctuate strongly (much in contrast to ore flotation). Surely, the degree of hydrophobicity (wettability) of the particle surface (contact angle, Θ) will be of importance. Furthermore, the pH value, the concentration of the flocculant (polyelectrolyte), $c_F$, the portion of solids, φ, in the system, the weight difference, $g\Delta\rho$,

between the bacteria and the liquid – just to mention a few – will play an important role.

In contrast, it is easy to list all of the process parameters involved: liquid input, $q_{in}$, which leaves the cell divided into the flotate discharge, $q_{Fl}$, and the processed liquid output, $q_{out}$; releasable gas content of the liquid feed, $q_{gas}/q_{in} = Hy\ \Delta p/\rho_G$; gravitational acceleration g. (Hy is the Henry's law constant)

The relevance list now reads:

$$\{A; D; \Theta, pH, c_F, \varphi; q_{in}, q_{aut}; q_G/q_{in}, g\Delta\rho\} \tag{5.10}$$

This relevance list, which is certainly incomplete with respect to physical properties, can be streamlined significantly by introducing two intermediate quantities:
1. the *superficial velocity*, v, in the annulus of the flotation cell (Fig. 3 a):

$$v = f_1\ (q_{in}\ ,\ D) \quad \text{and} \tag{5.11}$$

2. the *rising velocity*, w, of the flocks:

$$w = f_2\ (\Theta, pH, c_F, \varphi, q_G/q_{in}, g\Delta\rho) \tag{5.12}$$

(The rising velocity of the flocks has to be determined with an appropriate measuring device.)

The 10-parametric relevance list in eq. (5.10), which has been assumed to be fairly complete, now reduces to only a 5-parametric one:

$$\{A, v, w, q_{in}, q_{out}\} \tag{5.13}$$

This relevance list delivers the following simple 3-parametric pi-set:

$$\{A, w/v, q_{in}/q_{out}\} \tag{5.14}$$

In this pi-space, measurements were evaluated which were performed in a bench-scale flotation cell (Fig. 3 a) of D = 0.6 m. The flotation cell input consisted of biologically purified waste water, containing ≈ 3 g TS/l activated sludge (TS – total solids), which was processed in the 30 m high bubble columns, the so-called "Tower Biology" of BAYER AG/Leverkusen, Germany.

The result in **Fig. 3 b** cannot be called satisfying. This is certainly not surprising, because the processed waste waters of this chemical giant originated from ca. 150 production sites and constantly changed their composition. Nevertheless, at least it can be seen that the process parameters are correctly taken into account by the ratio v/w. (The rising velocity, w, was varied each day to a small extent by the addition of different amounts of polyelectrolitic flocculants.)

The results of this examination show that biologically purified waste water can be completely freed from activated sludge under the precondition that the superficial

velocity of the input amounted to the half value of the rising velocity of the flocks. (The fact that A = 100 % was never achieved is understandable, because in the determination of the solids content the dissolved inorganic salts were also measured, which of course cannot be removed by flotation.)

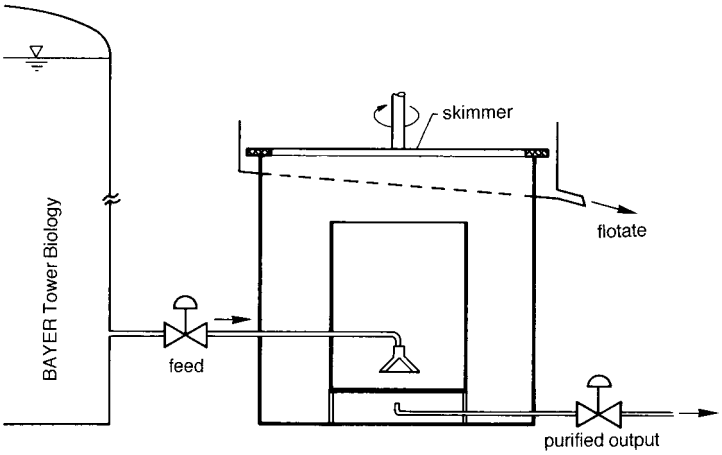


**Fig. 3 a** Sketch of a flotation cell with spacially separated aeration and separation zones for the dissolved air flotation

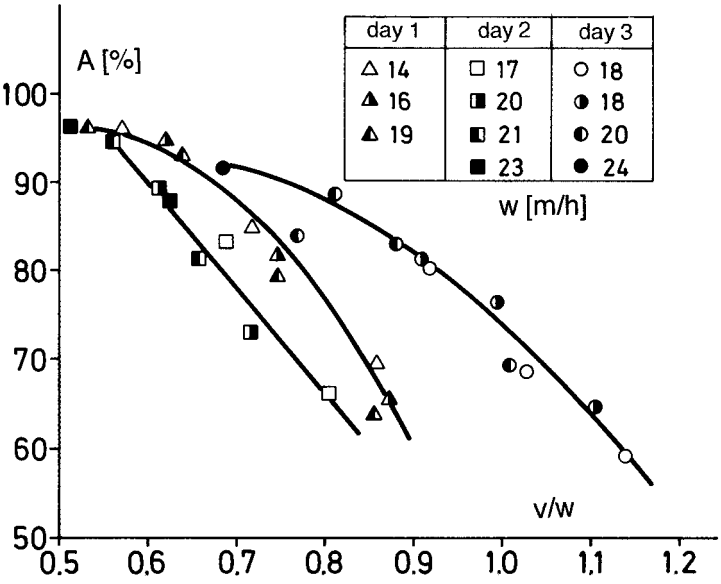


**Fig. 3 b** Correlation between the activated sludge discharge A and the ratio v/w of the superficial velocity, v, to the rising velocity of flocks, w; from [16].

*Scale-up in Chemical Engineering.* Marko Zlokarnik


ISBNs: 3-527-30266-2 (Hardback); 3-527-60056-6 (Electronic)

# 6
# Important Aspects Concerning the Scale-up

## 6.1
## Scale-up Procedure at Unavailability of Model Material Systems

To be able to adjust the process point of the pertinent pi-space in the model experiment, one has to chose an appropriate model material system.

In order to conduct model measurements in only one model device, the numerical values of the pi-numbers in question (i.e. the fixation of the operational process point of the system) must be adjusted by the appropriate selection of the numerical values of the process parameters and/or of the model material system. If this is not feasible, then the process characteristic has to be evaluated from model experiments in devices of different scales or the operational process point has to be extrapolated from measurements in differently sized model devices.

When model material systems are not available (e.g. with non-Newtonian fluids) or the relevant material parameters are unknown (e.g. with foams, slimes and sludges), model measurements must be carried out in models of various sizes.

The unavailability of the model material systems can sometimes limit the application of the dimensional analysis. In such cases it is, of course, absolutely wrong to speak of "*limits of the dimensional analysis*".

The following example will show how design and scale-up data can be obtained by model measurements with the same material system in differently sized laboratory devices.

**Example 8**: Scale-up of mechanical foam breakers

In certain chemical and biological as well in some unit operations, foaming occurs to such an extent that the process is severely impaired or even comes to a complete standstill. For example, chemical reaction systems tend to foam if a gas is formed in nascent state, because such minute gas bubbles do not coalesce to form larger ones and therefore remain in the system. Expulsion of residual monomers after emulsion polymerization often involves serious foaming problems because, in this case, very fine gas bubbles are formed in a material system which contains emulsifiers, i.e. foam producing surfactants.

In microbiological processes, foaming occurs more often than in chemical ones since many metabolic processes produce surfactants, the process frequently takes place in a 3- or 4-phase systems (G/L/(S)/microorganisms) and intensive aeration or gas evolution (fermentation processes) is often involved. This often leads to the situation that foam evolution cannot be controlled any more.

Finally, unit operations (gas absorption, distillation) may cause foaming or are even based on foaming (flotation, foam fractionation).

Mechanical foam breaking is the method most frequently used to cope with these problems. It is largely based on subjecting the foam lamellae to shear stress and to rapidly alternating pressure fields generated within the foam breaker. In addition, compressed secondary foam, which is ejected from the foam breaker, strikes against primary foam in the gas head or against the vessel wall. The task of the foam breaker is to compress the voluminous primary foam ($d_b$ > 1 mm) to an easy flowing secondary foam ($d_b$ > 0.05–0.1 mm). This can then be returned back into the gas space of the vessel.

This aim fully describes the target quantity of a foam centrifuge, s. sketch in **Fig. 4**. One has to determine the minimum rotational speed, $n_{min}$, required to set the foam flowing. (According to [17], a resulting foam density of ca. $\rho$ = 0.50 kg/l should suffice.)

The characteristic geometric parameter is undoubtedly the diameter, d, of the foam centrifuge (here the diameter of the cone base).

Density, viscosity and elasticity of the *foam lamellae*, as essential physical properties of the foam, cannot be measured. They all depend on the physical properties of the investigated multiphase material system, including the type and concentration of surfactants. These properties can usually not be measured, particularly not if they are produced *in situ* by the bacterial culture. We will therefore introduce into the relevance list the sum of all physical properties, $S_i$, which affect the destructibility of the foam as well as the concentration, $c_T$ (e.g. in [ppm]), of a known tenside used in the tests.

The process parameters are first represented by the minimum rotational speed, $n_{min}$ (as a target number), and then by the temporal foam evolution, $q_f$, which equals the gas throughput: $q_f \triangleq q$. In the original publication [17], the acceleration due to gravity, g, was not introduced into the relevance list on the grounds that it is the centrifugal acceleration which causes foam breaking and this exeeds gravitational acceleration by a multiple. This is indeed true, but it also has to be taken into consideration that the state of the foam upon entry into the foam centrifuge very much depends upon the force field in which it has been produced.

This reasoning leads to the following relevance list of the problem:

$$\{n_{min};\ d;\ S_i,\ c_T;\ q,\ g\} \tag{6.1}$$

and delivers the following pi-space:

$$Q^{-1} = f(Fr,\ S_i^*,\ c_T) \quad \text{with} \tag{6.2}$$

$$Q^{-1} \equiv \frac{n_{min}\, d^3}{q} \quad \text{and} \quad Fr \equiv \frac{q^2}{d^5 g}$$

$Q^{-1}$ represents the reciprocal value of the well known gas throughput number Q. Fr is the Froude number, here formed with the gas throughput and $c_T$ is the dimensionless concentration (in ppm) of the foaming agent in the liquid. $S_i$* are the physical properties which affect foam stability. Because they are neither known by number (i) nor by kind, instead of $S_i$* the type of the foaming agent (name and chemical structure) must be given.

The model measurements [17] were performed on three geometrically similar appliances in the scale-ratio $\mu = 1 : 1.5 : 2$. Fig. 4 shows the dependence, eq. (6.2), for the foaming agent Mersolat®H (BAYER/Leverkusen, Germany). The process equation reads:

$$Q^{-1} = 1.37\ Fr^{-0.40}\ c_T^{0.32} \tag{6.3}$$

For the five foaming agents examined in [17] the following exponents in

$$Q^{-1} = Fr^{-a}\ c_T^{b} \tag{6.4}$$

were found: $a = 0.40–0.45$ and $b = 0.1–0.36$.

The correlation $Q^{-1} \propto Fr^{-a}$ can be reduced after remodeling and, with respect to the exponent a, to the following dependences:

$$a = 0.5:\ n^2 d/g = c_T^{b} \tag{6.5}$$

$$a = 0.4:\ n\,d\ = q^{0.2}\ g^{0.4}\ c_T^{b} \tag{6.6}$$

In the first case, eq. (6.5), the necessary centrifugal acceleration $n^2d$ only depends on the foam parameters $S_i$* and $c_T$, these being independent of gas throughput $q \triangleq q_f$. These foams can be easily controlled. (With the exception of Mersolat®H ($a = 0.40$), the foaming agents investigated in [17] did not comply with this behaviour, here $a = 0.45$)

In the second case, eq. (6.6), which applies to Mersolat®H (Fig. 4), the tip speed, n d, necessary to control the foam is, to a small degree, also dependent upon q.
Since the exponent, a, of Fr in the process equation (6.4) exhibits a numerical value of $a = 0.45$ for four foaming agents and only $a = 0.40$ for Mersolat®H, see [17], the numerical value of the constant at Fr = const can be plotted for all five foaming agents as a function of the foaming agent concentration. In such a way the mechanical stability of foams produced by individual surfactants can be quantified. (It is shown in [17] that the effect of the type of foaming agent on the foam stability is surprisingly low.)

In order to design and to scale-up a foam centrifuge of the type presented, measurements with the material system in question would have to be performed on a appropriate model appliance. In this manner, the design of the full-scale foam centrifuge presents no problem. Apart from that, these tests and their representation in the sense of Fig.4 give the manufacturers of foaming agents a quantifiable assessment of the mechanical stability of the foams produced.

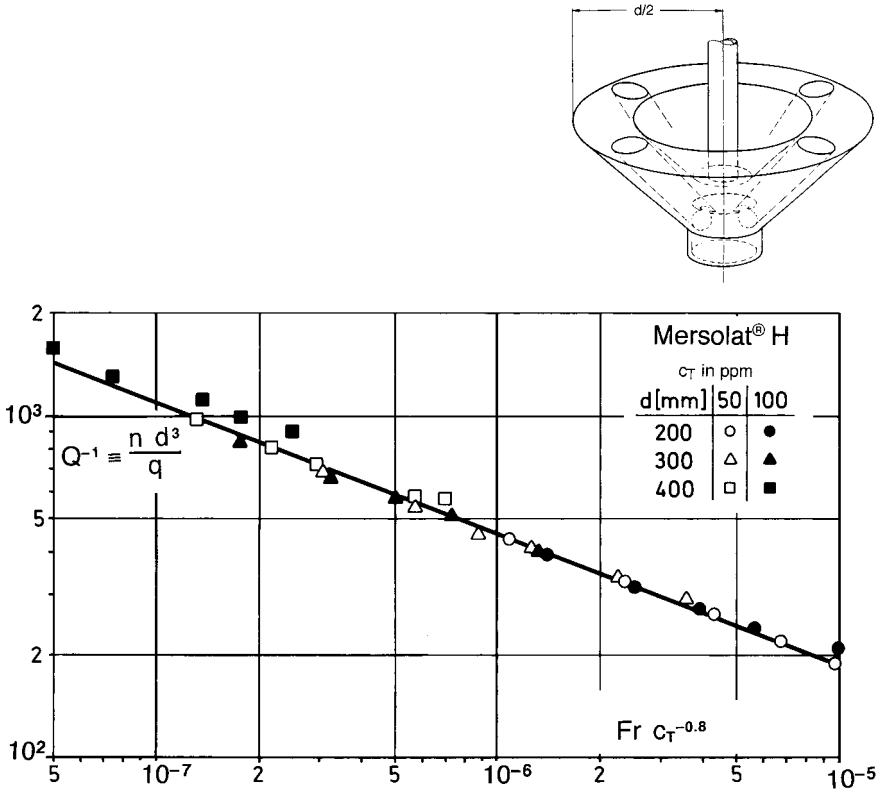


**Fig. 4** Process characteristic of a foam centrifuge (sketch) for a given foaming agent (Mersolat®H) in two concentrations ($c_T$ in ppm); from [17]

## 6.2 Scale-up Under Conditions of Partial Similarity

When appropriate material systems are not available for model experiments, accurate simulation of the working conditions of an industrial plant on a laboratory- or bench-scale may not be possible. Under such conditions, experiments on differently sized equipment are customarily performed before extrapolation of the results to the full-scale operation. Sometimes this expensive and basically unreliable procedure can be replaced by a well-planned experimental strategy. Namely, the process in question can be either divided up into parts which are then investigated separately (Example 9: Drag resistance of a ship's hull after *Froude*) or certain similarity criteria can be deliberately abandoned and then their effect on the entire process checked (Example 41/2: Simultaneous mass and heat transfer in a catalytic fixed bed reactor after *Damköhler*).

Several "rules of thumb" for dimensioning different types of process equipment are, in fact, scale-up rules based unknowingly on partial similarity. These rules

include the so-called *mixing power per unit volume*, P/V, widely used for scaling up mixing vessels, and the *superficial gas velocity*, v, which is normally used for scaling up bubble columns and fluidized beds (Example 10).

**Example 9**: Drag resistance of a ship's hull

This problem represents the dawn of scale-up methodology and is closely linked to the name of *William Froude* (1810 – 1879). We are very much indebted to this brilliant researcher because he treated this significant scale-up problem with a clear physical concept and carefully executed experiments to go with it.

We shall first treat this problem by using dimensional analysis. The drag resistance, F, of a ship's hull of a given geometry (characteristic length being its length, l, and a given displacement volume, V) depends on the speed of the ship, v, the density, ρ, and kinematic viscosity, ν, of the water and – because of the bow wave formation – also on the acceleration due to gravity, g. The list of relevant quantities is thus:

$$\{F; l, V; \rho, \nu; v, g\} \tag{6.7}$$

The following – conveniently drawn up – dimensional matrix leads to, after only two linear transformations, the unity matrix (rank r = 3) and the residual matrix:

| | ρ | ***l*** | ***ν*** | ***F*** | ν | ***g*** | ***V*** |
|---|---|---|---|---|---|---|---|
| mass M | 1 | 0 | 0 | 1 | 0 | 0 | 0 |
| length L | –3 | 1 | 1 | 1 | 2 | 1 | 3 |
| time T | 0 | 0 | –1 | –2 | –1 | –2 | 0 |
| | core matrix | | | residual matrix | | | |

| | ρ | ***l*** | ***ν*** | ***F*** | ν | ***g*** | ***V*** |
|---|---|---|---|---|---|---|---|
| M | **1** | 0 | 0 | 1 | 0 | 0 | 0 |
| 3M + L + T | 0 | **1** | 0 | 2 | 1 | –1 | 3 |
| –T | 0 | 0 | **1** | 2 | 1 | 2 | 0 |
| | core matrix | | | residual matrix | | | |

From this, after the well known procedure, the following four pi-numbers result:

$\Pi_1 \equiv F/(\rho\, l^2\, v^2) \equiv Ne$ (Newton number)

$\Pi_2 \equiv \nu\, /l\, v \equiv Re^{-1}$ (Reynolds number)

$\Pi_3 \equiv g\, l/v^2 \equiv Fr^{-1}$ (Froude number)

$\Pi_4 \equiv V/l^3$ – dimensionless diplacement volume

The problem is consequently completely defined by the pi-set

$$\{\mathrm{Ne}, \mathrm{Re}, \mathrm{Fr}, V/l^3\} \tag{6.8}$$

The model theory requires that in the scale-up from model- to the full-scale not only the geometric similarity ($V/l^3$ = idem) is maintained, but also that all the other pi-numbers describing the problem keep the same numerical values (pi = idem). This implies that, for example, in the measurements with the boat and ship models both process numbers

$$\mathrm{Fr} \equiv v^2/(l\,g) \quad \text{and} \quad \mathrm{Re} \equiv v\,l/\nu \tag{6.9}$$

be idem. However, this demand cannot be fulfilled.

Because the acceleration due to gravity cannot be varied on Earth, Fr = idem is adjusted in model experiments by the model speed $v_M$. Thereafter, Re = idem has to be met by the adjustment of the model fluid viscosity. Supposing that the size of the model is only 10 % of the full-scale size (scale-up factor $\mu = I_T/I_M = 10$), then the requirement Fr = idem results in the speed of the model $v_M = 0.32\ v_T$. From this, the kinematic viscosity, $\nu_M$, of the model fluid can be calculated:

$$\nu_M/\nu_T = (v_M/v_T)\ (I_M/I_T) = 0.32 \times 0.1 = 0.032 \tag{6.10}$$

However, there is no fluid with a viscosity which is only 3 % of that of water. (At $\mu = 100$ it follows $\nu_M/\nu_T = 1 \times 10^{-3}$, i.e. the viscosity of the model fluid may be only $1 \times 10^{-3}$ of the water value.)

If the scale-up factor didn't have to be that small and models were not so expensive to build, experiments could be run with models of various sizes in water at the same value of Fr and then the results could than be extrapolated to $\mathrm{Ne}_T$ at $\mathrm{Re}_T$. In view of the powerful model reduction and the resulting extreme differences in the Reynolds number

$$\mu = 1\ ;\ 10\ ;\ 100 \quad \rightarrow \quad \mathrm{Re}_M/\mathrm{Re}_T = 1\ ;\ 3.2 \times 10^{-2}\ ;\ 1 \times 10^{-3} \tag{6.11}$$

extrapolation appears to be a risky undertaking, particularly when the cost of the motor used in the full-scale application is considered.

Naturally, the results of dimensional analysis discussed above and their consequences were not known to the ship builders of the 19th century. Since the time of *Rankine*, the total drag resistance of a ship has been divided into three parts: the surface friction, the stern vortex and the bow wave. However, the concept of *Newtonian* mechanical similarity, known at that time, only stated that for mechanically similar processes the forces vary as $F \propto \rho\ l^2\ v^2$. Scale-up was not considered for assessing the effect of gravity.

*Froude* observed that the resistance due to the stern vortex was relatively small compared to the other two sources of resistance. Therefore, he decided to combine it with the bow wave resistance to obtain the *form drag*, $F_f$. As a result of careful inve-

stigations and theoretical considerations, he realized that the wave formation of the ship could be simulated by using scale models. He arrived at the law of appropriate velocities: "The wave formations at the ship and the model are (geometrically) similar, if the velocities are in the ratio of the square root of the linear dimensions". He also found that for similar wave formations, the hull drag (*friction drag* $F_r$) behaves not as $F_r \propto \rho\, v^2\, l^2$, but as $F_r \propto v^{1.825}\, A\, \rho$ (A - surface area). Consequently, he developed computational methods for scaling down models and ships by length and the type of the wetted surface. In this way, he was in the position of being able to calculate the form drag, $F_f$, from the total drag after subtracting the predictable friction drag. He found: "If we adhere to the law of the appropriate velocities in scaling-up the ship, the form resistances will correspond to the cubes of their dimensions (that is to say, their displacement volumes)" [18]*)

In summary:

1. $F_{total} - F_r = F_f$
2. If $v^2 \propto l$, than $F_f \propto l^3$. (6.12)

Dividing this functional dependence (6.12) by $\rho\, l^2\, v^2$, in order to transform $F_f$ into the Newton number of form drag, leads to the following proportionality

$$\frac{F_f}{\rho\, l^2\, v^2} \propto \frac{l^3}{\rho\, l\, v^2} = \frac{l}{\rho\, v^2}$$

This means:

$$Ne_f = \text{idem} \quad \text{at} \quad Fr = \text{idem} \quad \text{with} \quad Fr \equiv v^2/l\, g \tag{6.13}$$

In order to verify these experimental results, the corvette "Greyhound" was towed by the corvette "Active" under the command of *Froude*, and the drag force in the tow rope was measured. *Froude* reported [19] that the observed deviations from the predictions of the model were in the range of only 7 – 10%.

*M. Weber* [20] pointed out that *Froude*'s procedure was not entirely correct and could never provide real proof, because complete similarity between the model and its full-scale counterpart cannot be achieved. The described procedure can therefore represent nothing more than an excellent approximation of reality. He continued by saying: "The fact that *Froude* was able to achieve his goal with such a large measure of success, despite all the difficulties, lies in his ingenuity which enabled him to itemize and to assess all the practical and theoretical details of drag resistance and finally to trace a clear picture of this intricate phenomenon." Nothing can be added to this assessment: *Froude*'s work represents a prime example of partial similarity. His performance can certainly be admired, especially in view of the measuring techniques available to him at that time.

*) The reference [18] includes the minutes of the session of The Institution of Naval Architects in London of April 7, 1870. During this session, W. Froude presented and defended the results of his modeling with great steadfastness and conviction; this represents the sidereal hour of the theory of models.

*J. Pawlowski* [21] discussed an interesting alternative experimental approach to this scale-up problem. He also started by splitting the drag resistance into friction, depending only on Re, and a bow wave resistance, depending only on Fr:

$$Ne_T = f_1\,(Re_T) + f_2\,(Fr_T) \tag{6.14}$$

However, he proposed a different strategy from that of *Froude*. In the *first* experiment, measurements were made with the model ship in water at $Fr_1 = Fr_T$, consequently $Re_1 = Re_T\,\mu^{-3/2}$, i.e., the measurement was carried out at a correct Fr value and a false Re value. As a result, also a false value of $Ne_1$ was obtained from the relationship:

$$Ne_1 = f_1\,(Re_1) + f_2\,(Fr_T)$$

*Two additional* experiments were carried out, not with the model ship, but with a totally immersed form (**Fig. 5**) whose shape was given by reflecting the immersed portion of a ship's hull at the water line (at $V/l^3$ = idem). In these experiments, the Froude number is irrelevant; the friction corresponding to the surface area of the model must be divided by 2.

The measurements in water were carried out at $Re_1$ and $Re_T$, thereby obtaining

$$Ne_2 = f_1\,(Re_T) \quad \text{and} \quad Ne_3 = f_1\,(Re_1)$$

The desired $Ne_T$ could then be calculated:

$$Ne_T = f_1\,(Re_T) + f_2\,(Fr_T) = Ne_1 - Ne_3 + Ne_2$$

The above alternatives for the determination of a ship's hull resistance illustrate an application of the method of partial similarity in which the process is divided into parts, this allowing them to be investigated independently.

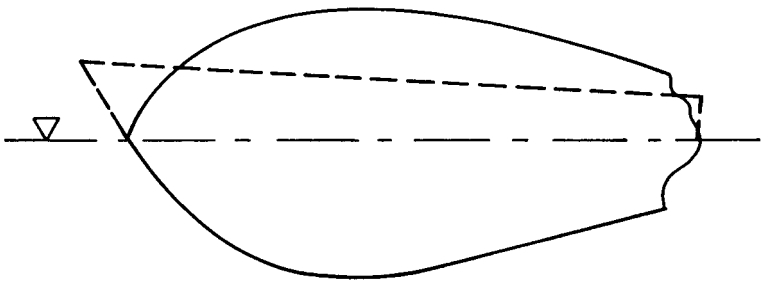

**Fig. 5** Sketch of the completely submersed streamlined body

**Example 10**: Rules of thumb for scaling up chemical reactors: Volume-related mixing power and the superficial velocity as design criteria for mixing vessels and bubble columns

In the introduction to this chapter it has been already pointed out that for the design of chemical process equipment "rules of thumb" exist. Upon closer examination, these rules provide conditions which unconsciously accept partial similarity. Actually, one cannot expect that complicated processes of fluid dynamics occurring during mass and heat transfer can be adequately described by criterions such as power per unit of volume, P/V, for mixing vessels and superficial gas velocity, $v \equiv q/S$, for bubble columns.

Each unit operation in process engineering obeys specific laws which demand a separate pi-space. It cannot be expected that different processes can be depicted by the same pi-space.

**Stirring vessels.** Upon the examination of different stirring operations it was indeed found that the *intensively* formulated process parameter P/V represented the pertinent scale-up criterion only if the stirring power has to be dissipated in the volume as evenly as possible (micro-mixing, isotropic turbulence). Examples of this are the dispersion of a gas in a liquid or the dispersion of immiscible liquids; s. [22].

In the most important stirring operation – the homogenization of liquid mixtures – the convective transport of liquid balls (macro-mixing) is of predominant importance. Thus, this process depends to a large degree on space geometry and type of stirrer. It is influenced by the *extensive* parameters such as stirrer speed, n, and stirrer diameter, d. Here, the similarity with respect to fluid dynamics is given by $Re \equiv n\, d^2\, \rho/\mu = \text{idem}$.

Convective bulk transport is also an extremely important factor in the suspension of solids in a stirred tank (this is also responsible for the flow pattern at the tank bottom). P/V cannot be used as a scale-up criterion in this process either. Measurements have shown that the minimum rotational speed, $n_{crit}$, of the stirrer which is necessary for the suspension (whirling-up) of particles in the turbulent regime is given by the appropriate Froude number:

$$Fr_{crit} \equiv n_{crit}^2\, d\, \rho/(g\, \Delta\rho) \tag{6.18}$$

Which consequences result from the "dimensioning criterion" P/V if the correct scale-up criterion is represented by Fr = idem?

Because the Froude number is the scale-up criterion here, we formulate it for a given material system by P/V as follows:

$$Fr \propto n^2\, d = \text{idem} \tag{6.19}$$

$$P/V \propto n^3\, d^2 \quad (P \propto n^3\, d^5 \text{ in the turbulent flow range; } V \propto d^3) \tag{6.20}$$

$Fr \propto n^2\, d = \text{idem}$ means that any power of Fr is equally idem:

$$Fr^{3/2} = (n^2\, d)^{3/2} = (P/V)\, d^{-1/2} = \text{idem} \tag{6.21}$$

The answer to the question of the relationship between P/V and Fr, at Fr = idem, reads:

$$[(P/V)\, d^{-1/2}]_T = [(P/V)\, d^{-1/2}]_M$$
$$Fr = \text{idem} \rightarrow (P/V)_T = (P/V)_M\, \mu^{1/2} \qquad \mu \equiv d_T/d_M \tag{6.22}$$

It should be pointed out that the scale-up rule Fr = idem results in costly consequences: The power input per unit volume increases by the square root of the scale-up factor μ.

**Bubble columns** are often designed on the basis of the superficial gas velocity $v \equiv q/S$ (q - gas throughput, S - cross-sectional area of the column). Many authors have found that the gas/liquid mass transfer in bubble columns is indeed governed by this quantity ($k_L$ - liquid side mass transfer coefficient; a - interfacial area per unit volume):

$$k_L a \propto v \;\rightarrow\; k_L a/v = \text{const.} \tag{6.23}$$

This interdependence is only understandable when one considers that the volume-related mass transfer coefficient is defined by $k_L a = G/(V\Delta c)$ and the superficial velocity, v, by $v = q/S$, as well the fact that volume $V = H \times S$ (H - height of the column):

$$\frac{k_L a}{v} = \frac{G}{H\, S\, \Delta c}\, \frac{S}{q} = \frac{G}{H\, q\, \Delta c} = \text{const.}$$

In words: The gas absorption rate $G[MT^{-1}]$ is directly proportional to the liquid height, H, the gas throughput, q, and the concentration difference, Δc [24]. (This is only valid under the conditions that the gas is not completely absorbed: $\Delta c > 0$.)
In contrast with this – and in analogy to the corresponding findings in the mixing vessel – the mixing (back-mixing) in bubble columns cannot be described by the intensively formulated quantity v. For this scale-up task, the Froude number is competent here.

Experiments [25] performed in bubble columns of different sizes gave the following expression for the mixing time, θ:

$$\theta\, (g/D)^{1/2} \propto Fr^{-1/4} \tag{6.25}$$

$Fr \equiv v^2/D\, g$ ; D – diameter of the bubble column

It follows that

$$\theta \propto v^{-1/2}\, D^{3/4} \quad \text{resp.} \quad \theta = \text{idem} \rightarrow v^{-1/2}\, D^{3/4} = \text{idem}$$

This leads to the conclusion that

$$v_T = v_M \, \mu^{1.5} \tag{6.26}$$

Thus, in a bubble column which has been geometrically scaled-up by a factor of $\mu = 10$, the same mixing time as in the model will be only obtained when the superficial velocity is increased by a factor of $10^{1.5} = 32$. Hence, v is not a scale-up criterion here.

- The correlations presented in example 10 show emphatically that a particular scale-up criterion, that is valid in a given type of apparatus for a particular process, is not necessarily applicable to other processes occurring in the same device.

*Scale-up in Chemical Engineering.* Marko Zlokarnik


ISBNs: 3-527-30266-2 (Hardback); 3-527-60056-6 (Electronic)

# 7
# Preliminary Summary of the Scale-up Essentials

## 7.1
## The Advantages of Using Dimensional Analysis

The advantages made available by correct and timely use of dimensional analysis are as follows:

1. Reduction of the number of parameters necessary to define the problem. The pi-theorem states that a physical relationship between n physical quantities can be reduced to a relationship between $m = n - r$ mutually independent pi-numbers. Herein, r represents the rank of the dimensional matrix which is formed by the physical quantities in question and corresponds, in most cases, to the number of base dimensions contained in their dimensions.
2. Reliable scaling-up of the desired operating conditions from the model to the full-scale plant. This is based on the scale invariance of the pi-space. According to the model theory, two processes may be considered to be similar if they take place under geometrically similar conditions and all dimensionless numbers which describe the process have the same numerical value.
3. A deeper insight into the physical nature of the process. By representing experimental data in a dimensionless form, physical states (e.g. turbulent or laminar flow range, suspension state, heat transfer by natural or by forced convection, and so on) can be delimited from each other and the limits quantified. In this manner, the domain of individual physical quantities also becomes apparent.
4. A greater flexibility in the choice of parameters and their reliable extrapolation within the range covered by the dimensionless numbers. These advantages become clear if one considers the well-known Reynolds number, $Re = v\, l\, \rho/\mu$, which can be varied by altering the characteristic velocity, v, characteristic length, l, or the kinematic viscosity, $\nu = \mu/\rho$. By choosing appropriate model fluids, viscosity can be very easily altered by several orders of magnitude. Once the effect of the Reynolds number is known, extrapolation of both v and l is permitted within the examined range of Re.

## 7.2
## Scope of Applicability of Dimensional Analysis

In order to describe a physico-technological problem by a complete set of pi-numbers, initially all essential ("relevant") physical quantities which describe the problem must be known. A prerequisite of this requirement is a thorough and critical knowledge of the process in question.

In fact, the applicability of dimensional analysis depends heavily on the knowledge available. The following five steps can be outlined, see also **Fig. 6**.

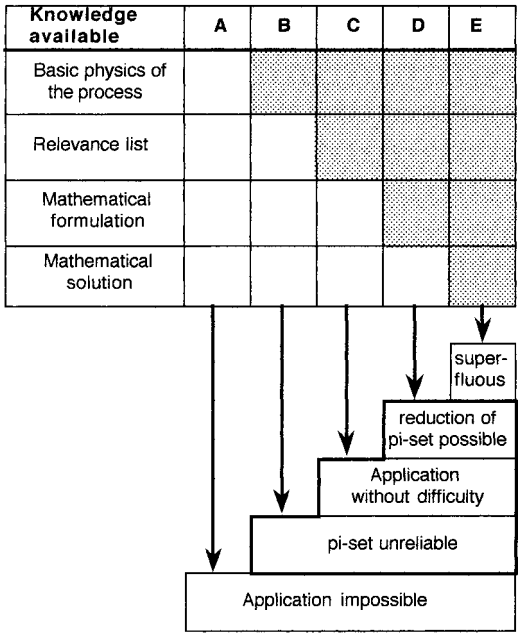


**Fig. 6** Applicability of dimensional analysis, as dependent on the knowledge available; after *J. Pawlowski* [26]

In words:

1. The physics of the basic phenomenon is unknown.
   **Result**: Dimensional analysis cannot be applied.
2. Enough is known about the physics of the basic phenomenon to compile a first, tentative relevance list.
   **Result** The resultant pi set is unreliable.[1)]

[1)] It must, of course, be said that approaching a problem from the point of view of dimensional analysis also remains useful even if all the variables relevant to the problem are not yet known: The timely application of dimensional analysis may often lead to the discovery of forgotten variables or the exclusion of artefacts.

3. All the relevant physical variables describing the problem are known.
   **Result**: The application of dimensional analysis is unproblematic.
4. The problem can be expressed in terms of a mathematical equation.
   **Result**: A closer insight into the pi relationship is feasible and may facilitate a reduction of the set of dimensionless numbers.[2)]
5. A mathematical solution of the problem exists.
   **Result**: The application of dimensional analysis is superfluous.

## 7.3 Experimental Techniques for Scale-up

In the Introduction, a number of questions were posed which are often asked in connection with model experiments. We are now in position to answer them.

- *How small can a model be?* The size of a model depends on the scale factor $\mu \equiv l_T/l_M$ and on the experimental precision of measurement. Where $\mu = 10$, a ± 10 % margin of error may already be excessive. A larger scale for the model will therefore have to be chosen to reduce the scale-up factor $\mu$.
- *Is one model scale sufficient or should tests be carried out with models of different sizes?* One model scale is sufficient if the relevant numerical values of the dimensionless numbers necessary to describe the problem (the so-called "process point" in the pi-space describing the operational condition of the technical plant) can be adjusted by choosing the appropriate process parameters or physical properties of the model material system. If this is not possible, the process characteristics must be determined in models of different sizes, or the process point must be extrapolated from experiments in technical plants of different sizes.
- *When must model experiments be carried out exclusively with the original material system?* When the material model system is unavailable (e.g., in the case of non-Newtonian fluids) or when the relevant physical properties are unknown (e.g., foams, sludges, slimes) the model experiments must be carried out with the original material system. In this case measurements must be performed in models of various sizes (cf. Example 8).

The unavailability of the model material systems can sometimes limit the application of dimensional analysis. In such cases it is of course absolutely wrong to speak of *"limits of the dimensional analysis"*.

[2)] In principle, in constructing a relevance list, one should take into consideration all the available information to possibly reduce it. In this context, reference is made to Example 33 (Description of particle separation by inertial forces after *Bürkholz*) and to Example 41/2 (Catalytic gas reactions in fixed beds after *Damköhler*)

*Scale-up in Chemical Engineering.* Marko Zlokarnik


ISBNs: 3-527-30266-2 (Hardback); 3-527-60056-6 (Electronic)

# 8
# Treatment of Variable Physical Properties by Dimensional Analysis

When using dimensional analysis to tackle engineering problems, it is generally assumed that the physical properties of the material system remain unaltered in the course of the process. Relationships such as the "heat transfer characteristic" of a wire in an air stream (Example 2) or of a mixing vessel

$$\mathrm{Nu} = f(\mathrm{Re}, \mathrm{Pr})$$

are valid for any material system with Newtonian viscosity and for any constant process temperature, i.e. for *constant* physical properties.

However, constancy of physical properties cannot be assumed in every physical process. A temperature *field* may well generate a viscosity *field* or even a density *field* in the material system treated. In non-Newtonian (pseudoplastic or viscoelastic) liquids, a shear rate can also produce a viscosity *field*.

Although most physical properties (e.g., viscosity, density, heat conductivity and capacity, surface tension) must be regarded as variable, it is particularly the value of viscosity that can be varied by many orders of magnitude under certain process conditions. Besides this, it shows the highest temperature coefficients. In the following, dimensional analysis will be preferentially applied to describe the variability of this one physical property. However, the same approach can be adapted for any other physical property.

The well-disposed reader will be surprised that this topic is given so much space in this book. An explanation is easy to give: A complete similarity requires a geometrical, material and process-related similarity, but the material similarity often cannot be easily obtained.

A problem arises, e.g., when model (laboratory, bench-scale) measurements are to be performed in a so-called "cold model", but the industrial plant operates at high temperatures (petrochemicals; $T \approx 800 - 1000$ °C). How can we ascertain that the laboratory model system behaves hydrodynamically similarly to that in the industrial plant? Here, different temperature dependence of physical properties (viscosity, density) may cause problems.

A problem also arises when laboratory measurements are to be performed with cheap and easy to handle model fluids in order to gain information about the scaling-up of an apparatus for treatment of cell cultures in biotechnology (mammal

and plant cells, aerobic cultures, yeasts), the rheological behavior of which is very complex (non-Newtonian: pseudoplastic and viscoelastic). Which model system may we choose?

The answer is clear and unambiguous: We may choose any model material system whose *dimensionless material function* in question is similar to that of the original material system. In this chapter the necessary procedures to obtain this information will be shown.

## 8.1 Dimensionless Representation of the Material Function

The variability of physical properties widens both the dimensional x- and the dimensionless pi-space. The process is not determined by the original material quantity x, but by its dimensionless reproduction. (*Pawlowski* [27] has clearly demonstrated this situation by the mathematical formulation of the steady-state heat transfer in an concentric cylinder viscometer exhibiting Couette flow). It is therefore important to carry out the dimensional-analytical reproduction of the material function uniformly in order to discover possibly existing, but under circumstances concealed, similarity in the behavior of different substances. This can be achieved only by the standard representation of the material function [5, 27].

- In the dimensional-analytical formulation of processes whose course depends on variable material properties, it is the dimensionless representation of the material function which counts.
- Analogous processes, in which the material properties vary in a different manner, can be described by the same process equation, only if the corresponding material functions can be represented by the same dimensionless material function. This point is particularly important for the selection of substances for model measurements.

Any material function s(p) – e.g. $\mu(T)$ – can be converted in its standard representation w = F(u) by standardization using two dimensional parameters a and b:

$$u \equiv \frac{p - p_0}{a}, \quad w \equiv \frac{s}{b} \tag{8.1}$$

Their meaning is:

$$a \equiv \frac{s_0}{(ds/dp)_{p=p_0}} \qquad \text{and} \qquad b \equiv s_0 = s(p_0) \tag{8.2}$$

A standard representation of any material function s(p) with the reference point $p_0$ is therefore given as

$$\Phi(u) \equiv \frac{1}{s(p_0)}\, s\left\{p_0 + u\,\frac{s(p_0)}{s'(p_0)}\right\} \tag{8.3}$$

This fulfils the standardization requirements

$$\Phi(u)_{u=0} = \left(\frac{\partial \Phi}{\partial u}\right)_{u=0} = 1 \tag{8.4}$$

**Example 11**: Standard representation of the temperature dependence of viscosity

The temperature dependence of the viscosity $\mu(T)$ is expressed by the temperature coefficient $\gamma_0$ of viscosity:

$$\gamma_0 \equiv \left(\frac{1}{\mu}\,\frac{\partial \mu}{\partial T}\right)_{T_0} < 0 \tag{8.5}$$

The standard representation of $\mu(T)$ is gained by transforming the function $\mu(T)$ into a function $\mu/\mu_0 = \Phi[\gamma_0(T-T_0)]$ and subsequently representing it graphically. The transformation parameters a and b, read here

$$a \equiv \gamma_0^{-1} \text{ and } b \equiv \mu(T_0) \equiv \mu_0 \tag{8.6}$$

Consequently, w and u have here the following meaning

$$w = \frac{\mu}{\mu_0} \qquad \text{and} \qquad u = \gamma_0\,(T - T_0) \tag{8.7}$$

In **Fig. 7** the dependence $\mu(T)$ is shown for 16 different liquids with extremely different $\gamma_0$ values. At room temperature they display $\mu$ values which cover five decades.

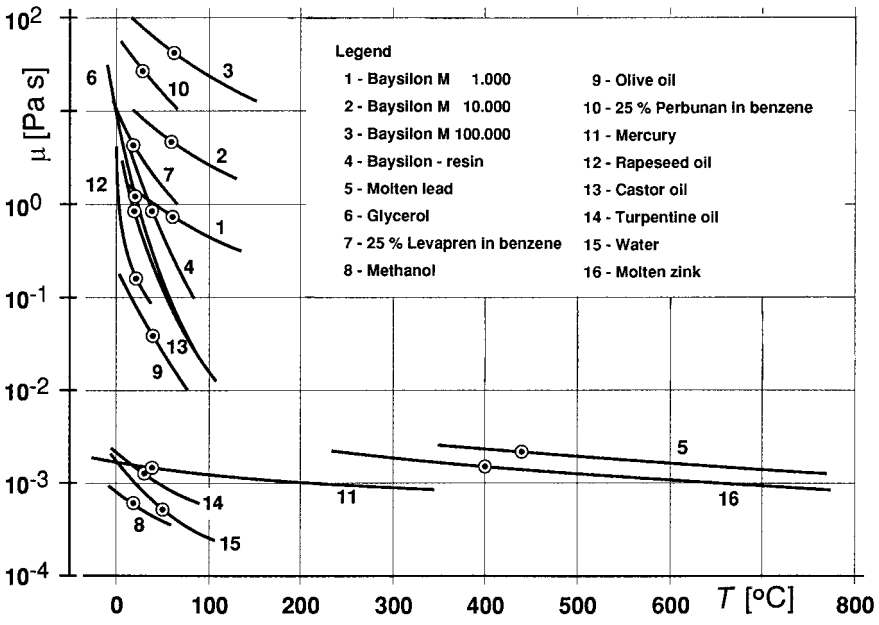


**Fig. 7** Dependence $\mu(T)$ for 16 different liquids; from [27]

**Fig. 8 a** shows these data in the framework $\mu/\mu_0 = f[\gamma_0 (T - T_0)]$. The reference temperature chosen is indicated by •. The *solid* curve **a** represents the so-called "reference-invariant approximation" of this function:

$$\mu/\mu_0 = \Phi[\gamma_0 (T - T_0)] \tag{8.8}$$

We will refer to this correlation later on.

The *dotted* curve corresponds to the representation preferred by engineers

$$\mu/\mu_0 = \exp[\gamma_0 (T - T_0)] \tag{8.9}$$

As can be seen from Fig. 8a, the experimental data under consideration cannot be approximated very well by this function. Nevertheless, it does seem to be suitable for smaller $\gamma_0 \Delta T$ intervals.

For the description of the material function $\mu(T)$, the so-called Arrhenius relationship can also be used

$$\frac{E_0}{\mathbf{R}} \equiv \left(\frac{1}{\mu} \frac{\partial \mu}{\partial (1/T)}\right)_{T_0} = \left(\frac{\partial \ln \mu}{\partial (1/T)}\right)_{T_0} \tag{8.10}$$

by which the temperature dependence of viscosity is expressed as

$$\mu/\mu_0 = \Phi_1 \left[\frac{E_0}{\mathbf{R}T_0}(T_0/T - 1)\right] = \Phi_1 \left[\mathrm{Arr}_0 (T_0/T - 1)\right] \tag{8.11}$$

(In this way *Svante Arrhenius* (1889) described the temperature dependence of the reaction rate constant k: $k(T) = k_\infty \exp(E/\mathbf{R}T)$.)

In this case it delivers an even better an approximation than the representation in Fig. 8 a (see **Fig. 8 b**). From

$$\mathrm{Arr} \equiv E/\mathbf{R}T \text{ and } u = \gamma_0 (T - T_0) \tag{8.12}$$

it follows that between the Arrhenius number Arr and $\gamma_0 T$ the relationship exists:

$$\mathrm{Arr} \equiv E/\mathbf{R}T = -\gamma_0 T \tag{8.13}$$

In addition, it should be pointed out that for a dimensionless representation of the dependence $\mu(T)$ two methods can be used. Only the first possibility has been discussed so far. It consisted of the choice of two additional quantities (transformation parameters) with the dimensions of $\mu$ and $T$, these already being contained in the material function. In the case treated above, this has been accomplished by the introduction of $\mu_0$ and $\gamma_0$ or $E/\mathbf{R}$ respectively. *Pawlowski* [5, 27] terms this representation a *genuine* one. Due to the fact that its definition is already contained in the material function, it has a higher significance in the dimensionally analytical treatment of a process.

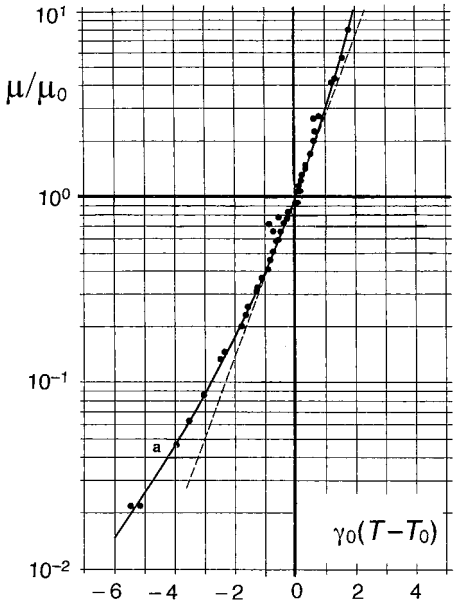


**Fig. 8 a** Standard representation of the temperature dependence of viscosity in the form of the relationship $\mu/\mu_0 = f[\gamma_0 (T - T_0)]$. The solid curve **a** represents the reference-invariant approximation by the $\chi$-function (see section 8.2), whereas the dotted line corresponds to the engineering representation, eq. (8.9); from [27].

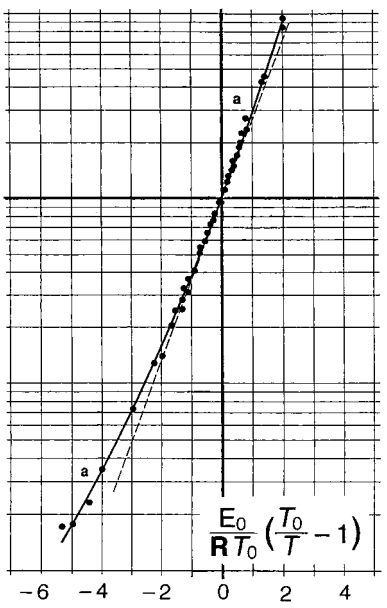


**Fig. 8 b** Standard representation of the temperature dependence of viscosity in the form of the relationship
$\mu/\mu_0 = \Phi_1 [\frac{E_0}{RT_0} (T_0/T - 1)]$.
For further explanations see Fig. 8 a.

In contrast to this approach, the parameters with the dimensions of $\mu$ and $T$, these being necessary for the dimensionless representation of the process, can also be formed by the parameters influencing the process in question. In this case, one can speak of the *process-related* representation of the material function.

**Example 12**: Standard representation of the temperature dependence of the density

The temperature dependence of density $\rho(T)$ is expressed in an analogous manner by the temperature coefficient of density:

$$\beta_0 \equiv \left(\frac{1}{\rho}\frac{\partial\rho}{\partial T}\right)_{T_0} \tag{8.14}$$

The standard representation of the material function $\rho(T)$ is analogous to $\mu(T)$. The transformation parameters are

$$a \equiv \beta_0^{-1} \text{ and } b \equiv \rho(T_0) \equiv \rho_0 \tag{8.15}$$

Consequently, w and u have here the following meaning:

$$w = \rho/\rho_0 \text{ and } u = \beta_0 (T - T_0) \tag{8.16}$$

The standard representation reads

$$\rho/\rho_0 = f[\beta_0 (T - T_0)] \tag{8.17}$$

**Fig. 9 a** shows the $\rho(T)$ dependence for four liquids. It can be seen that $\beta_0$ values are two decades lower than in the case of $\gamma_0$.

**Fig. 9 b** shows the standard representation of the above relationship. $\rho(T)$ curves for propene, toluene and $CCl_4$ coincide. The similarity of the respective $\rho(T)$ curves is clearly shown – this was also intended by this representation. These three fluids can therefore be used as mutual model fluids within the whole measured $T$ range. For water this is *not* the case. The expected correlation performed by the transformation parameters a and b is achieved only in the region close to the "standardization range" (at $u = \beta_0(T - T_0) \approx 0$).

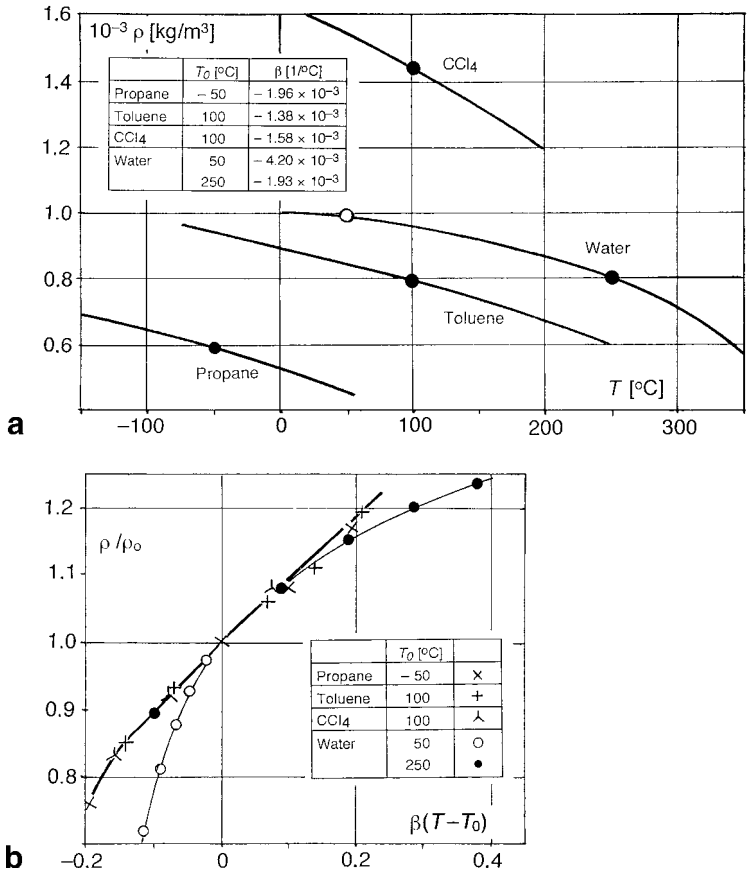


**Fig. 9** (**a**) $\rho(T)$ dependence for four liquids and (**b**) their standard representation

At this point the remarks given in the introduction to this chapter should be recalled: Water is of no use to investigate the performance of a petrochemical plant in a "cold model".

## 8.2
## Reference-invariant Representation of a Material Function

In general, standard representation depends upon the choice of the reference point. The question is posed: Do mathematical functions exist whose standard representations do not depend on the choice of the reference point and therefore could be named *"reference-invariant functions"*? In case of an affirmative answer on the one hand the reference point $p_0$ – here $T_0$ – could be omitted (constriction of the pi-space by one pi-number) and on the other hand the dimensionless representation of the material function would stretch over the entire recorded range.

It is mathematically proven that only one class of reference-invariant standard representations exists and that this can be represented by one-parametric $\chi\,(u, \psi)$ functions:

$$\begin{aligned} w &= \chi\,(u, \psi) \equiv (1 + \psi\, u)^{1/\psi} && \text{for } \psi \neq 0 \\ w &= \chi\,(u, \psi) \equiv \exp\,(u) && \text{for } \psi = 0 \end{aligned} \tag{8.18}$$

$\psi$ is a numerical value which can be determined numerically or graphically.

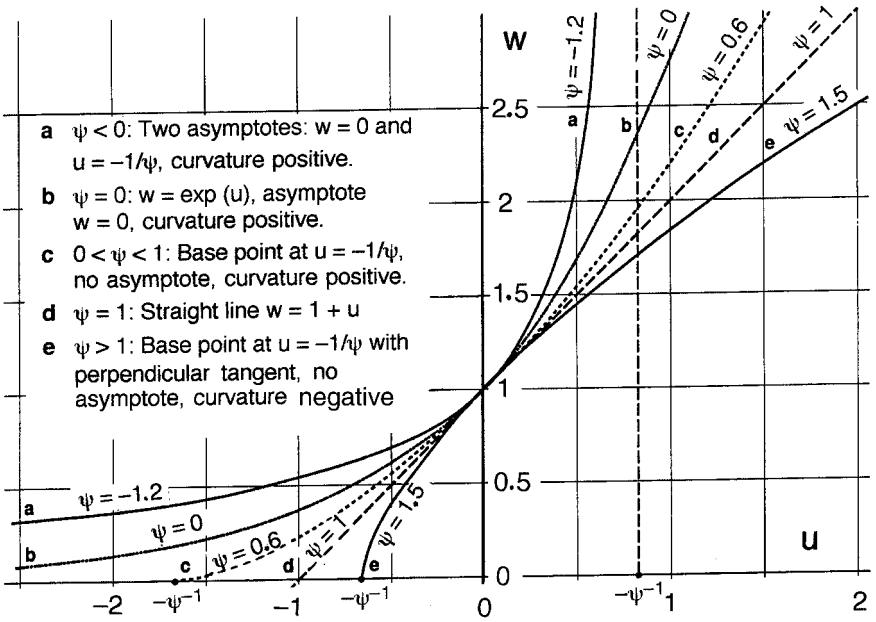


**Fig. 10** Ranges of existence and appearance of reference-invariant functions $\chi\,(u, \psi)$ [27]

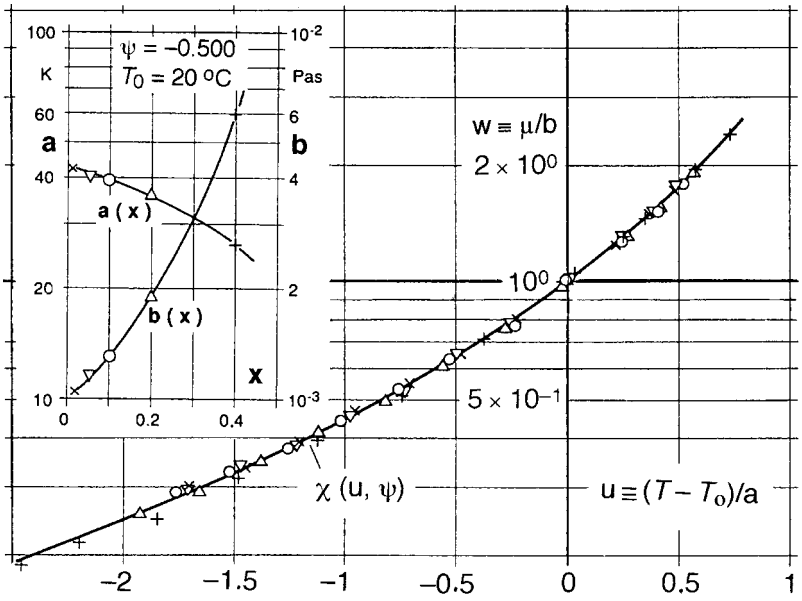


**Fig. 11** Standard representation of the temperature dependence of viscosity of aqueous sugar solutions of different concentrations as well as their reference-invariant approximation using $\psi = -0.500$ (solid curve). For key parameters a(x) und b(x) see the auxiliary diagram; from [27].

The regions of existence and appearance of reference-invariant functions $\chi\ (u, \psi)$ are represented in **Fig. 10**. Curves with maxima and minima cannot be described in a reference-invariant manner. In this case, both the dimensional-analytical representation and the model material system are confined to the region close to the "standardization range".

The reference-invariant representations of the temperature dependence of viscosity in Fig. 8 a and b were obtained by $\psi = -0.179$ and $-0.106$ respectively.

For the determination of $\psi$, two procedures are discussed in [27]: The 3-point approximation (N = 3) and the approximation with the smallest relative standard deviation (N > 3).

**Example 13:** Reference-invariant representation of the material function $\mu(T, x)$

Fig. 11 shows the reference-invariant representation of the temperature dependence of viscosity of aqueous sugar solutions of different concentration (x – mass portion of cane sugar). To obtain this correlation, $\mu$ and $(T - T_0)$ had to be transformed by the transformation or key parameters $a = 1/\gamma_0$ [K] and b [Pa·s] as $w = \mu/b$ and $u = (T - T_0)/a$, whereby a and b are functions of x, see auxiliary diagram in Fig. 11. The reference temperature is $T_0 = 20$ °C.

**Example 14:** Reference-invariant representation of the material function $D(T, F)$

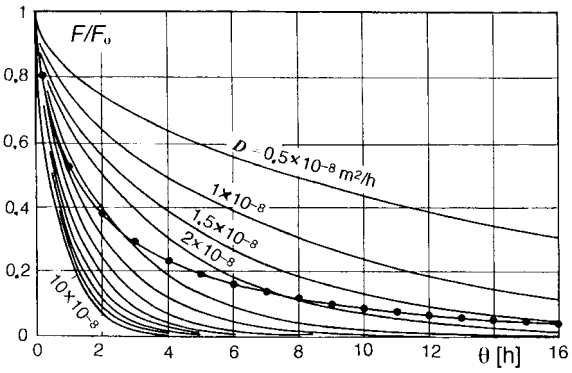


**Fig.12** Comparison of the measured course of drying (—•—) with the calculated one assuming constant diffusion coefficients ($10^8$ $D = 0.5 - 10$); from [28]

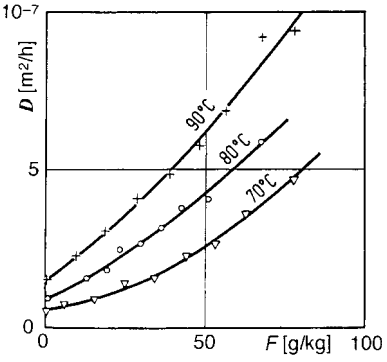


**Fig.13** The interrelation $D(F)$ for polyamide at three temperatures; from [28]

This example deals with the dependence of the diffusion coefficient, $D$, of water in polyamide (synthetic fiber Perlon®) on temperature and degree of moisture $F$ [g water/kg polyamide]. The knowledge of the correlation $D(T, F)$ is indispensable for the prediction of the course of drying shredded polyamide. This is convincingly shown in **Fig. 12**, in which the relative degree of moisture, $F/F_0$, in the course of drying an infinitely expanded sheet of polyamide with a thickness of 0.9 mm is calculated for different constant diffusion coefficients ($10^8$ $D = 0.5 - 10$). Only when the dependence $D(T)$ is taken into account (solid line), does the calculation of the drying progress correspond to the measured data (— • —). **Fig 13** shows $D(T, F)$ for the material system polyamide/water.

In **Fig. 14** the standard representation $w = \Phi(u)$ of the connection in Fig. 13 is given. The solid curve in Fig. 14 shows die invariant approximation of this correlation with $\psi = 0.61$. The correlations necessary to produce the standard representation between both key parameters a and b are represented in **Fig. 15**.

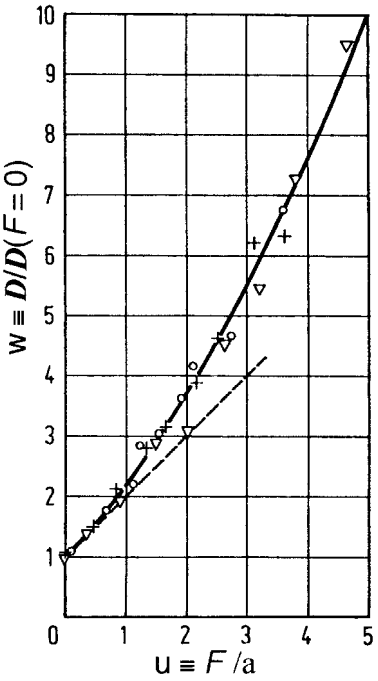


**Fig.14** Standard representation w = Φ (u) of the connection in Fig. 13; from [5]

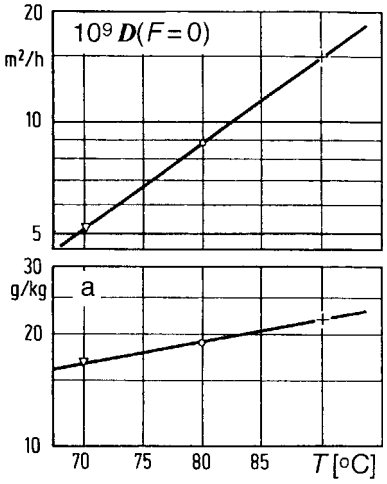


**Fig.15** Temperature dependence of both transformation or key parameters a = $D(F=0)/(\partial D/\partial F)_{F=0}$ and b = $D(F=0)$.

## 8.3 Pi-space at Variable Physical Properties

If the scale-up is performed in the pi-space with *constant* physical properties, the requirement "*idem*" concerns all pi-numbers involved, whereby the dimensional quantities contained in them can be deliberately varied. The dimensional-analytical validity range includes all physically convenient numerical values of these dimensional quantities.

If the scale-up is performed in the pi-space with *variable* physical properties, the requirement "idem" also concerns the form of the dimensionless formulated material function. This aspect can make the choice of the model material system considerably more difficult. This requirement is fulfilled, *a priori*, only if the interesting range Δu in the standard representation w = Φ (u) lies close to the standardization point, see the explanation concerning Fig. 9 b in the text.

With variable physical properties the relevance list widens by both key or transformation parameters a and b as well as by the reference point. In the dependence μ(*T*) this includes the quantities

$$a \equiv 1/\gamma_0 \; ; \; b \equiv \mu_0 \; ; \; p_0 \equiv T_0$$

The original relevance list now contains two additional quantities, $\gamma_0$ and $T_0$. Furthermore, $\mu_0$ has to replace μ. By this it follows that the 3-parametric pi-space

$$\{\mathrm{Nu}, \mathrm{Re}, \mathrm{Pr}\} \tag{8.19}$$

is transferred to the following 5-parametric one:

$$\{\mathrm{Nu}, \mathrm{Re}_0, \mathrm{Pr}_0, \gamma_0 T_0, \Delta T/T_0\} \tag{8.20}$$

If one takes into consideration that the standard representation of $\mu(T)$ is reference-invariant, see Fig. 8 a and 8 b

$$\mu/\mu_0 = \Phi(\gamma_0 \Delta T) \tag{8.21}$$

then the reference point $T_0$ is cancelled and the correlation (8.20) is reduced to

$$\mathrm{Nu} = f\{\mathrm{Re}_0, \mathrm{Pr}_0, \gamma_0 \Delta T\} \tag{8.22}$$

whereby $\mathrm{Re}_0$ and $\mathrm{Pr}_0$ are formed by $\mu_0$.

**Example 15**: Consideration of the dependence $\mu(T)$ using the $\mu_w/\mu$ term

In the treatment of heat transfer problems in the engineering literature, the process equation is, as a rule, extended by the parameter $\mu/\mu_0$ instead of $\gamma_0 \Delta T$. This is justified because between both terms, in accordance with the standard representation in Fig. 8a, a simple correlation exists:

$$\mu/\mu_0 = \Phi\,(\gamma_0 \Delta T) \quad \text{or} \quad \mu/\mu_0 = \exp\,(\gamma_0 \Delta T) \tag{8.23}$$

Both terms are equivalent to each other.

In heat transfer problems, the liquid bulk temperature is normally taken as the reference temperature $T_0$, whereas the temperature of the heat transfer surface (wall) $T_w$ is taken to describe the effective temperature difference, $\Delta T$, in the process. Therefore, the viscosity of the bulk liquid is taken as the reference viscosity: $\mu_0 = \mu$.

The inclusion of the *viscosity number*, $\mathrm{Vis} \equiv \mu_w/\mu$, in the process equation for heat transfer in pipes goes back to *Sieder* and *Tate* [29]. These researchers succeded to correlate experimental data obtained in pipe flow with the term $(\mu_w/\mu)^{-0.14}$. In this manner, the differences between the cooling and heating process were considered, these manifesting themselves by the differences in the thickness of the boundary layers. In heating, practically no boundary layer is present as compared to cooling.

The heat transfer characteristics read:

Laminar range*) ($\mathrm{Re} \leq 2\,320$):

$$\mathrm{Nu}\,(\mu_w/\mu)^{0.14} = 1.86\,(\mathrm{Re}\,\mathrm{Pr}\,\mathrm{d}/\mathrm{l})^{1/3} \quad \mathrm{Re}\,\mathrm{Pr}\,\mathrm{d}/\mathrm{l} = 10^1\text{–}10^4 \tag{8.24}$$

*) In this flow range the inlet effects make themselves felt until $\mathrm{d}/\mathrm{l} \approx 200$ (pipe diameter d, pipe length l)

Transition range ($Re = 2\,320–1 \times 10^4$):

$$Nu\,(\mu_w/\mu)^{0.14} = 0.12\,(Re^{2/3}–125)\,Pr^{1/3} \tag{8.25}$$

Turbulent range ($Re \geq 1 \times 10^4$):

$$Nu\,(\mu_w/\mu)^{0.14} = 0.1\,Re^{2/3}\,Pr^{1/3} \tag{8.26}$$

However, the power –0.14 of the Vis term in heat transfer process characteristics has not been confirmed by later researchers.

*Hruby* [30] found in cooling measurements with a Newtonian oil that the power m of the Vis term depends on its numerical value:

$$m = -0.215\,Vis^{-0.08} \qquad 0.32 < Vis < 320$$

For Vis = 3 it then follows that m = –0.20, for Vis = 200 in contrast m = –0.14.

*Hackl* [31] found insignificantly lower values:

$$m = -0.265\,Vis^{-0.14} \qquad 80 < Vis < 900$$

For Vis = 80 it is found that m = –0.14, for Vis = 900 in contrast m = –0.10.

These facts were examined in a later work [32], where two viscous mineral oils (Vis ≈ $1–10^4$) were used in cooling. It was found that power m attained for Vis = 1 – 100 was larger and for Vis = $10^2–10^4$ was lower than –0.14. A comparison of these findings is given graphically in **Fig. 16.**

For *Pawlowski* [27] a factorial inclusion of the Vis term into the heat transfer characteristic would make sense only if the temperature field is essentially restricted to

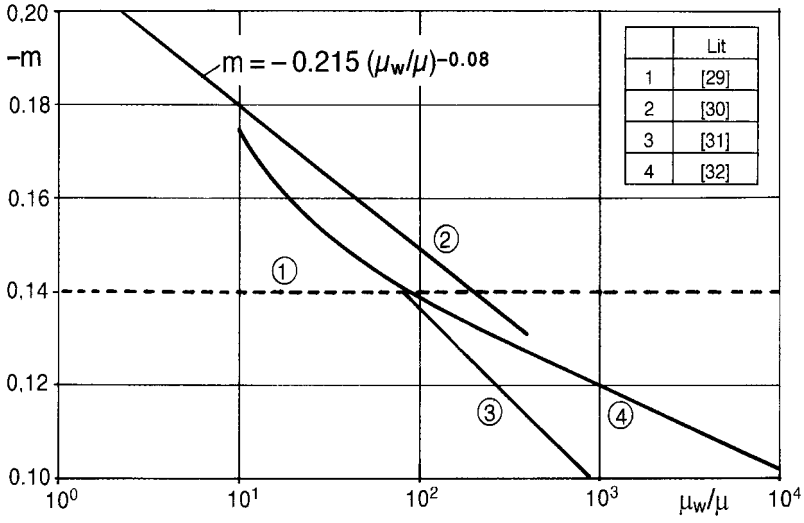


**Fig. 16** Comparison of the findings m(Vis) of different authors

the wall boundary layer, whereas the core flow would remain practically isothermal. This is certainly the case in the pipe flow at Re > 2.300.

According to this expectation, in stirring vessels equipped with close clearance anchor stirrers, the effect of the Vis term should not be observed. *Zlokarnik* [33] examined the heat transfer at cooling and heating in a stirring vessel equipped with a close clearance anchor stirrer. The eight liquids used displayed viscosities between 1 and $10^5$ *m*Pa·s at 20 °C and had extremely different temperature coefficients: $\gamma_0 = (1.5–11.2) \times 10^{-2}$ $K^{-1}$. It was found that the data for cooling could be correlated only insignificantly by $Vis^{-0.02}$ and for heating by $Vis^{0.073}$.

In contrast, *Dunlap* and *Rushton* [34] succeeded to correlate their measurements at cooling and heating in a vessel with a turbine stirrer and pipe bundle heat exchangers with $Vis^{-0.4}$ because a thick boundary layer developed around the tubes.

**Example 16**: Consideration of the dependence $\rho(T)$ by the Grashof number Gr

In contrast to $\mu(T)$, the relevance of $\rho(T)$ is considered in the engineering literature exclusively by the number $\beta\Delta T$. The ratio $\rho/\rho_0$ is used in heterogeneous material systems (solids/liquid or solids/gas) in which the density differences $\Delta\rho$ are occurring independently of the temperature differences.

Due to the fact that density differences can only have an effect when associated with acceleration due to gravity, both $\beta\Delta T$ and $\rho/\rho_0$ are consistently combined with the Galileo number $Ga \equiv Re^2/Fr \equiv g\, l^3/\nu^2$. Therefore, in the heat transfer under natural convection the

$$\text{Grashof number } Gr \equiv \beta\Delta T\, Ga \equiv g\beta\Delta T\, l^3/\nu^2 \tag{8.27}$$

plays a role, whereas in processes where buoyancy or sedimentation occurs, the

$$\text{Archimedes number } Ar \equiv (\Delta\rho/\rho)\, Ga \equiv g\Delta\rho\, l^3/(\rho\, \nu^2) \tag{8.28}$$

is added to the pi-space.

Examples of the application of the Grashof number in heat transfer problems can be found, for example, in [14]. For examples where the Archimedes number is applied in solid/liquid systems (suspensions) see [22] and for sedimentation as well as fluidization examples please refer to textbooks dealing with unit operations in chemical process engineering.

## 8.4
## Execution of Model Experiments with Newtonian Fluids Exhibiting Temperature Dependent Viscosity

### 8.4.1
### Pi-space and Requirements Concerning the Model Material System

We will start by discussing a pi-space in which an optional process in an apparatus of a given geometry takes place and where the hydrodynamics is coupled with a steady-state heat transfer [35]. The target pi-number will be laid down later on (Example 17). In case *temperature independent* materials take part, the process will be described by the following possible process-related and material pi-numbers:

$$\left\{ \underbrace{\frac{v\, l\, \rho_0}{\mu_0}}_{Re}, \underbrace{\frac{C_{p,0}\mu_0}{k_0}}_{Pr}, \underbrace{\frac{v^2}{l\, g}}_{Fr}, \underbrace{\frac{v^2 \mu_0}{k_0 \Delta T}}_{Br} \right\} \tag{8.29}$$

The Brinkman number, Br, is only relevant if the transformation of the mechanical energy into heat is important. All material properties are related to the characteristic temperature $T_0$.

If the problem is restricted to the *creeping* flow, the mass inertia (ρ) will not play a role. In this case, ρ must be combined with the quantities $C_{p,0}$ and g to give $\rho C_{p,0}$ and ρg. Consequently, the above pi-framework is reduced by one pi-number:

$$\left\{ \underbrace{\frac{v\, l (\rho\, C)_{p,0}}{k_0}}_{RePr}, \underbrace{\frac{v\, \mu_0}{l^2 \rho g}}_{Fr/Re}, \underbrace{\frac{v^2 \mu_0}{k_0 \Delta T}}_{Br} \right\} \tag{8.30}$$

However, if viscosity is *temperature dependent*, this has to be taken into account by an appropriate enlargement of the pi-space:

$$\left\{ \frac{v\, l (\rho\, C)_{p,0}}{k_0}, \frac{v\, \mu_0}{l^2 \rho g}, \frac{v^2 \mu_0}{k_0 \Delta T}, \frac{\Delta T}{T_0}, \mathrm{Arr}_0 \right\} \tag{8.31}$$

$\mathrm{Arr}_0$ is the Arrhenius number at $T_0$; see (8.13).

By the combining the three process numbers with $\Delta T/T_0$ a new pi-number is formed which, apart from reference temperature and acceleration due to gravity, *only* contains material properties:

$$\mathbf{B} \equiv \frac{\mathrm{Br}\, \Delta T/T_0}{(\mathrm{Re}\, \mathrm{Pr})^{4/3} (\mathrm{Fr}/\mathrm{Re})^{2/3}} \equiv \frac{\mathrm{Br}\, \Delta T/T_0}{(\mathrm{Re}\, \mathrm{Fr})^{2/3} \mathrm{Pr}^{4/3}} \equiv \frac{1}{T_0} \left( \frac{\mu_0\, k_0\, g^2}{\rho_0^2\, C_{p,0}^4} \right)^{1/3} \tag{8.32}$$

B becomes, at constant g, a pure material number which combines all the relevant material properties at the reference temperature $T_0$. B = idem will therefore define all the appropriate relevant model material properties.

If B is introduced into the pi-space (8.31), one optional process pi-number – e.g. Fr/Re – must be deleted. The advantage of the new pi-space

$$\{\mathrm{RePr},\ \mathrm{Br},\ \mathbf{B},\ \Delta T/T_0,\ \mathrm{Arr}_0\} \tag{8.33}$$

is that one of the three process numbers is replaced by a material number and, consequently, for the determination of the model fluid, as a *maximum requirement*, ($\mathrm{Arr}_0$, **B**, Φ) = idem is valid. In this case, the requirement Φ = idem must be considered at only higher u values ($u = \gamma_0 \Delta T$), i.e. far beyond the limits of the standardization range; see p. 52.

If the material function $\mu(T)$ can be represented in a reference-invariant manner, then the reference temperature $T_0$ is cancelled and the pi-numbers $\Delta T/T_0$ and $\mathrm{Arr}_0 \equiv E/\mathbf{R}T_0$ are combined to give

$$\mathrm{Arr}_0/(\Delta T/T_0) = E/\mathbf{R}\,\Delta T = -\gamma_0 \Delta T \tag{8.34}$$

see (8.13). The pi-framework is thereby reduced by one pi-number.

In this case, a pure material number can be formed instead of **B**, eq. (8.32), in which the temperature $T_0$ does not appear. Then $-\gamma_0 T_0$ is replaced by $-\gamma_0 \Delta T$ whereby $\Delta T$ represents the difference between two process-related temperatures (as in the Brinkman number):

$$\mathbf{B_1} \equiv \frac{\mathrm{Br}(-\gamma \Delta T)}{(\mathrm{ReFr})^{2/3}\,\mathrm{Pr}^{4/3}} \equiv -\gamma \left(\frac{\mu\, k\, g^2}{\rho^2 C^4}\right)^{1/3} \tag{8.35}$$

The resulting pi-set

$$\{\mathrm{RePr},\ \mathrm{Br},\ \mathbf{B_1},\ -\gamma_0 \Delta T\} \tag{8.36}$$

now consists of two process numbers (RePr and Br) and of two pure material numbers ($\mathbf{B_1}$ and $-\gamma_0 \Delta T$).

This pi-set is valid for any process involving creeping flow in which the conversion of the mechanical energy into heat is important (Br is relevant) and the material function $\mu(T)$ can be represented in a reference-invariant manner.

### 8.4.2
### Material Data Chart

In scaling up a process from the laboratory to the full-scale version, besides the geometrical similarity, process-related and material similarity must also be considered. In examining the demand for material similarity, it is expedient for the determination of model substances to start from a material data chart $\{\Gamma \equiv \mathbf{B_1} \times \mathrm{Pr}^{-1/3},\ \mathrm{Pr}\}$ with a parametrical temperature indication, see **Fig 17**. From this representation it can be discerned that mixtures of different materials are particularly suitable as model substances because they cover entire areas in this diagram and can therefore considerably widen the scope of material numbers.

The use of this material data chart will be explained by the Example 17.

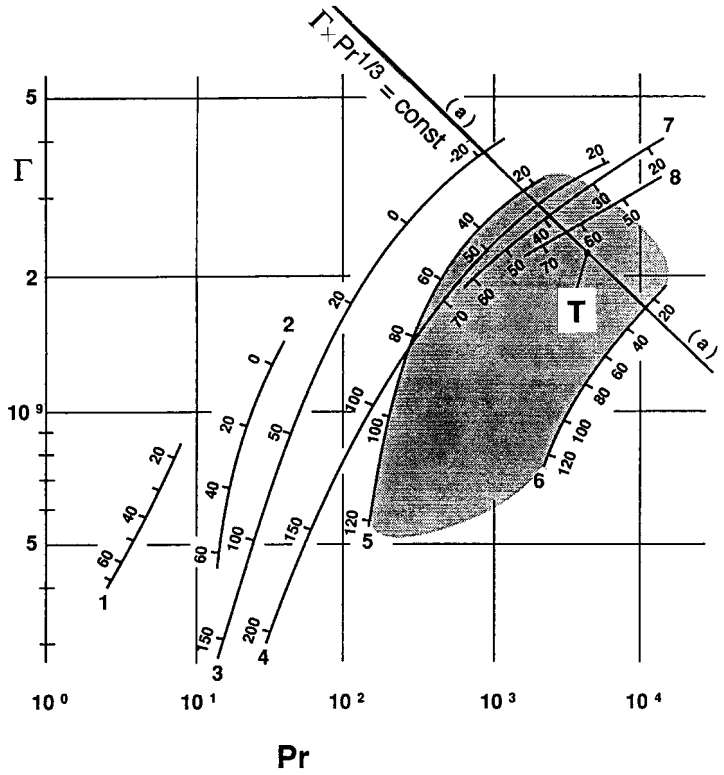


**Fig. 17** A material data chart for the evaluation of the appropriate model fluid and the assigned temperature $T_0$. Straight line (a) with $\Gamma^* \equiv \Gamma \times Pr^{1/3}$ = idem at creeping flow.
1 water 2 turpentine oil 3 engine oil Shell Thermia 11 4 Thermia 45
5 Baysilon M 10 6 Baysilon M 1000 7 glycerin 97 % 8 heavy machine oil
Hatched area: mixtures of different Baysilon oils
(Baysilon are silicone oils from Bayer AG, D – Leverkusen).

**Example 17**: Dimensioning of a wiped film heat exchanger [27]

With the help of model experiments, a wiped film heat exchanger, needed in a continuous production process to heat up a very viscous throughput, q, exhibiting Newtonian viscosity behavior, should be designed.

| Process parameters of the technical plant required | | |
|---|---|---|
| Diameter of the apparatus | $d_T$ | |
| Rotor speed | n | |
| Power | P | |
| **Process conditions:** | | |
| Input temperature | $T_{in}$ | = 102 °C |
| Output temperature | $T_{out}$ | = 112 °C |
| Wall temperature | $T_w$ | = 118 °C |
| Throughput | q | = 8 l/min = $1.33 \times 10^{-4}$ $m^3/s$ |

| | | |
|---|---|---|
| Physical properties of the input at | $T_0$ | = 110 °C: |
| Viscosity | $\mu$ | = 0.84 Pa·s |
| Temperature coefficient | $\gamma_0$ | = –0.083 K |
| Density | $\rho$ | = 897 kg/m$^3$ |
| Specific heat | $C_p$ | = 1570 J/(kg K) |
| heat conductivity | k | = 0.29 W/(m K) |
| Diameter of the model apparatus | $d_M$ | = 0.05 m |

The relevance list of the problem reads:

$$\{d, n, P, q, g, T_{in}, T_{out}, T_w, \mu, \gamma_0, \rho, C_p, k\} \tag{8.37}$$

The numerical values of the physical properties are valid for the mean process temperature which is defined by $T_0 = (T_{in} + T_w)/2$.

In association with four base dimensions contained in their dimensions, these 13 x-quantities yield the following 13 – 4 = 9 pi-numbers:

$$Re_n \equiv n\, d^2\, \rho/\mu \qquad Re_q \equiv q\, \rho/(d\, \mu) \qquad Fr \equiv n^2\, d/g \qquad Pr \equiv C_p\, \mu/k$$

$$Br \equiv (-\gamma_0)\, n^2\, d^2\, \mu/k \qquad Ne \equiv P/(\rho\, n^3\, d^5)$$

$$\theta_{in} \equiv \gamma_0\, (T_{in} - T_w) \qquad \theta_{out} \equiv \gamma_0\, (T_{out} - T_w) \qquad \theta_0 \equiv \gamma_0\, (T_0 - T_w) \tag{8.38}$$

If we assume that the material function can be approximated in a *reference-invariant* manner, then $T_0$ is irrelevant and the pi-number $\theta_0$ is cancelled. The pi-set contains now eight pi-numbers.

The further discussion is made essentially easier by remodeling the above pi-numbers in such a way that each pi-number contains only one process parameter:

$$\Pi_d \equiv (Re_n^2/Fr)^{1/3} = d\, \{g\, (\rho/\mu)^2\}^{1/3}$$

$$\Pi_q \equiv Re_q\, (Re_n^2/Fr)^{1/3} = q\, \{g\, (\rho/\mu)^5\}^{1/3}$$

$$\Pi_n \equiv (Fr^2/Re_n)^{1/3} = n\, \{g^{-2}\, (\mu/\rho)\}^{1/3}$$

$$\Pi_P \equiv Ne\, (Re_n^7\, Fr)^{1/3} = P\, \{g^{-1}\, (\rho^4/\mu^7)\}^{1/3} \tag{8.39}$$

Besides this – similar to the procedure in section 8.4.1 – one pure material number, $\Gamma$, is formed:

$$\Gamma \equiv \frac{Br(-\gamma_0 \Delta T)}{(ReFr)^{2/3}\, Pr^{5/3}} \equiv -\gamma_0 \left(\frac{k_0^2 g^2}{\rho^2 C_{p,0}^5}\right)^{1/3} \tag{8.40}$$

The pi-set of eight remodeled pi-numbers now reads:

$$\{\Pi_d, \Pi_q, \Pi_n, \Pi_P, \theta_{in}, \theta_{out}, \Gamma, Pr\} \tag{8.41}$$

In this pi-space the following pi-equations can be represented as:

$$\theta_{out} = f(\Pi_d, \Pi_q, \Pi_n, \theta_{in}, \Gamma, Pr) \quad \text{and} \tag{8.42}$$

$$\Pi_P = f(\Pi_d, \Pi_q, \Pi_n, \theta_{in}, \Gamma, Pr) \tag{8.43}$$

At this point, similar to section 8.4.1, we make the restriction that the state of flow in the process under examination is a *creeping* one. From this it follows that density can only appear as a product in $\rho C_p$ and $\rho g$. The Prandtl number is not an independent parameter any more and must be combined by the appropriate pi-numbers:

$$\begin{aligned}
\Pi_d^* \equiv \Pi_d\, Pr^{1/3} &= d\, g^{1/3} \{(C_p\, \rho^2/(k\, \mu)\}^{1/3} \\
\Pi_q^* \equiv \Pi_q\, Pr^{4/3} &= q\, g^{1/3} \{C_p{}^4\, \rho^5/(k^4\, \mu)\}^{1/3} \\
\Pi_n^* \equiv \Pi_n\, Pr^{1/3} &= n\, g^{-2/3} \{C_p\, \mu^2/(k\, \rho)\}^{1/3} \\
\Pi_P^* \equiv \Pi_P\, Pr^{5/3} &= P\, g^{-1/3} \{g^{-1}\, (C_p{}^5\, \rho^4/(k^5\, \mu^2)\}^{1/3} \\
\Gamma^* \equiv \Gamma\, Pr^{1/3} &= -\gamma_0 \{\mu\, k\, g^2/(\rho^2\, C_p{}^4)\}^{1/3} \equiv \mathbf{B}_1
\end{aligned} \tag{8.44}$$

The pi-set (8.41) is therefore reduced to seven pi-numbers:

$$\{\Pi_d^*, \Pi_q^*, \Pi_n^*, \Pi_P^*, \theta_{in}, \theta_{out}, \Gamma^*\} \tag{8.45}$$

and both process equations in examination read

$$\theta_{out} = f(\Pi_d^*, \Pi_q^*, \Pi_n^*, \theta_{in}, \Gamma^*) \quad \text{and} \tag{8.46}$$

$$\Pi_P^* = f(\Pi_d^*, \Pi_q^*, \Pi_n^*, \theta_{in}, \Gamma^*) \tag{8.47}$$

Of six pi-numbers in eq. (8.46) four are already known. $\theta_{in}$, $\theta_{out}$, $\Pi_q^*$ and $\Gamma^*$ are fixed by the process conditions of the full-scale plant and the material properties of the throughput. Therefore, only the functional interdependence

$$f(\Pi_d^*, \Pi_n^*) = 0 \tag{8.48}$$

must be found which consequently gives the dependence $f$ (d, n). Therefore, the dimensioning problem is not unambiguously fixed. It exhibits one degree of freedom and thus permits an optimization with respect to the power consumption.

**Conception of Model Experiments**

In the conception of model experiments we first regard a *general flow* state and will only later presuppose the *creeping flow.*

Pi-numbers which describe the general flow state (8.41) can be split into three groups:

a) pi-numbers which are known by the full-scale plant: $\Pi_q$, $\theta_{in}$, $\theta_{out}$, $\Gamma$, Pr ;
b) pi-numbers which can be adjusted by the choice of the model fluid: $\Pi_d$;
c) pi-numbers whose numerical values will be provided by the model experiment: $\Pi_n$, $\Pi_P$.

In the conception of model experiments the goal is to fix the model substance and the test conditions in such a way that a complete similarity is achieved between the processes in the full-scale plant ($_T$) and in the model ($_M$). In this case, all pi-numbers fulfil the requirement *idem*. In the discussed case the procedure is as follows:

a) $\Gamma$ = idem Pr = idem
b) $\Pi_d$ = idem
c) $\theta_{in}$ = idem $\quad \theta_{out}$ = idem $\quad \Pi_q$ = idem
d) $\Pi_n$ = idem $\quad \Pi_P$ = idem (8.49)

The requirements (8.49 a) are of prime importance, because they must be fulfilled in the search for a appropriate model fluid and the accompanying reference temperature $(T_0)_M$. Here, the material data chart (section 8.4.2) will help. Its use is described in the following:

Point T in Fig. 17 corresponds to the values of $\Gamma$ and Pr which result from the material values listed. According to the *idem* conditions (8.49 a), the identity line of the model fluid must pass this point, whereby the associated $T$ value delivers the reference temperature $(T_0)_M$. In our example, the Baysilon mixture (76 % M10 + 24 % M1000) at 25 °C fulfils this requirement.

After the model fluid has been found, the model temperature, $T_{0,M}$, and the physical properties of the model system assigned to it are fixed. With the given dimension, $d_M$, of the model apparatus, $\Pi_d$ also is fixed. The condition $\Pi_d$ = idem (8.49 b) also stipulates the size of the full-scale heat exchanger, $d_T$, before the model experiments have been performed:

$$d_T = d_M \, [(\rho/\mu)_M/(\rho/\mu)_T]^{2/3} \tag{8.50}$$

Due to the previously mentioned degree of freedom (8.48), a variety of alternatives with respect to $\{d_T, n_T, P_T\}$ can be established according to the model fluids used. All of them fulfil the requirements set above.

The *idem* conditions of the pi-numbers (8.49 c), whose numerical values are fixed by the process conditions of the full-scale device, are determining in association with (8.49 b) and the known temperature $(T_0)_M$ the conditions necessary for model experiments:

$$\gamma_{0,M}\,(T_{in} - T_w)_M = \theta_{in}$$

$$\gamma_{0,M}\,(T_{out} - T_w)_M = \theta_{out}$$

$$(T_{in} + T_w)_M = 2\,(T_0)_M \tag{8.51}$$

Employing $\Pi_q$, which is also given by the full-scale operational value, the throughput $q_M$ in the model apparatus can be determined according to (8.49 c):

$$q_M = \Pi_q\,[g\,(\rho/\mu)_M{}^5]^{2/3} \tag{8.52}$$

The only objective of the model experiments is now the determination of the rotational speed of the wipers (and the power $P_M$ necessary to operate them) required to achieve the calculated output temperature $(T_{out})_M$. When $n_M$ and $P_M$ are determined by the model experiment, the corresponding data for the full-scale device can be derived:

$$n_T = n_M \left(\frac{(\mu/\rho)_M}{(\mu/\rho)_T}\right)^{1/3} \quad \text{and} \quad P_T = P_M \left(\frac{(\rho^4/\mu^7)_M}{(\rho^4/\mu^7)_T}\right)^{1/3} \tag{8.53}$$

In obtaining this result, the discussion concerning the *general state* of flow is complete. In the following a *creeping flow* is presupposed. This facilitates the determination of the appropriate model fluid because instead of two, only one material number must be now idem, namely:

$$\Gamma^* \equiv \Gamma \times Pr^{1/3} = \text{idem},$$

see (8.44). This requirement is fulfilled not only in the point T in Fig. 17, but along the entire straight line (a). Therefore, several liquids with the respective temperatures can be considered. The determination of the parameters of both the model and full-scale device proceeds analogously to the general case.

## 8.5
## Material Function in non-Newtonian Liquids

In Newtonian liquids the shear stress $\tau$ [Pa] is proportional to the shear rate [$s^{-1}$]

$$\tau = \mu\,\dot{\gamma} \rightarrow \mu = \tau/\dot{\gamma} \tag{8.54}$$

and the proportionality constant is the dynamic viscosity $\mu$.

In non-Newtonian liquids $\mu$ actually depends on the effective shear rate $\dot{\gamma}$ and occasionally on its history as well. Such liquids are subdivided accordingly to their flow behavior into three classes:

1 The viscosity does not depend upon the duration of the shear
2 The viscosity depends upon the duration of the shear
3 The liquid partly behaves like a solid body

These interrelations are recorded in the rheological constitutive equations.

### 8.5.1 Pseudoplastic Flow Behavior

The *pseudoplastic* or shear-thining fluids represent the most important group within the 1st class of materials. Under shear stress aggregates of a dispersion liquid/solid or liquid/liquid (e.g. dyestuffs) disintegrate into single particles, which then orientate themselves in the direction of flow. Entangled chains of macromolecules of a polymer solution or melt are stretched, spherical erythrocytes of blood are elongated. In these cases viscosity is degraded by shear.

In most pseudoplastic liquids, Newtonian flow behavior is observed at sufficiently low and at high shear rates $\dot{\gamma}$, see **Fig. 18**. Viscosity approaching a constant value with low shear rates is called the zero-shear viscosity, $\mu_0$, and its constant value at very high shear rates is called the infinite shear viscosity, $\mu\infty$.

In a dimensional-analytical discussion of the rheological constitutive equations, *Pawlowski* [36] furnished the proof that the rank of the dimensional matrix is always two. By a convenient association of the quantities contained in them, two dimensional material parameters can be produced (see Fig. 18):

$$\mathrm{H}\ \text{– a characteristic viscosity constant, e.g. } \mu_0, \text{ and} \tag{8.55}$$

$$\Theta\ \text{– a characteristic time constant, e.g. } 1/\dot{\gamma}_0 \text{ or } 1/\dot{\gamma}_\infty \tag{8.56}$$

The relevance list of a process in which a rheological material participates is therefore extended by only two dimensional quantities. All the other material parameters can be transferred into dimensionless pi-numbers $\Pi_{\mathrm{rheol}}$.

Thus the rheological constitutive equation reads

$$\mu/\mathrm{H} = f(\dot{\gamma}\Theta, \Pi_{\mathrm{rheol}}) \quad \rightarrow \quad \mu/\mu_0 = f(\dot{\gamma}/\dot{\gamma}_0, \Pi_{\mathrm{rheol}}) \tag{8.57}$$

If the viscosity curve is plotted in a log-log scale and the transition range between $\mu_0$ and $\mu\infty$ is represented by a straight line with the slope $m < 1$, see **Fig. 18**, then one speaks about a *Ostwald-de Waele fluid* whose viscosity curve obeys the so-called "*power law*" ($\mu_{\mathrm{eff}}$ – effective viscosity, K – consistency index, m – flow index):

$$\mu_{\mathrm{eff}} = \mathrm{K}\,\dot{\gamma}^{\mathrm{m}-1} \tag{8.58}$$

Classical model fluids of this type are aqueous solutions of carboxy-methyl-cellulose (CMC), polyacrylamide (PAA), Carbopol® (acidic polymers of acrylic acid of Goodrich), and so on.

Shear rates normally appearing in mixing vessels are in the range of $\dot{\gamma} = 50\text{–}500\ \mathrm{s}^{-1}$, therefore many liquids behave like an *Ostwald-de Waele* fluid. This explains why the power law is so often used to describe rheological behaviour, see e.g. [37, 38].

Many years ago, *Pawlowski* [5; see there p. 124] pointed to the fact that the equation (8.58) injures the principle of consistency of physical quantities, because the dimension of $[\mathrm{K}] = \mathrm{M\,L^{-1}\,T^{m-2}}$ depends on the power m. In temperature dependent

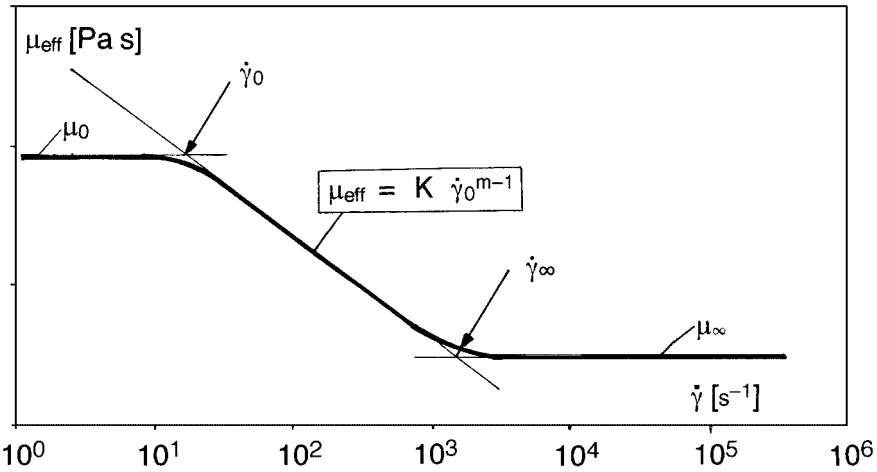


**Fig. 18** Typical course $\mu_{eff}(\dot{\gamma})$ in pseudoplastic fluids.

viscosities this entails that, for example, in a temperature field the quantity K changes its dimension from point to point and therefore neither *grad* K nor $K/K_0$ can be formed.

m is already a dimensionless parameter of the set $\Pi_{rheol}$. With the aid of parameters H and $\Theta$, eq. (8.55-56), the power law of *Ostwald-de Waele* can be transformed into a dimensionless form. The rheological constitutive equation of an *Ostwald-de Waele* fluid reads:

$$\frac{\mu}{H} = \frac{K}{H\Phi^{m-1}}(\dot{\gamma}\Phi)^{m-1} \quad \rightarrow \quad \frac{\mu}{\mu_0} = \frac{K}{\mu_0(1/\dot{\gamma}_0)^{m-1}}(\dot{\gamma}/\dot{\gamma}_0)^{m-1} \tag{8.59}$$

In the description of processes in which *Ostwald-de Waele* fluids take part, H and $\Theta$ are included into the relevance list. $\Theta$ can be formulated in a dimensionless manner as well as by other x quantities relevant to the process. In *pipe flow* it can be replaced by (l/v), whereby v and l are the characteristic flow velocity and length, respectively. The Reynolds number then has the following appearance:

$$Re_K \equiv \frac{\rho v^{2-m} l^m}{K} \tag{8.60}$$

In *stirring*, $\Theta$ is represented by $n^{-1}$, whereby n $[T^{-1}]$ stands for the stirrer speed. With d as the stirrer diameter, the Reynolds number then becomes:

$$Re_K \equiv \frac{\rho n^{2-m} d^2}{K} \tag{8.61}$$

For the effective viscosity in pipe flow from (5.59) it follows:

$$\mu_{eff} = K\,(v/l)^{m-1} \tag{8.62}$$

In the representation of power characteristics, Ne(Re) curves for stirrers in Newtonian and non-Newtonian liquids under identical geometric conditions coincide if the Reynolds number has been formed by the effective viscosity $\mu_{eff}$. According to the concept of *Metzner* and *Otto* [39], a direct proportionality between the stirrer speed, n, and the shear rate, $\dot{\gamma}$, exists:

$$\dot{\gamma} = k\,n \quad \rightarrow \quad \mu_{eff} = \frac{K}{\dot{\gamma}^{(1-m)}} = \frac{K}{(kn)^{(1-m)}} \tag{8.63}$$

The proportionality constant, k, depends on the stirrer type; for details see [22, p. 50].

If the Reynolds number is formed with the above formulated $\mu_{eff}$, then it follows that:

$$Re_{eff} \equiv \frac{nd^2\rho}{\mu_{eff}} = \frac{nd^2\rho}{K\,(kn)^{(m-1)}} = \frac{nd^2\rho}{K\,k^{(m-1)}n^{(m-1)}} = \frac{n^{(2-m)}d^2\rho}{K\,k^{(m-1)}} \tag{8.64}$$

If an analogy is assumed between the pressure drop characteristic of the pipe flow for a non-Newtonian fluid and the power characteristic of a stirrer, then $f\,(Re^*_{eff}, m)$ becomes the following expression:

$$Re^*_{eff} \equiv \frac{n^{(2-m)}d^2\rho}{K}\,8\left(\frac{m}{6m+2}\right)^m \tag{8.65}$$

which at $K = \mu$ and $m = 1$ yields $Re \equiv \frac{nd^2\rho}{\mu}$

Therefore, in stirring technology an alternative exists with respect to $\mu_{eff}$. One can take $\mu_{eff}$ either from the measured viscosity curve or from the corresponding *Ostwald-de Waele* "power law" (8.58) or else the concept of *Metzner* and *Otto* (8.63). With respect to the above explanations, the second alternative should be avoided. One should use $\mu_{eff}$ which corresponds to the effective shear rate in the measured viscosity curve $\mu_{eff}\,(\dot{\gamma}) \triangleq \mu_{eff}\,(k\,n)$.

According to (8.57), the material function of pseudoplastic fluids ($\Pi_{rheol} = m$), whose viscosity obeys the power law of *Ostwald-de Waele*, can be represented in the pi-space:

$$\{\mu/\mu_0,\ \dot{\gamma}/\dot{\gamma}_0,\ m\}$$

*Henzler* [40] correlated the viscosity behavior of aqueous CMC and Xanthan solutions in this pi-space with good success, as can be seen in **Fig. 19**. The fitting line corresponds to the process equation

$$\mu/\mu_0 = (1 + (\dot{\gamma}/\dot{\gamma}_0)^{2(1\,-\,m)})^{-1/2} \tag{8.66}$$

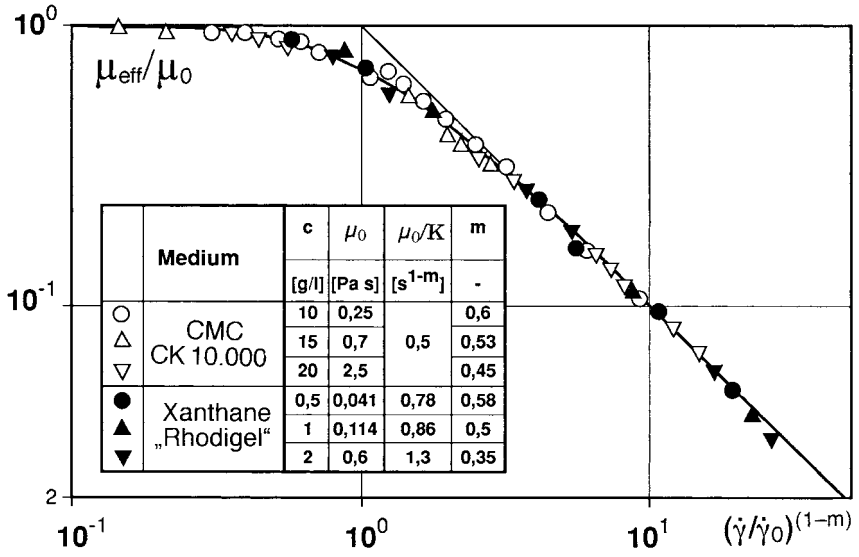


**Fig. 19** Dimensionless, standardized material function of some pseudoplastic fluids; from [40]. For the meaning of $\dot{\gamma}_0$ see Fig. 18.

### 8.5.2 Viscoelastic Flow Behavior

The *viscoelastic fluids* represent the 3rd material class of non-Newtonian fluids. Many liquids also possess elastic properties in addition to viscous properties. This means that the distortion work resulting from a stress is not completely irreversibly converted into frictional heat, but is stored partly elastically and reversibly. In this sense, they are similar to solid bodies. The liquid strains give way to the mechanical shear stress as do elastic bonds by contracting. This is shown in shear experiments (Fig. 1.27) as a restoring force acting against the shear force which, at the sudden ending of the effect of force, moves back the plate to a certain extent.

In viscoelastic fluids at steady-state laminar flow, besides shear stress $\tau = \sigma_{21} = \mu\,\dot{\gamma}$, normal stresses are observed in all three directions:

| | |
|---|---|
| in the direction of flow | $\sigma_{11} + p$ |
| perpendicular to the direction of flow | $\sigma_{22} + p$ and $\sigma_{33} + p$ |

(8.67)

The isotropic pressure, p, can be eliminated by the formation of normal stress differences:

1. normal stress difference $N_1 = \sigma_{11} - \sigma_{22}$ (8.68)

2. normal stress difference $N_2 = \sigma_{22} - \sigma_{33}$ (8.69)

$N_2$ values are always lower than $N_1$ values, see e.g. [40]. Therefore for many processes taking into consideration only $N_1$ will suffice. The normal stress differences are independent of the direction of flow and, in laminar flow (low $\dot{\gamma}$), are proportional to $\dot{\gamma}^2$. In following $\mu = \tau/\dot{\gamma}$ for a Newtonian fluid, normal stress coefficients $\psi_1 \equiv N_1/\dot{\gamma}^2$ and $\psi_2 \equiv N_2/\dot{\gamma}^2$ are occasionally used. Their dependence on the shear rate $\psi(\dot{\gamma})$ describes the non-linear viscoelastic behavior of the fluid.

For a correct dimensional-analytical representation of the viscoelastic behavior of a fluid, the ratio of normal stress to shear stress is used. The so-called Weissenberg number is defined as

$$Wi_1 \equiv N_1/\tau \tag{8.70}$$

In **Fig. 20** $Wi_1$ values as a function of $\dot{\gamma}$ are represented for aqueous CMC and PAA solutions.

Frequently, a characteristic relaxation time, $\lambda$, is used to describe viscoelastic behavior. It is a measure for the time needed to transform the reversibly-elastically stored energy into friction heat:

$$\lambda \equiv N_1/(2\,\tau\,\dot{\gamma}) = Wi_1/(2\,\dot{\gamma}) \tag{8.71}$$

If, according to the concept of *Metzner* and *Otto*, $\dot{\gamma}$ is replaced by the stirrer speed n, then (8.71) can also be written as

$$De \equiv \lambda\, n \triangleq \lambda\,\dot{\gamma} = Wi_1/2 \tag{8.72}$$

The product $n\,\lambda$ is named Deborah number, De.

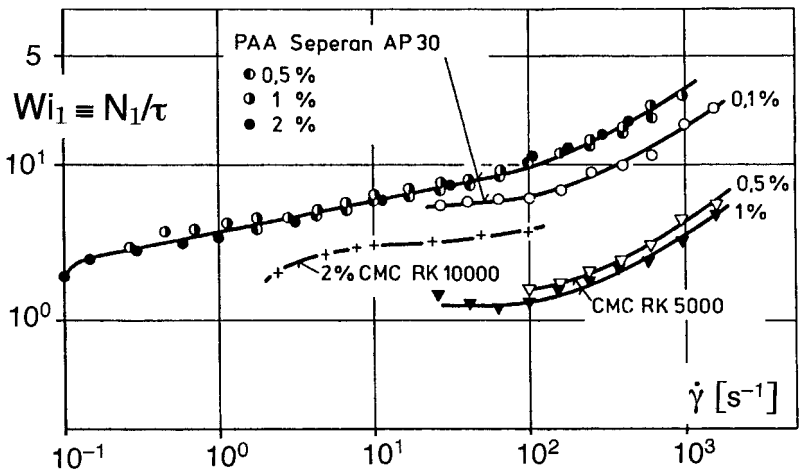


**Fig. 20** ($Wi_1$, $\dot{\gamma}_0$) dependence for CMC and Xanthan solutions; from [40].

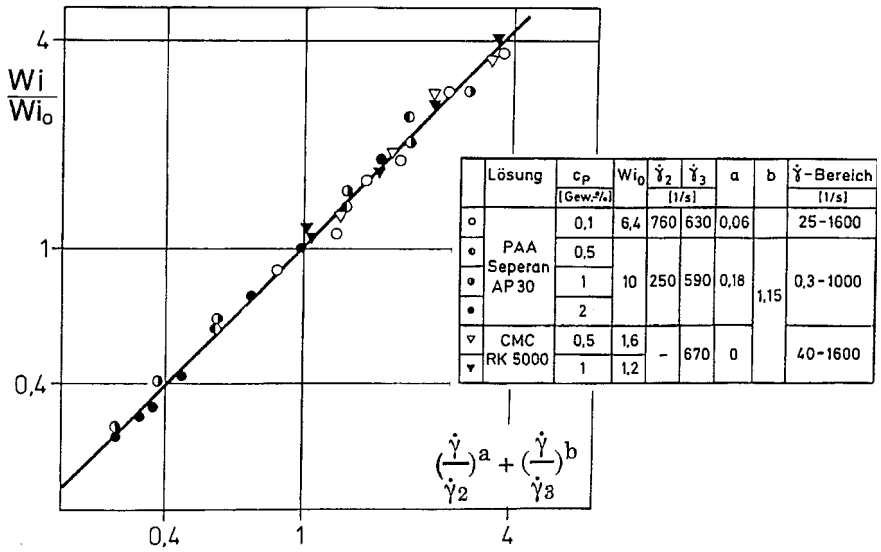


**Fig. 21** Dimensionless standardized material function of some viscoelastic fluids; from [40]

**Fig. 21** shows the dimensionless, standardized material function of two viscoelastic fluids, whose dependences $Wi_1$ ($\dot{\gamma}$) were given in Fig. 20. The fitting line corresponds to the process equation

$$Wi_{eff}/Wi_0 = (\dot{\gamma}/\dot{\gamma}_2)^a + (\dot{\gamma}/\dot{\gamma}_3)^b \tag{8.73}$$

(Exponents a and b have different values depending on the respective substance; see the inset in Fig. 21.)

## 8.6
## Pi-space in Processes with non-Newtonian Fluids

As previously mentioned, the transition from Newtonian to non-Newtonian fluids has the following consequences with respect to the enlargement of the pi-space:

a) All pi-numbers of the Newtonian case also appear in the non-Newtonian case, whereby $\mu$ is replaced by the quantity H (usually $\mu_0$) with the same dimension, see eq. (8.55).
b) An additional pi-number is included which contains $\Theta$ (usually $1/\dot{\gamma}_0$).
c) The pure material numbers are increased by $\Pi_{rheol}$.

This will be demonstrated on the heat transfer characteristics of a smooth straight pipe. **a** is valid for the temperature **in**dependent viscosity and **b** for the temperature dependent viscosity:

| | *Newtonian fluid* | *non-Newtonian fluid* |
|---|---|---|
| **a** | Nu, Re, Pr | Nu , $Re_H$, $Pr_H$, $v\Theta/L$, $\Pi_{rheol}$ |
| **b** | Nu, $Re_0$, $Pr_0$, $\gamma_0\Delta T$ | Nu, $Re_{Ho}$, $Pr_{Ho}$, $v\Theta_0/L$, $\gamma_{Ho}\Delta T$, $\gamma_\Theta/\gamma_H$, $\Pi_{rheol}$ |

(8.74)

In case b), $\mu_w/\mu$ and $\gamma_{Ho}\Delta T$, respectively, as well as $\gamma_\Theta/\gamma_H$ have to be added ($\gamma_\Theta \equiv \partial \ln\Theta/\partial T$).

In addition, it can happen that in the non-Newtonian case completely new phenomena take place (e.g. shaft climbing by a viscoelastic fluid against the acceleration due to gravity, the so-called Weissenberg effect), this calling for additional parameters (in this case g).

## 8.7 Scale-up in Processes with non-Newtonian Fluids

Due to the fact that the rheological properties are usually not fully known, one is forced to perform model experiments with the same substance which is used in the full-scale process. Thanks to

$$\Pi_{material} \text{ (here } Pr_H, \Pi_{rheol}) = \text{idem}$$

the process therefore takes place in a pi-space which is enlarged by only one pi-number (namely $v\Theta/L$) with respect to the Newtonian case, see (8.74).

However, in the transition from model to full-scale, a complete similarity cannot be achieved. This is because in using the same material system $Re_H \equiv \rho\, v\, L/H$ = idem, $v\,\Theta/L$ = idem cannot be ensured at the same time. It is recommended to use the same material system, but to change the model scale. An exception to this is represented by pure hydrodynamic processes in the creeping flow region ($\rho$ irrelevant) at steady-state and isothermal conditions. Here mechanical similarity can be obtained in spite of constant physical properties; see Example 26: Single-screw machines.

**Example 18**: Homogenization characteristics in viscoelastic liquids

Homogenization of miscible liquids, i.e. leveling out the concentration differences by stirring, is represented in Newtonian liquids by the pi-space

$$\{n\theta, \text{Re, type of stirrer, installation conditions}\}.$$

$\theta$ is the mixing time necessary for the attainment of a complete molecular-homogeneous mixture (see [22], chapter 3, and Example 21 in this book).

In non-Newtonian mixtures in the laminar and transition range this mixing operation requires considerably longer mixing times than in Newtonian liquids. This is due to the fact that in the catchment area of the stirrer higher shear rates and, there-

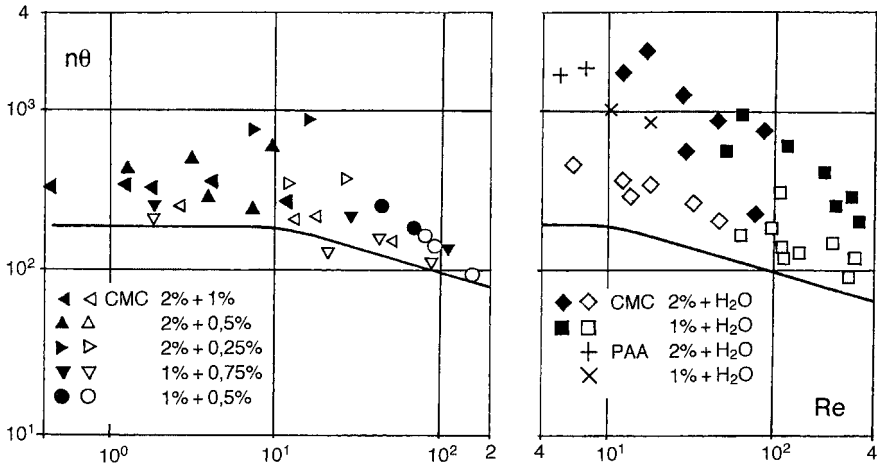


**Fig. 22** Representation of the test data in the pi-space {nθ, $Re_{eff}$} without taking into account the Wi number. $Re_{eff}$ is formed by the $\mu_{eff}$ of the homogenized mixture. *Full* signs: downflow, *hollow* signs: upflow. *Plotted curve*: Homogenization characteristics of Newtonian liquids, from [41].

fore, lower viscosities prevail as compared with the bulk of liquid. In addition, between neighboring flow threads viscous forces counteract the deformation due to shear whereas inside of these threads the elastic forces oppose the deformation due to stretching.

In the case of non-Newtonian mixtures, which also exert pseudoplastic and viscoelastic behavior, the pi-space is widened by the Weissenberg number, Wi. In addition, it has to be decided which effective viscosity, $\mu_{eff}$, has to enter the Reynolds number:

$$\{n\theta,\ Re_{eff},\ Wi,\ \text{type of stirrer, installation conditions}\} \tag{8.75}$$

*Ford* und *Ulbrecht* [41] performed homogenization measurements with aqueous CMC and PAA solutions in a vessel with a screw stirrer arranged in a central draught tube. The pumping direction of the screw could be changed as well. Initially, the liquid with a lower viscosity rested in a layer on top of the more viscous one (volume ratio $\varphi = 1$). The data measured were first represented in the space {nθ, $Re_{eff}$}, **Fig. 22**, whereby $\mu_{eff}$ was taken from the flow curve of the homogenized mixture at the shear rate of $\dot{\gamma} \approx 5\ s^{-1}$, which was effective in the draught tube.
The greater the difference in viscosity between both mixing components, the longer the mixing times. They can be extended by a factor of 10 as compared to the Newtonian case. The sense of conveying also has a big impact. If the liquid of higher viscosity is mixed into the less viscous one, then the mixing times are shorter as compared to the reverse addition order.

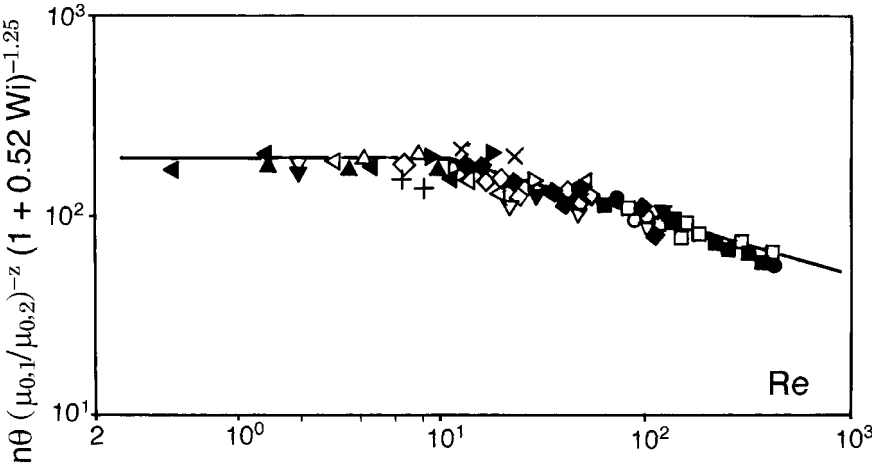


**Fig. 23** Homogenization characteristic of a screw stirrer in a draught tube for non-Newtonian liquids with pseudoplastic and viscoelastic properties. For the sign explanation see Fig. 22; from [41].

These test data are correlated satisfactorily by the Weissenberg number (here defined as $Wi \equiv \lambda n$) and the term $(\mu_{0,1}/\mu_{0,2})^z$ which accounts for the pumping direction, **Fig 23**. $\mu_0$ represents the starting viscosity of the lower, more viscous liquid (1), and the upper, less viscous (2) liquid. Upflow: $z = 0.059$, downflow: $z = 0.17$.

With respect to the consideration of effective viscosity, the concept of *Ford* and *Ulbrecht* seems not to be conveniently chosen, in spite of the fact that the results in Fig. 23 are really satisfying. *Opara* [42] noted that one should not expect to be able to correlate the mixing times using $\mu_{eff}$ and, consequently, $Re_{eff}$ according to the concept of *Metzner* and *Otto*, because their concept was founded on power dissipation: In this case, $\mu_{eff}$ is evaluated from shear rates which arise at the highest velocity differences, whereas for the homogenization process those areas are decisive which are close to the vessel wall, where the smallest velocity differences exist.

This alternative was examined in later experiments [43] with the same material system, but it did not produce a better correlation of the $n\theta$ values. It is not important whether or not $Re_{eff}$ is used whose $\mu_{eff}$ is determined by the shear rate $\dot{\gamma} = k\ n$ (eq. 8.63), or if one takes Rew whose $\mu_w$ has been determined by the shear rate at the vessel wall. For a satisfying correlation the Wi term is necessary.

Using the approach of *Ford* and *Ulbrecht*, influence of rheological properties (Newtonian, pseudoplastic, viscoelastic) on the homogenization characteristics was also satisfyingly taken into account for turbine stirrers [44] and other stirrer types [45].

*Scale-up in Chemical Engineering.* Marko Zlokarnik


ISBNs: 3-527-30266-2 (Hardback); 3-527-60056-6 (Electronic)

# 9
# Reduction of the Pi-space

Let us once more recall the statement of the pi-theorem (section 2.7):

Every physical relationship between n physical quantities can be reduced to a relationship between m = n – r mutually independent dimensionless groups, whereby r stands for the rank of the dimensional matrix, made up of the physical quantities in question and is generally equal to (or in some few cases smaller than) the number of the base quantities contained in their secondary dimensions.

In fact, this actually means that the pi-set could be reduced if one succeeds to enlarge the base dimensions of the dimensional system. However, it must be considered that in the enlargement (reduction) of a dimensional system the relevance list must also be enlarged (reduced) by the corresponding dimensional constant by which the number of the resulting pi-numbers is not changed. However, it can turn out that in the enlargement of the dimensional system the additional dimensional constant is, *a priori*, irrelevant to the problem. In this case, it need not be incorporated into the relevance list and the number of pi-numbers is, in fact, reduced by one.

## 9.1
## The Controversy Rayleigh – Riabouchinsky

In his famous and extremely short essay entitled "The principle of similitude" *Lord Rayleigh* [4] discussed 15 different physical problems which can be condensed to laws by using dimensional analysis without performing any experiments. The last of these examples concerned the "*Boussinesq* problem" of the steady-state heat transfer from a fixed body to a ideal liquid flowing with the velocity of v.

He considered, in his own words, "somewhat in detail, *Boussinesq*'s problem of the steady passage of heat from a good conductor immersed in a stream of fluid moving (at a distance from the solid) with velocity v. The fluid is treated as incompressible and, for the present as inviscid, while the solid has always the same *shape* and presentation to the stream. In these circumstances the total heat, Q, passing in unit time is a function of the linear dimension of the solid, l, the temperature difference, $\Delta T$, the stream velocity, v, the capacity for heat of the fluid per unit volume,

$\rho C_p$, and the conductivity, k. The density of the fluid clearly does not enter into the question." Thus, we obtain the following relevance list:

$$\{Q, l, \Delta T, v, \rho C_p, k\} \tag{9.1}$$

These six quantities contain four base dimensions [L, T, Θ, H], wherein H means the amount of heat with calorie as measuring unit. According to the pi-theorem, a dependence between two pi-numbers will result. *Rayleigh* obtained the following two pi-numbers which are today named: The Nusselt number Nu and the Péclet number Pe, the latter being the product of Reynolds and Prandtl numbers, Pe ≡ RePr:

$$\frac{Q}{l\,k\,\Delta T} \equiv \frac{h\,l}{k} = f\left(\frac{l\,\rho C_p\,v}{k}\right) \quad \rightarrow \quad Nu = f(RePr) \tag{9.2}$$

*Real* liquids display a physical property which is named viscosity. Only after the kinematic viscosity, $\nu \equiv \mu/\rho$, is introduced can the product RePr be taken apart:

$$\frac{Q}{l\,k\,\Delta T} \equiv \frac{h\,l}{k} = f\left(\frac{l\,\rho C_p\,v}{k};\ \frac{\rho C_p\,\nu}{k}\right) \rightarrow Nu = f(Re/Pr, Pr) \rightarrow Nu = f(Re, Pr) \tag{9.3}$$

Out of 7 x-quantities and 4 base dimensions we now obtain 7 – 4 = 3 pi-numbers.

*Lord Rayleigh* pointed out that one can deduce valuable information from the above interdependence (9.3) although it is an arbitrary function of the two variables. The latter of them appeared to be constant for any given kind of gas (compare to Example 5) and seemed to vary only moderately from one gas to another. Therefore, we are left with Nu = *f* (Re); for each v l = const therefore the functional dependence *f* remains unchanged.

Four months after this publication a "Letter to the Editor" of *D. Riabouchinsky* [46] appeared in *Nature*. He pointed out that *Lord Rayleigh* considered heat, temperature, length and time as four independent units. If we suppose that only three of these quantities are really independent, we obtain a different result. For example, if the temperature is defined as the mean kinetic energy of molecules, the principle of similitude allows us only to affirm that

$$\frac{Q}{l\,k\,\Delta T} = f\left(\frac{l\,\rho C_p\,v}{k},\ \rho C_p\,l^3\right) \tag{9.4}$$

If this is considered, then equation (9.2) is extended by another argument and, as a consequence, with two arguments is much more arbitrary than with one argument.

In his reply, *Lord Rayleigh* [47] referred this objection to the field of logic and explained that his conclusion has followed on the basis of the usual Fourier equations of heat, in which heat and temperature are regarded as *sui generis*. He added: "It would indeed be a paradox if the further knowledge of the nature of heat afforded by molecular theory put us in a worse position than before in dealing with a particular problem. The solution would seem to be that the Fourier equations embody something as to the nature of heat and temperature which is ignored in the alternative argument of Dr. Riabouchinsky."

(*Lord Rayleigh* is completely right with this latter sentence, as it will be shown later on.) After that, this problem was put aside as being unsolved and was called the "*Riabouchinsky* paradoxon". Obviously, this was to much for engineers, and physicists, who were spoken to, were not interested. However, the solution to this problem is in fact rather easy.

It is correct to state that according to the Theory of Gases energy can be expressed as temperature. However, this is advantageous and reasonable only if the physical process is governed by molecular events. For macroscopic interrelations like the *Boussinesq*'s problem, the molecular nature of the gas is irrelevant. Here, the microscopic parameters are replaced by mean values of the macroscopic ones, these appearing in measurable physical properties such as specific heat and heat conductivity. To equate energy with temperature as *Riabouchinsky* did, introduced irrelevant physics to the problem. See also the remarks of *L.I. Sedov* [48, p. 40+].

Furthermore, one has to bear in mind that relating energy with temperature implies the consideration of the *Boltzmann*'s constant, **k**. However, this natural constant will play a role in a physical problem only if the molecular nature of matter is involved, otherwise it is irrelevant.

**Example 19**: Dimensional-analytical treatment of the *Boussinesq*'s problem

In dealing with *Boussinesq*'s problem, *Lord Rayleigh* used the amount of heat H (measuring unit: calorie) as one of the then used base dimensions. Only since the introduction of SI (Système International d'Unités) it was required to make no distinction between heat and mechanical energy, because both were considered to be equal. In order to comply with this requirement, the *Joule* equivalent of heat **J** [$M\,L^2\,T^{-2}\,H^{-1}$] had to be introduced as a natural constant in the relevance list. If we proceed from the assumption of an "inviscid", *ideal* liquid, no mechanical heat can be converted into heat. In this case, **J** is irrelevant.

a) Procedure of *Lord Rayleigh*

Relevance list:

| | |
|---|---|
| Target quantity: | amount of heat, Q |
| geometric parameters: | characteristic measurement of length, l |
| material parameters: | volume-related heat capacity, $\rho C_p$ |
| | heat conductivity, k |
| process-related parameters: | velocity of flow, v |
| | temperature difference, $\Delta T$ |

$$\{Q, l, \rho C_p, k, \Delta T, v\} \tag{9.5}$$

| | *l* | *k* | $\Delta T$ | $\rho C_p$ | *Q* | *ν* |
|---|---|---|---|---|---|---|
| L | 1 | –1 | 0 | –3 | 0 | 1 |
| T | 0 | –1 | 0 | 0 | –1 | –1 |
| Θ | 0 | –1 | 1 | –1 | 0 | 0 |
| H | 0 | 1 | 0 | 1 | 1 | 0 |
| L + 2T + 3H | **1** | 0 | 0 | 0 | 1 | –1 |
| –T | 0 | **1** | 0 | 0 | 1 | 1 |
| Θ + H | 0 | 0 | **1** | 0 | 1 | 0 |
| H + T | 0 | 0 | 0 | **1** | 0 | –1 |

Formation of pi-numbers:

$$\Pi_1 \equiv \frac{Q}{l\,\Delta T\,k} \equiv Nu \qquad \Pi_2 \equiv \frac{v\,l\,\rho C_p}{k} \equiv RePr \equiv Pe \tag{9.6}$$

Conclusion: The carried out dimensional analysis fully proves *Lord Rayleigh*.

b) Procedure of *D. Riabouchinsky*

Relevance list: {Q, l, $\rho C_p$, k, v, $\Delta T$, **k**}
Dimensional matrix:

| | *l* | *k* | $\Delta T$ | $\rho C_p$ | *Q* | *ν* | *k* |
|---|---|---|---|---|---|---|---|
| L | 1 | –1 | 0 | –3 | 0 | 1 | 0 |
| T | 0 | –1 | 0 | 0 | –1 | –1 | 0 |
| Θ | 0 | –1 | 1 | –1 | 0 | 0 | –1 |
| H | 0 | 1 | 0 | 1 | 1 | 0 | 1 |
| L + 2T + 3H | **1** | 0 | 0 | 0 | 1 | –1 | 3 |
| –T | 0 | **1** | 0 | 0 | 1 | 1 | 0 |
| Θ + H | 0 | 0 | **1** | 0 | 1 | 0 | 0 |
| H + T | 0 | 0 | 0 | **1** | 0 | –1 | 1 |

Formation of pi-numbers:

$$\Pi_1 \equiv \frac{Q}{l\,k\,\Delta T} \equiv Nu \qquad \Pi_2 \equiv \frac{v\,l\,\rho C_p}{k} \equiv RePr \equiv Pe \qquad \Pi_3 \equiv \frac{\mathbf{k}}{l^3\,\rho C_p} \equiv \mathbf{k}^* \tag{9.7}$$

**k*** is the pi-number, which also *Riabouchinsky* would have obtained, only it must be cancelled here because of the irrelevance of **k**. Consequently, we are left with the pi-set obtained by *Lord Rayleigh*.

**Example 20**: Heat transfer characteristic of a stirring vessel

In *Rayleigh*'s treatment of the *Boussinesq*'s problem, we realized that Joule's heat equivalent had to be cancelled, because in this problem the liquid was supposed to be an ideal one. This is – of course – as with many problems arising in the areas of

the mechanical and thermal process engineering not the case. One only has to think of screw machines, where a large mechanical power input is transformed into heat. In such cases the **J** containing pi-number must not be disposed of. In this context, the heat transfer characteristics will be discussed, whereby from one part the dimensional system {M, L, T, Θ} and from the other {M, L, T, Θ, H} will be used.

Relevance list:

| | |
|---|---|
| target quantity: | heat transfer coefficient at the inner wall, h |
| geometric parameter: | vessel and stirrer diameters: D, d |
| material parameters: | density ρ; viscosity μ; temperature coefficient of viscosity, $\gamma_0$; heat capacity $C_p$; heat conductivity, k |
| process parameters: | stirrer speed, n<br>temperature difference, $\Delta T$, between wall and liquid |

The complete 10-parametric relevance list reads:

$$\{h; D, d; \rho, \mu, \gamma_0, C_p, k; n, \Delta T\} \tag{9.8}$$

**A** Dimensional system {M, L, T, Θ}

| | ρ | ***d*** | ***n*** | $\Delta T$ | ***h*** | $C_p$ | ***k*** | μ | ***D*** | $\gamma_0$ |
|---|---|---|---|---|---|---|---|---|---|---|
| M | 1 | 0 | 0 | 0 | 1 | 0 | 1 | 1 | 0 | 0 |
| L | –3 | 1 | 0 | 0 | 0 | 2 | 1 | –1 | 1 | 0 |
| T | 0 | 0 | –1 | 0 | –3 | –2 | –3 | –1 | 0 | 0 |
| Θ | 0 | 0 | 0 | 1 | –1 | –1 | –1 | 0 | 0 | –1 |
| M | **1** | 0 | 0 | 0 | 1 | 0 | 1 | 0 | 0 | 0 |
| L + 3M | 0 | **1** | 0 | 0 | 3 | 2 | 4 | 2 | 1 | 0 |
| –T | 0 | 0 | **1** | 0 | 3 | 2 | 3 | 1 | 0 | 0 |
| Θ | 0 | 0 | 0 | **1** | –1 | –1 | –1 | 0 | 0 | –1 |

The following six pi-numbers are produced:

$$\Pi_1 = \frac{h\,\Delta T}{\rho\, d^3 n^3} \qquad \Pi_2 = \frac{C_p\,\Delta T}{d^2 n^2} \qquad \Pi_3 = \frac{k\,\Delta T}{\rho\, d^4 n^3} \qquad \Pi_4 = \frac{\mu}{\rho\, d^2 n} \equiv Re^{-1}$$

$$\Pi_5 = D/d \qquad \Pi_6 = \gamma_0\,\Delta T$$

Pi-numbers $\Pi_1$, $\Pi_2$ and $\Pi_3$ have an unusual appearance. We shall first combine $\Pi_1$ and $\Pi_3$:

$\Pi_1\,\Pi_3^{-1} = h\,d/k \rightarrow h\,D/k \equiv Nu$ (Nusselt number).

Then, $\Pi_2$ will be transformed by $\Pi_3$ and $\Pi_4$ into a pure material number

$\Pi_2\,\Pi_3^{-1}\,\Pi_4^{-1} = C_p\mu/k \equiv Pr$ (Prandtl number).

Alas, we don't recognize the pi-number $\Pi_3$ and, therefore, have no idea about its significance. Otherwise, $\Pi_4$ is the inverse value of the Reynolds number and $\Pi_5$ as well $\Pi_6$ speak for themselves.

The dimensional analysis performed with the dimensional system {M, L, T, Θ} delivers, for the heat transfer characteristic of a stirring vessel, the following 6-parametric pi-set:

$$\{\mathrm{Nu}, \mathrm{Pr}, \Pi_3, \mathrm{Re}, \gamma_0 \Delta T, \mathrm{D/d}\} \tag{9.9}$$

whereby the significance of the pi-number $\Pi_3$ is not obvious.

**B** Dimensional system {M, L, T, Θ, H}

| | ρ | *d* | *n* | Δ*T* | *k* | *h* | $C_p$ | *J* | μ | *D* | $\gamma_0$ |
|---|---|---|---|---|---|---|---|---|---|---|---|
| M | 1 | 0 | 0 | 0 | 0 | 0 | – 1 | 1 | 1 | 0 | 0 |
| L | –3 | 1 | 0 | 0 | –1 | –2 | 0 | 2 | –1 | 1 | 0 |
| T | 0 | 0 | –1 | 0 | –1 | –1 | 0 | –2 | –1 | 0 | 0 |
| Θ | 0 | 0 | 0 | 1 | –1 | –1 | –1 | 0 | 0 | 0 | –1 |
| H | 0 | 0 | 0 | 0 | 1 | 1 | 1 | –1 | 0 | 0 | 0 |
| M | **1** | 0 | 0 | 0 | 0 | 0 | –1 | 1 | 1 | 0 | 0 |
| 3M + L + H | 0 | **1** | 0 | 0 | 0 | –1 | –2 | 4 | 2 | 1 | 0 |
| –T – H | 0 | 0 | **1** | 0 | 0 | 0 | –1 | 3 | 1 | 0 | 0 |
| Θ + H | 0 | 0 | 0 | **1** | 0 | 0 | 0 | –1 | 0 | 0 | –1 |
| H | 0 | 0 | 0 | 0 | **1** | 1 | 1 | –1 | 0 | 0 | 0 |

The following seven pi-number result from this:

$$\Pi_1 \equiv \frac{h\,d}{k} \equiv \mathrm{Nu} \qquad \Pi_2 \equiv \frac{C_p \rho d^2 n}{k} \qquad \Pi_3 \equiv \frac{J \Delta T k}{\rho d^4 n^3}$$

$$\Pi_4 \equiv \frac{\mu}{\rho d^2 n} \equiv \mathrm{Re}^{-1} \qquad \Pi_2 \Pi_4 \equiv C_p \mu / k \equiv \mathrm{Pr} \qquad \Pi_5 \equiv \frac{D}{d}$$

$$\Pi_6 \equiv \gamma_0 \Delta T \qquad \Pi_3^{-1} \Pi_4 \equiv \frac{\mu d^2 n^2}{J \Delta T k} \equiv \mathrm{Br}$$

In both dimensional systems, pi-number $\Pi_3$ has been produced which, after combination with the Reynolds number, can be recognized as Brinkman number Br. As long as the heat production can be neglected as compared with the heat removal, $\Pi_3$ and Br, respectively, also remain negligible and can therefore be deleted. The complete pi-set then reads:

$$\{\mathrm{Nu}, \mathrm{Pr}, \mathrm{Re}, \mathrm{D/d}, \gamma_0 \Delta T\} \tag{9.10}$$

In spite of the fact that both dimensional systems yield the same pi-sets, it is the second one which allows, by the appearance of **J** in one of the pi-numbers, its interpretation and the decision about its relevance.

*Scale-up in Chemical Engineering.* Marko Zlokarnik


ISBNs: 3-527-30266-2 (Hardback); 3-527-60056-6 (Electronic)

# 10
# Typical Problems and Mistakes in the Use of Dimensional Analysis

Occasionally, one could have read about the *failures* of the Theory of Similarity or of its *limits*. However, this criticism has arisen when, due to some physical reasons, a complete similarity could not be achieved (see e.g. remarks of *Damköhler* [113] on p. 183) or the scale-up criterion could not have been worked out with certainty because the measuring conditions did not allow it (false model scale, wanted sensitivity of the target quantity, non-availability of the model material system, ignorance about relevant physical properties, such as in foams and sludges, etc.).

When problems arise in model experiments for the above mentioned reasons, one cannot put the blame on an epistemologically and mathematically sound method.

The problems in connection with the non-availability of a model material system were already discussed in section 6.1. It has been shown how these problems can be handled by model measurements in differently scaled pieces of equipment. Only in cases where this option is too expensive (e.g. ship-building), can one depend on methods employing conditions of partial similarity (section 6.2).

In contrast, this chapter deals with widespread problems related to the measuring techniques. The majority of them have been taken from the area of stirring technology which is particularly familiar to the author, see [22] and [49].

## 10.1
## Model Scale and the State of Flow; Problems Concerning Mini Plants

Model measurements are normally executed in laboratories and the size of the laboratory equipment complies with the size of the premises. Usually, this is not a drawback, but in some cases the situation is grave. One of the main problems concerns the state of flow in the measuring device, this being exceedingly scale-dependent. Interestingly, this particular problem was never recognized by university researchers as such. Here, two typical problems are presented:

### 10.1.1 Bubble Columns

In the determination of the target quantities "gassed liquid height" and mass transfer coefficient, $k_La$, employing laboratory bubble columns with diameters of only a few centimeters, occasionally piston bubbles were observed. Above the gas sparger (mostly a sintered plate), primary tiny gas bubbles are produced and these coalesce to give bigger ones. Flow regions exist, where these big bubbles fill up the whole cross-sectional area of the column (so-called "piston bubbles"). It has been reported that the diameter of the column has to exceed D = 8 cm in order to avoid this situation.

There is no doubt that such state of flow cannot exist in an industrial bubble column of D » 1 m. If somebody wanted to scale-down the state of flow of a full-scale bubble column (the same process point in the pi-space) to a laboratory one, one would have to know what parameters in the full-scale bubble column are of real importance.

The proneness of the primarily produced minute gas bubbles to coalescence depends on three parameters: a) on the size of the primarily produced gas bubbles; b) on the material system; c) on the state of flow in the bubble column [50]. Therefore, fixing the minimum diameter of a bubble column is surely not a sufficient criterion. One would have to carry out preliminary tests in differently scaled columns to find out the necessary minimum size of the model bubble column, see also Example 34.

### 10.1.2 Stirring Vessels

In stirring, distinction is made between micro- and macro-mixing. Micro-mixing concerns the state of flow in the tiniest eddies. It is determined by the kinematic viscosity, $\nu$, of the liquid and by the dissipated power per unit of mass, $\varepsilon = P/\rho V$. Correspondingly, the so-called "*Kolmogorov*'s micro-scale $\lambda$ of the turbulence" is laid down as being $\lambda = (\nu^3/\varepsilon)^{1/4}$. (By the way, this equation is clearly derived from dimensional analysis!)

*Micro-mixing* is important in such stirring operations where the result depends upon the size of the smallest eddies, for example dispersion processes in liquid/liquid systems and shear damage to microorganisms. Therefore, it is not surprising that in such tasks it is the volume related power, P/V, that counts; it is an intensively formulated process quantity.

*Macro-mixing* concerns the state of flow produced by the stirrer in the vessel. The stirrer generates primary eddies whose size is of the same order of magnitude as the stirrer diameter d. The macro-scale, $\Lambda$, is therefore given by $\Lambda \propto d$. It is described by the hydrodynamical pi-numbers such as $Re \equiv n\, d^2/\nu$, $Fr \equiv n^2\, d/g$, and the like.

In the study of mixing operations which depend upon macro-mixing, the problem of the size of the experimental device therefore exists. *Kipke* [51] pointed out that in devices of industrial size with $D \geq 3$ m, the dimensions of the primary eddies,

$\Lambda_T$, broadly exceed those of the laboratory device, $\Lambda_M$. *Weber* [52] referred to the fact that in industrially sized reactors a highly turbulent state of flow corresponding to $Re \geq 10^6$ exists. To obtain this in a laboratory device, vessel sizes of $D_M \geq 1$ m are necessary.

This statement from *Weber* [52] hits the nail on the head. In a laboratory stirring vessel the state of flow corresponding to $Re \geq 10^6$ cannot be achieved, that is, the same Re value in the pi-space cannot be reproduced. If one would still want to achieve it by extremely intensive stirring, one would have to accept strong heat development and, because of this, an additional pi-number (here: Brinkman number) would come into play. In this case, the pi-space in the laboratory-scale would then be different to that in the industrial-scale.

From the viewpoint of dimensional analysis, the terms macro-mixing and micro-mixing used in the Theory of Turbulence are misleading, because they confuse the issue discussed above. In performing model experiments it does not matter whether the state of flow corresponds to the macro- or micro-mixing, but whether we succeeded in obtaining the working point of the same pi-space.

### 10.1.3
### Micro-reactors and Mini-plants

The above remarks throw a critical view onto the contemporary efforts to simulate entire chemical processes on the smallest possible scale. Beyond all doubt, this technology can produce the proof about the feasibility of a synthesis. In addition, all process steps carried out in a homogeneous medium and dependent on micro-mixing, will be correctly executed on the micro-scale. Furthermore, the scale-dependent process steps will also be carried out in a satifactory manner on the micro-scale, because their scale-dependence could not express itself. But: from these results no statement concerning the scale-up can be made! In other words: Mini-plants are not suitable to gain any scale-up rules for scale-dependent steps.

Additional aggravating circumstances arise from the fact that chemical steps which are transfer limited will proceed differently in the industrial plant than on laboratory-scale. The selectivity of multiple reactions such as competing consecutive and parallel reactions depend very much on the extent of micro-mixing in the system. These facts are well known from Chemical Reaction Engineering textbooks. Conversely, these reactions are carried out to obtain details about the extent of micro- and macro-mixing in stirring.

## 10.2
## Unsatisfactory Sensitivity of the Target Quantity

Due to the largely developed field of chemical process engineering, there are possibly only a few targets left whose sensitivity is not satisfying; from the area of stirring technology two of them will be presented in the following as examples.

### 10.2.1
### Mixing Time θ

In the leveling out of concentration differences in mutually soluble liquids to a molecularly homogeneous level by mixing ("homogenization"), the necessary homogenization or mixing time θ [T] is visually determined by a chemical decolorization method (e.g. neutralization reaction with phenolphthalein as indicator), see also Example 21. In the turbulent flow range ($Re > 10^4$) in the laboratory vessel, the mixing time only accounts for a few seconds. Because of this, measuring accuracy and the reliable determination of the scale-up rule suffer.

In order to obtain a reliable scale-up rule one would have to perform measurements in larger vessels (D > 1 m) [52]. Unfortunately, in this case, this otherwise outstanding and comprehensive decolorization method fails completely: thick water layers glimmer pale blue and the white painted vessels make the perception of the color change difficult. Consequently, in this field, computational fluid dynamics (CFD) will possibly provide a solution.

### 10.2.2
### Complete Suspension of Solids According to the 1-s Criterion

A further exceedingly important mixing operation consists of whirling up solid particles ("suspension of solids") to obtain their surfaces completely accessible to the surrounding liquid (dissolution of salts, solid catalyzed reactions in a S/L/G system, and so on). To work out the criteria important for this task, research concentrated on measuring the "critical stirrer speed" necessary for the flow state in which no particle lingered longer than 1 second on the bottom of the vessel.

Firstly, it has to be taken into account that criteria which characterize a state of flow have to be formulated in a dimensionless manner. Already *W. Froude* found in his experiments to determine the drag resistance of a ship's hull that the bow wave can only be reliably determined when the size of the ship model has the right proportions with respect to the travelling speed and channel width.

In case of "1-s criterion", we are dealing with an easy to allocate, but an inaccurate quantity with a low sensitivity: Who is able to decide, by purely visual means, if the time was 0.7 s or 1.3 s? Anyway, who is able to use this criterion in a vessel of D > 0,5 m?

However, the fact that this criterion is not dimensionless is not of great importance because of its low sensitivity.

If one would chose a dimensionless time, e.g. $t^* \equiv t\,(g/D)^{1/2}$ instead of t [T], no advantage would be gained (see **Table 4**). In this representation, for four differently sized vessels of D = 0.2–2.0 m, the left hand side indicates how the pi-number, t*, is changed for t = 1 s. In the transition from D = 0.2 → 1.0 m, t* is changed only by a factor of 2.2. The right hand side of the table shows how the 1-s-criterion should be changed in scale-up to satisfy t* = const.

**Table 4** Correspondence between 1-s criterion and the time number $t^* \equiv t\ (g/D)^{1/2}$ when D is changed by a scale factor of $\mu = 1{:}10$

| *D [m]* | *t [s]* | *t** | *t** | *t [s]* |
|---|---|---|---|---|
| 0.2 | 1 | 7.07 | 7.07 | 1.00 |
| 0.5 | 1 | 4.47 | 7.07 | 1.58 |
| 1.0 | 1 | 3.16 | 7.07 | 2.23 |
| 2.0 | 1 | 2.23 | 7.07 | 3.17 |

By the introduction of the 90 % "layer height ratio", $h^* \equiv h_s/H = 0.9$ ($h_s$ – height of the suspension layer, H – liquid height in the vessel), a convenient resort from the 1-s criterion has been found; see. [22].

## 10.3 Model Scale and the Accuracy of Measurement

In section 7.3 (Experimental Techniques for Scale-up), it has already been mentioned that the model size depends on the scale factor $\mu \equiv l_T/l_M$ and on the measuring accuracy attainable in the tests. At $\mu = 10$ a measuring accuracy of ± 10 % will possibly not suffice and one will therefore have to chose a larger model scale to reduce the scale factor $\mu$.

Measuring accuracy often depends on model scale. This is demonstrated with two examples taken from the area of stirring technology.

### 10.3.1 Determination of the Stirrer Power

Before a torsion shaft with strain gauges was employed to determine the torque on a rotating stirrer shaft, a swiveling motor had to be used and the torque measured by weighing.

In the latter case, friction loss in the motor and shaft bearings was automatically included in the measurement. In small stirrers, this was of the same order of magnitude as the power consumption of the stirrer. Therefore, at that time, rapidly rotating stirrers had to have diameters of $d > 10$ cm.

### 10.3.2 Mass Transfer in *Surface* Aeration

The determination of the overall mass transfer coefficient, $k_La$, using $O_2$ electrodes has an accuracy of ± 5 %. This suffices to determine the process characteristic in the so-called volume aeration in stirring vessels, as has been demonstrated by a comparative evaluation of measurements in vessel sizes covering liquid volumes from V = 2.5 liters to 906 $m^3$ [53].

Compared with this, so-called surface aeration brings about a comparatively modest oxygen uptake. Therefore, it is important to very accurately measure and/or to use a larger model scale. The latter is advisable because the diameters of the full-sized surface aerators amount to $d_T \geq 3$ m and, therefore, the scale factor surpasses $\mu = 10$, even if a relatively large laboratory stirrer diameter of $d_M = 0.3$ m is used.

In surface aeration, the absorption rate is also measured with $O_2$ electrodes in the liquid volume. By this method, the liquid-side overall mass transfer coefficient, $k_La$, is determined (a – volume-related mass transfer area = surface of all gas bubbles in the liquid volume). Due to the fact that the mass transfer in surface aeration occurs almost solely in the liquid surface, A, and by no means in the liquid volume, V, the measured $k_La$ has to be multiplied by V to obtain the target quantity $k_LA = k_La\ V$.

The evaluation of own measurements [54], which were performed on a laboratory scale of $d_M = 0.09$–$0.27$ m in the pi-space

$$(k_LA)^* = f(\mathrm{Fr}) \rightarrow \frac{k_LA}{d^3}\left(\frac{\nu}{g}\right)^{1/3} = f\left(\frac{n^2 d}{g}\right), \tag{10.1}$$

left open the question whether this pi-space is an applicable one or a further pi-number containing the diameter d must be added to properly accomplish the correlation, see **Fig. 24**.

If the correlation $(k_LA)^* = f(\mathrm{Fr})$ is taken as being valid, then this leads, in association with the known power characteristic of the surface aerators, to the devastating result that the efficiency E [kg $O_2$/kWh] of the surface aerators *diminishes* proportionally to the square root of the scale factor:

$$E_T = E_M\ \mu^{-1/2} \tag{10.2}$$

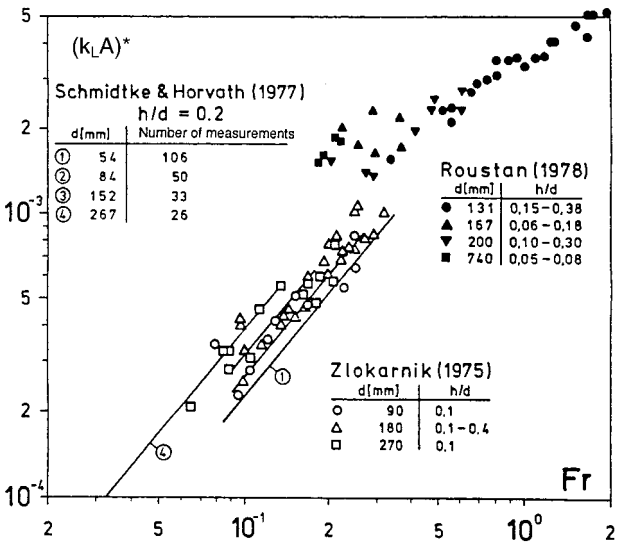


**Fig. 24** Mass transport characteristics of the turbine stirrer in surface aeration; from [54, 55]

In case of a realistic scale factor of $\mu = 10$, this means that the efficiency of the full-scale device would only be 32 % of that of model scale.

Not until the extremely accurate measurements of *Schmidtke* and *Horvat* [55] were published and, thereafter, evaluated by the author in the same pi-frame (see Fig. 24), was it possible to guarantee that the sorption characteristic is not given by $(k_L A)^* = f(\mathrm{Fr})$. Now, it turned out that an additional pi-number (the Galileo number $\mathrm{Ga} \equiv \mathrm{Re}^2/\mathrm{Fr} \equiv d^3 g/\nu^2$), containing the stirrer diameter, d, had to be introduced in order to satisfactorily complete the correlation. In plotting

$$(k_L A)^* \, \mathrm{Ga}^{-0.115} = f(\mathrm{Fr}) \tag{10.3}$$

the straight lines for different diameters coincide, whereas the correlation of the measuring points shown in Fig. 24 by different signs is not worth mentioning. This proves that their scattering is due to the inaccuracy of the measuring method.

From the accurate correlation, eq. (10.3), it follows that a completely different interrelation between the efficiency E [kg $O_2$/kWh] and the scale factor exists:

$$E_T = E_M \, \mu^{-0.155} \tag{10.4}$$

This states that at a scale factor of $\mu = 10$ the surface aerator would still have an efficiency 70% of that measured on a laboratory device.

## 10.4
## Change of Scale in Model Experiments to Locate the Correct Scale-up Rule

It has already been pointed out that experiments in differently scaled models are inevitable if physical properties cannot be changed and therefore one has to use the same material system (Example 8: Mechanical foam breaker, section 6.1). The same is true if the acceleration due to gravity is influencing the process under investigation. However, as we all know, gravity cannot be varied on Earth (Example: Surface aeration, section 10.3.2) .

There are some more dimensional-analytical problems whose clarification is indispensably dependent upon model experiments in differently sized models.

One of these will be introduced and discussed in the following section.

### 10.4.1
### Mass Transfer in *Volume* Aeration

Due to the approximate uniformity of the intensively mixed gas/liquid system and, therefore, the intensity character of the target quantity $k_L a$, the influencing process quantities (stirrer power P, air throughput q) have to be formulated in an intensive manner as well. Now, the question arises whether, in addition to the volume-related stirrer power, P/V, the gas throughput also has be formulated as a volume-related one (q/V), or if its inclusion as the so-called superficial velocity $v_G = q/S$ (as accurate

in bubble columns) is correct. A differentiation between q/V and q/S is impossible when experiments are performed on the same model scale. Here too, are model measurements in differently scaled vessels indispensable.

*Judat*'s [53] comparative evaluation of nine publications concerning mass transfer in the air/water system in vessels equipped with turbine stirrers has already been mentioned. The vessel sizes covered liquid volumes from V = 2.5 liters to 906 $m^3$ ($\mu = 1 : 71$). This evaluation unambiguously proved that the process equation is presented in the following pi-space

$$\{(k_L a)^*,\ (P/V)^*,\ v_G^*\} \quad \rightarrow \quad \left\{ k_L a \left(\frac{\nu}{g^2}\right)^{1/3},\ \frac{P/V}{\rho(\nu\, g^4)^{1/3}},\ \frac{v_G}{(\nu\, g)^{1/3}} \right\} \tag{10.5}$$

It is surely interesting to note that in volume aeration the sorption rate ($k_L a$) depends on the *volume*-related power P/V and on the *surface area*-related gas throughput $v_G = q/S$ (superficial velocity).

## 10.5
## Complete Recording of the Pi-set by Experiments

In this section the following question has to be clearly answered:

"Under which circumstances does a pi-relationship hold true if certain x-quantities are not varied in the respective experiments?"

This important question has been answered by *Pawlowski* [56] as follows:

- A pi-relationship is *not* secured if a pi-number can be produced out of parameters, which were not altered in the experiments, so that this pi-number remained unaltered.

This is illustrated by two examples:

a) The pertinent relevance list for the heat transfer at the wall of a stirring vessel reads:

$\{h; d; \rho, \nu, C_p, k; n\}$

and the corresponding pi-set follows to:

$\{Nu, Re, Pr\} \quad Nu \equiv h\, d/k\ ,\ Re \equiv n\, d^2/\nu\ ,\ Pr \equiv \rho C_p\, \nu/k$

Under which test conditions is this pi-relationship secured?

| *not varied x-parameters* | *varied x-parameters* | *pi-numbers remaining constant* | *result* |
|---|---|---|---|
| physical properties | d, n | Pr | negative |
| d, n | physical properties | no | positive |

b) Stirring power in a unbaffled vessel:

{P; d; ρ, ν; n, g}

and the corresponding pi-set:

{Ne, Re, Fr} $\quad Ne \equiv P/(\rho\, n^3\, d^5)$ , $Re \equiv n\, d^2/\nu$ , $Ga \equiv g\, d^3/\nu^2$

Under which test conditions is this pi-relationship secured?

| *not varied x-parameters* | *varied x-parameters* | *pi-numbers remaining constant* | *result* |
|---|---|---|---|
| d, g, ρ, ν | n | Ga | negative |
| d, n, g | physical properties | Fr | negative |
| d, g | physical properties, n | no | positive |
| g, physical properties | n, d | no | positive |

## 10.6 Correct Procedure in the Application of the Dimensional Analysis

In this section, a summary will be provided about how dimensional analysis can be properly utilized in order to obtain, with a minimum of time and expenditure, the results necessary for the determination of both the pi-relationship (process characteristic) of the process in question and a valid scale-up rule. In this context, nothing new will be imparted. All of this information has already been disclosed in previous chapters.

### 10.6.1 Preparation of the Model Experiments

Compiling the relevance list
Dimensional analysis should be carried out *before* the experiments are executed. The relevance list should be compiled as completely as possible and, on its foundation, the pi-set can then be determined. Depending on the circumstances, some orientating preliminary experiments will be necessary in order to verify or falsify the relevance of the one or other x-quantity.
Decision about the size of the model apparatus
The model scale depends on the size of the full-scale device and on the achievable measuring accuracy. Low measuring accuracy or a target quantity displaying a low sensitivity can be possibly counteracted by increasing the scale factor μ, in other words, the model scale should be as large as possible.

### 10.6.2
### Execution of the Model Experiments

It has already been pointed out that in model experiments the pi-number and not the x-quantity should be varied. This results in various advantages. On the one hand, the pi-number is varied by changing the most available, the most manageable or the cheapest x-quantity constituting it (example: changing the Reynolds number by varying the kinematic viscosity of the fluid). In addition, the evaluation of the test results is made easier, because in varying a certain pair of pi-numbers, the numerical values of all the other pi-numbers remain constant ($\Pi_i$ = idem).

### 10.6.3
### Evaluation of Test Experiments

The evaluation of the test experiments will be shown using an example (Example 34 "Gas hold-up in bubble columns"). It must be noted that this purposeful approach is often not complied with. It is simply false to plot a pi-number Y as a function of a pi-number X and to note that, in doing so, the one or the other dimensional quantity remained constant. In the representation Y(X) all remaining pi-numbers have to be constant ($\Pi_i$ = const)!

The author is aware of the fact that numerical data recording and processing enjoys great popularity these days. Numerical and graphical data processing can go well, but sometimes it's bound to go wrong.

A serious disadvantage of automated data processing is the fact that the researcher is deprived of those hours of leisure, in which he or she plotts results in silence and seclusion on the double-log scale and this opportunity is used to think over whether or not the data evaluated in this way make sense or if they should rather be represented in another fashion. No graphical representation of test data is in the first instance more suitable than that on the double-log scale. This approach shows better and quicker whether it is suitable for the description, or if a simple-log scale would possibly fit better. Furthermore, curves on the double-log scale can easily be converted into straight lines ($Y = aX^{\alpha} \pm b$) or in simple analytical expressions of the form ($Y = aX^{\alpha} \pm bX^{\beta}$). Of course, a statistical balancing of the coefficients and exponents can be left to the computer afterwards.

*Scale-up in Chemical Engineering.* Marko Zlokarnik


ISBNs: 3-527-30266-2 (Hardback); 3-527-60056-6 (Electronic)

# 11
# Optimization of Process Conditions by Combining Process Characteristics

In this chapter, three examples are introduced to exemplify the possibility of optimizing a process with respect to the desirable objective by the appropriate combination of process characteristics.

**Example 21**: Determination of stirring conditions in order to carry out a homogenization process with minimum mixing work

In order to design and dimension stirrers for the homogenization of liquid mixtures – and this is by far the most common task when it comes to stirring! – it is vital to know the *power characteristic* and the *mixing time characteristic* of the type of stirrer in question. If this information is available for various types of stirrers, it is possible to determine both the best type of stirrer for the given mixing task and the *optimum operating conditions* for this particular type.

a) *Power characteristic* of a stirrer
The power consumption, P, of a given type of stirrer under the given installation conditions depends on the following variables:

| | |
|---|---|
| geometric parameters: | stirrer diameter, d |
| physical properties: | density, $\rho$, and kinematic viscosity, $\nu$, of the liquid |
| process parameters: | stirrer speed, n. |

The relevance list therefore reads as follows:

$$\{P; d; \rho, \nu; n\} \tag{11.1}$$

The (appropriately assembled) dimensional matrix undergoes only one linear transformation to produce the two pi-numbers (Ne – Newton number; Re – Reynolds number):

| | ρ | ***d*** | ***n*** | ***P*** | ν |
|---|---|---|---|---|---|
| M | 1 | 0 | 0 | 1 | 0 |
| L | –3 | 1 | 0 | 2 | 2 |
| T | 0 | 0 | –1 | –3 | –1 |
| M | **1** | 0 | 0 | 1 | 0 |
| L + 3 M | 0 | **1** | 0 | 5 | 2 |
| –T | 0 | 0 | **1** | 3 | 1 |

$$\Pi_1 \equiv \frac{P}{\rho\, d^5\, n^3} \equiv Ne \quad \text{und} \quad \Pi_2 \equiv \frac{\nu}{d^2\, n} \equiv Re^{-1} \tag{11.2}$$

The experimentally determined *power characteristic*, Ne(Re), of a blade stirrer of a given geometry under the given installation conditions (see sketch in Fig. 27) is presented in **Fig. 25.**

From this representation a number of important points can be deduced:

1 $Re < 20$: $Ne \propto Re^{-1}$ and $NeRe \equiv P/(\mu\, n^2\, d^3) = \text{const}$, respectively, is valid. Density is irrelevant here – we are dealing with the *creeping flow* region.

2 $Re > 50$ (vessel with baffles) or $Re > 5 \times 10^4$ (unbaffled vessel): $Ne \equiv P/(\rho\, n^3\, d^5) = \text{const}$ is valid. In this case, viscosity is irrelevant, we are dealing with a *turbulent* flow region.

3 The influence of the baffles is, understandably, nil in the laminar flow region. However, it is extremely strong at $Re > 5 \times 10^4$. The installation of baffles under otherwise unchanged operating conditions increases the stirrer power by a factor of 20 here!

4 When stirred in an unbaffled vessel, fluid begins to circulate and a vortex is formed. The question whether gravitational acceleration, g, and hence the Froude number, $Fr \equiv n^2\, d/g$, plays a role under these circumstances can be

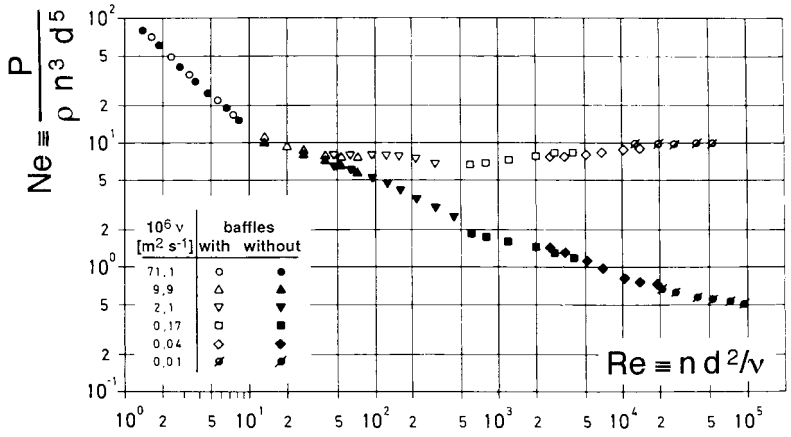


**Fig. 25** Power characteristic of a blade stirrer of a given geometry under the given installation conditions; from [57]

safely answered as being negative on the basis of the test results shown in Fig. 25: For confirmation, one only needs to look at the points on the lower Ne(Re) curve where the *same* Re value was set for fluids with *different* viscosities. This was only possible by a proportional alteration of the rotational speed of the stirrer. Where Re = idem, Fr was clearly not idem, but this has no influence on Ne: g is therefore irrelevant!

b) *Mixing time characteristic* of a stirrer
For our purposes, the mixing time, $\theta$, is the time required to mix two fluids of similar density and viscosity until they are molecularly homogeneous. (See [22] for practical determination of this quantity). In this case, the relevance list is as follows:

$$\{\theta; d; \rho, \nu, D; n\}$$

where $D[L^2\,T^{-1}]$ is the diffusivity of one fluid into the other.

Dimensional analysis of this example is associated by a reduction of the rank of the matrix, because the base dimension of mass is only contained in the density, $\rho$. From this it does not follow that the density wouldn't be relevant here, but that it is already fully considered in the kinematic viscosity $\nu$, which is defined by $\nu = \mu/\rho$. Therefore

$$\{n\theta;\ Re \equiv nd^2/\nu;\ Sc \equiv \nu/D\} \quad \text{resp.} \quad n\theta = f(Re, Sc) \tag{11.4}$$

represents the appropriate pi-space here. The corresponding pi-relationship, the *mixing time characteristic* of the blade stirrer for the geometric conditions given in Fig. 27, is shown in **Fig. 26**.

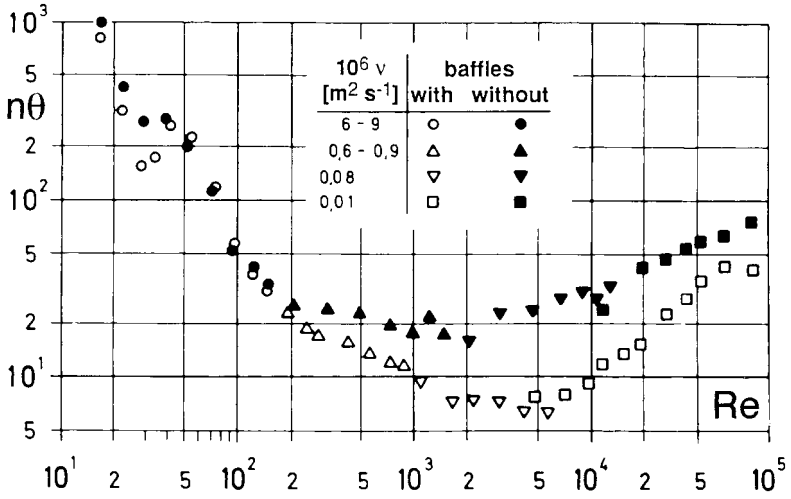


**Fig. 26** Mixing time characteristic of a blade stirrer
For installation conditions see Fig. 27; from [57].

The measured values demonstrate, in analogy to point 4 where power characteristic was discussed, that *D*, and consequently the Schmidt number, are not as relevant as assumed. (In the same system of materials - a mixture of water and cane syrup – at almost the same *D* value, the Schmidt number is varied by the kinematic viscosity, ν, over many orders of magnitude.)

c) *Optimum conditions* for the homogenization of liquid mixtures
If the power and mixing time characteristics are known for a series of common stirrer types under favorable installation conditions, see [57], one can go on to consider the optimum operating conditions by asking the question: Which type of stirrer operates within the desired mixing time θ with the lowest power consumption and hence the minimum mixing work (Pθ = min) in a given system of materials and a given vessel (vessel diameter D)?

In answering this question, we need not (at least for the moment) consider the diameter of the stirrer or its speed; the relevance list is as follows:

$$\{P, \theta; D; \nu, \rho\} \tag{11.5}$$

When the dimensional matrix has been assembled it becomes:

$$\Pi_1 \equiv \frac{P\,D}{\rho\,\nu^3} = \frac{P\,D\,\rho^2}{\mu^3} \quad \text{und} \quad \Pi_2 \equiv \frac{\theta\,\nu}{D^2} = \frac{\theta\,\mu}{D^2\rho} \tag{11.6}$$

| | ρ | ***D*** | ν | ***P*** | θ |
|---|---|---|---|---|---|
| M | 1 | 0 | 0 | 1 | 0 |
| L | –3 | 1 | 2 | 2 | 0 |
| T | 0 | 0 | –1 | –3 | 1 |
| M | **1** | 0 | 0 | 1 | 0 |
| L + 3 M + 2 T | 0 | **1** | 0 | –1 | 2 |
| –T | 0 | 0 | **1** | 3 | –1 |

These two pi-numbers can be formed from the known numerical values of Ne, nθ and Re with the help of D/d. The following interrelations exist:

$$\Pi_1 \equiv \mathrm{Ne}\,\mathrm{Re}^3\,\mathrm{D/d} \quad \text{and} \quad \Pi_2 \equiv \mathrm{n}\theta\,\mathrm{Re}^{-1}\,(\mathrm{D/d})^{-2} \tag{11.7}$$

**Fig. 27** shows this relationship for those stirrer types exhibiting the lowest $\Pi_1$ values within a specific range of the dimensionless number $\Pi_2$, i.e. the stirrers requiring the least power in this range.

This graph is extremely easy to use. The physical properties of the material system, the diameter of the vessel (D) and the desired mixing time (θ) are all known and this is enough to generate the dimensionless number $\Pi_2$. The curve $\Pi_1 = f(\Pi_2)$ in Fig. 27 then provides the following information:

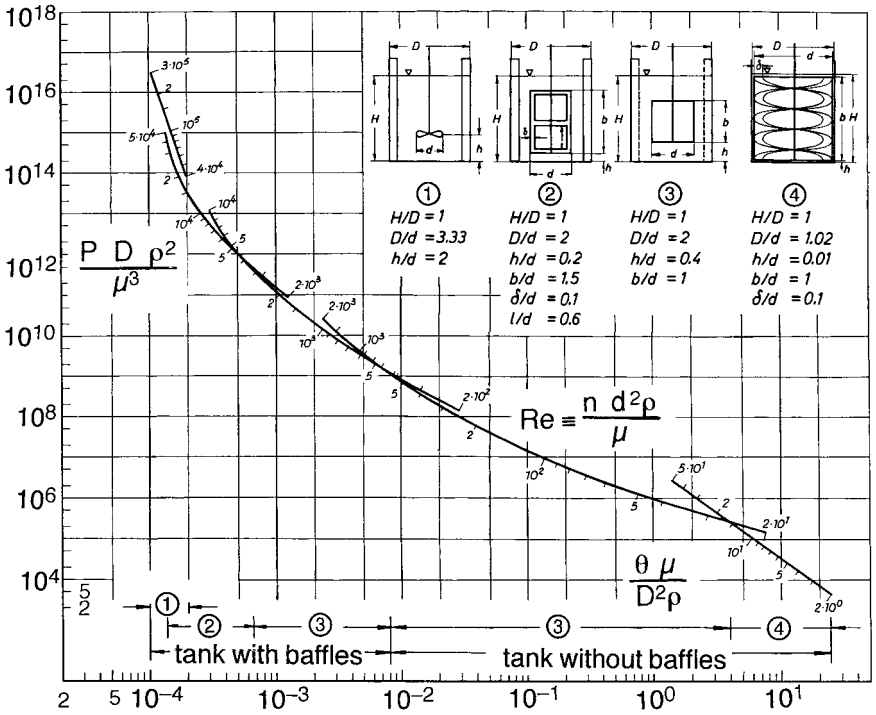


**Fig. 27** Working sheet for the determination of optimum working conditions for the homogenization of liquid mixtures in mixing vessels; from [57].

1 The *stirrer type* and baffling conditions can be read off the abscissa. The diameter of the stirrer can be determined from data on stirrer geometry in the sketch.
2 The numerical value of $\Pi_1$ can be read off at the intersection of the $\Pi_2$ value with the curve. The *power consumption*, P, can then be calculated from this.
3 The numerical value of Re can be read off the Re scale at the same intersection. This, in turn, makes it possible to determine the *stirrer speed*.

**Example 22**: Process characteristics of a self-aspirating hollow stirrer and the determination of its optimum process conditions

As a result of their form, hollow stirrers utilize the suction generated behind their edges (*Bernoulli* effect) to suck in gas from the head space above the liquid. As "rotating ejectors", they are stirrers and gas pumps in one and are therefore particularly suitable for laboratory use (especially in high pressure autoclaves) because they achieve intensive gas/liquid contacting via internal gas recycling without a separate gas pump [58/1]. A particularly effective type of this stirrer – the pipe stirrer – is depicted in **Fig. 28**.

In operating a hollow stirrer, both target quantities – gas throughput q and the stirrer power P – adapt themselves simultaneously. Both target quantities depend on the following parameters:

| | | |
|---|---|---|
| Geometry: | Stirrer diameter | d |
| Physical properties: | density | ρ |
| | viscosity | μ |
| Process parameters: | stirrer speed | n |
| | gravitational constant | g |

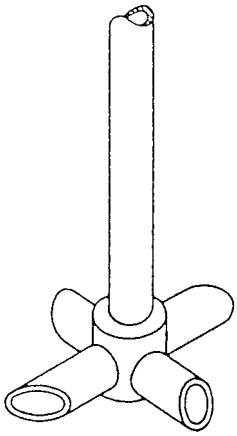

**Fig. 28** Sketch of the pipe stirrer

Thus we obtain two separate relevance lists:

$$\{q; d, \rho, \mu ; n, g\} \qquad (11.8)$$

$$\{P; d, \rho, \mu ; n, g\} \qquad (11.9)$$

| | ρ | ***d*** | ***n*** | ***q*** | μ | ***g*** |
|---|---|---|---|---|---|---|
| M | 1 | 0 | 0 | 0 | 1 | 0 |
| L | –3 | 1 | 0 | 3 | –1 | 1 |
| T | 0 | 0 | –1 | –1 | –1 | –2 |
| M | **1** | 0 | 0 | 0 | 1 | 0 |
| 3M + L | 0 | **1** | 0 | 3 | 2 | 1 |
| –T | 0 | 0 | **1** | 1 | 1 | 22 |

The first relevance list (11.8) leads to the following three pi-numbers:

$$\Pi_1 \equiv \frac{q}{n\,d^3} \equiv Q \quad \Pi_2 \equiv \frac{\mu}{\rho\,d^2 n} \equiv Re^{-1} \quad \Pi_3 \equiv \frac{g}{d\,n^2} \equiv Fr^{-1} \qquad (11.10)$$

$\Pi_1$ is named the gas throughput number Q, $\Pi_2$ is the inverse Reynolds number and Π3 is the inverse Froude number. The gas throughput characteristics of a hollow stirrer then reads:

$$\frac{q}{n\,d^3} = f_1\left(\frac{n\,d^2\rho}{\mu}, \frac{n^2 d}{g}\right) \rightarrow \quad Q = f_1(Re, Fr) \qquad (11.11)$$

The power characteristics – obtained from the relevance list (11.9) by a similar dimensional matrix – containing P instead of q – leads to:

$$\frac{P}{\rho\,n^3 d^5} = f_2\left(\frac{n\,d^2\rho}{\mu}, \frac{n^2 d}{g}\right) \rightarrow \quad Ne = f_2(Re, Fr) \qquad (11.12)$$

The pi-number containing P is termed the Newton number.
Model experiments with another type of hollow stirrer (3-edged stirrer, see sketch in Fig. 30) were performed in water/air under defined experimental conditions and the scale factor $\mu = d_T/d_M$ was changed in the range of μ = 1 : 2 : 3 : 4 : 5. The results

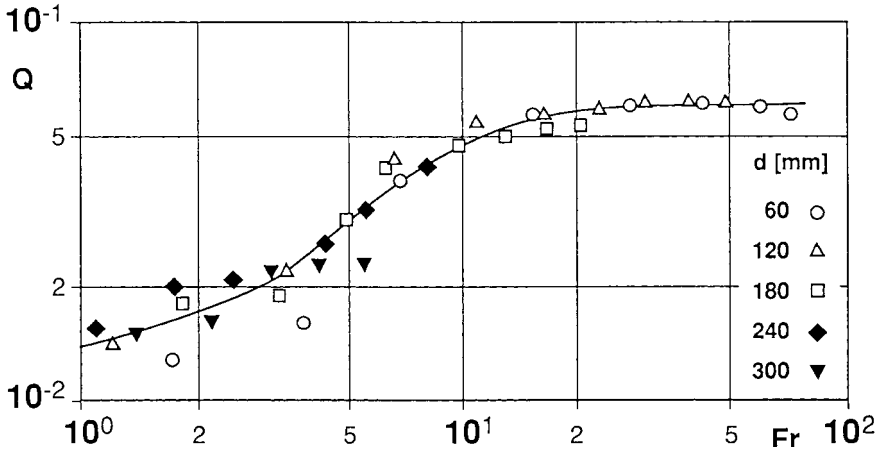


**Fig. 29** Gas throughput characteristic of a 3-edged stirrer; from [58/1].

demonstrate that the Reynolds number is irrelevant in the turbulent flow range ($Re > 10^4$) and the process is exclusively governed by the Froude number. Both process characteristics can therefore be represented as

$$Q = f_1 (Fr) \text{ and } Ne = f_2 (Fr)$$

see **Fig. 29** and **30**.

These results impressively demonstrate to which extent information can be compressed by dimensional analysis. – These process characteristics present a reliable basis for the scale-up of this hollow stirrer under the given geometric conditions. But they also allow a further optimization of this process as will be demonstrated by

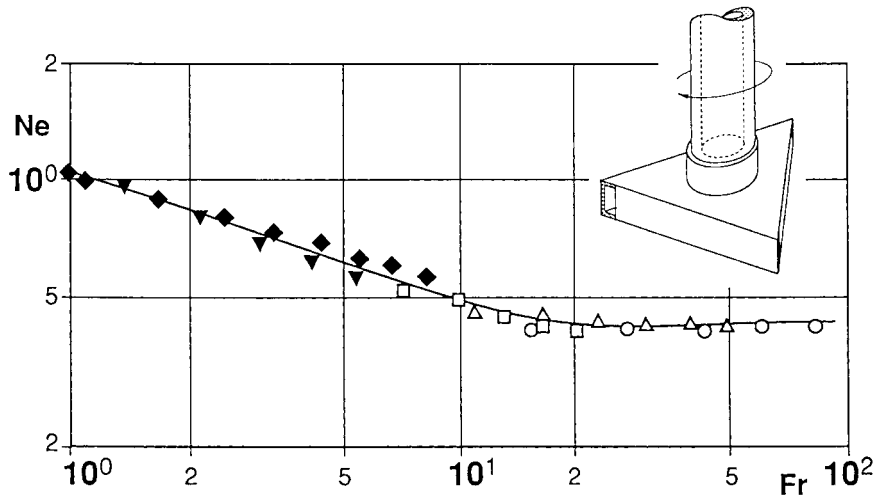


**Fig. 30** Power characteristic of a 3-edged stirrer. For the legend see Fig. 29; from [58/1].

the following additional treatment. A question must be answered with respect to the process conditions under which this stirrer will achieve a given gas throughput with the minimum power, P/q = min! This answer can be easily found by combining the above characteristics in Fig. 29 and 30 in such a way that a dimensionless expression for P/q is produced. This is the pi-number combination

$$\frac{\mathrm{Ne\ Fr}}{\mathrm{Q}} \equiv \frac{\mathbf{P}}{\mathbf{q}\,\mathrm{d}\,\rho g} = f_3(\mathrm{Fr}) \tag{11.13}$$

This new pi-number is, as are its constituents, also a function of the Froude number. This dependency is represented by **Fig. 31**. It can be seen that two sections exist:

$$\mathrm{Fr} \leq 10 : \mathrm{Ne\ Fr/Q} = \mathrm{const} \rightarrow \mathrm{P/q} \propto \mathrm{d}.$$

Here, P/q increases in direct proportion to scale (d).

$$\mathrm{Fr} \leq 10 : \mathrm{Ne\ Fr/Q} \propto \mathrm{Fr} \rightarrow \mathrm{P/q} \propto \mathrm{d}^2.$$

In this range, the hollow stirrer is still less effective, because the power per unit gas throughput increases with the square of the scale ($d^2$).

Under these circumstances, which can be described by "small is beautiful", it can be clearly shown that hollow stirrers are not suitable for sucking in large amounts of gas on a full-scale. In this case, it is advisable to decouple gas throughput and the power consumption by using a high speed stirrer (e.g. turbine stirrer) and supply it with gas from underneath it via a blower.

In transport limited reactions in gas/liquid systems, mass transfer is usually dimensioned according to P/V = idem and v = q/S = idem, see section 10.4.1. In scaling up, these conditions also speak in favor of decoupling the gas supply and

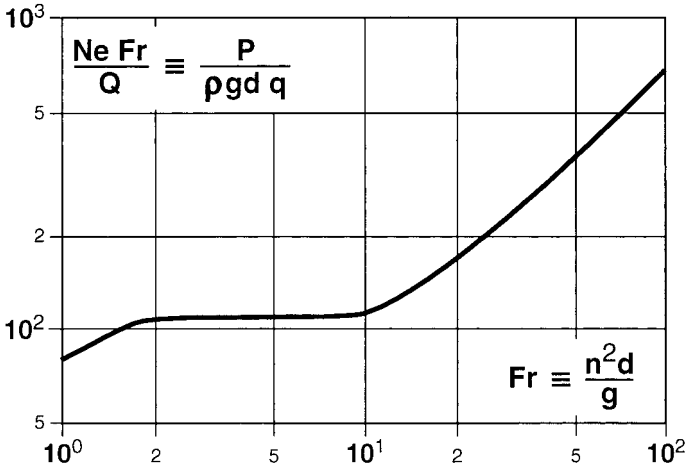


**Fig. 31** Dimensionless interdependence of P/q and d under different process conditions (Fr)

stirrer speed, because processes with two mutually independent process parameters can be more easily optimized than those having only one process parameter.

However, there are many chemical reactions in the G/L system in which the gas throughput plays no role because micro-kinetics is rate determining. In such cases, the hollow stirrers, due to their dual role as stirrers and gas conveyers, play a prime role, particularly in high pressure chemical engineering.

**Example 23**: Optimization of stirrers for a maximum removal of reaction heat

In the optimization of stirrers for an optimal heat transfer, it may not be forgotten that the removable heat flow, Q [kW], increases according to the heat transfer characteristic with $Re^{2/3} \propto n^{2/3}$, whereas the thereby associated stirrer power (stirring heat) increases substantially overproportionally according to the power characteristic of the stirrer with P [kW] $\propto n^3$. From this it follows that there is an optimum stirrer speed at which a maximum of process heat, e.g. chemical reaction heat, R, can be removed:

$$R \equiv Q - P \tag{11.14}$$

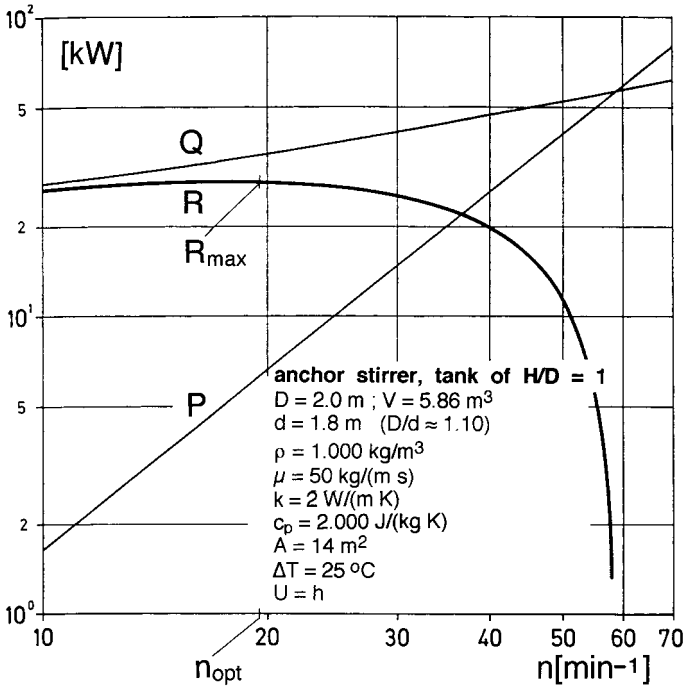


**Fig. 32** Graphical representation of the courses of R ≡ Q – P as a function of the stirrer speed for the example given in the plot; from [59]

**Figure 32** illustrates this situation with a concrete example. It shows that the optimum range with respect to the stirrer speed is very flat, 90% of the maximum value being removed in the range $n_{opt} = 20\ min^{-1} \pm 60\ \%$.

In the prediction of optimal conditions ($n_{opt}$, $R_{max}$), *Pawlowski* and *Zlokarnik* [59] applied the following procedure:

With $Q = h\ A\ \Delta T$ (in the laminar flow range the overall heat transfer coefficient $U \approx h$), the following expression follows from the relationship $R \equiv Q - P$

$$R/V = h\ A\ \Delta T/V - P/V \tag{11.15}$$

Formulation of this expression in terms of dimensional analysis yields:

$$\Pi_2 = Nu - (D/d)\ \Pi_1^{-1}\ Re^3\ Ne \tag{11.16}$$

where $\Pi_1$ and $\Pi_2$ stand for

$$\Pi_1 \equiv \frac{D^2 \rho^2 k\ \Delta T}{\mu^3} \frac{A}{D\,H} \quad \text{and} \quad \Pi_2 \equiv \frac{(R/V)D^2}{k \Delta T} \frac{V}{A\,D} \tag{11.17}$$

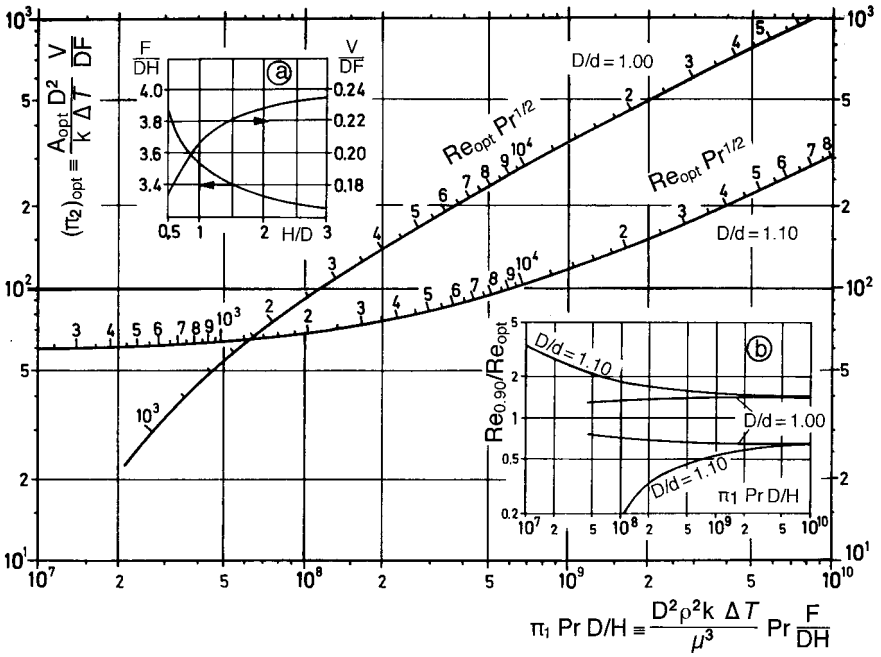


**Fig. 33** Work-sheet for determining optimal operating conditions for heat removal in a vessel with an anchor stirrer with two different wall clearances (D/d ≈ 1.00 – without wiper blades – and D/d = 1.10) in the laminar flow range (Re < 100); from [59]

If the known functions Nu = Nu (Re, Pr) and Ne = Ne (Re) are incorporated into the relationship (11.16), conditions are obtained for the sought optimum by differentiating this expression with respect to Re and setting its differential to zero.

The determination of these conditions for the optimum is made easier by the work-sheet in **Fig. 33**. It applies for two anchor stirrers with different wall clearances [D/d = 1.00 (no wiper blades!) and D/d = 1.10] in the laminar flow range (Re < 100).

The geometric parameters A/DH and V/DA for tanks with dished bottoms, which are necessary for utilizing the work-sheet, can be taken from the auxiliary diagram in inset (a) of Fig. 33 as functions of the aspect ratio H/D. Since the optimal stirrer speed determined can, in practice, only seldomly be realized, the Re and thereby the rotation speed range is given in the auxiliary diagram in inset (b) of Fig. 33. Within this range 90% of $(R/V)_{opt}$ (according to expression (11.15)) are attained.

Application example for Fig. 33:

The conditions used were those from which Fig. 32 is based. With $Pr = 5 \times 10^4$ and the abscissa value $\Pi_1\ Pr\ (H/D)^{-1} = 2.82 \times 10^8$, the optimum conditions $Re_{opt}\ Pr^{1/2} = 4.8 \times 10^3$ and the ordinate value $(\Pi_2)_{opt} = 8 \times 10^1$ follow from the work-sheet, producing $n_{opt} \approx 20\ min^{-1}$ and $R_{max} = (R/V)_{opt}\ V = 28.5$ kW (see the optimum operating point in Fig. 32). At this stirrer speed the stirrer power amounts to ca. 6 kW, which is ca. 20% with respect to the maximum removal of reaction heat. From the auxiliary diagram in inset (b), it can be inferred that the rotation speed interval, in which at least 90% of the maximum achievable value ($R_{90\%}$ = 25.6 kW) could be removed, lies between 8 and 32 $min^{-1}$.

If more than the determined amount $R_{max}$ has to be removed, an anchor stirrer with D/d = 1.1 can be replaced with one with D/d ≈ 1.0 (no wiper blades). Consequently, at a slightly lower optimum stirrer speed (n = 17 $min^{-1}$), the removal of $R_{max} \approx 60$ kW is possible.

Another option for raising $R_{max}$, this being a simpler option from a technical point of view, involves choosing a tank with a higher aspect ratio. For H/D = 2 and the same volume (V = 5.86 $m^3$) as above, a tank diameter D = 1.57 m is obtained. (For the given values of V and H/D the sought D is found with the assistance of the auxiliary diagram (a), if the H/D associated product $(A/DH)(V/DA)(H/D) \equiv V/D^3$ is generated. Therefore, in this case, $V/D^3 = 1.52$. With the new abscissa value $\Pi_1\ Pr\ (H/D)^{-1} = 1.7 \times 10^8$, it follows that the quantity $R_{max} \approx 39$ kW at $n_{opt} = 19.7\ min^{-1}$. For H/D = 3 (D = 1.37 m, d = 1.25 m), $R_{max} = 45.5$ kW at $n_{opt} = 20.6\ min^{-1}$ can be removed. In our example, $R_{max}$ increases with $(H/D)^{1/2}$. The calculated $R_{max}$ value of 60 kW for an anchor stirrer with D/d ≈ 1.00 is first achieved for H/D = 6.

In the range Re > 200 (turbulent range with respect to heat transfer), heat flux merely increases according to $R_{max} \propto (H/D)^{1/3}$. An effective increase of $R_{max}$ is only possible here by increasing $\Delta T$ or by using stirrers with wiper blades [22].

*Scale-up in Chemical Engineering.* Marko Zlokarnik


ISBNs: 3-527-30266-2 (Hardback); 3-527-60056-6 (Electronic)

# 12
# Selected Examples of the Dimensional-analytical Treatment of Processes in the Field of Mechanical Unit Operations

**Introductory remark**

Fluid mechanics and mixing operations in various types of equipment, agglomeration as well as disintegration and mechanical separation processes, just to mention a few, are described by parameters, the dimensions of which only consist of *three* base dimensions: Mass, Length and Time. An isothermal process is assumed: The physical properties of the material system under consideration are related to a *constant* process temperature. The process relationships obtained in this way are therefore valid for *any* constant, random process temperature to which the numerical values of the physical properties are related. This holds true as long as there is no departure from the scope of the validity of the respective process characteristic verified by the tests.

The scale-up can only present problems when model substances are not available. (Prime example: Drag resistance of a ship's hull and *Froude's* approach of this problem, Example 9).

**Example 24**: Power consumption in a gassed liquid. Design data for stirrers and model experiments for scaling up

Gas/liquid contacting is frequently encountered in chemical reaction and bioprocess engineering. For reactions in gas/liquid systems (oxidation, hydrogenation, chlorination, and so on) and aerobic fermentation processes (including biological waste water treatment), the gaseous reaction partner must first be dissolved in the liquid. In order to increase its absorption rate, the gas must be dispersed into fine bubbles in the liquid. A fast rotating stirrer (e.g. a turbine stirrer), to which the gas is supplied from below, is normally used for this purpose (see the sketch in Fig. 34).

For a given geometry of the set-up, the relevance list for this problem contains the power consumption, P, as the target quantity, the stirrer diameter, d, as the characteristic length and a number of physical properties of the liquid and the gas (the latter are marked with an apostrophe): Densities, $\rho$ and $\rho'$, kinematic viscosities, $\nu$ and $\nu'$, surface tension, $\sigma$, and an unknown number of still unknown physical properties, $S_i$, which describe the coalescence behaviour of finely dispersed gas bubbles and by this, indirectly, their hold-up in the liquid. The process parameters are the stirrer speed, n, and the gas throughput, q, which can be adjusted independently, as

well as the gravitational acceleration, g, which is implicitly relevant because of the large density difference. (We should actually have written $g\Delta\rho$ here – see Section 5.1 – but, since $\Delta\rho = \rho - \rho' \approx \rho$, the dimensionless number would contain $g\Delta\rho/\rho \approx g\rho/\rho = g$.) The relevance list is therefore:

$$\{P; d; \rho, \nu, \sigma, S_i, \rho', \nu'; n, q, g\} \tag{12.1}$$

In this case, the relevance list contains at least eleven variables – more than twice the number required for the power consumption in the homogeneous liquid system (Example 21, eq. (11.1)).

Before employing the dimensional analysis for generation of the dimensionless numbers, it is worthwhile anticipating obvious numbers such as $\rho'/\rho$ and $\nu'/\nu$. $S_i$ are physical properties of unknown dimension and number. Therefore they cannot be included in the dimensional matrix. However, this is no problem since, with the known relevant physical properties $\rho$, $\nu$ and $\sigma$, one will always be able to transform $S_i$ to the dimensionless numbers $S_i^*$. The above relevance list can therefore be reduced to

$$\{P; d; \rho, \nu, \sigma; n, q, g\} \quad \text{for anticipated} \quad \rho'/\rho, \nu'/\nu, S_i^* \tag{12.2}$$

Here, the simplest dimensional matrix is also the best one because it leads directly to the common, named dimensionless numbers.

| | $\rho$ | ***d*** | ***n*** | ***P*** | $\nu$ | $\sigma$ | ***q*** | ***g*** |
|---|---|---|---|---|---|---|---|---|
| M | 1 | 0 | 0 | 1 | 0 | 1 | 0 | 0 |
| L | –3 | 1 | 0 | 2 | 2 | 0 | 3 | 1 |
| T | 0 | 0 | –1 | –3 | –1 | –2 | –1 | –2 |
| M | **1** | 0 | 0 | 1 | 0 | 1 | 0 | 0 |
| L + 3M | 0 | **1** | 0 | 5 | 2 | 3 | 3 | 1 |
| –T | 0 | 0 | **1** | 3 | 1 | 2 | 1 | 2 |

$$\Pi_1 \equiv P/(\rho\, d^5\, n^3) \equiv Ne \quad \text{(Ne – Newton number)}$$

$$\Pi_2 \equiv \nu/(d^2\, n) \equiv Re^{-1} \quad \text{(Re – Reynolds number)}$$

$$\Pi_3 \equiv \sigma/(\rho\, d^3\, n^2) \equiv We^{-1} \quad \text{(We – Weber number)}$$

$$\Pi_4 \equiv q/(d^3\, n) \equiv Q \quad \text{(Q – throughput number)}$$

$$\Pi_5 \equiv g/(d\, n^2) \equiv Fr^{-1} \quad \text{(Fr – Froude number)}$$

Taking the anticipated numbers into account, it follows that:

$$Ne = f(Re, We, Q, Fr, \rho'/\rho, \nu'/\nu, S_i^*) \tag{12.3}$$

However, we can now see that the important process parameter, the stirrer speed, n, is present in *all* numbers: Their numerical value is changed with each change in speed. This is not advantageous for the planning and evaluation of experiments. Our aim is therefore to transform Re and We, which contain the physical properties ν and σ, to dimensionless material numbers through combination with other numbers.

Firstly, we form two combinations of the dimensionless numbers which do not contain n:

$$\mathrm{Re}^2/\mathrm{Fr} \equiv \frac{g\, d^3}{\nu^2} \equiv \mathrm{Ga}\ (\text{Galilei number}) \tag{12.4}$$

$$\mathrm{We}/\mathrm{Fr} \equiv \frac{\rho\, d^2 g}{\sigma} \tag{12.5}$$

Then we combine these two new numbers in such a way as to eliminate d:

$$\{(\mathrm{Re}^2/\mathrm{Fr})^{2/3}\ (\mathrm{Fr}/\mathrm{We})\} \equiv (\mathrm{Re}^4\ \mathrm{Fr})^{1/3}\ \mathrm{We}^{-1} \equiv \frac{\sigma}{(\rho^3 \nu^4 g)^{1/3}} \equiv \sigma^* \tag{12.6}$$

By this means it is possible to transform the We number into a pure material number, $\sigma^*$, the numerical value of which is dependent only on the material system. In contrast, the only advantage of the Ga number over Re is that it does not contain the stirrer speed. Let us stay with Re and base our considerations on the following pi-space:

$$\mathrm{Ne} = f\,(\mathrm{Q}, \mathrm{Fr}, \mathrm{Re}; \sigma^*, \rho'/\rho, \nu'/\nu, \mathrm{S_i^*}) \tag{12.7}$$

In this case, the pi-space consists of a target number (Ne), three process numbers (Q, Fr, Re) and a series of pure material numbers ($\sigma^*$, $\rho'/\rho$, $\nu'/\nu$, $\mathrm{S_i^*}$).

The first question, we must ask, is: Are laboratory tests performed in *one single piece* of laboratory equipment – i.e. on one single scale – capable of providing reliable information on the decisive process number (or combination of numbers)? Although we can change Fr by means of the stirrer speed, Q by means of the gas throughput and Re (or Ga) by means of the liquid viscosity independent of each other, we must accept the fact that a change in viscosity will alter not only Re but also the numerical values of the material numbers, $\sigma^*$, $\nu'/\nu$, and, very probably, $\mathrm{S_i^*}$.

In contrast to the gas density, $\rho'$ (hydrogen is by a factor of 16 lighter than air, its bubbles therefore have a stronger buoyancy and will escape the liquid quicker!), an influence of the gas viscosity, $\nu'$, on the stirrer power is not to be expected ($\nu'/\nu$ = irrelevant). Preliminary tests with methanol/water mixtures showed [60] that σ does not influence the stirrer power either, therefore $\sigma^*$ is irrelevant. Furthermore, measurements revealed that the coalescence behaviour of the material system is not affected if aqueous glycerol or cane syrup mixtures are used to increase viscosity. This means that the influence of $\mathrm{S_i^*}$ on Ne cannot be significant. These results alone give us the right to perform model experiments in *one single piece* of apparatus in order to elaborate the process relationship. The following pi-space is then used as the basis

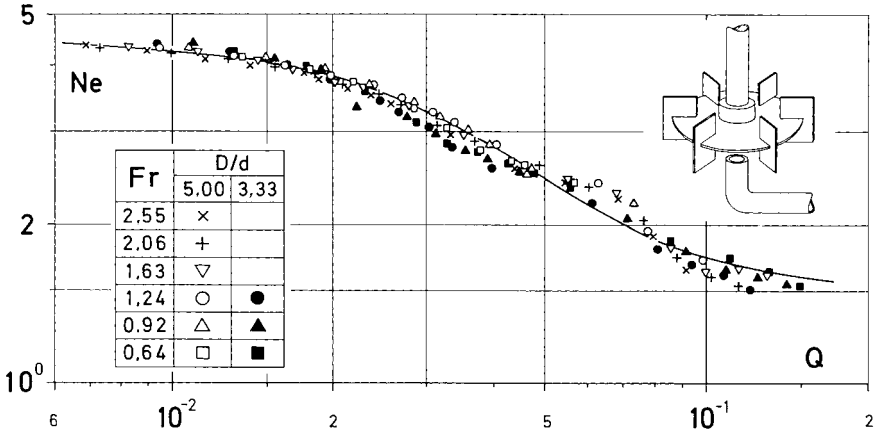


**Fig. 34** Power characteristic of a turbine stirrer under industrially interesting flow conditions ($Re \geq 10^4$; $Fr \geq 0.65$; $\rho'/\rho = 1.20 \times 10^{-3}$ ); from [60]

$$Ne = f(Q, Fr, Re) \tag{12.8}$$

and only *one* gas (air) is used, $\rho'/\rho = 1.20 \times 10^{-3} = \text{const.}$

The results of these model experiments are described in detail in [60]. For our consideration based on the theory of similarity, it is sufficient to present only the main result here. This states that, in the industrially interesting range ($Re \geq 10^4$ und $Fr \geq 0.65$), Ne is only dependent on Q; see **Fig. 34**.

Knowledge of this power characteristic, the analytical expression for which is

$$Ne = 1.5 + (0.5\, Q^{0.075} + 1600\, Q^{2.6})^{-1} \quad Re \geq 10^4;\ Fr \geq 0.65;\ \rho'/\rho = 1.20 \times 10^{-3} \tag{12.9}$$

can be used to reliably design a stirrer drive for conducting reactions in the gas/liquid system (e.g. oxidation with $O_2$ or air, fermentation etc.) as long as the physical, geometric and process-related (Re and Fr range) boundary conditions comply with those of the model measurement.

At this point we should ask ourselves how we would perform the scale-up if we did not know anything about the above functional relationship! Let us therefore try to determine the stirrer power of a given stirrer for a specified, large fermenter (e.g., $V = 100\ m^3$; $H/D = 3$; $D = 3.5$ m) on the basis of model measurements where the physical properties of the system and the gas throughput of interest are known. With a freely selectable stirrer speed, we can presuppose that, apart from the numerical value of Nu, the numerical values of all other dimensionless numbers are known. (Of course we do not know anything about the coalescence phenomena – this corresponding to the state of knowledge existing about 30 years ago.)

Our considerations are therefore based on the following relationship:

$$Ne = f(Q, Fr, Re; \sigma^*, \rho'/\rho, \nu'/\nu) \tag{12.10}$$

Naturally we will perform the model experiments (e.g., on a scale of $\mu = 1{:}10$, i.e. $V = 0.1\ m^3 \rightarrow D = 0.35$ m) with the industrially interesting material system; in this way, at least, the numerical values of the three material numbers remain constant. However, this means that Re (resp. Ga) *and* Fr can no longer be adjusted *independently* of each other because only the rotational speed of the stirrer is available for their realization.

Therefore, we can only realize *partial similarity* in the model: We can either set Q and Re = idem or Q and Fr = idem. We will opt for the second case (Q and Fr = idem) because we expect g and hence Fr to be more important then $\nu$ and hence Re in an aeration process.

From the scale-up rules

$$Fr \propto n^2\, d = idem \rightarrow n_M = n_T\, \mu^{1/2} \quad \text{and} \tag{12.11}$$

$$Re \propto n\, d^2 = idem \rightarrow n_M = n_T\, \mu^2 \quad (\mu = d_T/d_M) \tag{12.12}$$

it follows that, in order to maintain Fr = idem, the stirrer speed in the model is only faster by a factor of $\mu^{1/2}$ than in the full-scale application. However, the condition Re = idem requires a stirring rate which is faster by a factor of $\mu^2$. This means that if we carry out the model measurement at Fr = idem, we are running the risk of the flow condition shifting substantially towards the laminar region with respect to Re: That is to say, if we perform the model experiments, which are characterized with Fr = idem, $n_M = n_T\, \mu^{1/2}$ and $d_M = d_T\, \mu^{-1}$, the following is valid for the Re number under these conditions:

$$ReM \propto n_M\, d_M^2 = n_T\, \mu^{1/2}\, (d_T\, \mu^{-1}) \propto Re_T\, \mu^{-3/2} \tag{12.13}$$

In our example ($\mu = 1{:}10$), the Re number would only be approximately 1/30th of the value obtained in the full-scale application! In view of this fact, the following approach would seem to be sensible, see **Fig. 35**:

1. The first measurement point is determined at $Re_{M1}$ and Fr, Q = idem (*filled* circle in the figure).
2. In the course of further measurements at Fr, Q = idem, the viscosity of the experimental liquid is reduced stepwise to raise Re towards $Re_T$; compare the three *hollow* circles. The smaller the selected model-scale, the greater is the danger of this approach also finally leading to false extrapolation to $Ne(Re_T)$: We do not know that Re is no longer relevant at $Re \geq 10^4$!
3. Since the material numbers are changed by the approach described in point 2, we will perform another model experiment on a larger scale at $Re_{M2}$, just to be on the safe side, see the filled triangle. Although we may confirm preceding measurement results, this does not reduce the risk of *extrapolation* to $Re_T$, as shown by comparison with the actual state of affairs (curve in Fig. 34).

This example is not intended as a deterrent against measurements under the conditions of partial similarity in general since these – when performed with care – can

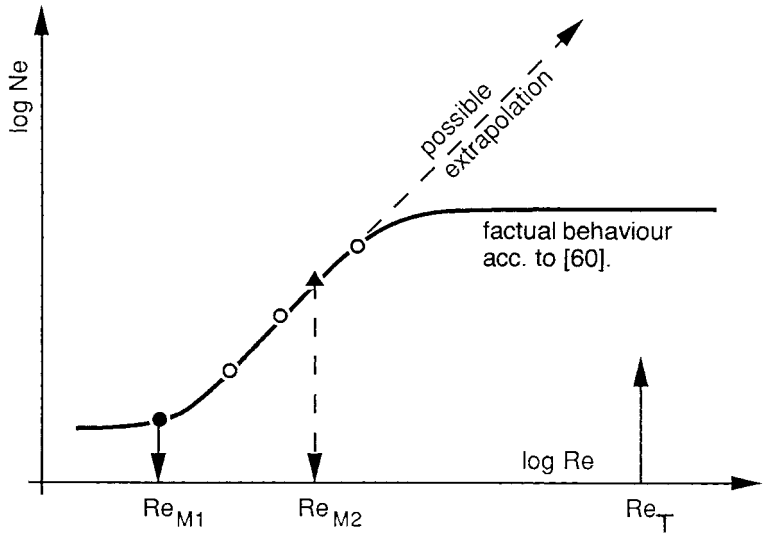


**Fig. 35** Presentation of the Ne(Re) curve for Q, Fr = idem kept constant. Illustration of model experiments. For explanation see text.

frequently provide valuable information. The purpose of this consideration is merely to show that there can be no substitute for *complete* information about a technical matter in the pertinent pi-space.

**Example 25**: Scale-up of mixers for mixing of solids

In the final state, the mixing of solids (e.g., powders) can only lead to a stochastically homogeneous mixture. We can therefore use the theory of random processes to describe this mixing operation. In the present example from [61] we will concentrate on a mixing device in which the position of the particles is adequately given by the x coordinate. Furthermore, we will assume that the mixing operation can be described as a stochastic process without "after-effects". This means that only the actual condition is important and not its history. The temporal course of this so-called *Markov* process can be described with the 2nd *Kolmogorov* equation. In the case of a mixing process without selective convectional flows (requirement: $\Delta\rho \approx 0$ and $\Delta d_p \approx 0$; see [62]), the solution of *Fick*'s diffusion equation gives a cosine function for the local concentration distribution, the amplitude of which decreases exponentially with the dimensionless time $\theta\ D_{eff}/(\pi^2\ L^2)$, see **Fig. 36**. (The variation coefficient or the relative variation, v, is defined as the standard deviation divided by the mean value: $v \equiv \sqrt{s^2}/\bar{x}$.)

Let us now consider this process using dimensional analysis. We have the following parameters:

| | | |
|---|---|---|
| Target quantity: | v | variation coefficient as a measure for the mixing quality |

| | | |
|---|---|---|
| Geometric parameters | D, L | diameter and length of the drum |
| | d | diameter of the mixing device |
| | $d_p$ | mean particle diameter |
| | $\phi$ | degree of fill of the drum |
| Material properties | $D_{eff}$, | effective axial dispersion coefficient |
| | $\rho$ | density of the particles |
| Process parameters | n | rotational speed of the mixer |
| | $\theta$ | mixing time |
| | $g\rho$ | solid gravity |

The relevance list contains 11 parameters

$$\{v; D, L, d, d_p, \phi; D_{eff}, \rho; n, \theta, g\rho\} \tag{12.14}$$

After the exclusion of the dimensionless quantities v and $\phi$ and the obvious geometric pi-numbers L/D, d/D and $d_p$/D, the following 3 pi-numbers are obtained:

| | $\rho$ | ***D*** | ***n*** | $\theta$ | $D_{eff}$ | $g\rho$ |
|---|---|---|---|---|---|---|
| M | 1 | 0 | 0 | 0 | 0 | 1 |
| L | –3 | 1 | 0 | 0 | 2 | –2 |
| T | 0 | 0 | –1 | 1 | –1 | –2 |
| M | **1** | 0 | 0 | 0 | 0 | 1 |
| L + 3M | 0 | **1** | 0 | 0 | 2 | 1 |
| –T | 0 | 0 | **1** | –1 | 1 | 2 |

| | |
|---|---|
| $\theta$ n | Mixing number |
| $D_{eff}/D^2$ n $\equiv$ $Bo^{-1}$ | Bo – Bodenstein number |
| $g\rho/\rho D\ n^2 \equiv Fr^{-1}$ | Fr – Froude number |

The complete pi-set reads:

$$\{v, L/D, d/D, d_p/D, \phi, \theta n, Bo, Fr\} \tag{12.15}$$

To obtain the rotational speed of the drum in only one number (the process number Fr), we combine the other two accordingly with Fr and get: $\theta\ D_{eff}/D^2$ und $g\ D^3/D_{eff}^2$.

The experimental results presented in **Fig. 36** were obtained in one single model (D = 0.19 m) with different lengths (L/D = 1; 1.5; 2; 2.5). The geometric and material numbers d/D, $d_p$/D, $\phi$ and $g\ D^3/D_{eff}^2$ remained unchanged as did Fr because of the constant rotational speed of the drum n = 50 $min^{-1}$. As a result, the measurements can only be depicted in the pi-space

$$\{v, \theta D_{eff}/D^2, L/D\} \tag{12.16}$$

whereby d/D, $d_p$/D, $\phi$, $g\ D^3/D_{eff}^2$, Fr = idem.

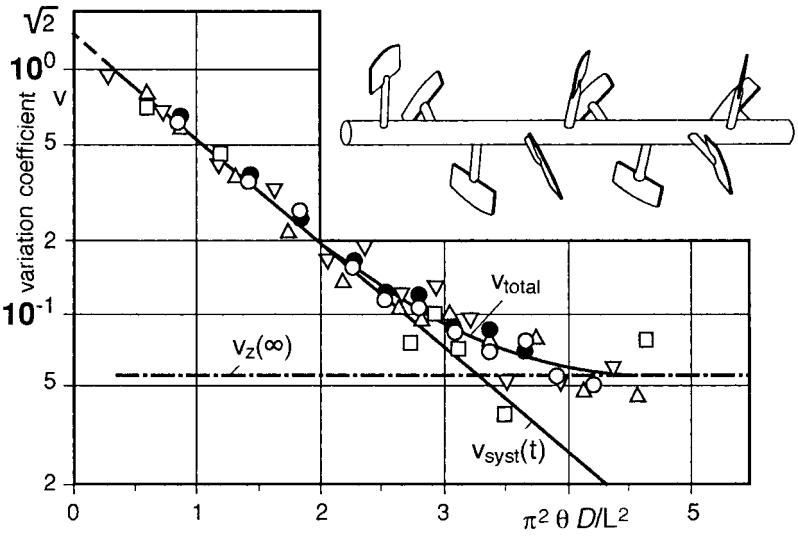


**Fig. 36** Mixing quality as a function of the dimensionless mixing time for different l/D ratios.Copper and nickel particles of $\delta = 300 - 400\ \mu m$, fill degree of the drum $\phi = 35\%$, Froude number of the drum Fr = 0.019. From [61].

The result of these measurements is

$$v = f(\theta D_{eff}/L^2) \tag{12.17}$$

In other words, the mixing time (at Fr = const), required to attain a certain mixing quality, increases with the square of the drum length L. In order to reduce the mixing time, the component to be mixed would have to be added in the middle of the drum or simultaneously at several positions.

Fig. 36 shows experimental results in a single logarithmic graph. They are compared with the theoretical prediction of a stochastic *Markoff*'s process. For details see [61].

*Entrop* [63] reported the process characteristics of the *Nauta*® mixer. The *Nauta*® mixer utilizes an orbiting action of a helical screw rotating on its own axis to carry material upward, while revolving about the centerline of the cone-shaped shell near the wall for top-to-bottom circulation., see the sketch in Fig. 37. *Nauta*® mixers of different sizes are not build geometrically similar to each other: The diameter of the helical screw and its pitch are kept equal.

Mixing time characteristic of the *Nauta*® mixer

Relevance list: In case of a pure convective mixing and $\Delta\rho \approx 0$ as well as $\Delta d_p \approx 0$, the particle size $d_p$ is of no influence.

| | | |
|---|---|---|
| Target quantity: | $\theta$ | mixing time |
| Geometric parameters | d, l | diameter and length of the helical screw |
| Material properties | $\rho$ | solid density |

| | | |
|---|---|---|
| Process parameters | n, $n_b$ | rotational speed of the helical screw and of its beam |
| | g | gravitational acceleration |

$$\{\theta; d, l; \rho; n, n_b, g\} \tag{12.18}$$

The base dimension M is contained only in the density ρ. Therefore, this quantity has to be deleted from the relevance list. 6 – 2 = 4 numbers will be produced. The pi-set reads:

$$\{n\theta, l/d, n_a/n, Fr \equiv n^2 d/g\} \tag{12.19}$$

The measurements were executed under following conditions: Mixer volume V = 0.05–10 $m^3$; diameter of the helical screw d = 0.15–0.63 m; rotational speed of the helical screw n = 30–120 $min^{-1}$; $n_a/n$ = 20–70; Fr = 0.24–4. Material systems: sand and fine-grained limestone.

The mixing time characteristic of the *Nauta*® mixer is given in **Fig. 37**. It can be shown that the type of material has a neglegible influence (proof that the density ρ is irrelevant indeed!). Likewise, the number $n_a/n$ has, within the used range, no effect. In contrast, the influence of the parameter l/d is very pronounced. The process equation reads:

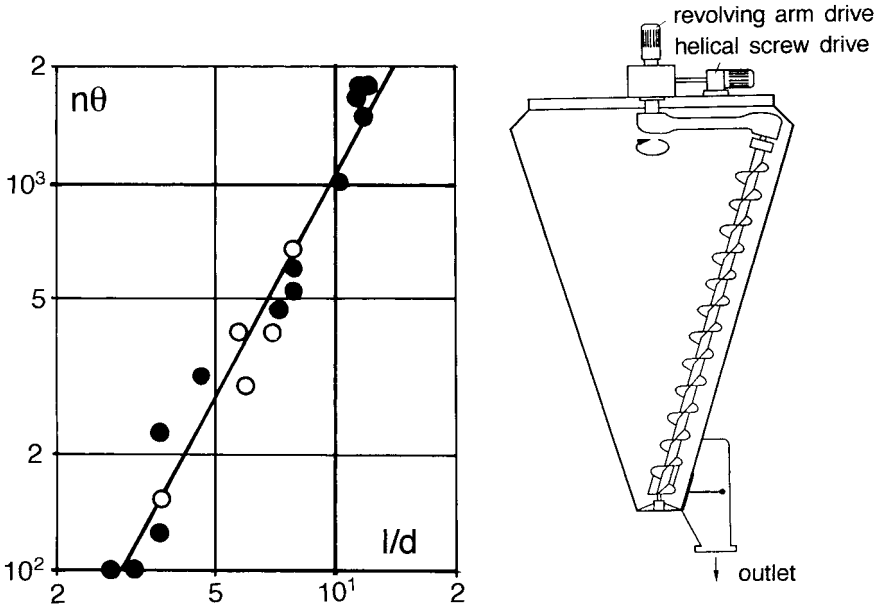


**Fig. 37** Mixing time characteristic of the *Nauta*® mixer and its drawing; from [63].
(Sign legend is missing in the original publication.)

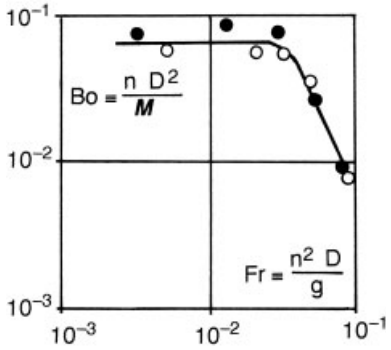


**Fig. 38** Mixing time characteristic of a plow-share mixer. Material: Cooper shot and corn shoot. D = 0.2 and 0.4 m; degree of fill φ = 0.35 and 0.4–0.65; from [64]. (Sign legend is missing in the original publication.)

$$n\theta = 13\ (l/d)^{1.93} \qquad n_a/n = 20\text{–}70 \quad Fr = 0.24\text{–}4 \tag{12.20}$$

This means, in practice, that the mixing time is lengthened by the square of the length (compare to the eq. (12.17)).
For the power characteristic of the *Nauta*® mixer has been found [63]:

$$Ne\ Fr \equiv \frac{P}{n\ d^4\ g\rho} \propto (l/d)^{1,62} \tag{12.21}$$

By multiplication of the process characteristics (12.20) and (12.21), the expression for the mixing work, W, can be obtained, this being necessary for a given mixing quality:

$$W = P\ \theta \propto d^{0.45}\ l^{3.55}\ \rho g \tag{12.22}$$

From the energetic point of view, it is therefore advantageous to construct mixers of low heights and to provide them with helical screws of large diameters.

In the study of plow-share mixers (centrifugal mixers) a different data processing method has been used [64]. From the concentration distribution of the material travelling through the drum, an effective Bodenstein number, $Bo \equiv v\ L/M$ (v – travelling velocity of the material to be equilized; L – drum length; *M* – mixing coefficient, comparable to the dispersion coefficient $D_{eff,\ ax}$), is determined and *M* calculated from it. With these *M* values a different Bodenstein number, $Bo \equiv n\ D^2/M$, is now formed and plotted against the Froude number $Fr \equiv n^2\ D/g$. **Fig. 38** shows that for $Fr \leq 0.038$ the Bodenstein numbers remain constant but afterwards they decrease proportionally to $Fr^2$. At this border value of the Froude number, the flow behavior changed completely.

According to *Müller* [64], the manufacturers of mixing equipment comply with the scale-up rule: u = const (u = πnd – tip speed of the mixing device). From this, the following applies for the mixing time θ:

$$\mathrm{Fr} \le 0.038: \theta = D/u \ (L/D)^2 \tag{12.23}$$

$$\mathrm{Fr} \ge 0.038: \theta = D^3/u^5 \ (L/D)^2 \tag{12.24}$$

At the same standardized L/D value and an equal tip speed, u, for $\mathrm{Fr} \le 0.038$ mixing time increases proportionally to the drum diameter, D. For $\mathrm{Fr} \ge 0.038$, mixing time increases proportionally to $D^3$. In this range, however, even a minute change in the rotational speed of the mixing device exerts a strong influence on the mixing time.

**Example 26**: Conveying characteristics of single-screw machines

Screw machines are important appliances used for the production (mass polymerization) and processing (mixing, extrusion) of plastics. They play also an important role in the food industry (chocolate, pasta). A distinction is made between single-screw and multiple-screw machines (e.g., self-wiping twin-screws) and between conveying, mixing and kneading screw machines. The conveying characteristics are represented for all types of screw machines in the same pi-space. In the following, they will be given and discussed for single-screw machines.

The conveying properties of a single-screw machine of given screw geometry are represented in the creeping range ($\mathrm{Re} < 100$) of Newtonian liquids by following characteristics [5, 65]:

*Pressure* characteristic: $$\mathrm{Eu\ Re\ d/L} \equiv \frac{\Delta p\ d}{\mu\ n\ L} = f_1\,(Q) \tag{12.25}$$

*Axial force* characteristic: $$\mathrm{NeF\ Re\ d/L} \equiv \frac{F}{\mu\ n\ d\ L} = f_2\,(Q) \tag{12.26}$$

*Power* characteristic: $$\mathrm{NeF\ Re\ d/L} \equiv \frac{P}{\mu\ n^2\ d^2\ L} = f_3\,(Q) \tag{12.27}$$

Q represents the flow rate number $Q \equiv q/(nd^3)$. These three characteristics are illustrated in **Fig. 39** for a screw of given geometry. They are linear dependences which are described by analytical expressions in the form:

$$\frac{1}{y_1} Y + \frac{1}{q_1} Q = 1 \tag{12.28}$$

where $y_1$ and $q_1$ are the respective axis intercepts.

In scrutinizing the conveying characteristics in Fig. 39, one discovers three typical ranges in which the screw machine can function. They are outlined in **Fig. 40**. In this representation, the throughput number Q is standardized by the intercept $A_1$. In other words, this is the numerical value of Q where the screw machine is conveying without pressure formation. With this "flow-kinematic" parameter, $\Lambda \equiv Q/A_1$, the state of flow of a screw machine can be outlined more distinctly.

The two intercepts $A_1$ and $A_2$ are called profile parameters of a screw machine because their numerical values depend on the screw geometry ("screw profile"), for details see [5, 65].

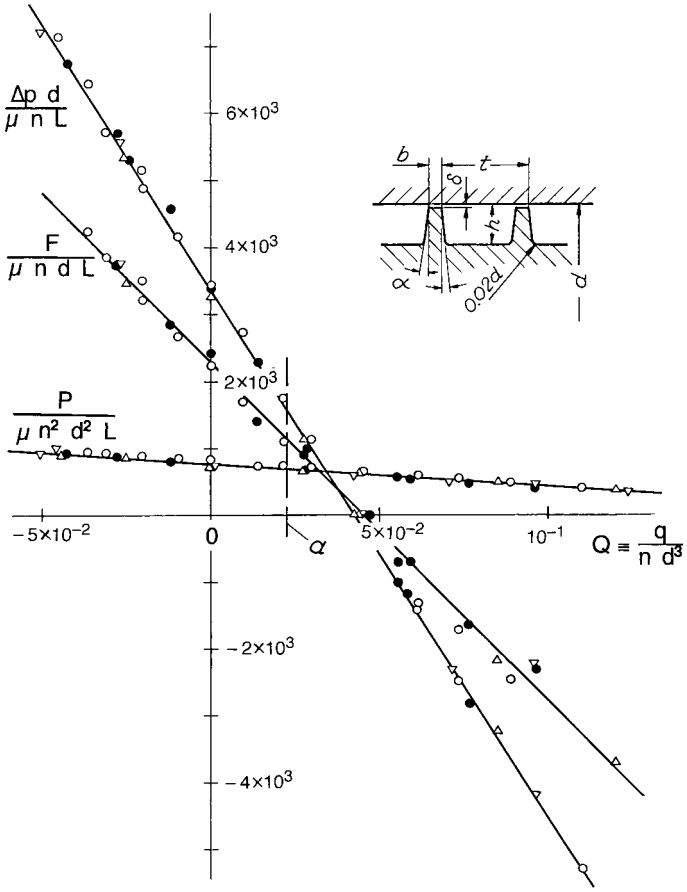


**Fig. 39** Conveying characteristics of a single-screw machine of given screw geometry, taken from [5].

From the three ranges of the conveying characteristics, only the middle one $0 < \Lambda < 1$ (the so-called active conveying range of the screw machine) can be implemented by suitable throttling and/or a change in the rotational speed alone, without an additional conveying device. At $\Lambda = 0$ the screw machine is fully choked and the highest pressure builds up. At $\Lambda = 1$ the highest throughput is achieved without a pressure build up.

In order to implement the other two ranges, it is necessary to couple the screw machine with an additional conveying device (e.g., a positive displacement gear-type rotary pump). If the pump transports the liquid in the same direction as the screw, the range $\Lambda > 1$ results. Here, the conveying action of the screw machine is "run over" by the conveying action of the pump. At $\Lambda < 0$, the pump pushes the liquid against the conveying sense of the screw. The screw machine is then only a mixing device.

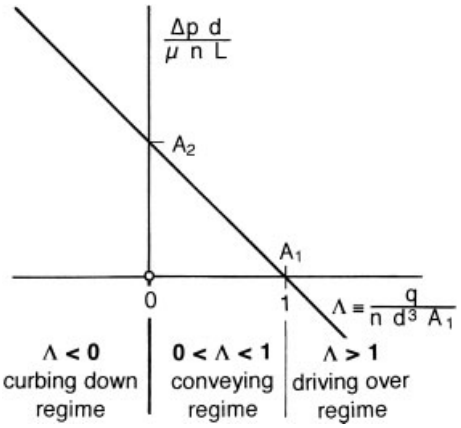


**Fig. 40** Subdivision of the typical working ranges of a screw machine by the "flow-kinematic" parameter Λ.

It has been already pointed out that the conveying properties of a single-screw machine can be described by linear dependencies of the type shown in eq. (12.28), this only being valid in the creeping range (Re < 100) of Newtonian liquids. The proof for this is given in **Fig. 41**. It represents the pressure characteristics of a single-screw machine of a given screw geometry in dependence of the Reynolds numbers. It can be seen that at Re ≥ 240 this linearity does not exist any more.

In case of a non-Newtonian liquid, the pressure characteristic is depicted by the pi-set:

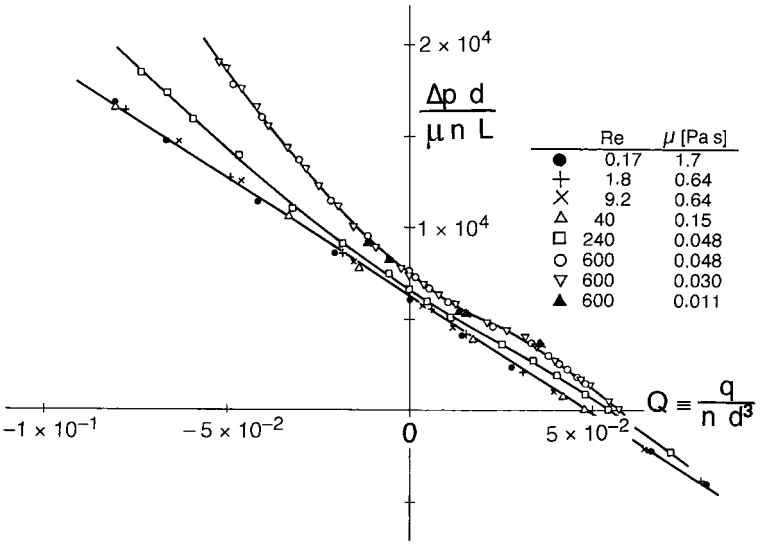


**Fig. 41** Dependence of the pressure characteristics of a single-screw machine on the state of flow (Re); from [5].

$$\{\Delta p\, d/(H\, n\, L),\ Q,\ n\Theta,\ \Pi_{rheol}\} \tag{12.29}$$

In this type of liquid, in which the viscosity curve corresponds to that shown in Fig. 18, the pi-space is given by

$$\{\Delta p\, d/(\mu_\infty\, n\, L),\ Q,\ n\dot{\gamma}_\infty\} \tag{12.30}$$

**Fig. 42** shows this relationship for such a liquid (lubricant for steam engines with ca. 7 % Al stearate, $\mu_\infty$ = 9.7 Pa s, $\dot{\gamma}_\infty$ = 0.205 $s^{-1}$). This was established with two differently sized (d = 60 and 90 mm) single-screw machines with the same profile geometry using two rotational speeds (n = 1.65 and 25 $min^{-1}$). Independent of the screw diameter, the curves coincide for $n\dot{\gamma}_\infty$ = const. The higher the rotational speed, the higher is the shear stress; the straight line (a), which is also valid for Newtonian liquids, adjusts as the limit case ($\mu = \mu_\infty$).

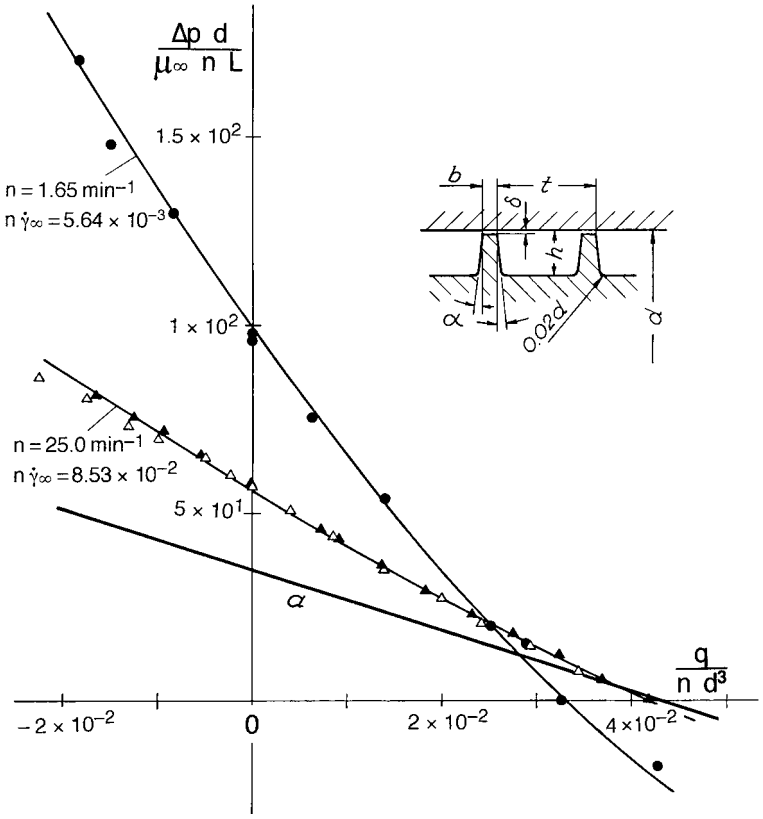


**Fig. 42** Pressure characteristic of a screw machine of given screw geometry for a non-Newtonian liquid (see text). Full signs: d = 60 mm, hollow signs: d = 90 mm; for $\mu_\infty$ and $\dot{\gamma}_\infty$ see Fig. 18; from [5].

When conducting extremely exothermic reactions in a screw machine as chemical reactor, operating conditions at which a minimum of power is dissipated in the liquid (≙ lowest thermal load of the liquid throughput) are of interest. The dissipated power, $H$, is obtained from the difference between the power, P, of the motor drive and that of the pump, $q\Delta p$:

$$H = P - q\Delta p \tag{12.31}$$

A dimensionless formulation of this relationship is possible using the conveying characteristics of the screw machine in question, see Fig. 39. In the active conveying range, $0 < \Lambda = 1$, the dissipation characteristic passes through a minimum in which the lowest power dissipation $H$ occurs for the given values of q and $\Delta p$, this corresponding to $H/q = \min$.

In Sect. 8.7 it was pointed out that in even using the same non-Newtonian liquid, complete similarity of the model and the full-scale counterpart can only be attained if there is a creeping, steady-state and isothermal flow condition. Scale-up is then carried out as follows:

The non-Newtonian liquid and the parameters $q_T$ and $\Delta p_T$ of the industrial facility are given. We are searching for the variable d and the rotational speed n of the technical device, whereby P = min is required. Corresponding to the above pi-set for non-Newtonian liquids, it follows that:

$$L/d,\ n,\ \Delta p = \text{idem} \quad \rightarrow \quad q/d^3;\ P/q = \text{idem} \tag{12.32}$$

In the model screw machine, the dependences q(n) and P(q) are established and depicted as $P/q = f_1(n)$ and $q/d^3 = f_2(n)$. This situation also applies to the full-scale appliance. The possibly existing minimum of P/q gives the optimum rotational speed $n_{opt}$, which is also valid for the technical device. The corresponding values $d_{opt}$ and $P_{opt}$ for the technical device are obtained from the values $(q/d^3)_{opt}$ and $(P/q)_{opt}$ by setting $q = q_T$. We have therefore solved the task.

A consequent dimensional-analytical treatment of the homogenization process, residence time distribution and heat transfer behavior in single-screw machines was performed by *Pawlowski* and was published in a sequence of scientific papers. A summary of this work is printed as a monograph [65].

**Example 27**: Dimensional-analytical treatment of liquid atomization

Liquid atomization (liquid-in-gas-dispersion) is an important unit operation which is employed in a variety of processes. They include: fuel atomization, spray drying, the spraying of a lime suspension into combustion gases in power stations for $SO_2$ removal, powder metallurgy (metal powder production), coating of surfaces by spraying, and so on.

In all these tasks the achievable (as narrow as possible) droplet size distribution represents the most important target quantity. It is often described merely by the mean droplet size, the so-called "*Sauter* mean diameter" $d_{32}$ [67], which is defined as

the sum of all droplet volumes divided by their surfaces. Mechanisms of droplet formation are:

1. Liquid column formed by a pressure nozzle is inherently unstable. The breakup of the laminar column occurs by a symmetrical oscillation, a sinusoidal oscillation and, finally, atomization.
2. Liquid sheet formation by an appropriate nozzle is followed by rim disintegration, aerodynamic wave disintegration and turbulent breakup.
3. Liquid atomization by a gas stream.
4. Liquid atomization by centrifugal acceleration.

For all of these operations process equations exist; some of them will be represented in the following.

As discharge velocity at the nozzle outlet increases, the following states appear in succession: dripping, laminar jet breakup, wave disintegration and atomization. These states of flow are described in a pi-space {Re, Fr, $We_p$}, whereby $We_p \equiv \rho\, v^2\, d_p/\sigma$ represents the Weber number, formed by the droplet diameter, $d_p$. To eliminate the flow velocity, v, these numbers are combined to give

$$\text{Bond number} \qquad Bd_p \equiv \frac{We}{Fr} \equiv \frac{\rho g\, d_p^2}{\sigma} \qquad \text{and} \tag{12.33}$$

$$\text{Ohnesorge number} \qquad Oh_p \equiv \frac{We^{1/2}}{Re} \equiv \frac{\mu}{(\sigma\, \rho\, d_p)^{1/2}} \tag{12.34}$$

The subscript p indicates that these pi-numbers are formed with the droplet diameter.

For a liquid, dripping from a tiny capillary with diameter, d, it follows (see Example 2 and [2]):

$$\frac{d_p}{d} = 1.6\left(\frac{\rho g\, d^2}{\sigma}\right)^{-\frac{1}{3}} = 1.6\,Bd^{-\frac{1}{3}} \tag{12.35}$$

Broader tubes (Bd > 25) exert no influence of d. Then we obtain:

$$Bd_p \equiv \rho g\, d_p^2/\sigma = 2.9\text{–}3.3 \tag{12.36}$$

On the jet suface, waves are formed which, at wave lengths of $\lambda > \pi d_j$ ($d_j$ – jet diameter), grow rapidly. The fastest wave disturbance takes place at the optimum wave length of

$$\lambda_{opt}/\pi d_j = \sqrt{2 + 6\ Oh} \tag{12.37}$$

For a low liquid viscosity $d/d_j \approx 1.9$ applies. If liquid output pulsates, uniformly spaced droplets are obtained; here $d/d_j \approx 1$. Another possibility to produce monosized droplets consists in using pneumatic extension nozzles [317].

With higher discharge velocities laminar jets are produced, which disintegrate to droplets in a certain distance from the capillary. The transition from dripping to liquid jet desintegration occurs at higher Weber numbers:

$$We \equiv \rho\, v^2\, d/\sigma = 8\text{–}10 \tag{12.38}$$

At We < 8, gravitational acceleration also has to be considered, thereby the Bond number has to be included into the process equation.

The working principle of hollow cone nozzles is that the liquid throuhgput is subjected to rotation by a tangential inlet and is then further accelerated in the conical housing towards the orifice; see the sketch in Fig. 43. A liquid film with a thickness, δ, is thereby produced, which, at the discharge from the orifice, spreads to a hollow cone sheet and disitegrates to droplets.

At low discharge velocities and low film thicknesses, the sheet disintegration is due to the oscillations caused by air motion. In this case, the film thickness has a large impact on the droplet size. In contrast, it is insignificant whether a pure liquid or a lime-water suspension (mass portion $\phi$ = 16-64 %) is treated, see **Fig. 43**.

The fitting line corresponds to the analytical expression for the wave disintegration of pure liquids by hollow cone nozzles:

$$\frac{d_{p,max}}{\delta} = 1.13 \left(\frac{\rho_L}{\rho_G}\right)^{1/6} \left(\frac{\sigma}{\rho_L v^2 \delta}\right)^{1/3} \left(\frac{2r_i}{\delta\, tg\alpha}\right)^{1/3} \left(\frac{\rho_G v\, \delta}{\mu_G}\right)^{1/5} \tag{12.39}$$

($r_i$ – orifice radius; $\alpha$ – angle of the hollow conical liquid sheet produced)

This pi-equation, taken from [68], represents a physical correlation. It is *absolutely useless* for scaling up purposes: To predict the target quantity $d_{p,max}$, knowledge of another target quantity, namely the film thickness, δ, is also necessary!

By exceeding a certain discharge velocity, turbulence forces increase to such an extent that film disruption takes place immediately at the orifice. Now, the droplet

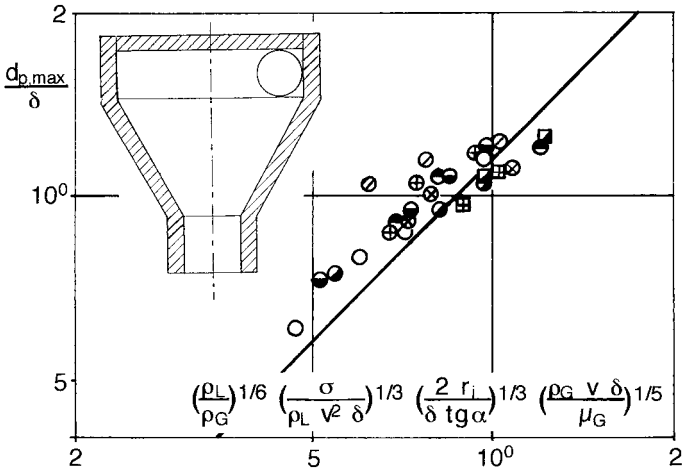


**Fig. 43** Film disintegration by wave oscillation. Measurements with hollow cone nozzles of different geometry and with lime-water-suspensions. For an explanation of signs see the original publication [68]. The fitted line is valid for pure liquids.

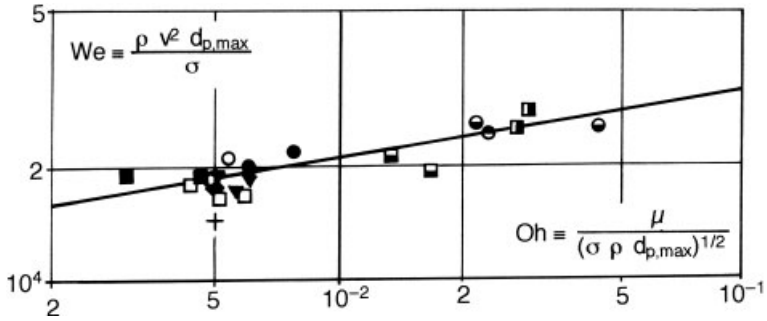


**Fig. 44** Liquid film atomization by turbulent forces. For an explanation of signs see the original publication [68].

size is independent of the film thickness. This state of atomization is described by the critical Weber number. Measuring data obtained with hollow cone nozzles of different geometry and pure liquids as well as lime-water-suspensions are represented in **Fig. 44**. $We_{p,crit}$ and the Ohnesorge number are formed by the largest stable droplet diameter, $d_{p,max}$. The pi-equation reads:

$$We_{p,crit} = 4.5 \times 10^4 \, Oh_p^{1/6} \tag{12.40}$$

This equation, also taken from [68], is equally useless for scaling up purposes, because the (unknown!) target quantity $d_{p,max}$ appears in both dimensionless numbers. In the combination

$$We_{p,crit} \, Oh_p^2 \equiv We/Re \equiv v \, \mu/\sigma$$

a new pi-number is obtained which does not contain $d_{p,max}$:

$$We_{p,crit} = 1.97 \times 10^4 \, (v \, \mu/\sigma)^{0.154} \tag{12.40a}$$

This process equation can now serve for scaling up $d_{p,max}$.

**Example 28**: The hanging film phenomenon

In a countercurrent flow of liquid and gas in a vertical tube, at a critical gas velocity, $v_G$, a situation arrises at which the liquid supply to the tube is interrupted and the liquid film inside the wall is held at rest; see sketch, **Fig. 45**. Increasing the gas velocity above $v_G$ causes the film attachment point to rise in the tube. Lowering gas velocity below $v_G$ causes the liquid film to move down the tube. Most of the researchers reported little or no difference between these two critical $v_G$ values. However, *Wallis* and *Makkenchery* [69] stated that, for small tube diameters (D = 6 mm) and air-water mixtures, the velocities differed by a factor of about two. These researchers found that the lower critical $v_G$ increased with pipe diameter, D, and was independent of it for large values of D. For acrylic glass the final result was found to be:

$$\mathrm{Ku} \equiv \frac{\rho_G^{1/2} v_G}{(\sigma\, g\Delta\rho)^{1/4}} \approx 3,2 \qquad \mathrm{Bd} \equiv D \left(\frac{g\Delta\rho}{\sigma}\right)^{1/2} > 40 \tag{12.41}$$

To obtain a linear expression for the characteristic lengths (D), the square root of the usual Bond number was used. $\mathrm{Ku} \equiv (\mathrm{Fr}^{*}\mathrm{We})^{1/4}$ is the Kutateladze number. Physical properties of the liquid have no subscript, $g\Delta\rho \equiv g(\rho - \rho_G)$.

Russian researchers [70] have found that in glass tubes the same Ku value is obtained at Bd > 6. This discrepancy caused *Eichhorn* [71] to carry out a detailed dimensional-analytical examination. He first discovered that the lower critical $v_G$ corresponded to a critical film thickness and to a critical shear rate in the phase boundary G/L. Therefore, there are three parameters independent of each other, which could be regarded as target quantities. However, $v_G$ can be measured more accurately and more easily than the others, therefore, it is accepted as the target quantity.

The contact angle, Θ, between the liquid and the tube wall is viewed as an essential material parameter. With this quantity, the wettability of the tube wall is taken into account. Therefore, the relevance list reads:

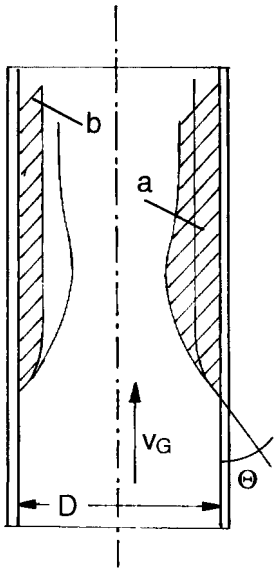


**Fig. 45** Schematic representation of the hanging film phenomenon (as sketched in [69])

$$\{v_G;\ D;\ \rho_G,\ \rho,\ \mu_G,\ \mu,\ \sigma,\ \Theta;\ g\Delta\rho\} \tag{12.42}$$

9 – 3 = 6 dimensionless numbers will be produced. Three of them are: $\rho_G/\rho$, $\mu_G/\mu$, Θ.

With the remaining six x-quantities a dimensional matrix is formed $\{\rho,\ D,\ \mu|\ v_G,\ \sigma,\ g\Delta\rho\}$ which is transformed, in three steps, to the matrix of unity. Following pi-numbers are produced:

$$\Pi_1 \equiv \frac{v_G\ \rho\ D}{\mu} \equiv \mathrm{Re}; \quad \Pi_2 \equiv \frac{\sigma\ \rho\ D}{\mu^2}; \quad \Pi_3 \equiv \frac{g\Delta\rho\ \rho\ D^3}{\mu^2} \tag{12.43}$$

To obtain the two pi-numbers presented in (12.41), these numbers are combined as follows:

$$\mathrm{Bd} \equiv (\Pi_3\, \Pi_2^{-1})^{1/2}; \quad \mathrm{Ku} \equiv \Pi_1\, (\Pi_2\, \Pi_3)^{-1/4}\, (\rho_G/\rho)^{1/2} \tag{12.44}$$

As the third pi-number, a pure material number can be produced out of the three:

$$\Pi_3\, \Pi_2^{-3} \equiv \frac{g\Delta\rho\ \mu^4}{\sigma^3 \rho^2} \equiv \mathrm{CB} \tag{12.45}$$

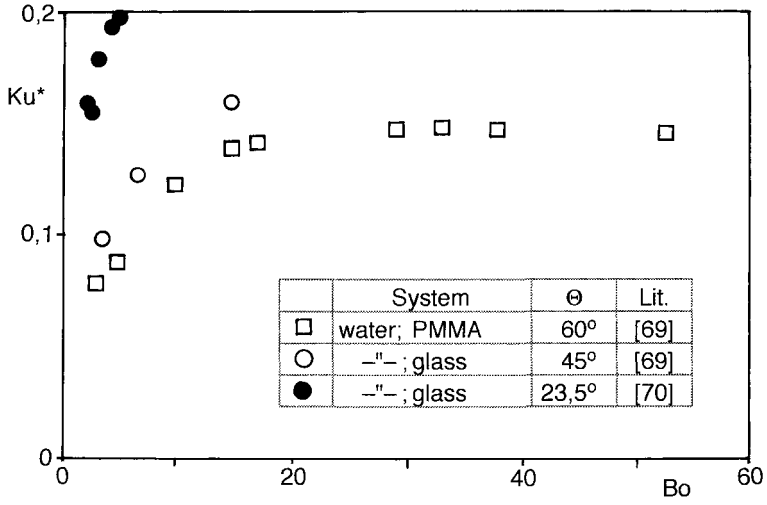


**Fig. 46** The correlation $Ku^* = f(Bd)$ for the hanging film at the *lower* critical air velocity

*Eichhorn* [71] names it the "capillarity-buoyancy number" CB.

From (12.42) we obtain the following pi-set:

$$\{Ku, Bd, CB, \rho_G/\rho, \mu_G/\mu, \Theta\} \tag{12.46}$$

*Eichhorn* [71] considers the air velocity, $v_G^*$, to be a more appropriate parameter, this corresponding to the gas-sided friction at a dry tube wall. (An explanation for this dicission is not clear: in the turbulent flow range the gas friction number, $\zeta$, is practically independent of the Reynolds number!)

$$\frac{\zeta}{2} \equiv \frac{\tau_w}{\rho_G v_G^2} = \left(\frac{v_G^*}{v_G}\right)^2 \tag{12.47}$$

Considering (12.47), the Ku number is transformed to

$$Ku^* \equiv Ku\sqrt{\zeta/2} \equiv \left(\frac{\tau_w^2}{\sigma g \Delta\rho}\right)^{1/4} \tag{12.48}$$

The experimental data [69, 70] are given in **Fig. 46** in the form $Ku^* = f(Bd)$. This means that the contact angle, $\Theta$, has not yet been considered. The discrepancy due to the different $\Theta$ values can be clearly seen.

**Fig. 47** clearly shows that the contact angle, $\Theta$, is satisfactorily taken into account by the function $Ku^* \times \sin\Theta = f(Bd)$. Only now it is also obvious that the "capillarity-buoyancy number" CB exerts no influence on the hanging film. The liquid viscosity, $\mu$, proves to be irrelevant. This is not surprising because of the fact that the respective measurement were executed in the turbulent flow range, $Re = 4.15 \times 10^3$–$1.42 \times 10^5$.

The fitted line in Fig. 47 corresponds to the process equation

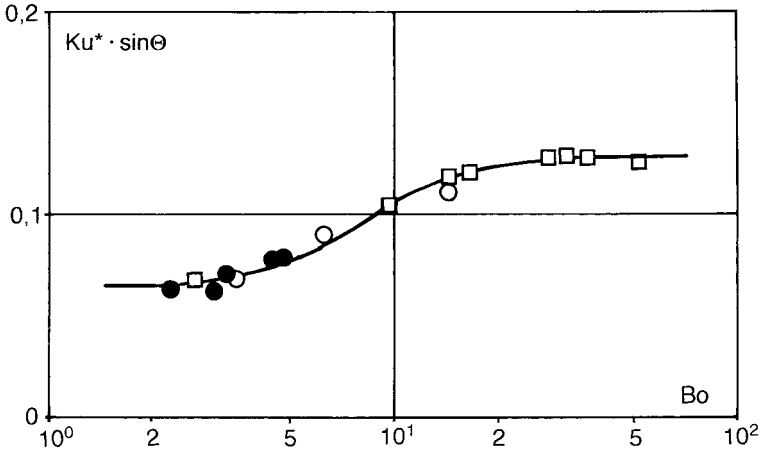


**Fig. 47** The correlation $Ku^* \times \sin \Theta = f\,(Bd)$. The fitted line corresponds to eq. (12.49), from [71].

$$Ku^* \times \sin \Theta = 0.096 \left(1 + \frac{1}{3}\left[\frac{(Bd/8)^3 - 1}{(Bd/8)^3 + 1}\right]\right) \tag{12.49}$$

This example also proves that in physics small causes (here the contact angle, $\Theta$) can result in major effects.

**Example 29**: The production of liquid/liquid emulsions

Liquid/liquid emulsions consist of two (or more) non-miscible liquids. Classical examples for this are oil in water (O/W) emulsions, for example milk, mayonnaise, lotions, creams, water soluble paints, photo emulsions, and so on. As appliances, teeth-rimed rotor-stator emulsifiers and colloid mills, as well as high-pressure homogenizers are used.

All of them utilise a high energy input to produce very fine droplets of the disperse (mostly oil) phase. The aim of this operation is, likewise in Example 27, the narrowest possible droplet size distribution. It is normally characterised by the "Sauter mean diameter" $d_{32}$ [67] or by the median $d_{50}$ of the size distribution. $d_{32}$ and $d_{50}$, respectively, therefore represent the target quantity of this operation.

The *characteristic length* of the contacting chamber, e.g. the slot width between rotor and stator in teeth-rimed emulsifiers or the nozzle diameter in high pressure homogenizers (utilizing the shear of the high-speed liquid jet ) will be denoted as d.

As *material parameters*, the densities and the viscosities of both phases as well as the interfacial tension $\sigma$ must be listed. We incorporate the material parameters of the disperse phase $\rho_d$ and $\mu_d$ in the relevance list and note separately the material numbers $\rho/\rho_d$ and $\mu/\mu_d$. Additional (dimensionless) material parameters are the volume ratio of both phases, $\varphi$, and the mass portion $c_i$, of the emulsifying agent (surfactant) [e.g. given in ppm].

The *process parameters* have to be formulated as intensive quantities. In appliances which display *two* degrees of freedom, where the liquid throughput, q, of both liquids which have to be emulsified is adjusted independently from the power input P, the power per liquid volume, P/V, as well as the duration of it, namely the residence time of the throughput, $\tau = V/q$, must be considered:

$$(P/V)\,\tau = E/V\ [M\ L^{-1}\ T^{-2}] \tag{12.50}$$

In appliances with only *one* degree of freedom (e.g. high-pressure homogenizers) power is being introduced by the liquid throughput itself. Here, the relevant intensively formulated quantity is therefore jet power per liquid throughput, P/q. Due to the fact that in nozzles $P \propto \Delta p\ q$, this results in

$$P/q = (\Delta p\ q)/q = \Delta p\ [M\ L^{-1}\ T^{-2}] \tag{12.51}$$

Therefore, the volume-related energy input E/V and the throughput-related power input P/q ($\triangleq \Delta p$) represent homologuos quantities of the same dimension. For the sake of simplicity, $\Delta p$ will be introduced in the relevance list.

Now, this six parametric relevance list (the dimensionless parameters $\rho/\rho_d$, $\mu/\mu_d$, $\varphi$, $c_i$ are anticipated) reads

$$\{d_{32};\ d;\ \rho_d,\ \mu_d,\ \sigma;\ \Delta p\} \tag{12.52}$$

The corresponding dimensional matrix

| | $\rho_d$ | $d$ | $\sigma$ | $\Delta p$ | $\mu_d$ | $d_{32}$ |
|---|---|---|---|---|---|---|
| M | 1 | 0 | 1 | 1 | 1 | 0 |
| L | –3 | 1 | 0 | –1 | –1 | 1 |
| T | 0 | 0 | –2 | –2 | –1 | 0 |
| M + T/2 | **1** | 0 | 0 | 0 | 1/2 | 0 |
| 3M + L + 3 T/2 | 0 | **1** | 0 | –1 | 1/2 | 1 |
| –T/2 | 0 | 0 | **1** | 1 | 1/2 | 0 |

delivers the remaining three dimensionless numbers:

$$\Pi_1 \equiv \frac{\Delta p\, d}{\sigma} \equiv \quad \text{Eu We} \equiv \text{La} \qquad \text{(Laplace number)}$$

$$\Pi_2 \equiv \frac{\mu_d}{(\rho_d d\sigma)^{1/2}} \equiv \frac{We^{1/2}}{Re} \equiv \text{Oh} \qquad \text{(Ohnesorge number)}$$

$$\Pi_3 \equiv d_{32}/d$$

The complete pi-set is given as

$$\{d_{32}/d,\ La,\ Oh,\ \rho/\rho_d,\ \mu/\mu_d,\ \varphi,\ c_i\} \tag{12.53}$$

Assuming a quasi-umiform power distribution into the throughput or into the volume, a characteristic length of the contacting chamber becomes irrelevant. In the relevance list, eq. (12.52), the parameter d must be cancelled. The target number $\Pi_3 \equiv d_{32}/d$ has to be dropped and the dimensionless numbers $La^*$ and $Oh^*$ are formulated with $d_{32}$ instead of d. At given constant material conditions ($\rho/\rho_d$, $\mu/\mu_d$, $\varphi$, $c_i$ = const), the process characteristics will be represented in the following pi-space:

$$Oh^{*-2} = f(La^* Oh^{*2}) \rightarrow d_{32}\left(\frac{\rho_d \sigma}{\mu_d^2}\right) = f\{\Delta p\left(\frac{\mu_d^2}{\rho_d \sigma^2}\right)\} \tag{12.54}$$

*Schneider* and *Roth* [72] confirmed this dependence with two colloid mills using the scale $\mu = 1 : 2.2$, see **Fig. 48**. For the material system vegetable oil/water and $\varphi = 0.5$ they found the following process equation:

$$d_{32} = 4.64 \times 10^5\ \Delta p^{-2/3} \qquad d_{32}\ [\mu m];\ \Delta p\ [M/(L T^2)] \tag{12.55}$$

*H. Karbstein* [73, 74] investigated two rotor-stator emulsifiers (teeth rings, ZKDM), two colloid mills (CM) and a high pressure homogenizer (HPH). She also proved that the results ($d_{32}$) from both of the first mentioned emulsifiers *did not* depend on the chamber size and were only slightly dependent on the type of apparatus. Therefore, eq. (12.54) is confirmed. In contrast, in the case of HPH as well the nozzle diameter as the application of counter-pressure plays a role, see **Fig. 49**. (For details of the geometry of the contacting chamber see [73].)

The measurements were executed with the material system 30 % vegetable oil/water under the addition of a fast absorbing emulsifying agent (Laurylethylenoxid

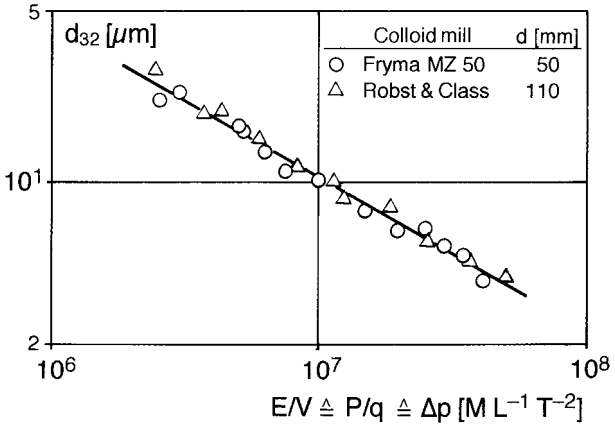


**Fig. 48** Relationship $d_{32} = f(\Delta p)$ for two colloid mills of different size. Material system: vegetable oil/water and $\varphi = 0.5$; from [72].

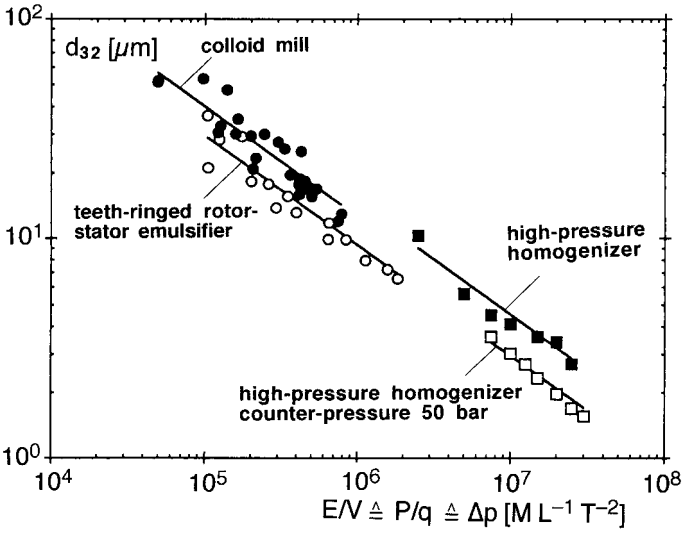


**Fig. 49** Relationship $d_{32} = f(\Delta p)$ for different emulsifiers. ZKDM – teeth ringed rotor-stator emulsifier, CM – colloid mill, HPH – high pressure homogenizer. Details on the material system in text; from [74]

LEO-10). The viscosity of the emulsion was 30 *m*Pa s at $\dot{\gamma} = 1/s$. $\varphi_d$ as well as $\mu/\mu_d$ were proved to be irrelevant. In all measurements a weaker dependence $d_{32}$ ($\Delta p$) than in Fig. 48 was found:

$$d_{32} \propto \Delta p^{-1/2} \tag{12.56}$$

The serious disadvantage of dimensional representations $d_{32}(\Delta p)$, eq. (12.55-56), as compared to the dimensionless one, eq. (12.54), is that these relationships are solely valid for the material system used, for which the physical properties ($\sigma$, $\rho_d$, $\eta_d$) were not even specified. Therefore, a belated conversion in the pi-space, eq. (12.54), is not feasible.

Jet emulsifiers belong to high pressure homogenizers, see **Fig. 50**. They display only one degree of freedom. For them, the same pi-space, eq. (12.53), applies. The coarse emulsion, produced by a nozzle, is conveyed under high pressure through the tiny bore-holes of the jet emulsifier. Extremely high shear forces disintegrate the primary droplets into finer ones and, in this manner, produce a stable, extremely fine emulsion.

**Fig. 51** represents the correlation $d_{32}/d = f(La)$ produced by the emulsification of the material system paraffin oil/water ($\varphi = 0.5$; $\sigma = 0.7$ *m*N/m; emulsifying agent Tween 80/Arlacel 80) in a jet emulsifier with bore-holes of d = 0.75 mm. (In these measurements, d has not been varied!)The result reads [75]:

$$d_{32}/d = 9.15\ La^{-0.6} \qquad Oh,\ \mu_d/\mu = const \tag{12.57}$$

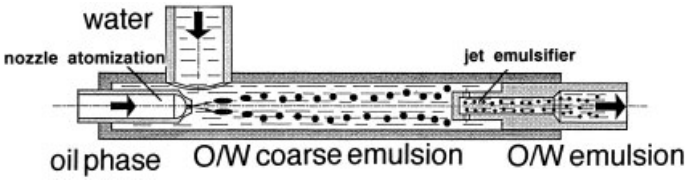


**Fig. 50** Sketch of the jet emulsifier; from [75].

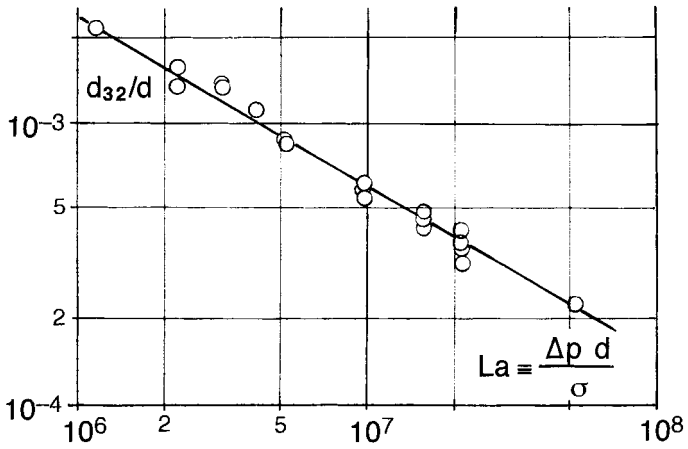


**Fig. 51** Process equation in emulsification with jet emulsifier according to Fig. 50; from [75].The fitting line corresponds to the eq. (12.75).

In [76], the production of an extremely fine polyisocyanate emulsion in polyol with a jet emulsifier is reported. The results obtained are evaluated in the pi-space (12.53). The process equation reads:

$$d_{32}/d = \text{const}\ La^{-0.6}\ Oh^{0.47}\ (\mu_d/\mu)^{0.025} \tag{12.58}$$

Here, the constant is only dependent on the type of apparatus. The remaining pi-numbers, see eq. (12.53), have presumably not been varied.

**Example 30**: Fine grinding of solids in stirred media mills

The fine grinding of solids in mills of different shape and mode of operation is used to produce very fine particles with a narrow particle size distribution. Therefore, as in the previous example, the target quantity is the median value $d_{50}$ of the particle size distribution.

The characteristic *length* of a given mill type is d.

The *physical properties* are given by the particle density, $\rho_p$, the energy per fissure area, $\beta$, and the tensile strength, $\sigma_Z$, of the material. Should there be additional rele-

vant material parameters, these can be easily converted to dimensionless material numbers by the above mentioned ones.

As process parameter, the energy input per unit mass, $E/\rho V$, must be taken into account. The relevance list reads:

$$\{d_{50};\ d;\ \rho_p,\ \beta,\ \sigma_Z;\ E/\rho V\} \tag{12.59}$$

| | $\rho_p$ | $d$ | $\beta$ | $E/\rho V$ | $\sigma_Z$ | $d_{50}$ |
|---|---|---|---|---|---|---|
| M | 1 | 0 | 1 | 0 | 1 | 0 |
| L | –3 | 1 | 0 | 2 | –1 | 1 |
| T | 0 | 0 | –2 | –2 | –2 | 0 |
| M + T/2 | **1** | 0 | 0 | –1 | 0 | 0 |
| 3M + L + 3 T/2 | 0 | **1** | 0 | –1 | –1 | 1 |
| –T/2 | 0 | 0 | **1** | 1 | 1 | 0 |

The pi-set reads

$$\{d_{50}/d,\ (E/\rho V)\rho_p d/\beta,\ \sigma_Z\, d/\beta\} \tag{12.60}$$

Assuming a quasi-uniform energy input in the mill chamber, its characteristic diameter, d, will be irrelevant. Then the pi-set can be reduced to

$$\{(E/\rho V)\rho_p d_{50}/\beta,\ \sigma_Z\, d_{50}/\beta\} \ \rightarrow\ d_{50}(\sigma_Z/\beta) = f\{(E/\rho V)(\rho/\sigma_Z)\} \tag{12.61}$$

In case of unknown physical properties, $\sigma_Z$ and $\beta$, the above dependence is reduced to $d_{50} = f\,(E/\rho V)$ which can then be used for scale-up of a given type of mill and a given grinding material.

For fine and very fine grinding of, e.g., limestone for paper and pottery manufacturing, *bead mills* are widely used. The beads of steel, glass or ceramic have diameters of 0.2–0.3 mm and occupy up to 90 % of the total mill volume ($\phi = 0.9$). The are kept in motion by perforated stirrer discs while the liquid/solid suspension is pumped through the mill chamber.

Mill types frequently in use are the stirred disc mill, centrifugal fluized bed mill, and annular gap mill.

*H. Karbstein* et al. [77] pursued the question of the smallest possible size of a laboratory bead mill which would still deliver reliable data for scale-up. In differently sized model appliances (V = 0.25–25 l), a sludge consisting of limestone ($d_{50}$ = 16 μm) and a 10 % aqueous Luviscol solution (mass portion of solids $\varphi = 0.2$) was examined.

In **Fig. 52** the dependence $d_{50} = f\,(E/\rho V)$ is shown for four stirred disk mills of different sizes. The correlation

$$d_{50} \propto (E/\rho V)^{-0.43} \qquad E/\rho V \leq 10^4 \tag{12.62}$$

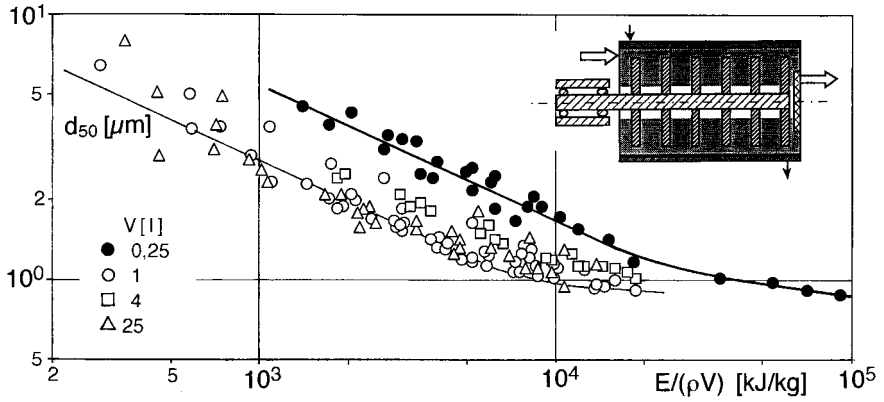


**Fig. 52** Correlation $d_{50}$ (E/ρV) for four differently shaped stirred disk mills; from [77].

also applies to the smallest mill shape (V = 0.25 l), but to obtain the same $d_{50}$ values, a threefold energy input is necessary.

Furthermore, it was found that the correlation (12.62) is valid only for $d_{50} \geq 1$ μm. To obtain even finer particles, a considerably higher energy input as according to (12.62) is necessary. A possible reason for this finding could be that, in this size range, the particle strength has a greater effect. It is also possible that the finest particles escape faster from the working zone between two beads [77].

The same result is also found in centrifugal fluidized bed mills, **Fig. 53**. Finer particles than 1 μm are not produced.

These facts and the scattering of results in differently sized mills made a systematic investigation of the grinding process necessary [78]. The grinding process in bead mills is determined by the frequency and the intensity of the collision between beads and grinding medium. According to this assumption, the grinding result

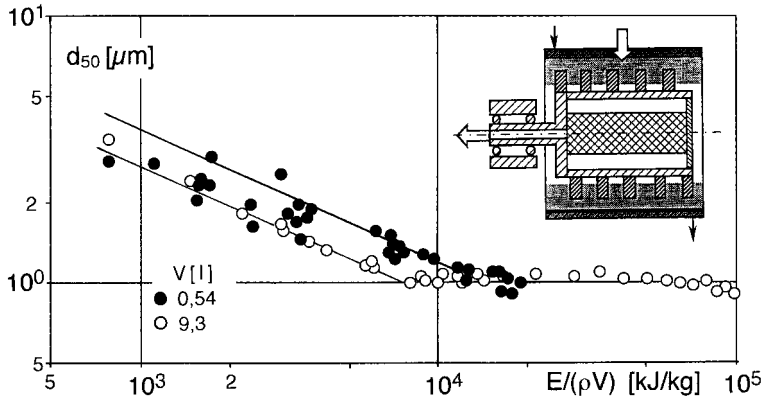


**Fig. 53** The relationship $d_{50}$ (E/ρV) for two centrifugal fluized bed mills of different size, from [77].

remains constant, if both of these quantities are kept constant. The intensity of the collision between beads is essentially given by the kinetic energy of the beads:

$$E_{kin} \propto m_M u^2 \propto V_M \rho_M u^2 \propto d_M^3 \rho_M u^2 \tag{12.63}$$

($d_M$, $\rho_M$ – diameter and density of the beads, u – tip velocity of the stirrer). On the other hand, the collision frequency also depends on the size of the mill chamber and on the overall mass-related energy input. To achieve the same grinding result in differently sized bead mills, $E_{kin}$ as well as $E/\rho V$ have to be kept idem.

The input of mechanical energy can be measured from the torque and the rotational speed of the perforated discs. The kinetic energy can be calculated from eq. (12.63).

The above assumption [78] was convincingly confirmed in a stirred media mill with a perforated stirrer disc of given size (V = 5.54 l) at a constant energy input per unit mass, $E/\rho V = 10^3$ kJ/kg. In batch-wise performed measurements, the kinetic energy of the beads has been varied by the tip speed of the perforated disk stirrers as well as by the density of the grinding media (glass, steel) and, in particular, by the bead diameter ($d_M$ = 97–4 000 μm).

With increasing $E_{kin}$ the particle size diminishes at first, but afterwards increases from a certain $E_{kin}$ value onwards. If one considers the implemented specific energy to be a *product* of the intensity and frequency of the collision between beads and grinding medium, it follows that, at $E/\rho V$ = const and an increasing intensity of the collision, the frequency has to diminish and this results in a coarser product. This also explains why, in the previously discussed investigation [77], particles no finer than $d_{50} \approx 1$ μm were found, see Fig. 52 and 53.

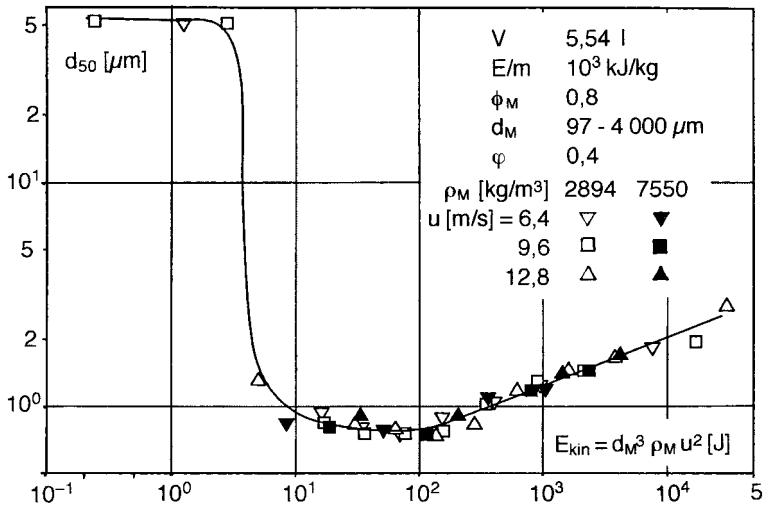


**Fig. 54** The relationship $d_{50}$ ($E_{kin}$) at $E/\rho V = 10^3$ kJ/kg in a stirred media mill with perforated stirrer disc (V = 5,54 l). Limestone/water ($\varphi$ = 0.4; $\phi$ = 0.8); from [78].

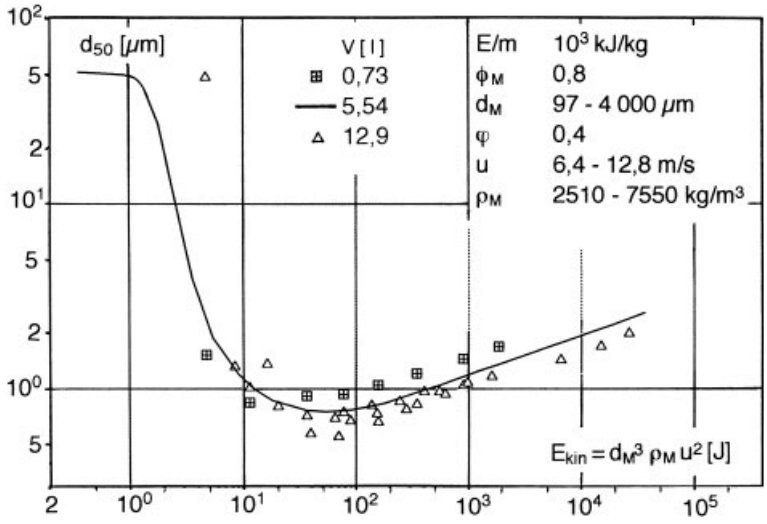


**Fig. 55** The relationship $d_{50}$ ($E_{kin}$) at $E/\rho V = 10^3$ kJ/kg for three differently sized stirred media mills with perforated stirrer discs; from [78].

In **Fig. 55**, the results shown were obtained in three stirred media mills with a perforated stirrer disc of different sizes (V [l] = 0.73; 5.54; 12.9). The results are not satisfactory with respect to the scale-up rule. Here, too, it can be seen that small mills (V < 1 l), under otherwise identical conditions, produce a coarser product than larger ones. A satisfying correlation is achieved by plotting the median particle size, $d_{50}$, versus the mean stress intensity. This is defined as stress intensity of the grinding media multiplied by the term which takes into account the stress intensity distribution [138].

Due to the fact that [78] the energy input was split into mass-related ($E/\rho V$) and kinetic ($E_{kin}$) energies, an earlier paper concerning the emulsification process should also be referred to [79]. As emulsifyer, a teeth-rimed rotor-stator machine was used and the results ($d_{50}$) were correlated with both power per unit volume ($P/V$) and work per unit volume ($P\tau/m^3$). This paper is also of special interest because the evaluation is performed in a dimensional-analytical manner. The dimensionally formulated result reads.

$$d_{50} \propto (E/V)^{-0.3}\,(P/V)^{-0.1} \qquad (12.64)$$

**Example 31**: Scale-up of flotation cells for waste water purification

In this example, the development of a new flotation technique for waste water treatment is discussed. Dimensional analysis has been used since the onset of this work. It concerns the so-called Induced Air Flotation, IAF, which is an alternative to the well-known Dissolved Air Flotation, DAF, the latter being already discussed in Example 7.

This example is divided into three parts. In (a), the development of a new, self-aspirating and radially discharging funnel-shaped nozzle is presented. In (b), a flotation cell with two spatially separated spaces is described. The inner chamber is used for contacting gas bubbles with flocks and the annular ring around it is needed for the tranquilization of liquid throughput. This facilitates the complete separation of the flocks from the biologically purified waste water. It is shown how the flotation kinetics can be determined in this continuously run cell and how this knowledge is used to scale-up a full-scale flotation plant. On the contrary, in (c), data from batch-wise performed experiments are used to evaluate the flotation kinetics and to scale-up continuously run full-scale flotation cells.

**a) Development of a self-aspirating and radially discharging funnel-shaped nozzle**

The funnel-shaped nozzle has been conceived as a means for gas/liquid contacting in a new class of flotation cells for waste water purification and for the removal of activated sludge from biologically purified waste water, see **Fig. 56**. It essentially consists of a cone with an angle of 90° which serves as the deflecting element for the liquid propulsion jet. It is surrounded by a housing which forms, with the cone, an annular channel. According to the *Bernoulli* principle, pressure drop develops at this point and this is used to suck in the gas. The gas/liquid dispersion formed in this manner is discharged radially with a low clearance over the floor of the whole flotation cell. After loosing the kinetic energy of the free jet, it disintegrates to a swarm of tiny gas bubbles which then slowly rise to the surface of the liquid.

The channel of the funnel-shaped nozzle, shown in **Fig. 56 a** [80], displays a constant hydraulic diameter, $D_h = D_a - D_i$. Therefore, the annular cross-sectional area steadily increases towards the cone base; a diffusor is formed.

It turned out that this nozzle produces coarse bubbles which are not able to float very fine or strongly hydrophilic flocks. A nozzle which displays a channel with a constant hydraulic cross-sectional area, $S_h \approx D_a^2 - D_i^2$, see **Fig. 56 b**, serves this purpose better [81]. It also exerts a stronger suction and produces a larger gas throughput. This has to be throttled in order to prevent tiny gas bubbles to coalesce

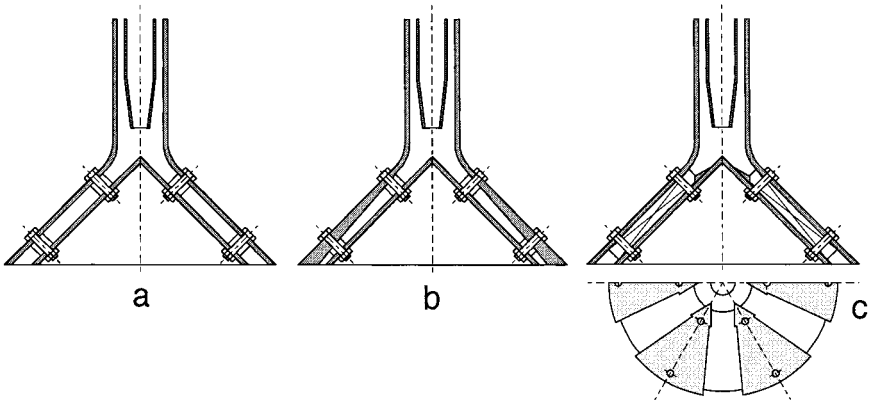


**Fig. 56 a – c** Different designs of the funnel-shaped nozzle for induced air flotation; from [80, 81, 82].

to bigger ones: The gas-side pressure drop, $\Delta p_G$, represents therefore an additional, freely eligible, parameter here.

However, this design has an inherent disadvantage, namely the annular channel at the cone base is compulsorily narrow. With cone base diameters of $D_c >> 0.5$ m, a possible clogging can take place, especially if the nozzle is used for waste water treatment.

The ring channel can be enlargerd to a sufficient extent, if one starts from a constant hydraulic diameter (Fig. 56 a) and divides it into segments ("star-shaped nozzle"); see **Fig. 56 c**. In addition, by the widening of the cone angle at the top of the cone, a trip edge [82] is formed, by which the impinging liquid jet is better spread out over the entire cross-sectional area of the annulus.

The relevance list for the suction characteristic of the "star-shaped nozzle":

| | |
|---|---|
| Target quantity: | self aspirated gas throughput, $q_G$ |
| Geometric parameters: | diameter of the propulsion jet nozzle, d |
| | cross-sectional area of the annular channel, s |
| | number of the segments, z |
| | diameter of the cone base, $D_c$ |
| | ($\triangleq$ channel length $L_c = \sqrt{2}\, D_c/2$) |
| Material parameters: | liquid density, $\rho$ |
| Process-related parameters: | liquid throughput, $q_L$ |
| | liquid head above the nozzle, H′ |
| | gravitational acceleration, g |

This gives:

$$\{q_G, d, s, z, D_c, \rho, q_L, H', g\} \tag{12.65}$$

These nine dimensional parameters deliver the following six pi-numbers:

$$\{q_G/q_L,\ q_L^2/(d^5\, g) \equiv Fr,\ H'/d,\ s^{0.5}/d,\ D_c/d,\ z\} \tag{12.66}$$

Self aspirating devices (hollow stirrers, ejectors, funnel-shaped nozzles) have to overcome the hydrostatic pressure $\Delta p_{hydr} = \rho g\, H'$. This is taken into account by the combination $Fr' \equiv Fr\ (d/H')$. By the way, this extended Froude number, Fr′, represents the reciprocal value of the Euler number, Eu:

$$Fr' \equiv Fr\ (d/H') \equiv \frac{q_L^2}{d^5\, g}\frac{d}{H'} = \frac{q_L^2}{d^4 H' g} = \frac{q_L^2 \rho}{d^4 H' g \rho} = \frac{q_L^2 \rho}{d^4 \Delta p_{hydr}} \equiv Eu^{-1} \tag{12.67}$$

It turned out [81] that the result $(q_G/q_L)$ is independent of whether or not the nozzle *pushes* the gas against the hydrostatic pressure or *sucks* it from a space with lower pressure, $\Delta p_G$. Both pressures have to be taken as sum: $\Sigma\Delta p = \rho g H' + \Delta p_G$. Therefore, the process number Fr′ is expanded as follows:

$$Fr^* \equiv \frac{q_L^2 \rho}{d^4 (\rho g H' + \Delta p_G)} \tag{12.68}$$

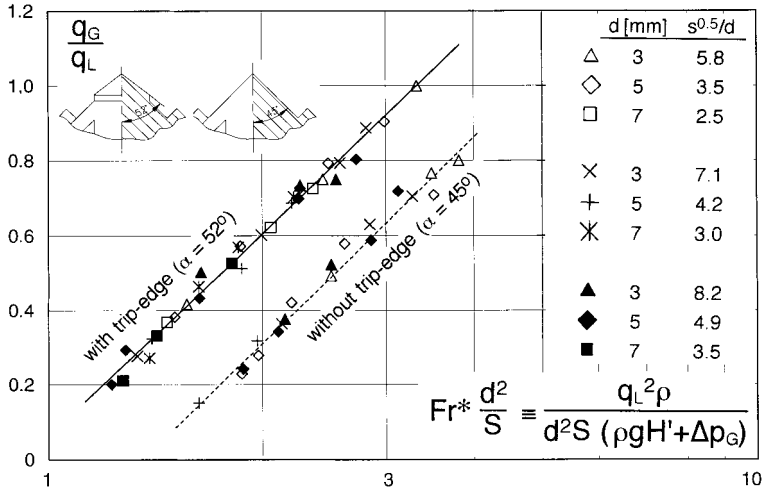


**Fig. 57** Sorption characteristic of the "star-shaped nozzle" with and without a trip edge; after [83].

Furthermore, the number of channels, z, produced by segmentation is combined with the cross-sectional area of the channel, s, to produce the total cross-sectional area, $S = z \times s$, of the "star-shaped nozzle". Preliminary measurements showed that $D_c/d$ does not influence the sucking performance, as long the channels are filled with the dispersion G/L. Therefore, the above 6-parametric pi-space (12.66) is reduced to only a 3-parametric one:

$$\{q_G/q_L, Fr^*, S/d^2\} \tag{12.69}$$

Experiments were carried out with three diameters of the propulsion jet nozzle, d, with different number of channels, z, as well with or without the trip edge. The result is represented in **Fig. 57**. It verifies that the trip edge essentially improves the sucking performance. The fitting line corresponds to the process equation:

$$q_G/q_L = 0.97 \ln (Fr^* d^2/S) + 0.06 \tag{12.70}$$

The parameter $S^{0.5}/d$ was varied within the limits 2.5–8.2. The best result was obtained at the lowest value.

**b) Scaling up a flotation cell with spatially separated aeration and tranquilisation space for continuously carried out induced air flotation (IAF) in waste water treatment**

Following the biological waste water purification, an easy separation of activated sludge flocks can be achieved by flotation. To facilitate this separation, the flotation cell is subdivided into two parts, each having equal superficial areas, **Fig. 58**. The inner cylindrical vessel serves as the aeration chamber, this being equipped with the forementioned funnel-shaped nozzle. Here, particles are brought into intimate con-

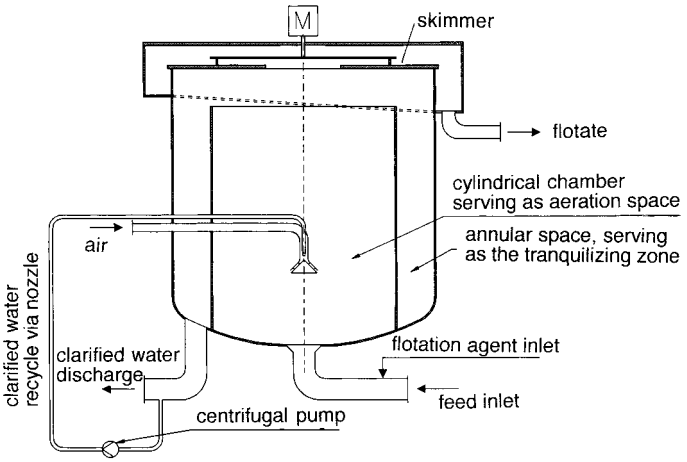


**Fig. 58** Sketch of a flotation cell with spatially separated aeration and final solids separation space; from [84].

tact with gas bubbles, which cause them to float to the surface and are subsequently removed from it with a skimmer. The liquid throughput, already largely freed from solids, passes the adjacent tranquilising annular space from top to bottom (in a counter-current sense to the floating residual flocks). In the upper area of the annular space, the flocks form a filter which supports the separation.

If we assume that the current in the annulus is not back-mixed, then it has a residence time characteristic of an ideal plug flow. Due to the fact that flotation is a depletion process which obeys the 1st order time law, the flotation kinetics is given by the correlation

$$-\ln \frac{\varphi_t - \varphi_\infty}{\varphi_0 - \varphi_\infty} = k_f \tau \tag{12.71}$$

$k_f$ [$T^{-1}$] is the flotation rate constant, $\tau$ [T] is the mean residence time, $\tau = V/q$, and $\varphi$ is the mass portion of solids in the liquid. When liquid samples are taken along the annulus and $\varphi$ is plotted on a single-log-scale according to (12.71), a straight line with the slope of $k_f$ must result in case the above assumptions are fulfilled. In our case, this is fully confirmed, see **Fig. 59**. This graph verifies that the fastest flotation occurs at the lowest gas throughput, because here the bubble coalescence is least marked.

In scaling up of this type of flotation cell, the following must be considered: Both cell spaces should have a flow with a superficial velocity of $v \approx 10$ m/h (resulting in a total superficial velocity of $v \approx 5$ m/h). This guarantees a satisfying separation of the flotate from the liquid throughput. In adddition, the state of flow in the annular space must be laminar. To achieve $Re \approx 2\,000$, an insertion of a tranquilizing grid will possibly be necessary.

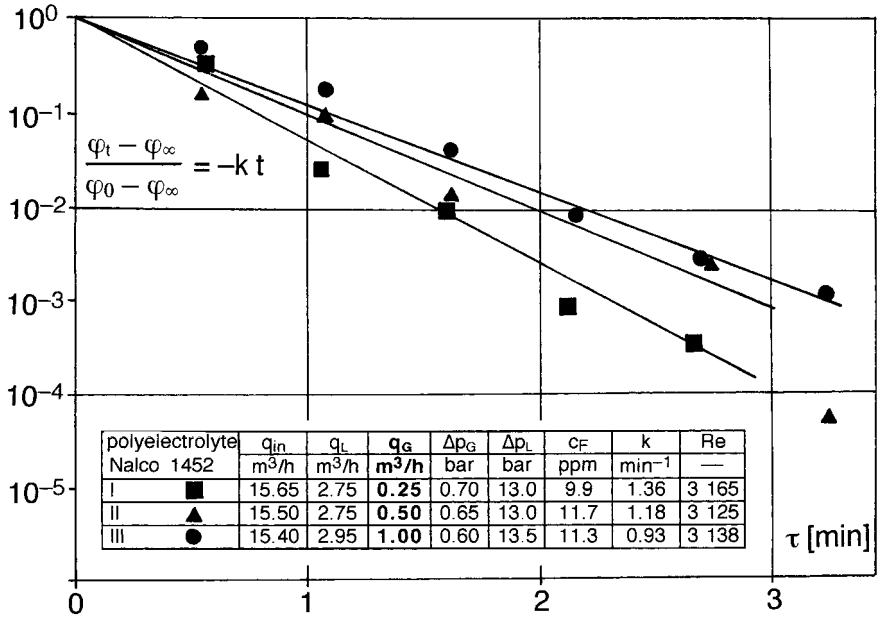


| polyelectrolyte Nalco 1452 | $q_{in}$ $m^3/h$ | $q_L$ $m^3/h$ | $q_G$ $m^3/h$ | $\Delta p_G$ bar | $\Delta p_L$ bar | $c_F$ ppm | k $min^{-1}$ | Re — |
|---|---|---|---|---|---|---|---|---|
| I ■ | 15.65 | 2.75 | **0.25** | 0.70 | 13.0 | 9.9 | 1.36 | 3 165 |
| II ▲ | 15.50 | 2.75 | **0.50** | 0.65 | 13.0 | 11.7 | 1.18 | 3 125 |
| III ● | 15.40 | 2.95 | **1.00** | 0.60 | 13.5 | 11.3 | 0.93 | 3 138 |

**Fig. 59** Flotation kinetics in the material system activated sludge/biologically purified waste water; from [84]. Parameter: gas throughput, $q_G$.

For a given liquid throughput, the superficial area of the flotation cell and its diameter can be calculated from the above details. The cell height, H, results from the measured $k_F\tau$ values according to the following reasoning:

$$\tau = V/q_L = S\,H/q_L;\ q_L = v\,S;\ \tau = H/v \rightarrow H = (k\,\tau)\,v/k_f \qquad (12.72)$$

(S – superficial area) As a rule, the height of the flotation cell will amount to H < 2 m.

Example: $k_f = 1\ min^{-1}$; v = 10 m $h^{-1}$; depletion $\varphi_t/\varphi_0 = 1.0 \times 10^{-4}$: H = 1.53 m

**c) Scaling up of a continuously operating flotation cell on the basis of model experiments performed in batch experiments**

In a laboratory flotation cell (e.g. $200^{\varnothing} \times 300$ mm) with only one space for aeration and flotation (full back-mixing), samples are taken during the flotation experiment and the mass portion of solids in liquid, φ, is determined. In the representation $ln\ \varphi/\varphi_0 = f\,(t)$ a straight line with the slope $k_f$ (flotation rate constant $k_f$ ) results. $k_f$ depends on the material system, on the concentration and nature of flotation aids (flocculants) as well on the process parameters $q_L$, $q_G$ and g. Interestingly, in all investigated material systems (dye pigments, plastic particles, printers ink, film emulsions, i.e. Hg halogenides in gelatine) the same proportionality was found:

$$k_f \propto q_G\, q_L^2 \tag{12.73}$$

see **Fig. 60**. This expression (12.73) reads in a dimensionless form as:

$$k_f^* \propto \frac{q_G}{q_L}\, Fr^{3/2} \tag{12.74}$$

$k_f^*$ indicates that $k_f$ [$T^{-1}$] can always be transformed into a pi-number with the aid of pertinent material parameters (this has been omitted here for simplicity). The inspection of this correlation in two geometrically similar flotation cells ($\mu = 1 : 2$) gave proof that this approach is correct, see **Fig. 61**.

If the dependence (12.74) is known, a batch-wise operated full-scale flotation cell can be scaled up according to (12.74).

A continuously operated flotation cell with fully back-mixed contents – or a cells-in-series arrangement with N equally sized cells, respectively – is scaled up according to the same recipe as 1st order chemical reactions:

$$N = 1:\ \tau \equiv \frac{V}{q} = \frac{1}{k_f}\frac{\varphi_0 - \varphi}{\varphi} \tag{12.75}$$

$$N = N:\ \tau \equiv \frac{V}{q} = \frac{1}{k_f}\frac{\varphi_{N-1} - \varphi_N}{\varphi_N} \tag{12.76}$$

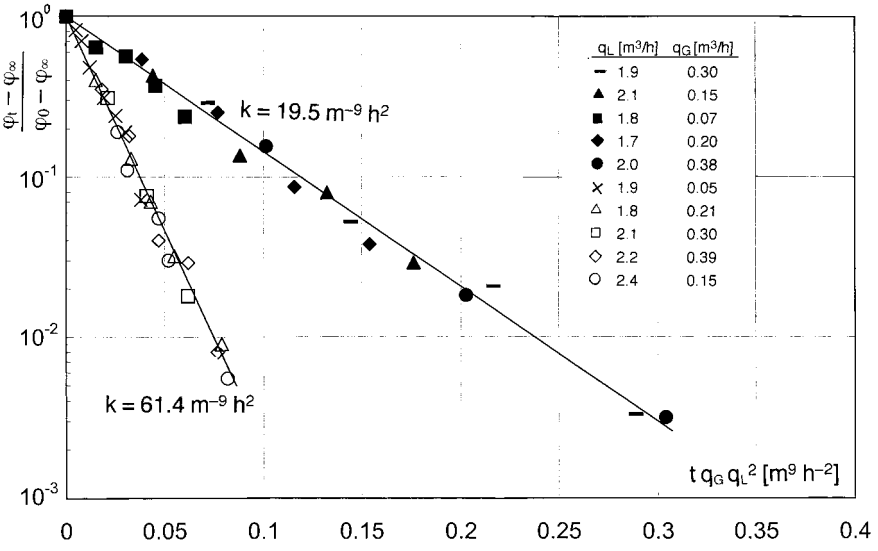


**Fig. 60** Dependence of flotation kinetics on process conditions ($q_G$, $q_L$) in a batch process. *Full signs*: Cell (0.5$^{\varnothing}$ × 0.6 m) with a "star-shaped nozzle" according to Fig. 52 c, $D_c$ = 80 mm; throttling of $q_G$. Material system: waste water from a printing works with 5–6 g TS/l, flocculant: 45 ppm Peratom 815 of Henkel/Düsseldorf; from [83].

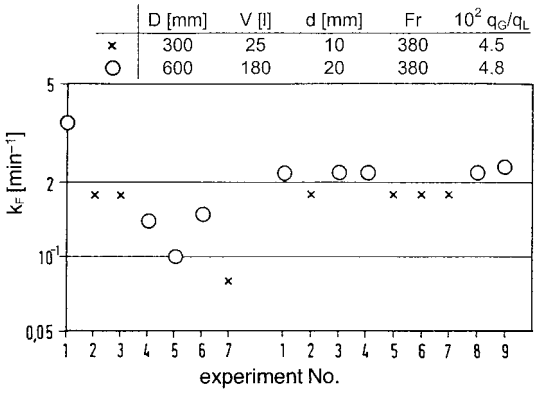


**Fig. 61** Checking of the correlation $k_f \propto (q_G/q_L)\ Fr^{3/2}$ in two geometrically similar flotation cells ($\mu = 1 : 2$). Material system: Washing water from the production of the film emulsion (AGFA) with ca. 25 mg Ag/l; from [86].

For the mass portion of solids, $\varphi_N$, in the outlet from a N cells-in-series it follows:

$$\varphi_N = \frac{\varphi_0}{(1+k_f\tau)^N} \tag{12.77}$$

*Remaining signs*: Cell ($0.2^{\varnothing} \times 0.2$ m) with a funnel-shaped nozzle according to Fig. 52 a, $D_c$ = 60 mm; no throttling of $q_G$. Material system: Process waters from Novodur® pigment production with ca. 4 g TS/l, flocculant: 410 ppm RO + 15 ppm 417 S of Stockhausen/Krefeld; from [85].

With the aid of correlations (12.75) and (12.76) as well as knowing the $k_f$ value and the accepted $\varphi$ value of the outlet ($\varphi$ or $\varphi_N$), the mean residence time, $\tau$, of the liquid throughput, q, as well the liquid volume of the flotation cell, $V = \tau\, q$, can be calculated. To ascertain the same $k_f$ value in all cells, $(q_G/q_L)\ Fr^{3/2}$ = idem must be kept.

**Example 32**: Description of the temporal course of spin drying in centrifugal filters

The centrifugal filter represents the most frequently used filter centrifuge operating on a horizontal axis. The operating cycle consists of loading, wet spin, cake wash, dry spin, and unloading (peel out). The dry spin requires most time. It consists of the rapid draining of the mother liquor from the capillary spaces and the slow draining of the surface liquor. The dry spin, which governs the flow rate, has been completed when the equilibrium residual moisture, $w_\infty$, is attained in the filter cake.

Before considering the dry spin process in a dimensional analysis, some terms have to be explained and defined.

1. Centrifugal acceleration, b [$LT^{-2}$], is expressed by the multiple (z) of gravitational acceleration g: $b = z\ g$
2. The specific filter cake resistance, $\alpha$ [$L^{-2}$], is defined with the equation describing the pressure loss, $\Delta p$, of the liquid in the porous filter cake at laminar flow:

$$\Delta p = \alpha\, v\, \mu\, h \tag{12.78}$$

$v \equiv q/S$ – liquid flow rate q related to the filter surface S; h – cake height; $\mu$ – dynamic viscosity.

3. The porosity, $\varepsilon$ [–], of the filter cake is defined as the ratio of pore volume to total volume.
4. The residual moisture, w [–], of the filter cake reflects the ratio of liquid mass to solid mass.
5. The degree of saturation, S [–], is defined as the ratio of the pore volume filled with liquid to the total pore volume:

$$S = w \frac{\rho_s}{\rho_w} \frac{(1-\varepsilon)}{\varepsilon} = \frac{w}{w_{max}} \tag{12.79}$$

whereby $\rho_s$ and $\rho_w$ are the densities of solid matter and water, respectively, and $w_{max}$ is the cake moisture at saturation.

Equilibrium saturation of the cake, $S_\infty \equiv w_\infty/w_{max}$, will initially depend on the physical properties of the filter cake. They are characterized by $\alpha$, $\varepsilon$, $\Theta$ and K. $\Theta$ represents the contact angle (degree of wettability) and K any other grain parameters such as roughness and so on. Furthermore, the physical properties of the wash liquid (density, $\rho$, and surface tension, $\sigma$) and, finally, centrifugal acceleration, b, as process parameter will be of importance:

$$\{S_\infty;\ \alpha,\ \varepsilon,\ \Theta,\ K,\ \rho,\ \sigma;\ b\} \tag{12.80}$$

Four of these eight process-relevant variables are dimensionless, the other four form only one further pi-number:

| | $\rho$ | $\alpha$ | ***b*** | $\sigma$ |
|---|---|---|---|---|
| M | 1 | 0 | 0 | 1 |
| L | –3 | –2 | 1 | 0 |
| T | 0 | 0 | –2 | –2 |
| M | **1** | 0 | 0 | 1 |
| –(3M + L + T/2)/2 | 0 | **1** | 0 | –1 |
| –T/2 | 0 | 0 | **1** | 1 |

$$\Pi_1 \equiv \frac{\sigma\, \alpha}{\rho\, b}$$

From the relevance list (12.80) it follows that:

$$S_\infty \equiv w_\infty/w_{max} = f\,(\Pi_1, \varepsilon, \Theta, K) \tag{12.81}$$

Tests [87] have shown that this relationship is described by the analytical expression

$$S_\infty = \Pi_1^{0.2}\, f\,(\varepsilon, \Theta, K) = \left(\frac{\sigma\, \alpha}{\rho\, b}\right)^{0.2} f\,(\varepsilon, \Theta, K) \tag{12.82}$$

and hence by

$$S_\infty = \text{const}\ (1/z)^{0.2} \tag{12.83}$$

whereby $z = b/g$. Of course, the numerical values of the constants and the exponent are dependent on the material system under examination.

In order to track the time course of the dewatering process up to an average degree of saturation, $S_m \equiv w_m/w_{max}$, the parameters time t, viscosity μ of the wash liquid and the geometric parameters of the cake (cake height, h, and cake residual height, $h_0$, remaining after peel out) must be added to the above relevance list. Since we are dealing with a creeping flow in the centrifugal field, ρ is only effective in combination with b: ρb; compare the form of $\Pi_1$. Apart from the obvious geometric numbers $h/h_0$ and $\alpha h^2$ and the dimensionless parameters $S_m$, ε, Θ, K, two further numbers will be involved:

| | ρ***b*** | α | ***t*** | σ | μ |
|---|---|---|---|---|---|
| M | 1 | 0 | 0 | 1 | 1 |
| L | –2 | –2 | 0 | 0 | –1 |
| T | –2 | 0 | 1 | –2 | –1 |
| M | **1** | 0 | 0 | 1 | 1 |
| –(2 M + L)/2 | 0 | **1** | 0 | –1 | –1/2 |
| 2 M + T | 0 | 0 | **1** | 0 | 1 |

$$\Pi_1 \equiv \frac{\sigma\alpha}{\rho b} \qquad \Pi_2 \equiv \frac{\mu\alpha^{1/2}}{\rho b t} \tag{12.84}$$

$\Pi_1$ is the same number as that formed before. The complete pi-set is now:

$$\{S_m,\ h/h_o,\ \alpha h^2,\ \varepsilon,\ \Theta,\ K,\ \Pi_1,\ \Pi_2\} \tag{12.85}$$

The tests [87] were performed with small acryl glass spheres of $d_p = 20$–$50$ μm. The material numbers ε, Θ, K remained unchanged. However, $h/h_0$, $\alpha h^2$, $\Pi_1$ and $\Pi_2$ were varied by changing b, t and h. It was found that the test results can be correlated in the pi-space $\{S_m, \Pi_2, \alpha h^2\}$, i.e., neither $\Pi_1$ nor $h/h_0$ is significant. **Fig. 62** shows this result. The reciprocal value of $\Pi_2$ $(\alpha h^2)^{0.5} \equiv [\rho b\ t/(\mu\ \alpha\ h)]^{-1}$ is plotted on the abscissa. The process equation reads:

$$S_m = 0.26\ \left(\frac{\rho\ b\ t}{\mu\ \alpha\ h}\right)^{-2/3} \tag{12.86}$$

The irrelevance of $h_0$ is not surprising if the solid particles are neither damaged nor compressed in the peel out process and if the capillary rise height is $<< h_0$. The above pi-space should also apply for filter cakes which can be compressed to a greater extent [87]. The fact that $\Pi_1$ is not significant at total wetting, can only document the irrelevance of σ during the dry spin process.

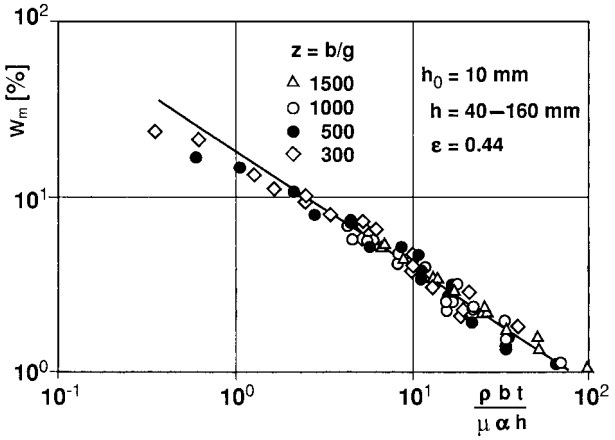


**Fig. 62** Temporal course of the average residual moisture, $w_m$, as a function of $\rho b\, t/(\mu\, \alpha\, h)$ for given geometric and material conditions at centrifugal accelerations of b = 300–1500 g; from [87].

**Example 33: Description of particle separation by means of inertial forces**

Let us consider the separation of aerosols (droplet size $d_P$ = 0.2 – 20 μm) from a gas stream in a dust separator (e.g. wire filter, cyclone, etc.). The result, the *"fractional degree"* $\eta_f$, is characterized by $\eta_f = (\varphi_{in} - \varphi_{out})/\varphi_{in}$.

This target quantity is dependent on the following quantities:

| | |
|---|---|
| g*eometric* parameters: | particle diameter, $d_P$ and a characteristic length, D, of the separator |
| p*hysical* properties: | particle density, $\rho_p$, density, ρ, and viscosity, μ, of the gas |
| p*rocess* parameters: | gas velocity, v, *or* the pressure drop $\Delta p \propto v^{\alpha}$ ($\alpha$ = 1–2) because this variable is characteristic of the separating device. |

This seven parametric relevance list

$$\{\eta_f;\ d_p,\ D;\ \rho_p,\ \rho,\ \mu;\ \Delta p\} \tag{12.87}$$

can be streamlined by a closer examination of the problem and by preliminary tests:

1. For sufficiently small particles *Stokes*'s law applies. According to this, the *frictional force* is $F_{fr} = 6\,\pi\, r\, \mu\, v = 3\,\pi\, d_P\, \mu\, v$. At the same time, the *inertial force* is $F_{mass} = m\, b = (\pi/6)\, \rho_p\, d_p^3\, b$.
   In the steady-state $F_{fr} = F_{mass}$. For the *settling velocity*, it follows that $v = \rho_p\, d_p^2\, b/(18\, \mu)$. From this we can deduce that $v \propto \rho_p d_p^2$.
2. The gas velocity, v, and the pressure drop, Δp, these being necessary for the separation of a specific limiting droplet size (e.g., $d_{50}$), decrease with $d_p$ and

are strongly dependent on the type of separator device: $\Delta p \propto d_p^{-3} \rightarrow \Delta p\, d_p^3 = \text{const}$ (geometry).

Since the particle size is bound by both $\rho_p\, d_p^2$ and $\Delta p\, d_p^3$, we can combine these two requirements to obtain:

$$\rho_p^3\, d_p^6\, \Delta p^2 \tag{12.88}$$

As a result of closer examination (1) and preliminary tests (2), the above 7-parametric relevance list can be reduced to the following 5-parametric one:

$$\{\eta_f;\ D;\ \rho,\ \mu;\ \rho_p^3\, d_p^6\, \Delta p^2\} \tag{12.89}$$

Since the target number $\eta_f$ is dimensionless, we only have to form one single process number:

| | $\rho$ | $D$ | $\mu$ | $\rho_p^3\, d_p^6\, \Delta p^2$ |
|---|---|---|---|---|
| M | 1 | 0 | 1 | 5 |
| L | –3 | 1 | –1 | –5 |
| T | 0 | 0 | –1 | –4 |
| M + T | **1** | 0 | 0 | 1 |
| 3 M + L + 2 T | 0 | **1** | 0 | 2 |
| –T | 0 | 0 | **1** | 4 |

$$A \equiv \frac{\rho_p^3\, d_p^6\, \Delta p^2}{\rho D^2\, \mu^4} \tag{12.90}$$

We will first draw the square root of this dimensionless group and then relate it to the well-known Euler, Reynolds and Stokes numbers:

$$Eu \equiv \Delta p/(\rho\, v^2); \quad Re \equiv v\, D\, \rho/\mu; \quad Sto \equiv \rho_p\, d_p^2\, v/(D\, \mu).$$

It follows that

$$A^{1/2} \equiv \frac{d_p^3\, \rho_p^{3/2}\, \Delta p}{\rho^{1/2} \mu^2 D} \equiv Eu\, Re^{1/2}\, Sto^{3/2}. \tag{12.91}$$

*Bürkholz* [88] calls this combination of dimensionless numbers the "deposition number" ${\Psi_A}^{3/2}$.

Furthermore, the dimensionless number $A^{1/2}$ indicates the existence of the relationship $\Delta p \propto D$. For each desired fractional degree of separation, the necessary pressure drop, $\Delta p$, is proportional to the characteristic linear dimension D. Different separator types can therefore be compared if D is selected sensibly, see [88].

The significance of this "deposition number" is impressively demonstrated by the comparison in **Fig. 63**. To obtain the particle diameter $d_p$ with the 1st power, the abscissa is transformed to $A^{1/6} \triangleq {\Psi_A}^{1/2}$.

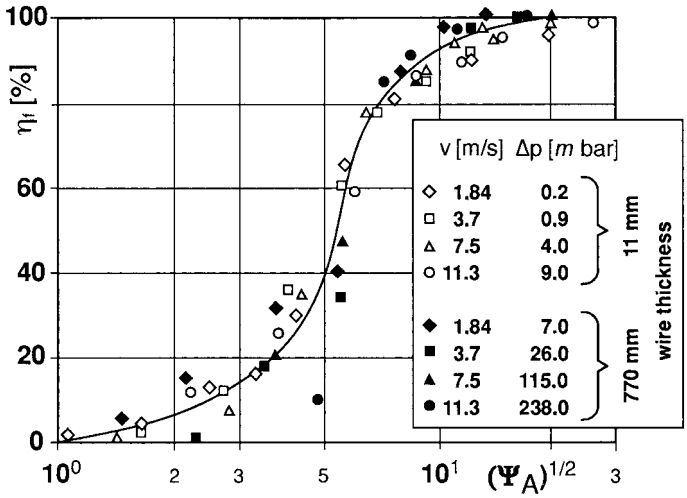


**Fig. 63** Fractional degree of separation, $\eta_f$, of two differently thick filters (11 and 770 mm) having the same wire thickness. Correlation of the measurements by means of the number $A^{1/6} \triangleq \Psi_A{}^{1/2}$; from [88].

**Example 34**: Gas hold-up in bubble columns

Bubble columns are important appliances for the absorption of gases in liquids and, consequently, for the execution of chemical reactions in gas/liquid system. In this context, the attainable interface (≙ sum of the surfaces of all gas bubbles) is of most interest because it affects the mass flow in a directly proportional manner. If a gas throughput q is introduced into a bubble column with the diameter D and the liquid height H, the liquid height rises by the amount occupied by the gas bubbles in the liquid. The gas fraction in the liquid, the so-called gas hold-up $H^*$ can be determined from the liquid height $H_b$ of the gassed and the non-gassed liquid (see sketch).

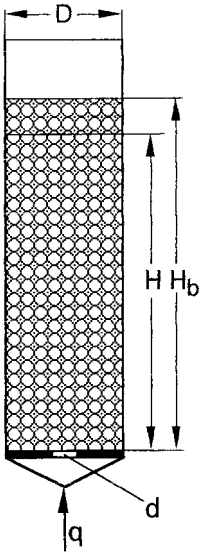


$$H^* \equiv \frac{V_G}{V_L} = \frac{H_b - H}{H} \tag{12.92}$$

In the course of extensive measurements on bubble columns with different dimensions [89], the gas hold-up $H^*$ proved to be directly proportional to the volume-related mass transfer coefficient $k_La$. For this reason, $H^*$ will be the *target number* in the following considerations.

Bubble columns with a single-hole plate as gas distributor (see sketch) were used in these investigations. D, H and d (= hole diameter) therefore describe their *geometry* in full.

The densities (ρ and ρ′) and the viscosities (ν and ν′) of both phases (′ gas) and the surface tension, σ, must be taken into account as *physical properties*.

The *process parameters* are the gas throughput q and, on account of the extreme differences in density, the gravity difference $g\Delta\rho = g\,(\rho - \rho')$.

The complete relevance list is therefore:

$$\{H^*;\ D,\ H,\ d;\ \rho,\ \rho',\ \nu,\ \nu',\ \sigma;\ q,\ g\Delta\rho\} \tag{12.93}$$

If we exclude the target number $H^*$ and the trivial numbers H/D, d/D, $\rho'/\rho$ and $\nu'/\nu$, the remaining relevance list is

$$\{D;\ \rho,\ \nu,\ \sigma;\ q,\ g\Delta\rho\} \tag{12.94}$$

from which, via the dimensional matrix, the following three dimensionless numbers result:

| | $\rho$ | ***D*** | $\nu$ | $\sigma$ | ***q*** | $g\Delta\rho$ |
|---|---|---|---|---|---|---|
| M | 1 | 0 | 0 | 1 | 0 | 1 |
| L | –3 | 1 | 2 | 0 | 3 | –2 |
| T | 0 | 0 | –1 | –2 | –1 | –2 |
| M | **1** | 0 | 0 | 1 | 0 | 1 |
| 3M + L + 2 T | 0 | **1** | 0 | –1 | 1 | –3 |
| –T | 0 | 0 | **1** | 2 | 1 | 2 |

$$\Pi_1 \equiv \frac{\sigma D}{\rho\nu^2} \equiv \frac{Re^2}{We} \qquad \Pi_2 \equiv \frac{q}{D\nu} \equiv Re \qquad \Pi_3 \equiv \frac{g\Delta\rho D^3}{\rho\nu^2} \equiv Ar \equiv \frac{Re^2}{Fr} \tag{12.95}$$

This dimensional analysis produces two dimensionless numbers, $\Pi_1$ and $\Pi_3$, which, apart from the column diameter, contain only physical properties, and the Reynolds number $\Pi_2$ as the process number (because it contains q).

However, this is unsatisfactory because we must expect the hydrodynamics of a bubble column to be substantially governed by $g\Delta\rho$. Consequently, the process number must contain $g\Delta\rho$. We must therefore combine $\Pi_2$ and $\Pi_3$ in order to obtain the modified Froude number $Fr^*$, which is probably the *true process number*:

$$\Pi_2^2\,\Pi_3^{-1} \equiv \frac{q^2\rho}{D^5 g\Delta\rho} \equiv Fr^* \tag{12.96}$$

The complete pi-set now becomes:

$$\{H^*;\ H/D,\ d/D;\ \rho'/\rho,\ \nu'/\nu,\ Fr^*,\ Re,\ We\}$$

Comprehensive measurements [89] were performed to verify this pi-space and to evaluate the following process characteristics:

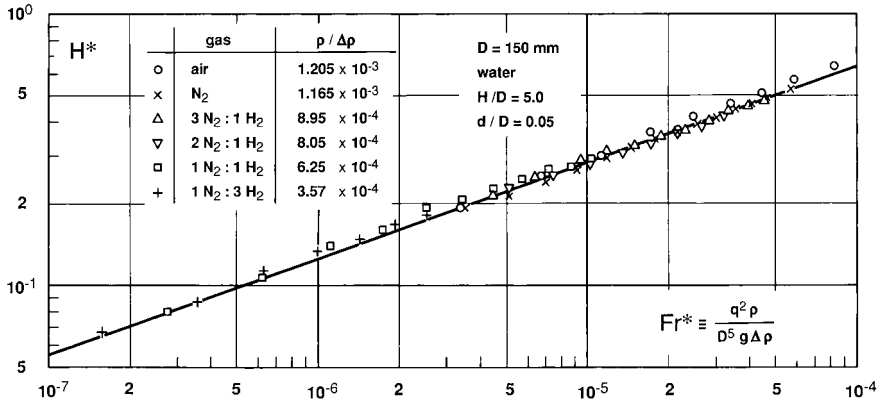


**Fig. 64** The relationship $H^*(Fr^*)$ confirms the expectation that the gas hold-up $H^*$ in a bubble column is dependent on the process number $Fr^*$; from [89].

a) The relationship $H^* = f(Fr^*)$ was examined using a bubble column of given geometry; water was used as the liquid and the physical properties of the gas were varied over a wide range. Air, nitrogen and nitrogen/hydrogen mixtures were used. The result in **Fig. 64** demonstrates that $Fr^*$ takes full account of the influence of both densities and that $\nu'/\nu$ is obviously irrelevant. The process equation is:

$$H^* = 15.0\ Fr^{*0.35} \tag{12.97}$$

b) Further measurements were carried out with one single material system (water/air) in bubble columns of different geometries, see **Fig. 65**. The extended process relationship now reads:

$$H^* = 16.7\ Fr^{*0.35}\ (H/D)^{-0.25}\ (d/D)^{-0.125} \tag{12.98}$$

As far as the scale-up of a bubble column from a laboratory to an industrial scale is concerned, one will have to keep in mind that the scale-up rule is not $v$ = idem, as is often stated in the chemical-engineering literature, but $Fr \equiv v^2/(d\,g)$ = idem. This means:

$$v_T = v_M \sqrt{d_T/d_M} = v_M\ \mu^{0.5} \tag{12.99}$$

c) The influence of the physical properties of the liquid phase was also investigated in one single model bubble column using water and, in addition, 12 different pure organic liquids, the physical characteristics of which varied substantially, see Table 2 in [89]. The result of these measurements is presented in **Fig. 66**. The dimensionless numbers had to be combined as follows in order to correlate the measured values:

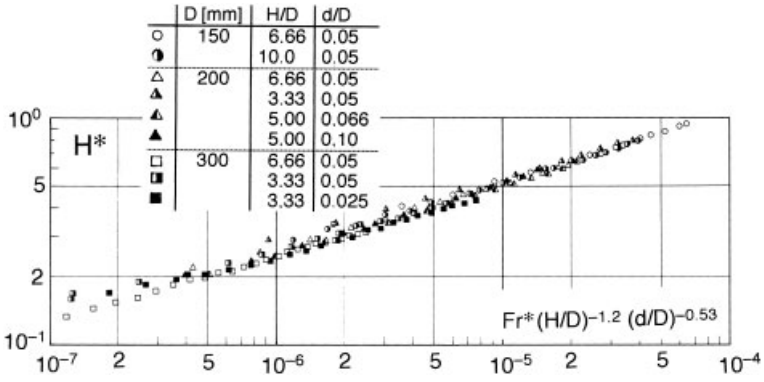


**Fig. 65** Dependence of the gas hold-up $H^*$ on the geometry of the column; from [89].

$$B \equiv \frac{\rho/\rho' \, Fr^*}{ReWe^{0.5}} \equiv \frac{\nu(\sigma\rho)^{0.5}}{D^{2.5} g \Delta\rho} \tag{12.100}$$

The disadvantage of the resulting number combination B is that it is not a pure material number, but still contains the column diameter, D. For safe scale-up, the validity of this correlation will therefore have to be checked on columns of different diameters and with simultaneous alteration of the material system.

The correlation from Fig. 66 may give the impression that it will always be possible to depict an n-digit pi-space two-dimensionally using the analytical evaluation. This is not necessarily the case. The more complicated the physical facts are, the more incomplete the analytical description and depiction will be. Indeed, it is quite easy to imagine situations where this will not even be possible. One example is the pressure drop characteristic of the straight, smooth pipe in Fig. 1, the analytical reproduction of which is likely to cause considerable problems!

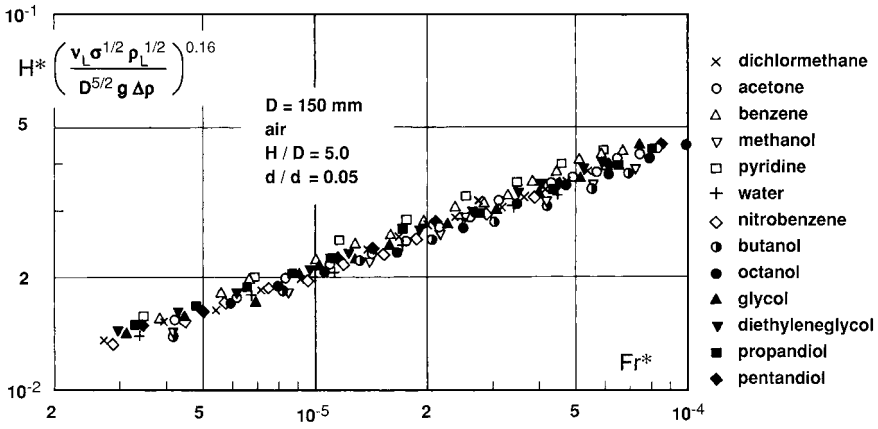


**Fig. 66** Influence of the physical properties of both phases on the gas hold-up $H^*$ in a bubble column of given geometry, from [89].

*Scale-up in Chemical Engineering.* Marko Zlokarnik


ISBNs: 3-527-30266-2 (Hardback); 3-527-60056-6 (Electronic)

# 13
# Selected Examples of the Dimensional-analytical Treatment of Processes in the Field of Thermal Unit Operations

**Introductory remark**

Besides fluid mechanics, thermal processes also include mass transfer processes (e.g. absorption or desorption of a gas in a liquid, extraction between two liquid phases, dissolution of solids in liquids) and/or heat transfer processes (energy uptake, cooling, heating, drying). In the case of thermal separation processes, such as distillation, rectification, extraction, and so on, mass transfer between the respective phases is subject to *thermodynamic laws* (phase equilibria) which are obviously not scale dependent. Therefore, one should not be surprised if there are no scale-up rules for the pure rectification process, unless the hydrodynamics of the mass transfer in plate and packed columns are under consideration. If a separation operation (e.g. drying of hygroscopic materials, electrophoresis, etc.) involves simultaneous mass and heat transfer, both of which are scale-dependent, the scale-up is particularly difficult because these two processes obey different laws.

Heat transfer processes are described by physical properties and process-related parameters, the dimensions of which not only include the base dimensions of Mass, Length and Time but also Temperature, $\Theta$, as the fourth one. In the discussion of the heat transfer characteristic of a mixing vessel (Example 20) it was shown that, in the dimensional analysis of thermal problems, it is advantageous to expand the dimensional system to include the amount of heat, H [kcal], as the fifth base dimension. *Joule*'s mechanical equivalent of heat, **J**, must then be introduced as the corresponding dimensional constant in the relevance list. Although this procedure does not change the pi-space, a dimensionless number is formed which contains **J** and, as such, frequently proves to be irrelevant. As a result, the pi-set is finally reduced by one dimensionless number.

**Example 35**: Steady-state heat transfer in bubble columns

The heat transfer characteristic of a mixing vessel (Example 20) is represented by the pi-space:

$$\{\mathrm{Nu}, \mathrm{Pr}, \mathrm{Re}, \mathrm{D/d}, \gamma_0 \Delta T\}$$

see eq. (9.10). Instead of $\gamma_0 \Delta T$ the pi-number Vis $\equiv \mu_w/\mu$ is normally used (see Example 15). Due to the material system water/air, in this example this number will be ignored.

The pi-space of a heat transfer characteristic of a bubble column is different to that of a mixing vessel in that the pertinent process quantity is the gas throughput q. In addition, because of the extremely large density differences in the material system G/L, $g\Delta\rho$ will also play a decisive role:

| | |
|---|---|
| Target quantity: | heat transfer coefficient, h |
| Geom. parameter: | column diameter, D |
| Physical properties: | density, $\rho$, and viscosity, $\mu$, of the liquid |
| | heat capacity, $C_p$, and conductivity, k |
| Process parameters: | Gas throughput, q |
| | Gravity difference, $g\Delta\rho$ |

$$\{h; D; \rho, \mu, C_p, k; q, g\Delta\rho\} \tag{13.1}$$

This 8-parametric set delivers the following four pi-numbers:

| | |
|---|---|
| $Nu \equiv h\ D/k$ | Nusselt number |
| $Pr \equiv C_p\ \mu/k$ | Prandtl number |
| $Re \equiv q\ \rho/(D\ \mu)$ | Reynolds number |
| $Fr^* \equiv q^2\ \rho/(D^5\ g\Delta\rho)$ | Froude number |

$$\{Nu, Pr, Re, Fr^*\} \tag{13.2}$$

*W. Kast* [90] found that in bubble columns the intensity variable superficial velocity, $v \propto q/D^2$, is also decisive for heat transfer. (The same was found for mass transfer in bubble columns, see Example 10 and Example 38). From the dimensional analysis point of view, v is an intermediate variable, the introduction of which reduces the above 4-parametric pi-space to a 3-parametric one. For this purpose, first the two q containing numbers have to be formulated with v instead of q:

| | |
|---|---|
| $Re \equiv v\ D\ \rho/\mu$ | Reynolds number |
| $Fr^* \equiv v^2\ \rho/(D\ g\Delta\rho)$ | Froude number |

By the combination of the three D containing numbers (Nu, Re, $Fr^*$), D can be eliminated, which leads to the following two pi-numbers:

$$St \equiv \frac{Nu}{RePr} = \frac{h}{v\rho C_p} \quad \text{Stanton-Kennzahl}$$

$$ReFr^* \equiv \frac{v^3}{vg}\ \frac{\rho}{\Delta\rho}$$

This leads to the following pertinent pi-space:

$$\{St, Pr, ReFr^*\} \tag{13.3}$$

We would have obtained this 3-parametric pi-set if we had correspondingly rearranged the relevance list:

$$\{h; \rho, \mu, C_p, k; \nu, g\Delta\rho\} \tag{13.4}$$

| | $\rho$ | $\mu$ | $g\Delta\rho$ | $C_p$ | $h$ | $k$ | $\nu$ |
|---|---|---|---|---|---|---|---|
| M | 1 | 1 | 1 | 0 | 1 | 1 | 0 |
| L | –3 | –1 | –2 | 2 | 0 | 1 | 1 |
| T | 0 | –1 | –2 | –2 | –3 | –3 | –1 |
| $\Theta$ | 0 | 0 | 0 | –1 | –1 | –1 | 0 |
| $Z_1$ | **1** | 0 | 0 | 0 | 1/3 | 0 | –2/3 |
| $Z_2$ | 0 | **1** | 0 | 0 | 1/3 | 1 | 1/3 |
| $Z_3$ | 0 | 0 | **1** | 0 | 1/3 | 0 | 1/3 |
| $-\Theta$ | 0 | 0 | 0 | **1** | 1 | 1 | 0 |

$Z_1 = M + T + A - 4/3\ \Theta \qquad Z_2 = 3M + L + T + A + 2/3\ \Theta$
$Z_3 = A + 2/3\ \Theta \qquad A = -1/3\ (3M + L + 2T)$

$$\Pi_1 = \frac{h}{(\rho\,\mu\,g\Delta\rho)^{1/3} C_p} \qquad \Pi_2 = \frac{k}{\mu\, C_p} \qquad \Pi_3 = \frac{\nu\rho^{2/3}}{(\mu\, g\Delta\rho)^{1/3}}$$

$$\Pi_1 \Pi_3^{-1} = \frac{Nu}{RePr} \equiv St \qquad \Pi_2 \equiv Pr^{-1} \qquad \Pi_3^3 \equiv ReFr^*$$

This dimensional analysis is only briefly presented here, because it leads to pi-expressions with broken exponents.

The evaluation of test results [90] in **Fig. 67** shows that the 3-dimensional pi-space can be further reduced to a 2-dimensional one through the product combination of Re Fr $Pr^2$. Apart from his own measurements, *Kast* also included extensive experimental material by *Kölbel* et al. [91]. The correlation

$$St \propto \left[\sqrt[3]{(ReFr^*)Pr^2}\right]^{2/3}$$

leads to the dependence $h \propto \nu^{1/3}$ when the same material system is used.

*Zlokarnik* [58/2] determined the heat transfer characteristic of a mixing vessel, equipped with a self-aspirating hollow stirrer, using the material system water/air. This enables a direct comparison between the heat transfer behavior in a stirring vessel at gassing and a bubble column. **Fig 68** shows that in gas/liquid contacting in a mixing vessel, approximately twice as much heat can be transferred through the

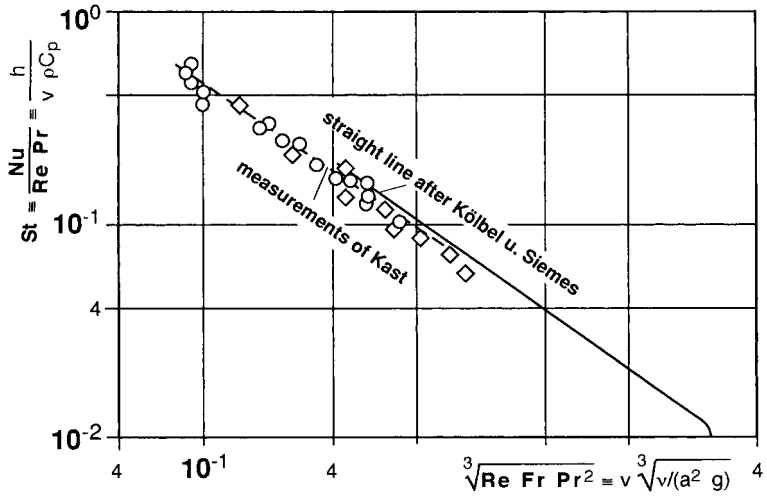


**Fig. 67** Heat transfer characteristic of a bubble column, from [90]. $a \equiv k/(\rho C_p)$ – thermal diffusivity

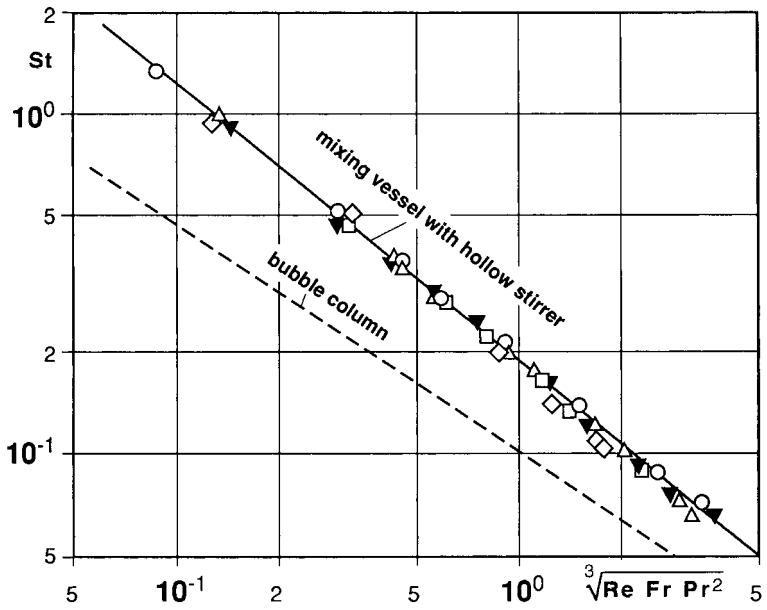


**Fig. 68** Comparison of the heat transfer behaviour of a mixing vessel with a self-aspirating hollow stirrer [58/2] and a bubble column [90].

wall as in a bubble column. Besides this, $h \propto v^{1/5}$ applies here. This also confirms that the hydrodynamics in a gassed stirred vessel is more strongly influenced by the stirrer than by the gas throughput.

**Example 36**: Time course of temperature equalization in a liquid with temperature-dependent viscosity in the case of free convection

Temperature equalization is to be measured with respect to time in a viscous Newtonian liquid located in a thin-walled copper cylinder. Heat will be transferred alternately from one thermostat, with $T_1$, to another where $T_2 > T_1$. In this example, two questions arise:

a) How can the measured $T$(t) curve at a selected measuring point (e.g. axis) be described by means of a dimensional analysis ?
b) Do identical $T$(t) curves result when measured under the conditions required by similarity criteria? This question is particularly important if the temperature coefficients of viscosity of the liquids employed substantially differ.

The *target quantity* in this process is the temperature, $T$, of the liquid. We will include the cylinder diameter, d, as characteristic *geometric parameter* in the relevance list. The *physical properties* are the density, $\rho$, the viscosity, $\mu$, the heat capacity, $C_p$, the thermal conductivity, k, and the temperature coefficients of viscosity, $\gamma_0$, and of density, $\beta_0$. The *process parameters* are the experimental time, t, gravitational acceleration, g (because of the density differences on account of the temperature field) and the two characteristic temperatures:

$$T_0 = (T_1+T_2)/2,$$

to which the numerical values of all physical properties are related and

$$\Delta T = T_2 - T_1,$$

the maximum temperature difference for the respective temperature equalization.

This leads to the following 12-parametric relevance list:

$$\{T;\ d;\ \rho,\ \mu,\ C_p,\ k,\ \gamma_0,\ \beta_0;\ g,\ T_0,\ \Delta T,\ t\} \tag{13.5}$$

from which eight dimensionless numbers will be obtained in conjunction with the dimensional system [M, L, T, $\Theta$]. One of these numbers will represent energy dissipation which cannot be of relevance in this process. To simplify matters, it is advisable to use the dimensional system which has been extended to include the amount of heat [M, L, T, $\Theta$, H], as already demonstrated in Example 20 on page 80. In this case, the mechanical equivalent of heat, **J**, must be incorporated and this identifies the superfluous dimensionless number.

| | ρ | *d* | μ | Δ*T* | $C_p$ | *t* | *g* | *k* | *J* | $\gamma_0$ | $\beta_0$ | *T* | $T_0$ |
|---|---|---|---|---|---|---|---|---|---|---|---|---|---|
| M | 1 | 0 | 1 | 0 | –1 | 0 | 0 | 0 | 1 | 0 | 0 | 0 | 0 |
| L | –3 | 1 | –1 | 0 | 0 | 0 | 1 | –1 | 2 | 0 | 0 | 0 | 0 |
| T | 0 | 0 | –1 | 0 | 0 | 1 | –2 | –1 | –2 | 0 | 0 | 0 | 0 |
| Θ | 0 | 0 | 0 | 1 | –1 | 0 | 0 | –1 | 0 | –1 | –1 | 1 | 1 |
| H | 0 | 0 | 0 | 0 | 1 | 0 | 0 | 1 | –1 | 0 | 0 | 0 | 0 |
| $Z_1$ | **1** | 0 | 0 | 0 | 0 | 1 | –2 | 0 | –2 | 0 | 0 | 0 | 0 |
| $Z_2$ | 0 | **1** | 0 | 0 | 0 | 2 | –3 | 0 | –2 | 0 | 0 | 0 | 0 |
| $Z_3$ | 0 | 0 | **1** | 0 | 0 | –1 | 2 | 1 | 2 | 0 | 0 | 0 | 0 |
| $Z_4$ | 0 | 0 | 0 | **1** | 0 | 0 | 0 | 0 | –1 | –1 | –1 | 1 | 1 |
| $Z_5$ | 0 | 0 | 0 | 0 | **1** | 0 | 0 | 1 | –1 | 0 | 0 | 0 | 0 |

In addition to the obvious dimensionless numbers $\gamma_0\Delta T$, $\beta_0\Delta T$ (or $\beta_0/\gamma_0$), $T/\Delta T$ and $T_0/\Delta T$, the following four dimensionless numbers appear:

$$\Pi_1 = \frac{t\mu}{\rho d^2} \quad \Pi_2 = \frac{g\rho^2 d^3}{\mu^2} = \frac{gd^3}{\nu^2} \equiv Ga \quad \Pi_3 = \frac{k}{\mu C_p} \equiv Pr^{-1} \quad \Pi_4 = \frac{J\rho^2 d^2 \Delta T C_p}{\mu^2}$$

This 8-parametric pi-set can be streamlined by the following, physically founded, considerations:

1 $\Pi_4$ is irrelevant: The dissipated energy is negligibly small in the case of free convection.
2 $T_0/\Delta T$ is superfluous because the material function, $\mu(T)$, can be represented invariantly with respect to $T_0$, see Sect. 8.1.
3 The gravitational acceleration, g, and hence the Galileo number, Ga, only occur together with $\gamma_0\Delta T$ as the Grashof number, $Gr \equiv \gamma_0\Delta T\,Ga$ (see Example 16).
4 In the case of *creeping* motion, it is necessary a) to transform the mass-related heat capacity $C_p$ in $\Pi_3$ into a volume-related one ($\rho C_p$) and b) g and ρ can only occur as gravity gρ. These two requirements have been fulfilled when Gr has been multiplied with Pr and $\Pi_1$ has been combined with $\Pi_3$ (= $Pr^{-1}$) to give the Fourier number Fo:

$$\Pi_1\ \Pi_3 \equiv \frac{tk}{\rho C_p d^2} \equiv Fo \tag{13.6}$$

Finally, once the target number $T/\Delta T$ has been replaced by a temperature number

$$\Theta \equiv \frac{T}{\Delta T} - \frac{T_0}{\Delta T} + \frac{1}{2} = \frac{T - T_1}{\Delta T} \tag{13.7}$$

which is standardized to one, the complete pi-set becomes

$$\{\Theta, Fo, GrPr, \gamma_0\Delta T, Pr, \beta_0/\gamma_0\} \tag{13.8}$$

The following remarks apply to the *influential range* of individual dimensionless numbers:

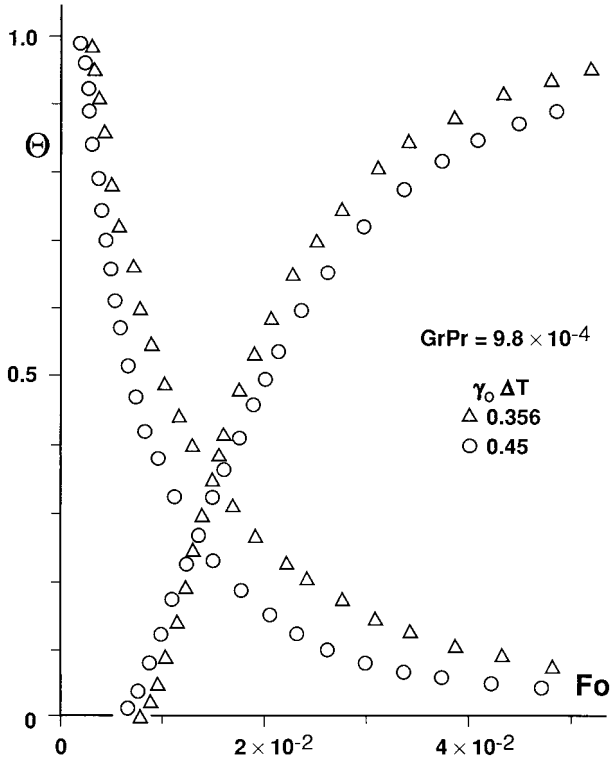


**Fig. 69** Θ(Fo) courses for the cooling and heating of a single liquid (superheated steam cylinder oil) at GrPr = idem and two different $\gamma_0 \Delta T$ values; from [27].

1 Free convection does not come into play at very small values of Gr. In this case, temperature equalization takes place as in a solid body according to the process equation: $\Theta = f(\mathrm{Fo})$.
2 In the range of creeping flow, as a result of free convection, the process equation $\Theta = f(\mathrm{Fo}, \mathrm{GrPr})$ is applicable for small values of $\gamma_0 \Delta T$.
3 The following applies only for larger values of $\gamma_0 \Delta T$: $\Theta = f(\mathrm{Fo}, \mathrm{GrPr}, \gamma \Delta \mathrm{T})$.

In order to verify these facts, measurements were performed in three geometrically similar copper cylinders with D = 30.0; 37.8 and 47.2 mm and five different liquids (glycerol, superheated steam cylinder oil, silicone oil Baysilon M 1.000, Desmophen 1.100 and HD oil SAE 90). The standard representation of their material functions $\mu(T)$ almost corresponds well (see Example 11).

**Fig. 69** shows the Θ(Fo) curves for heating and cooling of superheated steam cylinder oil at constant values of GrPr but two different $\gamma_0 \Delta T$ values. Because $\gamma_0 \Delta T$ is not constant, the respective curves do not correlate, this being documented in **Fig. 70**. This shows the temperature courses of four different liquids. These were measured at GrPr = idem and $\gamma_0 \Delta T$ = idem but display different Pr and $\beta_0/\gamma_0$ values.

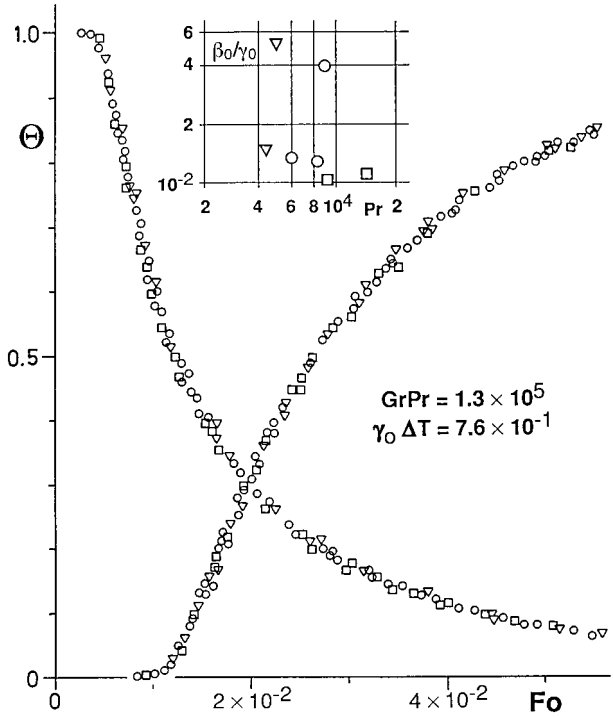


**Fig. 70** Θ(Fo) courses for the cooling and heating of four different liquids at GrPr and $\gamma_0 \Delta T$ = idem, but Pr, $\beta_0/\gamma_0 \neq$ idem, from [27].

**Example 37**: Mass transfer in stirring vessels in the G/L system (bulk aeration) Effects of coalescence behavior of the material system

The mass transfer process (absorption, desorption: "sorption") in gas/liquid contacting is described according to the Two-Film Theory with the general mass transfer equation:

$$G = k_L A \Delta c$$

where:

| | | |
|---|---|---|
| G | – | mass transfer rate [kg $s^{-1}$] through the phase boundary |
| $k_L$ | – | liquid-side mass transfer coefficient [m $s^{-1}$] |
| A | – | interfacial area (sum of the surfaces of all gas bubbles) [$m^2$] |
| $\Delta c$ | – | characteristic concentration difference [kg $m^{-3}$] of the dissolved gas between the phase boundary and the liquid bulk |

For bulk aeration, an uniform distribution of gas bubbles in the liquid is assumed and the mass transfer is therefore related per unit volume:

$$G/V = k_L\,(A/V)\,\Delta c = k_L\,a\,\Delta c$$

Since both $k_L$ and the volume-related interfacial area, $a \equiv A/V$, are not easily accessible for measurement, they are combined to form the "overall mass transfer coefficient $k_La$" which is then defined with the above overall mass transfer equation:

$$k_L a \equiv \frac{G}{V\Delta c}$$

Since part of the gas mixture (e.g. air) is absorbed as it bubbles through the liquid column, the composition of the gas mixture changes. Furthermore, the pressure in the liquid is higher at the gas inlet than in the head space above it. This difference in partial pressure is taken into account by the mean logarithmic concentration difference, $\Delta c_m$:

$$\Delta c_m = \frac{c_1 - c_2}{\lg\left(\frac{c_1 - c}{c_2 - c}\right)} = \frac{\Delta c_1 - \Delta c_2}{\lg\left(\frac{\Delta c_1}{\Delta c_2}\right)} \qquad \Delta c_{1,2} = c_{1,2} - c$$

$c_1$ and $c_2$ are the saturation concentrations under the (p, T, x) conditions at gas inlet (1) and gas outlet (2); c is the concentration of the gas dissolved in the liquid bulk, x is the mol fraction of the absorbed component of the gas mixture.

The selection of the volume-related and, therefore, intensively formulated variable $k_La$, this being the *target* quantity of the mass transfer process, implies the following consequences:

1 Since a quasi-uniform material system is assumed, $k_La$ should not depend on *geometric* parameters.
2 On account of $k_G >> k_L$, $k_La$ must be independent of the *physical* properties of the gas phase.
3 Since the target quantity $k_La$ is an intensity variable, the *process* parameters must also be formulated intensively.

According to these premises, the relevance list must be formed with the following parameters: *Target quantity*: $k_La$; *physical properties*: density $\rho$, viscosity $\mu$, diffusivity *D* and the coalescence parameters $S_i$ of the liquid phase. Despite extensive research, coalescence phenomena have still not been clarified to such an extent as to permit explicit formulation of the coalescence parameters (see [22], section 4.10). *Process parameters*: volume-related mixing power P/V, superficial velocity v of the gas and gravitational acceleration g. (The decision in favour of P/V and v instead of P/q and q/V was based on extensive research results obtained in the last three decades, see Section 10.4.1)

$$\{k_La,\ \rho,\ \mu,\ D,\ S_i,\ P/V,\ v,\ g\} \tag{13.9}$$

| | $\rho$ | $\mu$ | $g$ | $k_La$ | $P/V$ | $v$ | $D$ |
|---|---|---|---|---|---|---|---|
| M | 1 | 1 | 0 | 0 | 1 | 0 | 0 |
| L | –3 | –1 | 1 | 0 | –1 | 1 | 2 |
| T | 0 | –1 | –2 | –1 | –3 | –1 | –1 |
| $Z_1$ | **1** | 0 | 0 | 1/3 | 2/3 | –1/3 | –1 |
| $Z_2$ | 0 | **1** | 0 | –1/3 | 1/3 | 1/3 | 1 |
| $Z_3$ | 0 | 0 | **1** | –2/3 | 4/3 | 1/3 | 0 |

$$Z_1 = M + T + 2A \qquad Z_2 = 3M + T + A \qquad Z_3 = A = -1/3\,(3M + L + 2T)$$

$$\Pi_1 = (k_La)^* \equiv k_La\left(\frac{\mu}{\rho g^2}\right)^{1/3} = k_La\left(\frac{\nu}{g^2}\right)^{1/3}$$

$$\Pi_2 = (P/V)^* \equiv \frac{P/V}{(\rho^2\mu g^4)^{1/3}} = \frac{P/V}{\rho(\nu g^4)^{1/3}}$$

$$\Pi_3 = v^* \equiv \frac{v\rho^{1/3}}{(\mu g)^{1/3}} = \frac{v}{(\nu g)^{1/3}} \qquad \Pi_4 \equiv Sc^{-1} \equiv \frac{D\rho}{\mu} = \frac{D}{\nu}$$

The following pi-set resulted here:

$$\{(k_La)^*, (P/V)^*, v^*, Sc, S_i^*\} \tag{13.10}$$

**Fig. 71** shows a correlation of the mass transfer measurements in this pi-space. The measurements were performed under unsteady-state conditions by several authors in the water/air system which is a coalescent one, using the turbine stirrer (see sketch in Fig. 34) as a mixing device. The measurements cover an extreme experimental scale of $\mu \approx 1$–80. The geometric parameters were broadly varied: d = 0.05–3.1 m; D = 0.15–12.2 m; H = 0.15–6.1 m. Between B and $v^*$ the following correlation exists: $B = (\pi/4)\, v^*$.

In contrast, **Fig. 72** shows the results of mass transfer in the system: aqueous 1-n sodium sulphite solution/air. These measurements were carried out under steady-state conditions in vessels with hollow stirrers on the scale $\mu = 1 : 5$ [58/1, 92]. In this material system, the high salt concentration (70 g/l) fully suppresses bubble coalescence. In the case of the self-aspirating hollow stirrer (see Fig. 28), the stirrer power and gas throughput were coupled via the stirrer speed and were therefore dependent on each other. Consequently, $v^*$ does not occur explicitly in the representation in Fig. 72, because it is a function of $(P/V)^*$.

These results can be summarized as follows: In case of a coalescent material system, for example in pure liquids of low viscosity (e.g. water), the absorption rate depends to an equal extent on P/V and on $v \propto q/D^2$:

$$(k_La)^* \propto (P/V)^{*0.4}\, v^{*0.5} \tag{13.11}$$

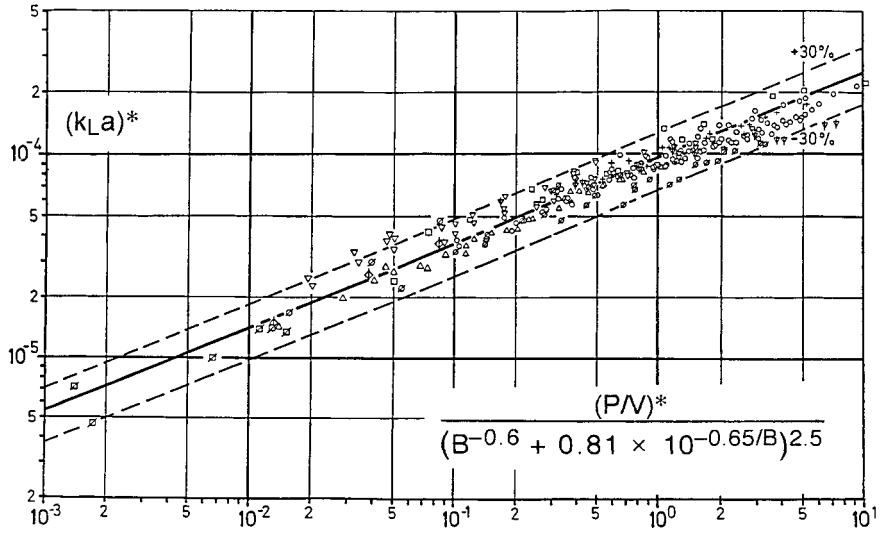


**Fig. 71** Sorption characteristic of a mixing vessel with turbine stirrer for a coalescing material system (water/air), from [53].
$B = (\pi/4)\ v^*$

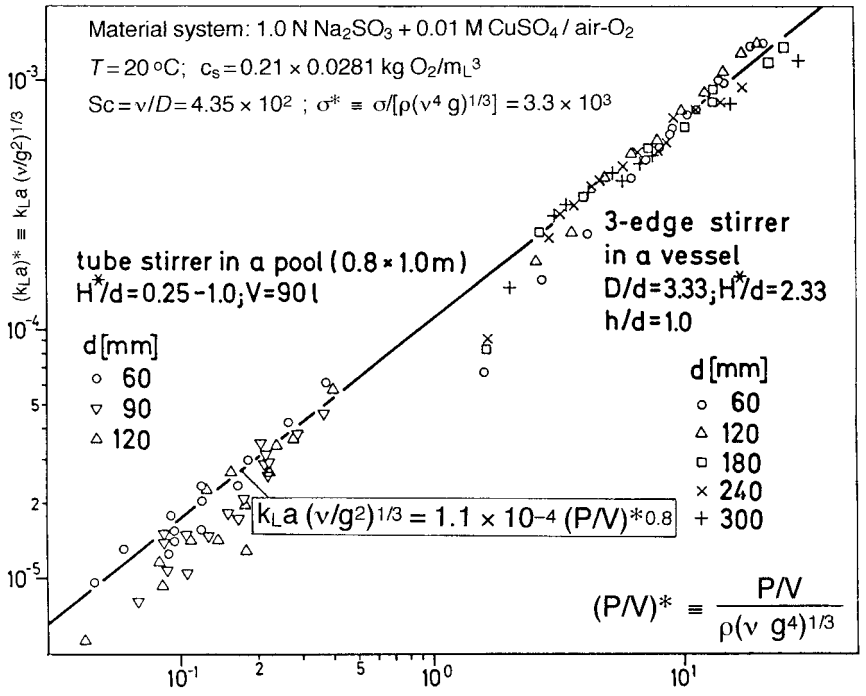


**Fig. 72** Sorption characteristic of a mixing vessel with a self-aspirating hollow stirrer in a material system (70 g $Na_2SO_3$/l) with fully suppressed coalescence; taken from [58/2, 92].

In completely coalescence suppressed systems, for example in many highly concentrated aqueous salt solutions – see [22], Section 4.10 – in contrast to the above, the following applies:

$$(k_La)^* \propto (P/V)^{*0.7}\, v^{*0.2} \tag{13.12}$$

Only with self-aspirating hollow stirrrers, where $v^*$ is not an independent process parameter, the following correlation was found:

$$(k_La)^* \propto (P/V)^{*0.8}. \tag{13.13}$$

This is impressively demonstrated by Fig. 72.

From the above, the following conclusion can be made: High power inputs (P/V) are justified only in coalescence inhibited material systems. In other words, the generation of very fine primary gas bubbles in coalescent-prone systems is not economically justified.

**Example 38**: Mass transfer in the G/L system in bubble columns with injectors as gas distributors. The effects of coalescence behavior of the material system

Injectors are two-component nozzles which utilize the kinetic energy of the liquid propulsion jet to disperse the gas continuum into very fine gas bubbles and to distribute them into the liquid. (In contrast, with *ejectors*, the kinetic energy is utilized to produce *suction*.) Their *advantage* over stirrers is that the liquid jet causes gas dispersion directly while the stirrer has to set the entire contents of the vessel in motion in order to generate the necessary shear rate in the liquid. Their *disadvantage* is the predominance of severe coalescence on account of the high gas bubble density in the free jet of the G/L dispersion. However, in contrast to stirrers, the injector cannot cause redispersion of the large gas bubbles.

Design data for the so-called slot injector – see the sketch in **Fig. 74** – are presented in the following. The shape of its mixing chamber performs two different functions:

(a) Due to the converging walls of the casing, the shear rate of the free jet increases along the mixing chamber. However, because the cross-sectional area of the mixing chamber remains unchanged, this does not result in an additional pressure drop.
(b) The free jet of the G/L dispersion leaves the slot-shaped mouthpiece in the form of a ribbon which mixes more quickly into the surrounding liquid than a jet with a circular cross-section. This counteracts bubble coalescence.

For optimum design of injectors for G/L contacting their pressure drop and sorption characteristics must be known. The first is needed to dimension the conveying devices (pumps and blowers), the latter to establish the necessary gas and liquid throughputs.

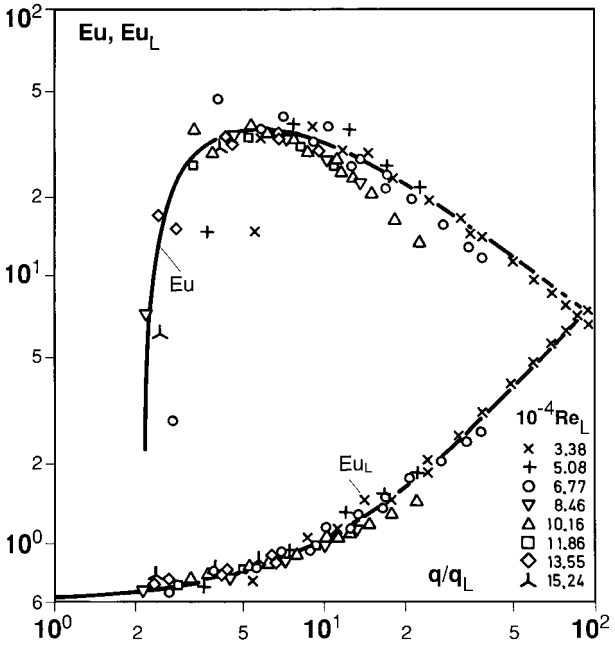


**Fig. 73** Pressure drop characteristics of an injector; q is related to standard conditions (20 °C, 1 bar)

a) The *pressure drop characteristics* of an injector are based on the following relevance lists:

for the *gas throughput* : $\{\Delta p;\ d_M;\ \rho,\ \nu_L;\ q,\ q_L\}$ (13.14)

for the *liquid throughput*: $\{\Delta p_L;\ d,\ \rho_L,\ \nu_L;\ q,\ q_L\}$ (13.15)

$\Delta p$ – pressure drop of the respective medium in the propulsion jet nozzle of diameter, d, in the mixing chamber of diameter, $d_M$; q – throughputs; $\rho$ and $\nu$ densities and kinematic viscosities of the respective medium. (Gas: without subscript, Liquid: subscript L). The following pi-sets result:

for the *gas throughput*: $$\{Eu \equiv \frac{\Delta p d_M^4}{\rho q^2},\ \frac{q}{q_L},\ Re \equiv \frac{q_L}{\nu_L d_M}\} \quad (13.16)$$

for the *liquid throughput*: $$\{Eu_L \equiv \frac{\Delta p_L d^4}{\rho_L q_L^2},\ \frac{q}{q_L},\ Re \equiv \frac{q_L}{\nu_L d}\} \quad (13.17)$$

Measurements have shown that Re is irrelevant in the range of $Re > 10^4$. Therefore, in both cases, $q/q_L$ is the only process number effecting Eu; see **Fig. 73**.

b) The *sorption characteristic* of an injector is formed with intensively formulated process parameters. The gas throughput, q, will be replaced by superficial

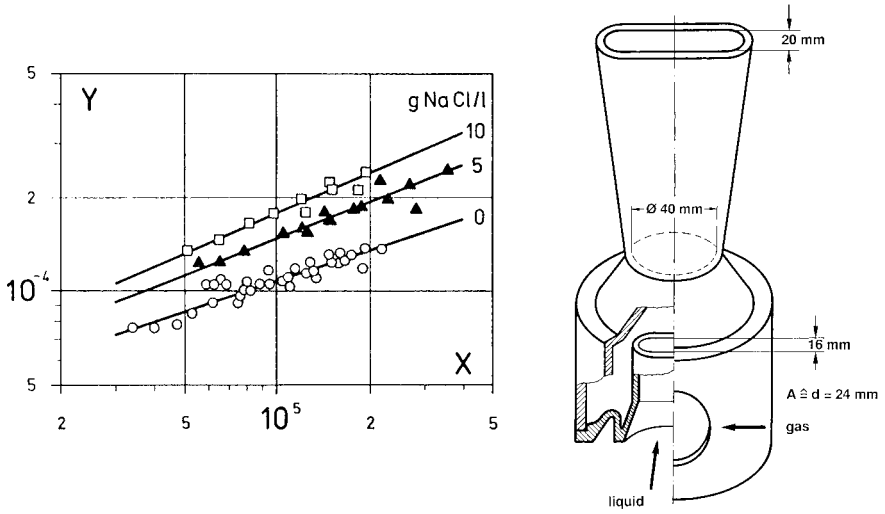


**Fig. 74** Sorption characteristics of a slot injector of industrial-size (sketch) in dependence upon the coalecence degree of the system; from [93].

velocity, $v \approx q/D^2$, since it has proved suitable for the correlation of $k_La$ values in laboratory bubble columns: $k_La/v$ = const. (see Example 10, bubble column). Following the sorption characteristics of a mixing vessel, instead of the liquid throughput, $q_L$, we will use the power of the liquid jet, $P_L = \Delta p_L q_L$, per gas throughput, q: $P_L/q$ [93]. Including the physical parameters, the following relevance list results:

$$\{k_La/v;\ \rho,\ \nu,\ D,\ S_i;\ P_L/q,\ g\} \tag{13.18}$$

This leads to the following pi-set:

$$\{(k_La/v)^*,\ (P_L/q)^*,\ Sc,\ S_i^*\} \tag{13.19}$$

pi-numbers indicated by * have the following meaning:

$$(k_La/v)^* \equiv \frac{k_La}{v}\left(\frac{\nu^2}{g}\right)^{1/3} \equiv \quad Y - \text{sorption number}$$

$$(P_L/q)^* \equiv \frac{P_L/q}{\rho(\nu g)^{2/3}} \quad \equiv \quad X - \text{dispersion number}$$

The sorption characteristics of an industrial-sized slot injector were measured in a bubble column of technical size ($3^{\varnothing} \times 8$ m), as dependenent on the common salt (NaCl) content, this influencing the coalescence behavior of the material system, see **Fig. 74**. The results demonstrate that already small amounts of cooking salt (5 g/l ≙ 0.5 %) suffice to increase the absorption rate by ca. 30 %. The following correlations were found:

| g NaCl/l | |
|---|---|
| 0 | $Y = 2.4 \times 10^{-6}\, X^{0.33}$ |
| 3 | $Y = 2.2 \times 10^{-6}\, X^{0.37}$ |
| 5 | $Y = 2.0 \times 10^{-6}\, X^{0.39}$ |
| 10 | $Y = 1.5 \times 10^{-6}\, X^{0.43}$ |

When the coalescence of the primary gas bubbles is more strongly suppressed, the power input of the propulsion jet (P/q) is more efficiently utilized. The above table shows how with increasing salt concentration (increasing suppression of coalescence), the power of X also increases.

In the following, it will be explained why these characteristics can be used solely as design data for optimizing the running conditions of this *particular size* of injector and why they are certainly not suitable for a scale-up of this device.

In fact, the concept of the quasi-homogeneous gas/liquid mixture, on which also the formulation of the target pi-number $Y \equiv (k_L a/v)^*$ with intensity quantities is based, and which was fully verified in bubble columns with perforated plates as gas distributors, proves to be *totally inappropriate* when injectors are used as gas dispersers. The explanation for this fact is that in the case of injectors the coalescence takes place both in the free jet of the G/L dispersion and at its disintegration into a bubble swarm, while in the case of gas distribution with perforated plates this process has already been completed just above the perforated plate.

This is verified by the measuring data obtained in a column of 1.6 m ∅, in which a slot injector was installed with a bottom clearance of 1 m and an angle of 25° towards the bottom. The liquid head H above the injector was varied in the range H = 1–7 m. It is shown that the influence of the bubble coalescence in the G/L free jet on the mass transfer – which occurs in a short distance from the nozzle orifice – is equilized only after H = 3 m; see **Fig. 75**. This finding proves that the pi-set, eq. (13.19), is not complete but has to be widened by a pi-number which essentially contains liquid height H. It can be formulated by $H^* \equiv H\,(g/\nu^2)^{1/3}$.

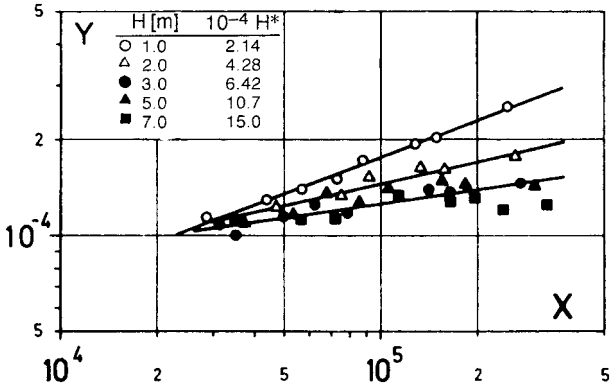


**Fig. 75** Dependence of the sorption characteristic Y(X) on the liquid head above the injector [93].

Furthermore, it is clear that the scale-up of an injector inherently lessens its efficiency. This is caused by the fact that the dispersing effect of the liquid propulsion jet is restricted to its circumference which, in the case of geometrically similar scale-up, increases only linearly ($u = \pi d$) while its cross-sectional area increases quadratically ($S = \pi\, d^2/4$). This means that with increasing diameter of the device, an increasingly smaller fraction of the liquid throughput is dispersed: The dispersion efficiency of injectors inherently diminishes with increasing scale.

This is confirmed by mass transfer measurements conducted with three differently shaped slot injectors, see **Fig. 76**. Two of them have been geometrically similarly scaled up (scale $\mu = 1 : 2$). The smaller one (d = 2 cm ∅; o signs) was installed in a bubble column of D = 1.6 m, the larger one (d = 4 cm ∅; Δ signs) in a bubble column of D = 2.8 m. In both cases, the liquid head above the injectors was equal (H = 7 m). Both injectors were attached to the vessel wall with a bottom clearance of 1 m and inclined with an angle of 25° and 35°, respectively, towards the bottom. In this manner was ensured that the free jet desintegrated into a bubble swarm just above the bottom. The result of these measurements is represented as Y(X) in Fig. 76. It proves that the larger injector has an efficiency which is approximately 30 % lower than the smaller version thereof. A correlation of both of these straight lines can be obtained by the representation: $Y\,[d\,(g/\nu^2)^{1/3}]^{2/3} = f(X)$.

A solution to this problem was to avoid scaling-up under geometrically similar conditions and to increase only the diameters and not the lengths of the mixing chamber by a factor of 2. As a result, all angles are doubled: the shear rates are enhanced and the free jet fans out more which further suppresses coalescence. The result (d = 4 cm ∅; × signs) shows that this injector is, at last from $X = 2 \times 10^5$ on, equal to the small one. The positive aspects of this scale-up approach are counteracting the negative ones discussed before.

An enlargement of an injector is necessary if it is to be implemented in waste water treatment plants. In this case it must be prevented that the propulsion jet nozzle is clogged by solid particles contained in the waste water.

Last but not least, the influence of bubble coalescence in the treatment space should be addressed. The pi-set for the sorption characteristic only takes account of gas dispersion and not of bubble coalescence in the treatment space. According to

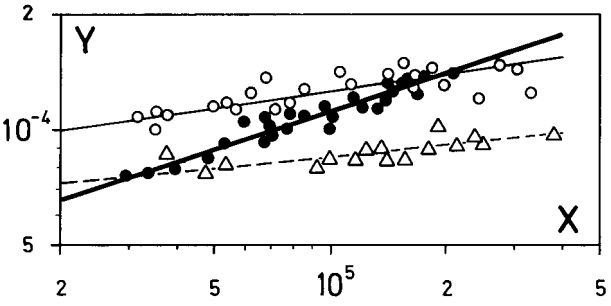


**Fig. 76** Sorption characteristics of three slot injectors of different shape and size (explanation in text); from [93].

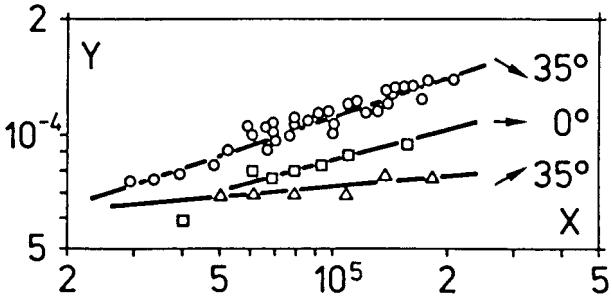


**Fig. 77** Influence of the inclination angle of the free jet on bubble coalescence and, consequently, on Y(X); from [93].

the laws governing the free jet, the free jet of the G/L dispersion sucks in the liquid which surrounds it and in succession it loses its kinetic energy and decomposes into a gas bubble swarm. This process is extremely scale dependent and would need to be considered in a separate relevance list in which all the relevant geometric parameters are included.

To give an example of the dramatic influence which the geometric parameters can have on coalescence behavior, **Fig. 77** shows Y(X) correlations for the industrial-size slot injector which were obtained in a vessel of $3^{\varnothing} \times 8$ m water height. The injector was positioned 1 m above the bottom at the vessel wall in such a way that its axis formed an angle of 0°, + 35° resp. – 35° with the horizontal. Only in the last case, the free jet was pointed towards the floor and decomposed into the bubble swarm just above it. Near the floor, the suction of the free jet is weakest on account of bottom friction. Furthermore, the bubble swarm which has formed does not exert a "chimney effect" there. Consequently, liquid entrainment into the free jet is suppressed at exactly that point at which it would be particularly supportive of coalescence on account of the weakened kinetic energy of the free jet.

Therefore, the sorption characteristics Y(X) presented in **Fig. 74–77** can only be used as design data for the injector type measured in the respective case. They can not be used for scale-up!

In view of the fact that injectors exhibit favorable characteristics for G/L contacting which makes them superior to stirrers with respect to power consumption, systematic research in this area would be most desirable. However, it has been pointed out that it is necessary to perform the measurements at least in the final stage in full-scaled plants in order to obtain reliable information on the bubble coalescence in the respective treatment space.

The data presented in Fig. 77 deal with flow states, these being far more complicated than those encountered in the ventilation technique. It would certainly be of interest to examine which tips and statements can be delivered here by the Computational Fluid Dynamics (CFD)!

**Example 39**: Scaling up of dryers

Drying belongs to those thermal unit operations in which a simultaneous heat and mass transfer occurs. Therefore, it is not surprising to learn that this complicated process has never been treated by dimensional analysis. Instead, intuition and practical experience are used to construct industrial devices. At the same time, mathematical models existed which treated single process steps (e.g. mass transfer from solid particles into air stream, heat transfer to the solid particles, product flow through the dryer, moisture mass bilances, etc.) present in the course of single drying periods. Today, these aspects can be treated with modern computers using numerical fluid simulation (CFD).

In 1994, two issues of the magazine *Drying Technology* were devoted to the dimensioning of dryers [94]. Their content verified the above conclusions.

In his introducing communication, *Kerkhof* [95] referred to the fact that the scaling up of dryers is made difficult by the non-linearity of the occurring physical processes. In addition, he reminded of the simultaneous changes of essential physical properties due to a permanent change of drying conditions in the course of drying. In a slow drying process, the heat uptake and the moisture removal are balanced. A flat moisture profile exists within the particle and the process is governed "externally". In a fast drying process, the moisture diffusion to the surface of the particle is not as fast as is its removal. Within the particle a sharp moisture profile exists and the process is governed "internally".

As a measure for the degree with which these states are governing the drying process, an extended Sherwood number $Sh^*$ is introduced ( called a "modified Biot number" in [95]):

$$Sh^* \equiv \frac{k_G d_p}{D_{eff}} \frac{\rho_{wG}}{\rho_S} \frac{1}{F^*_{crit}} \tag{13.22}$$

| | |
|---|---|
| $k_G$ | gas-side mass transfer coefficient |
| $d_p$ | particle diameter |
| $D_{eff}$ | effective diffusion coefficient |
| $\rho_{wG}$, $\rho_S$ | densities of the saturated wasser steam and of the solids |
| $F^*_{crit}$ | mass portion of the moisture in the solid particle |

As a rough estimate, the border line between both states will lie at $Sh^* = 1$.

In a spray drying process, the determining dimension is the particle diameter, $d_p$. With $d_p = 0.1$ mm and assuming conditions usually prevailing in spray dryers, $Sh^* \approx 70$. Therefore, this process will be diffusion-limited, that is "internally" governed.

*Genskow* [96] pointed out that a correct scale-up is of higher importance for a drying process than in many other unit operations. This is because this process is determining a variety of different product qualities, such as density, particle size distribution, wettability, flow ability, composition, taste, color, and so on. He also concluded that dimensional analysis should be introduced as a compulsory topic in the study of process engineering.

After a review of the customary calculation methods [97] for both essential classes of dryers (convective and contact dryers), the dimensioning methods for spray dryers [98, 99], fluidized and spouted bed dryers [100, 101, 102], cascading rotary dryers [103], pneumatic conveying dryers [104], conductive-heating agitated dryers [105] and layer dryers [106] were presented. They all confirmed the initially made conclusion that the scaling up of dryers is still made today without dimensional analysis and the model theory based thereupon.

Drying of solvent-moist films and coatings is an important task in the photochemical industry. If the film surface is sufficiently moist, evaporation from a free surface takes place. Consequently, the drying rate only depends on the mass and heat transfer at the surface ("surface evaporation", 1st drying period). After the critical humidity has been achieved, heat transfer and diffusion within the goods interior govern the drying process ("diffusion-limited", 2nd drying period).

*Y. Sano* [107] described the influence of the film thickness, $\delta$, on the drying course of water-moist polyimide films. In thick films ($\delta \approx 1$ mm), the liquid-side diffusion plays an important role from the very beginning. The surface concentration quickly drops off to an equilibrium value and the temperature at the film surface increases to the drying air temperature, without reaching a constant steady-state goods temperature. A period of constant drying rate does not appear.

The curves of the drying course for thicker polyimide films correlate, if the evaporated amount of the solvent is plotted against the Fourier number, Fo. This pi-number is defined as follows:

$$\mathrm{Fo} \equiv \frac{x\,a}{\delta^2\,v} = \frac{\text{momentary position on the belt} \times \text{thermal diffusivity}}{(\text{layer thickness at the beginning})^2 \times \text{belt velocity}} \tag{13.23}$$

From this relationship, the belt velocity of the dryer, necessary to achieve a certain degree of moisture, can be predicted.

In contrast, thin films ($\delta \approx 50$ μm) display, at the beginning of the drying process, a period of constant drying rate at which the evaporation takes place from the free liquid surface. Only when the film is impoverished on solvent, drying is governed by diffusion through the polymer matrix.

*H. Jordan* [109] experimentally investigated the drying course of a tetrahydrofuran/cyclohexane-moist film. The following assumptions were made:

1 The mass transfer rate is essentially dependent upon the degree of moisture $F^* \equiv F/F_0$. A diffusive mass transfer of solvent exists within the polymer film, whereby the diffusion coefficient depends on the degree of moisture, $D(F)$. (Later on, this situation will not be considered.)
2. The film base is impenetrable for the solvent, mass transfer occurs solely into the gas space.
3. Because the solvent transfer within the polymer film is rate determining, the temperature field within the film remains practicaly constant and equal to the temperature on the film surface.
4. The incoming drying gas is solvent-free. Outside the laminar boundary layer the solvent concentration is practically zero.

The course of drying is described by the following parameters:

| | |
|---|---|
| Target quantity: | degree of moisture $F^* \equiv F/F_0$ |
| Influencing parameters: | |
| geometric: | film thickness of dried film, $\delta$ |
| | film length, L |
| material: | densities of gas, $\rho$, and of solvent, $\rho_L$ |
| | kinematic viscosity of gas, $\nu$ |
| | heat capacities of gas, $C_p$, and of solvent, $C_{pL}$ |
| | thermal diffusivity of gas, $a$ |
| | diffusion coefficient of solvent in drying gas, $D$ |
| | mass transfer coefficient of solvent, $k_L$ |
| | vapour pressure of solvent, $p_L$ |
| | evaporation enthalpy of solvent per unit mass, $\Delta H$ |
| process related: | gas throughput, q |
| | pressure in gas space, p |
| | gas temperature, $T$ |
| | duration of drying, t |

The relevance list therefore consists of 17 parameters:

$$\{F^*;\ \delta,\ L;\ \rho,\ \rho_L,\ \nu,\ C_p,\ C_{pL},\ a,\ D,\ k_L,\ p_L,\ \Delta H;\ p,\ q,\ T,\ t\} \tag{13.24}$$

In connection with the dimensional system [M, L, T, $\Theta$], 13 pi-numbers will be produced. To facilitate the dimensional analysis, six of them can be anticipated as trivial pi-numbers:

$$\{F^*;\ \delta/L,\ \rho_L/\rho,\ C_{pL}/C_p,\ p_L/p,\ \nu/D\} \tag{13.25}$$

$\nu/D \equiv$ Sc – Schmidt number. The reduced relevance list only contains eleven parameters:

$$\{\delta;\ \rho,\ \nu,\ k_L,\ c_p,\ a,\ \Delta H,\ p,\ q,\ T,\ t\} \tag{13.26}$$

| | $\rho$ | $\delta$ | $t$ | $T$ | $\nu$ | $k_L$ | $C_p$ | $a$ | $\Delta H$ | $p$ | $q$ |
|---|---|---|---|---|---|---|---|---|---|---|---|
| M | 1 | 0 | 0 | 0 | 0 | 0 | 0 | 0 | 0 | 1 | 0 |
| L | –3 | 1 | 0 | 0 | 2 | 1 | 2 | 2 | 2 | –1 | 3 |
| T | 0 | 0 | 1 | 0 | –1 | –1 | –2 | –1 | –2 | –2 | –1 |
| $\Theta$ | 0 | 0 | 0 | 1 | 0 | 0 | –1 | 0 | 0 | 0 | 0 |
| M | **1** | 0 | 0 | 0 | 0 | 0 | 0 | 0 | 0 | 1 | 0 |
| 3M + L | 0 | **1** | 0 | 0 | 2 | 1 | 2 | 2 | 2 | 2 | 3 |
| T | 0 | 0 | **1** | 0 | –1 | –1 | –2 | –1 | –2 | –2 | –1 |
| $\Theta$ | 0 | 0 | 0 | **1** | 0 | 0 | –1 | 0 | 0 | 0 | 0 |

From this 11 – 4 = 7 pi-numbers result which can be combined to form known or practical pi-numbers (right hand side):

$$\Pi_1 \equiv \frac{\nu t}{\delta^2} \qquad \Pi_1 a/\nu \equiv \frac{at}{\delta^2} \qquad \equiv \text{Fo (Fourier)}$$

$$\Pi_2 \equiv \frac{k_L t}{\delta} \qquad \Pi_2 \Pi_4 a/D \equiv \frac{k_L \delta}{D} \qquad \equiv \text{Sh (Sherwood number)}$$

$$\Pi_3 \equiv \frac{C_p t^2 T}{\delta^2} \qquad \Pi_3^{-1} \Pi_2 \Pi_5^{-1} = \frac{k_L^2}{\Delta H}$$

$$\Pi_4 \equiv \frac{at}{\delta^2} \qquad \Pi_4^{-1} \Pi_1 \equiv \frac{\nu}{a} \qquad \equiv \text{Pr (Prandtl number)}$$

$$\Pi_5 \equiv \frac{\Delta H t^2}{\delta^2} \qquad \Pi_5 \Pi_3^{-1} \equiv \frac{\Delta H}{C_p T}$$

$$\Pi_6 \equiv \frac{p t^2}{\rho \delta^2} \qquad \Pi_6 \Pi_5^{-1} \equiv \frac{p}{\rho \Delta H}$$

$$\Pi_7 \equiv \frac{qt}{\delta^3} \qquad \Pi_7 \Pi_1^{-1} \delta/L \equiv \frac{q}{\nu L} \qquad \equiv \text{Re (Reynolds-Kennzahl)}$$

The complete set of 13 pi-numbers therefore consists of:

| | |
|---|---|
| target number: | $F^*$ |
| geometric pi-number: | $\delta/L$ |
| material pi-numbers: | $\rho_L/\rho$, $C_{p,L}/C_p$, $p_L/p$, Sc, Sh, $k_L^2/\Delta H$, Pr |
| process related pi-numbers: | Fo, $\Delta H/C_p T$, $p/\rho\Delta H$, Re |

In the diploma thesis conducted by *Jordan* [109], concerning the drying of tetrahydrofuran/cyclohexane-wetted polyvinylbutyral films, the influence of only a few of the given parameters, namely $\delta/L$, Re, $\Delta H/c_p T$, on the dependence $F^*$(Fo) could be experimentally examined. Their influence was then taken into account by simple power products, **Fig. 78**.

**Example 40**: Scale-up of a continuous, carrier-free electrophoresis

Electrophoresis makes use of differences in the electrophoretic mobility of electrically charged particles (biomolecules, micro-organisms etc.) as a means to separate them. For this purpose, a homogeneous, rectified electrical field is used. Thanks to the excellent resolution and mild operating conditions, this is currently the best analytical method for protein separation, purification and characterization. It is also used as a preparative separation method which allows a few grams per hour to be purified.

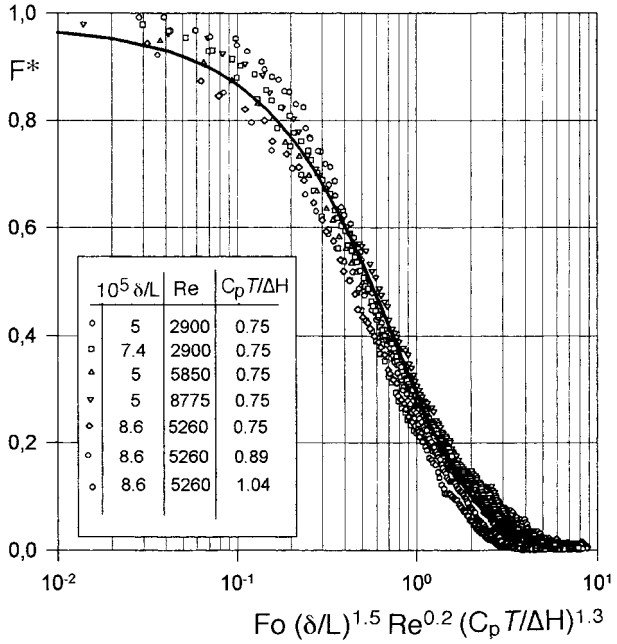


**Fig. 78** The correlation $\{F^*, \text{Fo}, \delta/L, \text{Re}, \Delta H/c_p T\}$ for the discussed material system

In the case of *carrier* electrophoresis, a sheet of paper, starch, polyacrylamide or agarose gel or similar materials, where the respective solid phase is saturated with buffer solution, are placed between the electrodes in order to generate a homogeneous, rectified electrical field. The mixture of substances to be separated is supplied as a single spot and the individual components are then separated in the course of time. Carrier electrophoresis is therefore a *discontinuous* separation process.

*Carrier-free, continuous* electrophoresis is utilized for preparative work [110]. In this process, the two electrodes form a parallel, plane slot or annulus of a few mm to a number of cm in width through which the buffer solution migrates. The material mixture to be fractionated is injected into the carrier solution at one point along this slot and, after its resolution into separate fractions, is then removed with the buffer solution at several points along the slot, see **Fig. 79**.

Before compiling the relevance list for this process, it must be considered in greater depth:

This resolution is characterized by a bandwidth, b (which is as small as possible), and a clearance, s, between the respective bands (which is as large as possible). Both parameters are dependent upon the same influencing variables. The *resolution effect* is therefore defined as the quotient s/b and is taken as the *target number* of the process.

One of the main material-related parameters will be *electrophoretic mobility*, $\mu$. It is defined as the velocity, v, of the particles in relation to the electrical field strength, E.

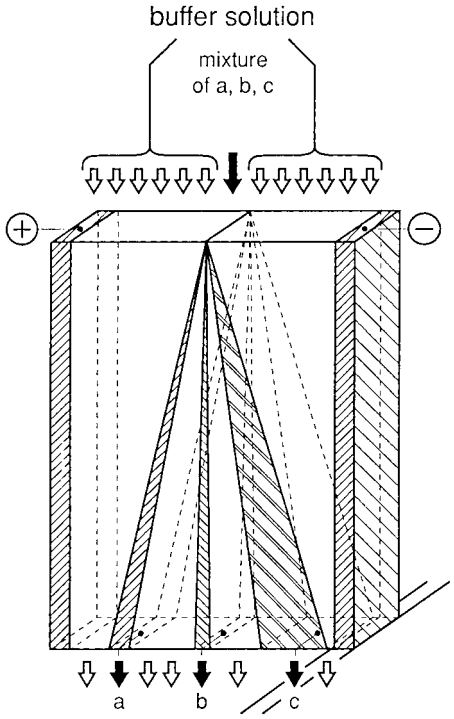


**Fig. 79** Sketch of a continuous, carrier–free electrophoresis cell

It results from the balance between the electrical field force, $F_{el}$, and the frictional force, $F_r$.

The following is valid for electrical field force, $F_{el}$:

$$F_{el} = e\ z\ E \tag{13.27}$$

where e [Coulomb = A s] is the electrical charge, z the number of charge carriers per particle (e.g. biomolecules) and E [V $m^{-1}$] the electrical field strength. The following is valid for frictional force, Fr:

$$F_r = 6\ \pi\ r\ \mu\ v \tag{13.28}$$

where r is the particle diameter and $\mu$ the dynamic viscosity of the medium.

The following results for electrophoretic mobility:

$$\mu = \frac{v}{E} = \frac{e\ z}{6\ \pi\ r\ \mu} \tag{13.29}$$

Furthermore, it is important to know that electrical power is fully converted into heat. In turn, this causes convective mass flows which disrupt the fractionation process.

We are going to consider two different operating modes. In the first, a *creeping flow* predominates between two plane-parallel electrodes. The electrodes are not cooled in this case; consequently $\Delta T$ is not a freely selectable process parameter. In the second operating mode, in contrast, the operating conditions are those of the so-called *Biostream separator*.

**Case 1**: *Creeping flow*
This boundary condition has the following consequences for this problem relevance list:

1 The density, $\rho$, as such, does not play any role.
2 The specific heat, $C_p$, must be formulated as per unit of volume: $\rho C_p$.
3 The temperature coefficient of density, $\beta_0$, only acts in conjunction with gravitational acceleration, g, and must be combined with the density: $\rho g \beta_0$

The influencing variables of this process are therefore:

1 *Geometric* parameters: Characteristic length of the channel, L
2 *Physical properties*: The dynamic viscosity $\mu$ of the buffer solution; the diffusivity *D* of the substances to be separated in the buffer solution; $\rho g \beta_0$, the specific heat $\rho C_p$ and the thermal conductivity k. (These three quantities are the only ones which contain temperature in their dimensions; therefore we will formulate them as quotients to obtain $k/\rho g \beta_0$ and the thermal diffusivity, $a \equiv k/\rho C_p$). The electrical properties are electrical conductivity, $k_{el}$ (current density/electrical field strength), and electrophoretic mobility, $\mu$.
3 *Process-related* parameters: liquid throughput, q, and electrical tension, $U \propto E$ L, because this, in contrast to E, is a directly adjustable process variable.

The relevance list of the problem is therefore:

$$\{s/b;\ L;\ \mu,\ D,\ k/\rho g \beta_0,\ a,\ k_{el},\ \mu;\ q,\ U\} \tag{13.30}$$

Without the (dimensionless) target number s/b, the dimensional matrix is:

| | $\mu$ | ***L*** | ***D*** | $\mu$ | $k/\rho g \beta_0$ | ***a*** | $k_{el}$ | ***q*** | ***U*** |
|---|---|---|---|---|---|---|---|---|---|
| M | 1 | 0 | 0 | –1 | 0 | 0 | –1 | 0 | 1 |
| L | –1 | 1 | 2 | 0 | 3 | 2 | –3 | 3 | 2 |
| T | –1 | 0 | –1 | 2 | –1 | –1 | 3 | –1 | –3 |
| I | 0 | 0 | 0 | 1 | 0 | 0 | 2 | 0 | –1 |
| $Z_1$ | **1** | 0 | 0 | 0 | 0 | 0 | 1 | 0 | 0 |
| $Z_2$ | 0 | **1** | 0 | 0 | 1 | 0 | –2 | 1 | 0 |
| $Z_3$ | 0 | 0 | **1** | 0 | 1 | 1 | 0 | 1 | 1 |
| $Z_4$ | 0 | 0 | 0 | **1** | 0 | 0 | 2 | 0 | –1 |

$Z_1 = M + I$; $Z_2 = 3M + L + 2T - I$; $Z_3 = -M - T + I$; $Z_4 = I$

This dimensional matrix leads to the following pi-set:

$$\Pi_1 \equiv \frac{k}{\rho g\, \beta\, D\, L};\quad \Pi_2 \equiv \frac{a}{D} \equiv \mathrm{Le};\quad \Pi_3 \equiv \frac{k_{el} L^2}{\mu\, \mu^2};\quad \Pi_4 \equiv \frac{q}{L\, D} \equiv \mathrm{Bo};\quad \Pi_5 \equiv \frac{U\, \mu}{D}$$

Bo and $\Pi_5$ are the two process numbers.

$$\Pi_2 \equiv \mathrm{Le}\ (\text{Lewis number})\ \text{ and }\ \Pi_1 \Pi_3^{0,5} = \frac{k}{\rho g\, \beta\, D\, \mu} \left(\frac{k_{el}}{\mu}\right)^{0,5}$$

are the two material numbers, while the combination of numbers

$$\Pi_1^{-1} \Pi_3 = \frac{\rho g\, \beta\, D\, L^3}{\mu\, \mu^2}\, \frac{k_{el}}{k} \equiv \text{„Gr“}$$

provides a modified Grashof number, “Gr”.

Taking account of these alterations and the addition of the target number s/b, the above pi-set is as follows:

$$\frac{s}{b}; \frac{q}{L\, D} \equiv \mathrm{Bo};\quad \frac{U\mu}{D}; \frac{\rho g\, \beta\, D\, L^3}{\mu\, \mu^2}\, \frac{k_{el}}{k} \equiv \text{„Gr“}; \frac{k}{\rho g\, \beta\, D\, \mu} \left(\frac{k_{el}}{\mu}\right)^{0,5};\quad \frac{a}{D} \equiv \mathrm{Le} \qquad (13.31)$$

It is apparent that a change in scale, while keeping s/b = idem, implies the retention of *idem* for the mechanical process number Bo and, therefore, q ∝ L, i.e. an increase in q causes a corresponding increase in scale. However, this condition means that the numerical value of “Gr” is changed very substantially during scale-up. This dimensionless number could only be kept *idem* by changing the physical properties and this, of course, cannot be done.

A way out, which has frequently been considered but, understandably, still has not been realized, would be to eliminate the influence of “Gr” by exclusion of gravity in the “Spacelab”. The efforts to suppress smearing of the individual material bands by superimposing a shear flow crosswise to the volume flow in the annulus between the concentric electrodes would seem to be more an interesting alternative.

**Case 2**: The *Biostream Separator*

Indeed, the “Biostream Separator” [111] operates according to this principle. The device consists of two concentric cylinders; the inner one is made to rotate in order to generate a *Couette* flow. We are no longer dealing with a creeping flow, therefore the liquid density, ρ, is not negligible. The number of *process* parameters is increased from two to four. These are (1) the rotational speed, n, of the inner cylinder. (2) In addition, as a result of the possibility of cooling the outer cylinder wall, the temperature difference, $\Delta T$, is an additional process parameter which is freely adjustable.

The relevance list which has been extended in comparison to Case 1 now becomes:

$$\{s/b;\ L;\ \mu,\ D,\ k/\rho g\beta_0,\ a,\ k_{el},\ \mu;\ q,\ U,\ n,\ k\Delta T,\ \rho\}$$

The extended dimensional matrix supplies the three additional dimensionless numbers:

$$\Pi_6 \equiv \frac{nL^2}{D}; \quad \Pi_7 \equiv \frac{k\Delta T\, L^2}{\mu D^2}; \qquad \Pi_8 \equiv \frac{\rho D}{\mu} \equiv Sc^{-1}$$

To simplify test planning and execution, the complete pi-set – i.e., the already obtained numbers $\Pi_1$ to $\Pi_5$ and the three numbers $\Pi_6$ to $\Pi_8$ given above – is converted, as follows, to more sensible process and material numbers:

*Target* number: $\Pi_9 \equiv s/b$

*Process* numbers:

for n: $\Pi_6\Pi_8 \equiv \frac{nL^2}{\nu} \equiv$ Re (Reynolds number)

for q: $\Pi_4 \equiv \frac{q}{DL} \equiv$ Bo (Bodenstein number)

for E: $\Pi_5 \equiv \frac{U\mu}{D}$

for $\Delta T$: $\Pi_1^{-1}\Pi_7\Pi_8 \equiv \frac{g\beta\Delta T\, L^3}{\nu^2} \equiv$ Gr (Grashof number)

*Material* numbers:

$\Pi_2 \equiv \frac{a}{D} \equiv$ Le (Lewis number)

$\Pi_8^{-1} \equiv \frac{\nu}{D} \equiv$ Sc (Schmidt number)

$\Pi_1\Pi_3^{0,5} \equiv \frac{k}{\rho g\, \beta\, D\, \mu} \left(\frac{k_{el}}{\mu}\right)^{0,5}$ and

$\Pi_8^{-1}\Pi_6 \equiv \frac{\mu L^2 n^2}{k\, \Delta T} \equiv$ Br (Brinkman number)

The target number is dependent on four process numbers and three pure material numbers. Since the rotation of the inner cylinder generates a negligible "heat of agitation", the last number, the Brinkman number, can be considered to be irrelevant and can therefore be deleted.

Model tests employed to determine scale-up rules are, of course, performed with the same material system as that used in the prototype. This is because any alteration of a physical characteristic, e.g. the dynamic viscosity, automatically changes other physical properties, e.g. electrophoretic mobility, $\mu$.

In the model apparatus, it will be possible to adjust the four process numbers independent of each other without any problems. In this way, their influence on s/b will be clarified and optimum process conditions for the desired separation operation will be established. (We would like to assume that, in these tests, it will also be possible to determine the influence of Gr on s/b within certain limits by altering $\Delta T$.)

On the next-larger model scale, the process numbers for n, q and E can also be set to idem without any problems since they contain clear instructions as to how the respective process variables have to behave in the case of a change in scale. The adjustment of Gr = *idem*, in contrast, will be problematic, since *doubling* the slot width makes it necessary to set a temperature difference which is *smaller* by a factor of 8 on account of $\Delta T \propto L^{-3}$. As a result, the heat produced in the annulus can no longer be removed.

As a last resort, the cooling surface area can be increased. In [112], the slot between the electrodes was 6 mm wide and this was transformed into a heat exchanger. It consisted of teflon capillary tubes ($d_i$ = 0.4 mm, $d_o$ = 0.7 mm) aligned and spaced by woven Teflon mesh. 5 layers of tubes were separated and spaced by 6 layers of mesh. The bed performs cooling and, at the same time, suppresses the convection.

In [139] a new design of an electrophoresis cell with a flat rectangular chamber is presented in which the smallest cell dimension is arranged parallel and not perpendicular to the electric field. It is claimed that this arrangement allows a simple scale-up.

*Scale-up in Chemical Engineering.* Marko Zlokarnik


ISBNs: 3-527-30266-2 (Hardback); 3-527-60056-6 (Electronic)

# 14
# Selected Examples of the Dimensional-analytical Treatment of Processes in the Field of Chemical Unit Operations

**Introductory remark**

Chemical reactions obey the rules of chemical thermodynamics and chemical reaction kinetics. One can represent them easily in a dimensionless space. However, if they take place slowly and without significant heat of reaction in the homogeneous system ("micro-kinetics") they are not subject to any scale-up rules.

Nontheless, such a reaction course occurs only very infrequently in chemical reaction engineering. Most chemical reactions take place in heterogeneous material systems (G/L, L/L, G/S, L/S, G/L/S) and generate considerable amounts of reaction heat. Consequently, the genuine chemical action is accompanied by mass and heat transfer processes ("macro-kinetics") which are scale-dependent. The course of such chemical reactions will be similar on a small and large scale, if the mass and heat transfer processes are similar and the "chemistry" remains the same.

In a continuous reaction process, the actual residence time of the reaction partners in the reactor plays a major role. It is governed by the residence time distribution of the reactor which gives information on back-mixing (macro-mixing) of the throughput. This emphasizes the interaction between chemical reaction and fluid dynamics.

Chemical reactions exist in which mass and/or heat transfer represent the rate-controlling step. If both transfer processes occur *simultaneously,* special scale-up problems may arise because they obey different laws; see the reaction in a catalytic packed-bed reactor, Example 41/2.

From the point of view of dimensional analysis, a chemical engineering problem presents itself with the appearance of chemical parameters containing an additional base dimension, namely the amount of substance N in their respective dimensions (base unit: mole). Consequently, we then have to deal with a 5-parametric dimensional system [M, L, T, Θ, N].

**Example 41**: Continuous chemical reaction process in a tubular reactor

Historical credit goes to *Gerhard Damköhler* (1908–1944) who was the first to use the theory of similarity [113] to investigate a chemical process in conjunction with mass and heat transfer. In a purely theoretical way he examined the conditions under which scale-up would be possible in the case of (inevitably) partial similarity and he

checked the consequences which would result from such a procedure. However, before analysing his method, we shall discuss this problem from the point of view of dimensional analysis.

1. Homogeneous irreversible 1st order reaction

A homogeneous, constant-volume chemical reaction taking place in a tubular reactor is influenced by mass and heat transfer processes. The flow condition is described by

$$\{v, d, L, \rho, \mu\} \tag{14.1}$$

(v – flowrate, d, L – diameter resp. length of the tubular reactor, $\rho$, $\mu$ – fluid density resp. viscosity). All physical properties are related to the known inlet temperature $\boldsymbol{T}_0$. In contrast to the continuous reaction in the catalytic packed-bed reactor – see section 2 – it is assumed here that c and $T$ differences in radial direction are negligible (plug flow).

The chemical reaction and its conversion are characterized by the *inlet* and *outlet* concentrations $c_{in}$ and $c_{out}$ as well as by the effective reaction rate constants $k_{eff}$. It should be noted that the reaction order – here 1st order – governs the dimension of $k_0$! At the temperature field actually predominating in the reactor, the effective reaction rate constants $k_{eff}$ in the reactor will adjust themselves in accordance with Arrhenius' law:

$$k_{eff} = k_0 \exp(E/\mathbf{R}T) \tag{14.2}$$

The mass and heat transfer is described by

$$\{D, C_p, k, c_{in}\Delta H_R, T_0, \Delta T\} \tag{14.3}$$

($D$ – diffusion coefficient, $C_p$ – heat capacity, k – thermal conductivity, $c_{in}\Delta H_R$ – heat of reaction per unit time and volume, $T_0$ – inlet temperature, $\Delta T$ – temperature difference between fluid and tube wall). The complete relevance list is therefore:

$$\{v, d, L, \rho, \mu, c_{in}, c_{out}, k_0, E/\mathbf{R}, D, C_p, k, c_{in}\Delta H_R, T_0, \Delta T\} \tag{14.4}$$

Only 9 numbers are formed from these 15 dimensional parameters if the amount of heat, H, is added to the five primary quantities [M, L, T, Q, N] as the sixth base dimension: 15–6 = 9. If L/d, $c_{out}/c_{in}$, $E/RT_0$, and $\Delta T/T_0$ are anticipated as trivial numbers, the other five pi-numbers can be obtained using the following simple dimensional matrix:

| | $\rho$ | $L$ | $k_0$ | $T_0$ | $c_e\Delta H_R$ | $\nu$ | $\mu$ | $D$ | $C_p$ | $k$ |
|---|---|---|---|---|---|---|---|---|---|---|
| M | 1 | 0 | 0 | 0 | 0 | 0 | 0 | 0 | –1 | 0 |
| L | –3 | 1 | 0 | 0 | –3 | 1 | –1 | 2 | 0 | –1 |
| T | 0 | 0 | –1 | 0 | 0 | –1 | –1 | –1 | 0 | –1 |
| $\Theta$ | 0 | 0 | 0 | 1 | 0 | 0 | 0 | 0 | –1 | –1 |
| H | 0 | 0 | 0 | 0 | 1 | 0 | 0 | 0 | 1 | 1 |
| $Z_1$ | 1 | 0 | 0 | 0 | 0 | 0 | 1 | 0 | –1 | 0 |
| $Z_2$ | 0 | 1 | 0 | 0 | 0 | 1 | 2 | 2 | 0 | 2 |
| $Z_3$ | 0 | 0 | 1 | 0 | 0 | 1 | 1 | 1 | 0 | 1 |
| $Z_4$ | 0 | 0 | 0 | 1 | 0 | 0 | 0 | 0 | –1 | –1 |
| $Z_5$ | 0 | 0 | 0 | 0 | 1 | 0 | 0 | 0 | 1 | 1 |

$Z_1 = M;\qquad Z_2 = 3M + L + 3H;\qquad Z_3 = -T;\qquad Z_4 = \Theta;\qquad Z_5 = H$

The following dimensionless numbers result:

$$\Pi_1 = \frac{v}{Lk_0} = (k_0\,\tau)^{-1}$$ (mean residence time $\tau \equiv L/v$ at pipe flow!)

$$\Pi_2 = \frac{\mu}{\rho d^2 k_0} = (k_0\,\tau\,\mathrm{Re}\,L/d)^{-1}$$

$$\Pi_3 = \frac{D}{L^2 k_0} = (k_0\,\tau\,\mathrm{Re}\,\mathrm{Sc}\,L/d)^{-1}$$

$$\Pi_4 = \frac{\rho C_p T_0}{c_{in}\Delta H_R} = \mathrm{Da}^{-1}$$ (Da – Damköhler number)

$$\Pi_5 = \frac{kT_0}{c_{in}\Delta H_R d^2 k_0} = (k_0\tau\,\mathrm{Re}\,\mathrm{Pr}\,\mathrm{Da}\,L/d)^{-1}$$

The power products formed with the aid of the dimensional matrix can be traced back to known, mostly named numbers (Re, Pr, Sc). The only new dimensionless number here is the Damköhler number, Da, which will be discussed later. The numbers obtained, together with the four anticipated trivial numbers, give the following dimensional-analytical framework:

$$\{L/d,\ c_{out}/c_{in},\ E/\mathbf{R}T_0,\ \Delta T/T_0,\ k_0\tau,\ \mathrm{Re},\ \mathrm{Sc},\ \mathrm{Pr},\ \mathrm{Da}\} \tag{14.5}$$

The pi-space under consideration is described completely by this pi-set.

It is obvious that when scaling up chemical reactors it is generally unacceptable to change the reaction temperature $T_0$ because this would impede the reaction course (and hence $k_0$) or at least the selectivity of the reaction. For the same reason, it is not possible to vary the physical or chemical properties of the reaction partners.

If scale-up of the tubular reactor of the given geometry (L/d = idem) is performed at $T_0$ and $\Delta T/T_0$ = idem, taking account of these restrictions, the kinetic and material numbers $E/\mathbf{R}T_0$, Da, Sc, Pr remain unchanged. Therefore, to attain a specified degree of conversion $c_{out}/c_{in}$ = idem, it is only necessary to ensure that the other two numbers $Re = v\, d\, \rho/\mu$ and $k_0\tau \equiv k_0\, L/v$ are adjusted in such a way that they remain *idem*. However, it is immediately clear that this is an impossibility in the case of L/d = idem because

$$v\, d \rightarrow v\, L = \text{idem and } L/v = \text{idem}$$

cannot be fulfilled simultaneously in the tubular reactor! (In a mixing vessel this problem does not exist.)

In the scale-up of a tubular reactor, the problem is to increase the flowrate $q \propto v\, d^2$ by a factor $n$ (not to be confused with the scale μ!) while retaining the chemical efficiency (yield, conversion, selectivity, etc.):

$$q_T = n\, q_M \quad \rightarrow \quad v_T\, d_T{}^2 = n\, v_M\, d_M{}^2$$

How does this demand react with the conditions Re = idem and $k_0\tau$ = idem?

$$Re \propto v\, d = \text{idem} \quad \rightarrow \quad d_T = n\, d_M; \quad v_T = v_M/n$$

It follows that

$$V_T = n^3\, V_M \quad \text{and hence} \quad \tau_T = n^2\, \tau_M \quad (\tau = V/q)$$

The volume of the full-scale facility is $n^3$ times larger than that of the model. However, the flow through it is only $n\, q_M$ , consequently the residence time τ is $n^2$ times larger. From $k_0\tau$ = idem it follows that the reaction rate constant $k_0$ in the prototype would be smaller by a factor of $n^2$ and this contradicts the precondition stated above!

At this point, one will ask whether or not the demand for Re = idem is justified. In the last instance we are dealing with a fast reaction if we have selected a tubular reactor. Consequently, the flow through this pipe reactor will certainly be turbulent. It is well known that Re only has a slight influence in the turbulent flow regime!

2. Heterogeneous catalytic reaction of the 1st order

Let us now consider a "catalytic packed bed reactor", i.e. a tubular reactor filled with a grained catalyst through which the gas mixture flows. With the particle diameter of the catalyst, $d_p$, an additional dimensionless number $d_p/d$ is added to the pi-space; the Reynolds number is now expediently formed with $d_p$. The reaction rate is related to the unit of the bulk volume and characterized by an effective reaction rate constant $k_{0,eff} \equiv k^*$. The thermal conductivity (k) also has to be valid for the gas/bulk solids system and diffusion can be considered as being negligible (Sc is irrelevant). The complete pi-space is therefore:

$$\{c_{out}/c_{in},\ L/d,\ d_p/d,\ E/\mathbf{R}T_0,\ \Delta T/T_0,\ k^*\tau,\ Re,\ Pr,\ Da\} \tag{14.6}$$

Since the diameter of the catalyst grain has a considerable influence on the reaction rate, its variation will not be permitted during scale-up; this means that the geometrical similarity will *inevitably* be violated by $d_p/d \neq$ idem. Therefore, scale-up of the tubular reactor filled with catalyst is, at best, possible through adherence to partial similarity whereby it is necessary to check whether violation of geometric similarity alone is enough to guarantee scale-up.

The scale-up problem under discussion is completely covered by the given pi-space. However, it can be considered in greater depth by compiling fundamental differential equations which mathematically formulate the conditions for preservation of mass, impulse and energy (c.f. statement in Fig. 6).

*G. Damköhler* [113] used this possibility to develop *Navier-Stockes* differential equations of the mass and heat transfer for the case of an adiabatic reaction. Analytical solution of these differential equations is not possible. However, if they are made dimensionless, it becomes apparent that the pi-space is formed by the five dimensionless numbers listed below:

$$Re \equiv \frac{vL\rho}{\mu}$$

$$I \equiv \frac{k^* L}{v} \rightarrow k^*\tau \text{ (for the pipe flow)}$$

$$II \equiv \frac{k^* L^2}{D} = \frac{k^* L}{v}\ \frac{vL}{\nu}\ \frac{\nu}{D} = k^*\tau\ Re\ Sc$$

$$III \equiv \frac{k^* c_{in} \Delta H_R L}{\rho C_p T_0 v} = \frac{c_{in}\Delta H_R}{\rho C_p T_0}\ \frac{k^* L}{v} = Da\ k^*\tau$$

$$IV \equiv \frac{k^* c_{in} \Delta H_R d^2}{k T_0} = \frac{c_{in}\Delta H_R}{\rho C_p T_0}\ \frac{k^* L}{v}\ \frac{vL\rho}{\mu}\ \frac{C_p\mu}{k} = Da\ k^*\tau\ Re\ Pr$$

Although *Damköhler* traced numbers I to IV back to the above combinations of named dimensionless numbers known at that time, numbers I to IV have come to be known as the four Damköhler numbers $Da_I$ to $Da_{IV}$ in chemical literature. We will *not* identify them in this way, instead we will only refer to the new, genuine reaction kinetic pi-number

$$\frac{c_{in}\Delta H_R}{\rho C_p T_0} \equiv Da \tag{14.7}$$

as the Damköhler number Da.

In fact, the advantage of these combinations of numbers obtained by making differential equations dimensionless, over those combinations delivered by dimensional analysis, is that they characterize certain types of mass and heat transfer, respec-

tively. For example, III represents the ratio of the reaction heat to heat removal by convection, while IV expresses the ratio of the reaction heat to heat removal by conduction.

*G. Damköhler* bases his analysis of the scale-up problem relating to the catalytic tubular reactor on the following pi-set (*D* and hence number combination II are irrelevant):

$$\left\{\frac{L}{d},\ \frac{d_p}{d},\ \underbrace{\frac{v d_p \rho}{\mu}}_{\text{Re}},\ \underbrace{\frac{k^* L}{v}}_{\text{I}},\ \underbrace{\frac{k^* c_{in} \Delta H_R L}{\rho C_p T_0 v}}_{\text{III}},\ \underbrace{\frac{k^* c_{in} \Delta H_R d^2}{k T_0}}_{\text{IV}}\right\} \tag{14.8}$$

He knows that he may not vary the temperature $T_0$ and $d_p$ if he does not want to risk influencing the chemical course of the reaction. Consequently, as already mentioned, geometric similarity is inevitably violated during scale-up on account of $d_p/d \neq$ idem. *Damköhler* is therefore prepared to waive adherence to L/d = idem as well. However, he points out that this will necessarily lead to consequences for heat transfer behaviour. In this case, he uses the *hypothesis* that thermal similarity is guaranteed if the ratio of IV to III (heat conduction through the tube wall to heat removal by convection) is kept equal:

$$\frac{\text{IV}}{\text{III}} = \frac{k^* c_{in} \Delta H_R d^2}{k T_0} \frac{\rho C_p T_0 v}{k^* c_{in} \Delta H_R L} = \frac{\rho C_p v d}{k L} \equiv \text{Pe}\frac{d}{L} = \text{ idem}$$

Scale-up must therefore be effected in the pi-space $\{k^*\tau$, Re, Pe$\}$. It then follows that:

$\text{Re} = \text{idem} \rightarrow v = \text{idem}$

$k^*\tau = k^* L/v = \text{idem} \rightarrow L = \text{idem}$

$\text{Pe} = \text{idem} \rightarrow d = \text{idem}$

The requirement d = idem means $\mu$ = idem and this makes a change in scale impossible.

**Result**: Abandoning geometric similarity is not enough to guarantee chemical similarity which requires that $T_0$ and hence $k^*$ be idem.

*Damköhler* now proposes to abandon not only geometric, but also fluid dynamic similarity (Re = irrelevant). The scale-up should depend exclusively on thermal and reaction similarity. This means that, apart from $k^*\tau$, only III and IV must be kept constant. The pi-space is then:

$$\left\{\frac{k^* L}{v},\ \frac{k^* c_0 \Delta H_R L}{\rho C_p T_0 v},\ \frac{k^* c_0 \Delta H_R d^2}{k T_0}\right\} \tag{14.9}$$

Since, according to *Damköhler*, heat conductivity is approximately proportional to the flowrate ($k_{eff} \propto v$) in the turbulent flow regime and, from a certain small $d_p/d$ ratio, independent of it, the following scale-up rules result from the above pi-space:

$$Da_I \equiv k^* \tau \rightarrow L/v = \text{idem}$$

$$Da_{III} \rightarrow L/v = \text{idem}$$

$$Da_{IV} \rightarrow d^2/k \propto d^2/v = \text{idem}$$

In conjunction with the flow rate equation and the enlargement factor for the liquid throughput $n \equiv q_T/q_M$, it follows that

$$Da_{IV} = \text{idem} \rightarrow d_T = n^{1/4}\, d_M \quad \text{as well as } v_T = n^{1/2}\, v_M$$

$$Da_I = \text{idem as well as } Da_{III} = \text{idem} \rightarrow L_T = n^{1/2}\, L_M$$

Consequently,

$$(L/d)_T = n^{1/4}\, (L/d)_M \tag{14.10}$$

and, in conjunction with $\Delta p \propto L\, v^2$, the following is valid

$$\Delta p_T = n^{3/2}\, \Delta p_M$$

If one assumes that both hypotheses (irrelevance of both geometric and fluid dynamic similarity) are applicable, this result shows that the industrial tubulat reactor would be influenced by a pressure increase. This would not only incur costs but could also have an unknown effect on the course of reaction. Therefore, tube bundle reactors are more economic.

Scale-up at partial similarity was discussed in Sect. 6.2. It was pointed out that various strategies exist and Froude's method which is based on *dividing the process into parts* that can be investigated separately, was presented.

The present example illustrates another method for dealing with partial similarity. It is based on *deliberately abandoning certain similarity criteria* and theoretically and/or practically checking the effects on the entire process. *Damköhler*'s example convincingly demonstrates that valuable information concerning the scale-up of a complex chemical process can be deduced from theoretical considerations alone if the principles relating to the theory of similarity are used consistently.

However, *Damköhler* seems to have been very disappointed with the result of his study. His conclusions, in [113], as quoted below, cannot be interpreted any other way:

"Although it is basically possible to apply the theory of similarity to chemical processes and to scale up one of these processes in such a way that geometric, fluid dynamic, thermal and reaction-kinetic similarity is retained to a greater or lesser extent, these transformation processes are only of limited importance. They may be quite useful for increasing equipment performance two to five-fold but hardly to much larger amounts. This circumstance is of importance since *it is more or less equivalent to practical failure of the theory of similarity.* This, however, was not to be expected from the beginning, especially in view of the fact that the theory of simila-

rity proved itself brilliantly in the solution of other heat transfer problems where no additional chemical conditions had to be fulfilled".

The results of his studies and the efficiency of methods based on the theory of similarity have been assessed differently by posterity. If the method shows that scale-up is not possible, this by no means points to failure of the method but rather is a valuable indication of the given facts!

**Example 42**: Description of the mass and heat transfer in solid-catalyzed gas reactions by dimensional analysis

In this example, the composition of the catalyst surface is responsible for its activity. Therefore, catalysts are placed on porous supporting material (pellets) which have specific surface areas of some hundred $m^2/g$ pellet. Because the pellet core has the largest surface area, the reaction predominantely takes place here.

In solid-catalyzed gas reactions the rate equations have to be extended by the mass and heat transfer terms. The following has to be considered:

1 Diffusion resistance for educts in the gas film and in the catalyst pores;
2 Sorption processes and reaction on the catalyst surface;
3 Diffusion resistance for products in the gas film and in the catalyst pores.

If the reaction proceeds without a change in molar volume, steps 1 and 3 can be considered as countercurrent diffusion.

In this field, an intensive research has been carried out about 40–60 years ago, see e.g. [114–118]. The results of these studies are contained in textbooks on chemical engineering, see e.g. [119–121]. Only those results will be presented and discussed here, which are directly associated with dimensional analysis.

1 Outer transfer processes

The isothermal and the non-isothermal reaction with the diffusion resistance in the gas film will be treated in succession.

1.1 Surface reaction with diffusion resistance in the gas film

Here, we look at the conversion of a gaseous component A on a non-porous catalyst under isothermal conditions. In the steady-state, the volume-related rates of the gas-side mass transfer and the surface reaction are equal to each other:

$$k_G a\,(c_G - c_S) = k c_S \tag{14.12}$$

$k_G$ – gas side mass transfer coefficient; a – surface area per unit volume; k – reacton rate constant; subscripts: G – gas phase; S – solid phase.

Using this equation, the unknown gas concentration prevailing on the catalyst surface, $c_S$, can be expressed as

$$c_S = \frac{k_G a}{k + k_G a} c_G = \frac{1}{1 + k/k_G a} c_G \tag{14.13}$$

and the effective reaction rate $r_{eff} = kc_S$ formulated:

$$r_{eff} = \frac{k}{1+k/k_G a} c_G = k_{eff} c_G \tag{14.14}$$

At $k/k_G a << 1$, the chemical reaction is much slower than the mass transfer rate. In this case, concentration difference in the gas boundary layer does not exists. Therefore, $k/k_G a$ can be interpreted as the ratio of the reaction rate without transport limitation ($c_S = c_G$) to the reaction rate at transport limitation ($c_S \to 0$).

$k/k_G a$ is also named the 2. Damköhler number $Da_{II}$, because in $Da_{II} \equiv k_1 L^2/D$, the expression $(D/L)L^{-1}$ can be interpreted as $k_G a$: $D/L\, k_G$; $A/V \equiv a$ and $k_1$ is the reaction rate of a 1st order reaction.

The quotient from the effective reaction rate ($r_{eff}$) and that (r) without diffusion control ($c_G = c_S$) defines the outer catalyst effectiveness factor, $\eta_{ext}$:

$$\eta_{ext} \equiv \frac{r_{eff}}{r} = \frac{k_{eff} c_G}{k c_G} = k \frac{1}{1+Da_{II}} c_G \times \frac{1}{k c_G} = \frac{1}{1+Da_{II}} \tag{14.15}$$

Whether $r_{eff}$ is diffusion controlled or not, i.e., whether $\eta_{ext} = 1$ or $\eta_{ext} < 1$, $r_{eff}$ can be ascertained if the measured k value is first multiplied with the (solely known) $c_G$

$$r_{eff} = r\, \eta_{ext} = \eta_{ext}\, k c_G \tag{14.16}$$

and then divided by the maximum attainable mass transfer

$k_G a\, (c_G - c_S)$ at $c_S = 0$, i.e. with $k_G a\, c_G$

$$\frac{r_{eff}}{k_G a c_G} = \eta_{ext} \frac{k^* c_G}{k_G a c_G} = \eta_{ext} Da_{II} \tag{14.17}$$

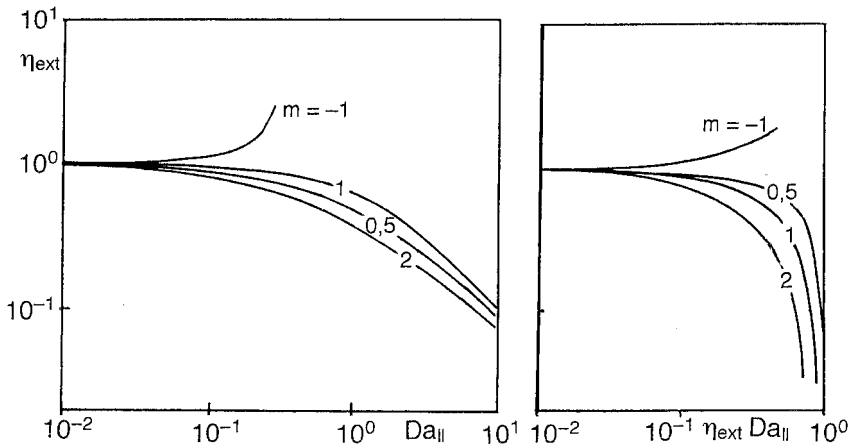


**Fig. 80** External catalyst effectiveness factor $\eta_{ext}$ as a function of the Damköhler-II number $Da_{II} \equiv k/k_G a$ and the reaction order m; from [118].

For this purpose the $k_G a$ value has to be determined separately: a can be measured and $k_G$ can be calculated. Then $\eta_{ext}$ can be determined from the correlation $\eta_{ext}$ ($\eta_{ext}$ $Da_{II}$) in **Fig. 80**.

1.2 Surface reaction with diffusion and heat transfer resistance

In fast exothermic reactions, in addition to grad c, also grad $T$ ($T_G \neq T_S$) is present in the boundary layer between the gas bulk phase and the catalyst surface. For the outer effectiveness factor $\eta_{ext}$ this means that

$$\eta_{ext} = \frac{r_{eff}}{r} = \frac{k(T_S)c_S}{k(T_G)c_G} \tag{14.18}$$

The quotient $c_S/c_G$ corresponds to the expression

$$\frac{c_S}{c_G} = \frac{k_G a - \eta_{ext} k(T_G)}{k_G a} = 1 - \eta_{ext} \frac{k(T_G)}{k_G a} = 1 - \eta_{ext} Da_{II} \tag{14.19}$$

Coupling of (14.19) and (14.18) gives the sought after correlation between grad $T$ and $\eta_{ext}$:

$$\eta_{ext} = \frac{k(T_S)}{k(T_G)}(1 - \eta_{ext} Da_{II}) \tag{14.20}$$

The introduction of the Arrhenius term for k($T$) and the pi-number Arr ≡ E/**R**$T$ gives:

$$\eta_{ext} = \exp\left[Arr_G\left(1 - \frac{T_G}{T_S}\right)\right](1 - \eta_{ext} Da_{II}) \tag{14.21}$$

For the determination of $\eta_{ext}$, not only the accessible quantity $\eta_{ext}$ $Da_{II}$ but also $T_G/T_S$ must be known. This can be obtained by the following reasoning: In the steady-state, heat removal equals the heat production:

$$Q/V = h\,a\,(T_S - T_G) = r_{eff}\,(-\Delta H_R) \qquad (a \equiv A/V) \tag{14.22}$$

Resolved after $T_S/T_G$, the equation reads

$$\frac{T_S}{T_G} = 1 + \frac{r_{eff}(-\Delta H_R)}{T_G h a} \tag{14.23}$$

h can be expressed via analogy between mass and heat transfer according to the correlation Sh = Nu $(Sc/Pr)^n$ as follows:

$$h = k_G\,(k/D)\,Le^{-n} \qquad \text{(Lewis number Le} \equiv Sc/Pr)$$

Now, the reciprocal value of $T_S/T_G$ is formed, see eq. (14.23), and h is expressed by the just presented correlation:

$$\frac{T_G}{T_S} = \frac{1}{1 + \frac{r_{eff}(-\Delta H_R)}{T_G a k_G (k/D) Le^{-n}}} \tag{14.24}$$

A multiplication of the fraction in the denominator by $c_G$ finally gives:

$$\frac{T_G}{T_S} = \frac{1}{1+\frac{r_{eff}(-\Delta H_R)}{T_G a k_G (k/D)Le^{-n}} \times \frac{c_G}{c_G}} = \frac{1}{1+\frac{(-\Delta H_R)c_G}{(k/D)Le^{-n}T_G} \times \frac{r_{eff}}{k_G a c_G}} = \frac{1}{1+\beta \times \eta_{ext} Da_{II}} \quad (14.25)$$

The fraction surrounded by a box in eq. (14.25) is named Prater number β. It is formed with the gas-side values ($c_G$, $T_G$). The fraction on the right-side of the box is the already known pi-number combination $\eta_{ext}Da_{II}$. When this correlation is introduced into the equation for $\eta_{ext}$, then it follows that:

$$\eta_{ext} = \exp\left[-Arr_G\left(\frac{1}{1+\beta\eta_{ext}Da_{II}} - 1\right)\right](1 - \eta_{ext}Da_{II}) \quad (14.26)$$

Prater number β represents a combination of pi-numbers which can be traced back to the already known ones:

$$\beta \equiv \frac{Da_{IV}}{Da_{II}Le} \times Le^{-n} \quad \rightarrow \quad \beta \equiv Da \times Le^{-(1+n)} \quad (14.27)$$

For Da see the definition, eq. (14.7). From this it follows that the name "Prater number" is superfluous.

The eq. (14.26) is represented in **Fig. 81** for two different Arr values. It can be seen that the outer effectiveness factor $\eta_{ext}$ can attain values of >> 1. In such cases the reaction takes place on the surface of the catalyst at $T_S$>> $T_G$. The difference in $T$ can come to 10–30 K and more.

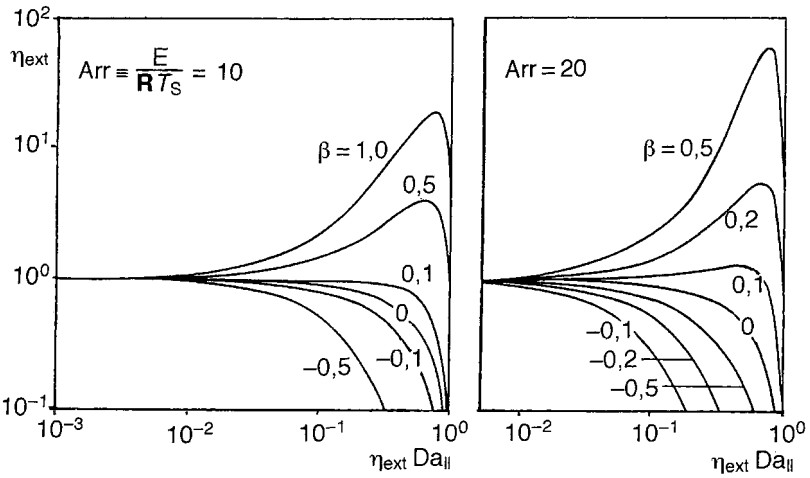


**Fig. 81** Outer catalyst effectiveness factor, $\eta_{ext}$, as a function of the measurable quantity $\eta_{ext}Da_{II}$ for two values of the Arrhenius number, Arr, and for different values of the Prater number $\beta \triangleq Da \times Le^{-(1+n)}$

2 Inner transfer processes

Analogous to above, the isothermal and the non-isothermal reaction will be treated in succession with respect to diffusion resistance in the catalyst pore.

2.1 Isothermal reaction with the diffusion resistance in the pore

Solving the differential equation for the mass balance at steady-state (output – input + disappearance by reaction = 0), see e.g. [119], in a volume element of the pore delivers an equation which describes the change of concentration in the pore as a function of its length, L:

$$\frac{c}{c_S} = \frac{\cosh\ m(L-x)}{\cosh\ mL} = \frac{\cosh[\Phi(1-x/L)]}{\cosh\ \Phi} \tag{14.28}$$

where $\Phi \equiv m\ L \equiv L\ \sqrt{k_1/D}$, a dimensionless number named the Thiele modulus, $\Phi$, was introduced. This naming is also completely superfluous: It could be replaced by $\sqrt{Da_{II}}$.

The effectivenes factor of the pore, $\eta_p$, is defined simislarly to $\eta_{ext}$ and is the ratio of $r_{eff}$ to r without any transport limitation. For a 1st order reaction, a simple correlation between $\eta_p$ and $\Phi$ exists, because here $r \propto c$ holds:

$$\eta_p = \frac{c}{c_S} = \frac{\tanh\ \Phi}{\Phi} = f(\Phi) \tag{14.29}$$

($c_S$ means c at the pore entrance) This correlation is valid for a straight cylindrical pore. To be also valid for a porous pellet, the molecular diffusivity *D* must be replaced by $D_{eff}$ in the porous pellet and the influence of the pellet shape taken into consideration by a characteristic length $L_C \equiv (V/S)_P$. Consequently, the modified Thiele modulus, $\Psi$, is given by

$$\Psi \equiv L_C \sqrt{k_1/D_{eff}} \tag{14.30}$$

The hitherto made statements are only valid for irreversible reactions of the 1st order. To obtain an expression which is also valid for optional reaction orders, m, a modification of the Thiele modulus has to be made:

$$\Psi \equiv L_C \sqrt{[(m+1)/2](k_1 c_S^{m-1}/D)} \tag{14.31}$$

If kinetic measurements have been obtained with a certain catalyst, the question arises as to whether or not these data have been influenced by the pore resistance. To answer this question, one has first to chose an optional reaction order and to suppose that the film resistance can be neglected. For a 1st order reaction:

$$-r = k_1\ c_S\ \eta_p \tag{14.32}$$

and eliminating the unknown rate constant $k_1$ using the Thiele modulus $\Phi$ we obtain:

$$\Phi \equiv L\sqrt{k_1/D_{eff}} \quad \rightarrow \quad k_1 = D_{eff}\Phi^2/L^2,$$

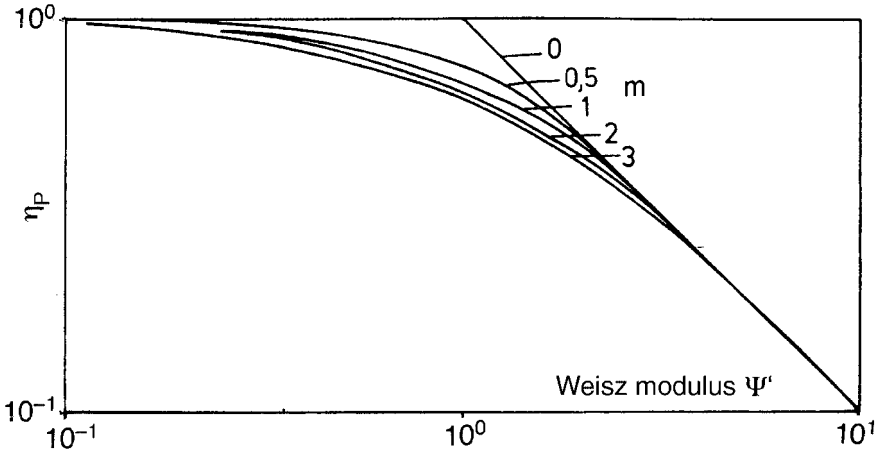


**Fig. 82** Catalyst effectiveness factor $\eta_p$ as a function of the Weisz modulus, $\Psi' \triangleq \eta_p\, Da_{II}$, and the reaction order, m.

Therefore, it follows from (14.32) that

$$\frac{-rL^2}{D_{eff}\, c_G} = \eta_p \Phi^2 \equiv \Psi' \qquad \Psi' - \text{Weisz-Modul} \tag{14.33}$$

Keeping in mind that the Thiele modulus, $\Phi \equiv L\sqrt{k_1/D}$, can be replaced by $\sqrt{Da_{II}}$, this means that the naming of Weisz modulus $\Psi'$ was also superfluous, because $\Psi' \equiv \eta_p\, Da_{II}$.

The correlation between $\eta_p$ and $\Psi'$ as being dependent on the reaction order, m, is represented in **Fig. 82**.

2.2 Non-isothermal reaction with the diffusion resistance in the pore

In an exothermal reaction, temperature gradients will arise within the pellet and, consequently, the temperature of pellet will be elevated compared with its surroundings. As a result, the reaction will be faster than the isothermal counterpart. $\Delta T$ in the film as well in the pellet can be theoretically predicted and, consequently, the maximum $\Delta T$ between the outer surface ($T_s$) and the inside of the catalyst ($T_{in}$) calculated, when there c = 0:

$$\frac{(T_{in} - T_S)max}{T_S} = \frac{(-\Delta H_R)c_S}{(k/D)_{eff}\, T_S} \equiv \beta \tag{14.34}$$

The Prater number β – in contrast to eq. (14.25) is related to $T_S$ and not to $T_G$ – and the Arrhenius number have a major influence on the development of the $T$ and c profiles. The pore utilization factor $\eta_p$ is therefore dependent upon Arr, β and Thiele modulus Φ. The correlation between these four pi-numbers is represented in **Fig. 83**. For $\eta_p$ and Φ the following definitions apply:

$$\eta_K \equiv \frac{r_{eff}}{r(T_s, c_s)} \quad \text{and} \quad \Phi^2 \equiv r_p^2 \frac{k_s c_s^{m-1}}{D_{eff}} \exp(-Arr) \tag{14.35}$$

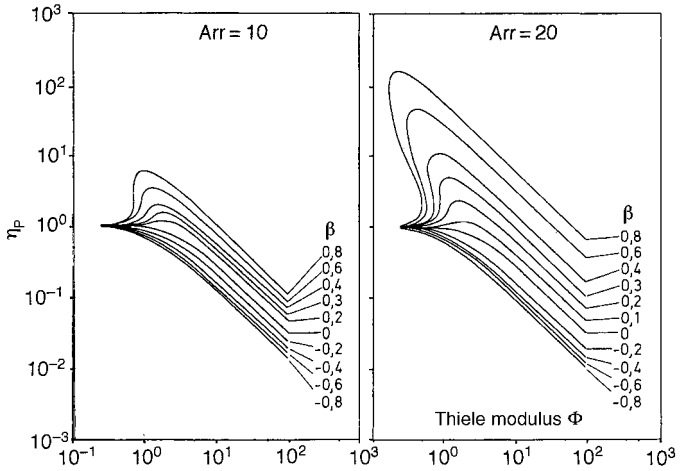


**Fig. 83** Catalyst effectiveness factor (pore utilization factor), $\eta_p$, for two Arrhenius numbers and different Prater numbers β as a function of the Thiele modulus, Φ.

However, a comparison of the numerical values of Φ, β and Arr, established in full-scale reaction plants for exothermal catalytic gas reactions, has revealed that due to mostly very low β values ($\beta \approx 0.01$–$0.1$), values of $\eta_p > 1$ do not appear. This means that within the paletts larger *T* gradients are not to be expected.

Finally, a few remarks should be made with respect to the naming of characteristic pi-numbers in the macro-kinetics. Pi-numbers are associated with researchers names in order to point clearly and easily to a particular dimensionless formulated context (e.g. Reynolds number). In doing so, it was primarily not intended to highlight the respective researcher in some manner. Seen from this point of view, the posthumous naming of the four Damköhler numbers seems unnecessary, particularly because even Damköhler himself referred to the fact that pi-numbers $k\ L/v \triangleq k\ \tau$ and $k\ L^2/D$ had already been introduced before him. Because these two pi-numbers are the most important pi-numbers in the field of chemical engineering, their handy naming after *Damköhler* as $Da_I$ and $Da_{II}$ represents no disadvantage. Whether one can say the same for Prater number and the Thiele and Weisz modulus is a question which everybody should answer for himself. (For comparison, see the listing of the important named pi-numbers in the appendix.)

**Example 43**: Scale-up of reactors for catalytic processes in the petrochemical industry

Today, solid-catalyzed gas reactions are executed to an extent of several billions of tonnes per annum. To name only a few important examples: Steam reforming of methane-rich natural gas to "synthesis gas" ($H_2$ + CO), conversion of CO with $H_2O$ to $CO_2$ + $H_2$, conversion of CO with $H_2$ to methane, ammonia synthesis, oxidation of $SO_2$ to $SO_3$ (sulphuric acid production), oxidation of $NH_3$ to NO (nitric acid production). The world production of ammonia in 1995 amounted to 90 m tonnes and

of sulphuric acid to 140 m tonnes. Alone BAYER AG, D–Leverkusen, produced 1.000 tonnes $H_2SO_4$/day in the early 1990is.

In this specific field, in particular the petrochemical industry is subjected to gigantism, due to the fact that the investment costs for petrochemical plants do not increase proportionally but to the 0.7 power of their capacity [122]. It is therefore profitable to build the production units as large as possible – market permitting.

In the development of these processes and their transference into an industrial-scale, dimensional analysis and scale-up based on it play only a subordinate role. This is reasonable, because one is often forced to perform experiments in a demonstration plant which copes in its scope with a small production plant ("mock-up" plant, ca. 1/10-th of the industrial scale). Experiments in such plants are costly and often time-consuming, but they are often indispensable for the lay-out of a technical plant. This is because the experiments performed in them deliver a valuable information about the scale-dependent hydrodynamic behavior (circulation of liquids and of dispersed solids, residence time distributions). As model substances hydrocarbons as the liquid phase and nitrogen or air as the gas phase are used. The operation conditions are ambient temperature and atmospheric pressure ("cold-flow model"). As a rule, the experiments are evaluated according to dimensional analysis.

*P. Trambouze* [122, 123] from Institut Français du Petrole (IFP) demonstrated on the basis of three petrochemical processes how "mock-up" plants enabled the acquisition of pertinent data for a reliable scale-up. This work will be presented here in greater detail because it shows that for a reliable scale-up of industrial plants in petrochemical industry – whose investment costs per plant often amount to a three digit million US$ sum – measurements on a large scale are often indispensable, leaving hardly place for a classical model scale-up. Seen from this point of view, the quotation in [122] is perfecty understandable:

"In pilot plants, scale-up does not correspond to a change in size that is achieved by multiplying characteristic dimensions by a factor greater than one."

1. **Hydrotreating petroleum cuts.** Catalytic hydrogenation of organic compounds containing S, N and O, into $H_2S$, $NH_3$ and $H_2O$, respectively, is necessary today for environmental reasons as well as to protect exhaust gas catalysts in automobiles. It is performed in catalytic fixed bed reactors through which the gaseous and liquid phases flow simultaneously in a cocurrent downflow. The flow of the liquid phase corresponds to the plug flow. Back-mixing is negligible for catalyst bed heights of > 1m. Problems are caused by a poor liquid distribution that leads to preferential paths. Certain portions of the catalyst bed may not even be wetted by the liquid. Reactions may take place in the dry zones involving the gas phase only, these are faster and liable to give rise to hot spots. Another problem is caused by the broader residence time distribution, which may have an effect when an extremely high conversion degree is required in order to remove traces of certain products.

In a mock-up plant the catalyst bed consists of the industrially used catalyst. As the liquid phase hydrocarbons and as the gas phase nitrogen are used. A geometric similarity cannot be kept because this would lead to a pilot reactor with the height of the industrial plant. The capacity of the pilot plant has to be reduced. In order to do

this, two alternatives exist. The first is to perform an operation with a cocurrent upflow, this makes sure that the catalyst bed is wetted by the liquid. The second possibility is to have a downflow operation. In this case the catalyst must be diluted with inert particles having a much smaller particle size distribution. This significantly increases the retention time of the liquid phase and, accordingly, the wetting of the catalyst.

The first alternative was examined. Measurements confirmed that the hydrodynamic conditions were compatible with the assumptions made for this model.

Recent studies (made public in 1988) revealed that the fixed bed technology was no longer the best, given the rapid deactivation of the catalyst that resulted from the deposition of metals contained in the feedstock. The moving bed alternative was therefore considered and countercurrent flow appeared to offer the optimal technology.

A feasibility study, carried out with mock-ups of various sizes, ensured that the catalyst bed could flow in countercurrent to the fluids (gas and liquid) and that the flow of the particulate solids was sufficiently close to plug flow. A moving bed reactor ($40^{\varnothing}$ cm × 20 m high) was succesfully operated as a demonstration plant for several months, whereby different heavy residues were treated.

2. **Regenerative catalytic reforming** serves to increase the fuel octane number. It is performed in catalyst fixed beds in the gas phase (ca. 500 °C, p = 10–50 bar). Thermal effects are fairly pronounced during the first phase of the conversion, which essentially corresponds to the dehydrogenation of the cycloparaffins.

Conventional technology, which has been employed for over 25 years, uses three or four fixed bed reactors in series, these operating under adiabatic conditions. They are preceeded by heating furnaces that compensate for the overall endothermicity of the reaction. Catalyst performance was investigated separately in a pilot plant under isothermal conditions, employing ca. 300–400 g of catalyst.

This process could cope with gasoline demand by only steadily improving the catalyst stability. Nevertheless, this process would reach its limits if process technology would remain unchanged. Consequently, moving bed technology, which allows continuous or semicontinuous regeneration of the catalyst, was developed.

Before building an industrial plant using this new technology, a number of investigations were obviously necessary. They had to be performed in mock-ups of different sizes in order to ascertain that a largely plug flow motion of the catalyst could be achieved.

After regeneration, the catalyst enters the first reactor at the top. It passes through the reactor by gravity and is then transferred from the bottom of each reactor to the top of the next by a gas-lift. To minimize the pressure drop across the bed, a crossflow technology was adopted: The catalyst flows downwards from the top of the reactor between two concentric cylinders made up of grids, this allowing the radial passage of the gas phase.

Therefore, it was possible to choose the direction of fluid flow. Firstly, either from the inside towards the outside or, secondly, from the outside towards the inside of the reactor. The interactions between the gas phase and the granular solid phase were liable to create irregularities in the solid downflow. The main risk was that the catalyst would be plastered against the grid and would no longer be able to move.

This question was also investigated in differently sized mock-ups, the largest having the geometry and dimensions of the planned industrial reactor. To reduce the catalyst and gas throughputs, only a cut-off section of the cylinder was used. The radial cross-sectional area was made of Plexiglas which permited the observation of the solid flow by means of a tracer technique (layer of colored spheres). This mock-up contained a solid volume of 2.5 $m^3$.

As solids, only spheres were used and these served as a support for the catalyst. The gas phase was air. The operation conditions were ambient temperature and atmospheric pressure.

3. **Catalytic cracking** (cleavage of C–C and C–H bonds in high boiling crude oil fractions to transform long chain hydrocarbons into short chain ones and, consequently, increase the fuel yield.) In this field, Institut Français du Petrole (IFP) together with "Total France" developed a new technique (R2R process) which utilizes a riser and two regenerators. Because the hydrodynamics of the three phase, gas-liquid-solid flow inside the riser could not be investigated on a small scale, a large mock-up had to be build. In addition, an injector was also developed. This introduced the cracking feed at the bottom of the riser and mixed it as rapidly and uniformly as possible with the catalyst.

**Example 44**: Dimensioning of a tubular reactor, equipped with a mixing nozzle, designed for carrying out competitive-consecutive reactions

This example deals with the dimensioning data for a chemical reactor intended to perform a homogeneous, competitive-consecutive chemical reaction. The reaction course is given by:

$$A + B \xrightarrow{k_1} P \text{ (desired)}$$

$$P + B \xrightarrow{k_2} R \text{ (undesired)}$$

This type of reaction is by no means rare. Many chlorinations, phosgenations, and so on, belong to this type. If a high selectivity with respect to P, $S_P$, is demanded, P may not come into contact with B. Therefore, a stirring vessel would be completely unsuitable for this task! It is recommended to perform this reaction in a continuous mode and to use a tubular reactor because it exhibits ideal plug-flow characteristics with respect to macro-mixing (i.e. no back-mixing). Fast micro-mixing of the reaction partners is taken care of by a propulsion jet nozzle installed at the inlet of the pipe, this impinges the smaller volume flow of B into the larger volume flow of A (stoichiometrically surplus component). A annular inset is installed at a short distance after the propulsion jet nozzle in order to prevent a possible back-mixing eddy which would mix the reaction mixture with the free jet. (This happens if the free jet is able to suck more liquid from its surroundings than is supplied with it at the inlet.)

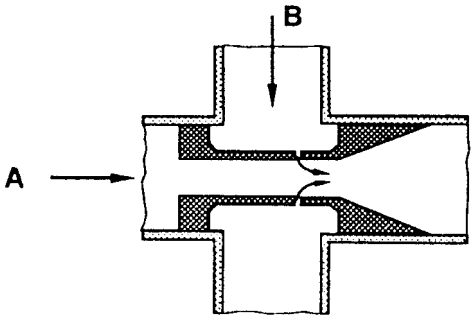


**Fig. 84** Sketch of the propulsion jet nozzle for a tubular reactor for carrying out competitive reactions

In experiments [125], a well known azo reaction (conversion of 1-naphthol with diazo sulphanilic acid into a simple coupled – desired product – and twice coupled product) is carried out. It allows the quantitative determination of micro-mixing on a "molecular scale". Its selectivity is determined following the proposal of *J.R. Bourne* [124] with respect to the undesired product, R. $S_R$ is defined by P and R, which only can be detected analytically, according to the relationship

$$S_R \equiv \frac{2R}{2R+P} = \frac{\text{mols B consumed for the formation of R}}{\text{total moles of B consumed}} \tag{14.36}$$

The reaction engineering task will be to *minimize* the quantity $S_R$.

We will start with the following relevance list:

| | |
|---|---|
| target quantity: | selectivity, $S_R$ |
| geom. parameter: | tube diameter, d (as the characteristic length) |
| physical properties: | $c_A$, $c_B$; $\rho_A$, $\rho_B$; $\nu_A$, $\nu_B$; $D$ |
| process parameters: | $k_1$, $k_2$; $q_A$, $q_B$. |

$c_i$ are the concentrations, $\rho_i$ and $\nu_i$ are the densities and kinematic viscosities of the educts, $D$ is the diffusion coefficient of A in B, $q_i$ are the liquid throughputs and $k_i$ [$L^3\,T^{-1}\,Mol^{-1}$] the reaction rate constants of 2nd order isothermal reactions.

From this relevance list, first the trivial pi-numbers can be anticipated:

$$S_R;\ \frac{c_A}{c_B},\ \frac{\rho_A}{\rho_B},\ \frac{\nu_A}{\nu_B},\ \frac{D}{\nu_B},\ \frac{k_1}{k_2},\ \frac{q_A}{q_B}$$

In the remaining relevance list

$$\{d,\ c_B,\ \rho_B,\ D,\ k_2,\ q_B\}$$

only $\rho_B$ contains the base dimension [M] and therefore has to be cancelled. Only $c_B$ and $k_2$ contain the base dimension [N]; this is eliminated in the combination $c_Bk_2$. The residual relevance list is then

$$\{d,\ D,\ c_Bk_2,\ q_B\}$$

The dimensional matrix with the rank 2 supplies two pi-numbers. They are the Reynolds number and the Damköhler-II number for a 2nd order reaction:

$$\mathrm{Re} \equiv \frac{q_B}{\nu d} \quad \text{und} \quad \mathrm{Da_{II}} \equiv \frac{d^2 c_B k_2}{D}$$

The complete pi-set is comprised of nine numbers

$$\left\{ S_R,\ \frac{c_A}{c_B},\ \frac{\rho_A}{\rho_B},\ \frac{\nu_A}{\nu_B},\ \frac{D}{\nu_B},\ \frac{k_1}{k_2}\ \frac{q_A}{q_B},\ \mathrm{Re},\ \mathrm{Da_{II}} \right\} \tag{14.38}$$

For the given reaction in the given material system, four pi-numbers display constant numerical values

$$\frac{\rho_A}{\rho_B},\ \frac{\nu_A}{\nu_B},\ \frac{D}{\nu_B},\ \frac{k_1}{k_2} = \text{const}$$

Therefore, only a dependence between five pi-numbers has to be investigated:

$$S_R = f\left(\frac{c_A}{c_B},\ \frac{q_A}{q_B},\ \mathrm{Re}, \mathrm{Da_{II}}\right) \tag{14.39}$$

This pi-space can be further reduced if the liquid throughput, $q_A$, forming the jet in the propulsion jet nozzle, is replaced by an intermediate quantity, jet power per unit throughput, $P/q_A$. Due to the relationship $P = q_A \Delta p$, $P/q_A$ corresponds to the pressure drop, $\Delta p$, in the propulsion jet nozzle. The reduction of the pi-space is now possible because by the introduction of $\Delta p$, not only $q_A$ is replaced, but also – due to the intensive character of this variable – d becomes irrelevant and must be deleted.

In order to replace $q_A$ by $\Delta p$, we combine the Euler and Reynolds numbers accordingly

$$\mathrm{EuRe}^2 \equiv \frac{\Delta p d^4}{\rho q^2} \frac{q^2}{\nu^2 d^2} \equiv \frac{\Delta p d^2}{\rho \nu^2}$$

and eliminate d from the resulting pi-number using $\mathrm{Da_{II}}$:

$$\mathrm{EuRe}^2 \mathrm{Da_{II}}^{-1} \mathrm{Sc} \equiv \frac{\Delta p d^2}{\rho \nu^2} \frac{D}{d^2 c_B k_2} \frac{\nu}{D} \equiv \frac{\Delta p}{\mu c_B k_2} \equiv \Psi$$

The sought after dependence for the selectivity, $S_R$, of a fast chemical reaction carried in a tubular reactor with a propulsion jet nozzle as a mixing device, is now represented by only a four-parametric pi-space:

$$S_R = f\left(\frac{c_A}{c_B},\ \frac{\rho_A}{\rho_B},\ \Psi\right) \tag{14.40}$$

Laboratory tests [125] were performed in glass tubes (d = 3–25 mm) with converging propulsion jet nozzles manufactured by the Schlick company (d′ = 0.3–1.6 mm). $q_B$ formed the propulsion jet. A temperature of 20 °C, pH = 10 and mole ratio of $\frac{c_A}{c_B}\frac{q_A}{q_B} = 1.05$ were kept constant, so that only a further reduced relationship of

$$S_R = f\left(\frac{\rho_A}{\rho_B}, \Psi\right) \tag{14.41}$$

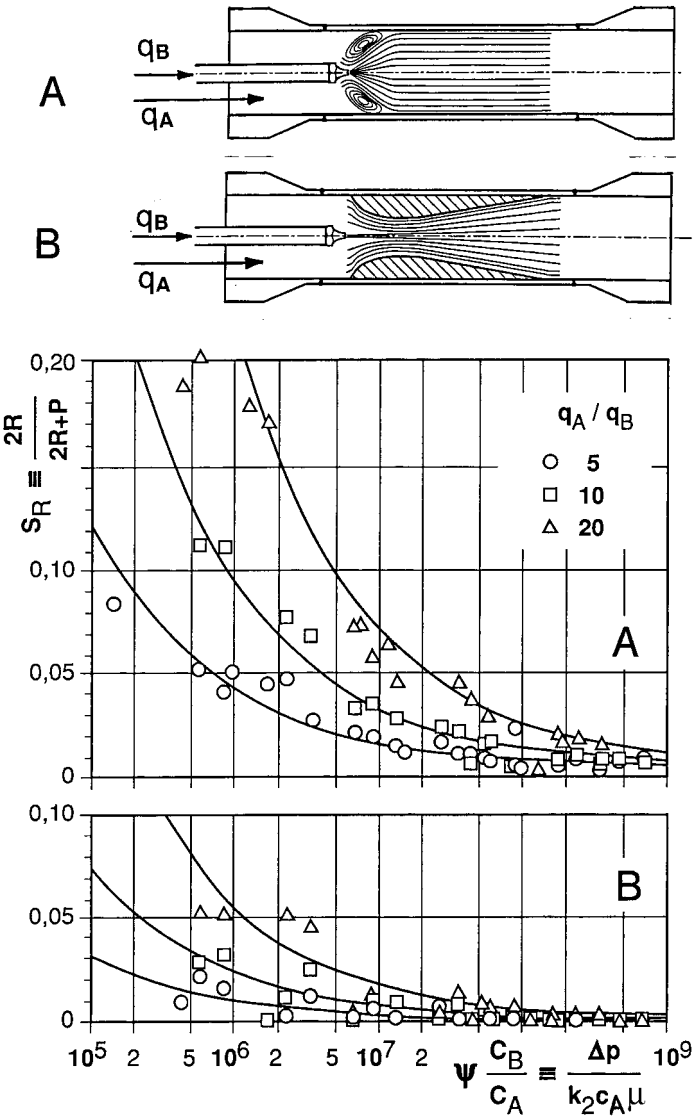


**Fig. 85** Selectivity $S_R$ of the undesired by-product R for a fast reaction taking place in a tubular reactor with a propulsion jet nozzle (Fa. Schlick) as mixing device as a function of $q_A/q_B$ and $\Psi \times c_B/c_A$. The upper graph is valid for developed, the lower graph for suppresed back-mixing.

could be investigated. Test conditions which permitted the formation of a back-mixing eddy in the pipe reactor and hence back-mixing of R and B were also adjusted.

The correlation between the three pi-numbers in (14.41) is presented in **Fig. 85**. The analytical expressions for the two groups of curves are:

without back-mixing: $S_R = 1.3\ (\Psi \times c_B/c_A)^{-0.5}\ (q_A/q_B)^{1.25} + 0.001$

with back-mixing: $S_R = 5.0\ (\Psi \times c_B/c_A)^{-0.5}\ (q_A/q_B)^{1.25} + 0.005$

Firstly, **Fig. 85** shows which $P/q_A$ value is necessary to obtain a high selectivity for P (correspondingly, an equally bad one for R!), whereby this information is scale-independent and therefore can be used for scaling up such reactors. Secondly, it is shown that by suppressing back-mixing it is already possible to obtain the same selectivity with $P/q_A$ values, these being two orders lower.

If these results are considered for the selectivity, $S_P$, with reference to the desired product P (in Fig. 85 the selectivity $S_R$ of the *un*desired by-product is plotted!), it becomes apparent that this increases with increasing $\Psi$ but decreases superproportionally with increasing the throughput ratio $q_A/q_B$. This is because the propulsion jet power related to the *total* liquid throughput $\Delta p q_B/(q_A+q_B)$ decreases with increasing $q_A/q_B$.

If the kinetic parameters $k_1/k_2 = 7300/1.63 = 4480$ and the mol ratio $c_A q_A/c_B q_B = 1.05$ are known, it is possible to calculate the selectivities $S_R$ which would result from the ideal plug-flow tubular reactor and in the completely back-mixed vessel. The corresponding values are 0.001 and 0.008 respectively. This is in good agreement with the results obtained for high values of $\Psi \times c_B/c_A$.

**Example 45**: Mass transfer limitation of the reaction rate of fast chemical reactions in the heterogeneous material system gas/liquid

To allow a chemical reaction to take place between a gaseous and a liquid reaction partner, the gaseous component must first be dissolved (absorbed) in the liquid. In this case, the overall reaction rate will depend on the rates of the mass transfer and the chemical reaction step.

The so-called "Two Film Theory" (*Lewis* and *Whiteman*, 1923–24) assumes the formation of laminar boundary layers on both sides of the interphase. Mass transfer through these boundary layers can only be effected by means of diffusion, while the phase transition is immeasurably fast, **Fig. 86**. Consequently, an equilibrium predominates in the interphase and the saturation concentration $c_G^*$ of the gas in the interphase (*) obeys *Henry*'s law:

$$p_G = Hy\ c_G^* \qquad (14.42)$$

(Hy – Henry coefficient, $p_G$ – partial pressure of the gaseous reaction partner; indices: G – gas, L – liquid)

The two mass transfer coefficients $k_G$ and $k_L$ give the ratio of the respective diffusion coefficients, $D_i$, to the respective boundary layer thickness, $x_i$:

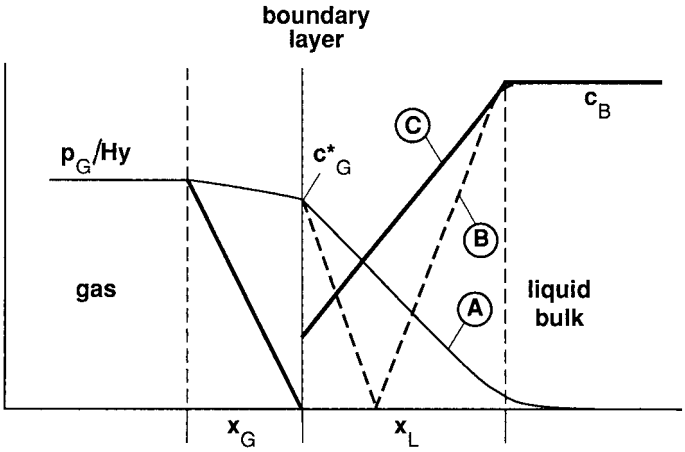


**Fig. 86** Graphic depiction of the concentration profiles on both sides of the interphase when the gas absorption is followed by (A) a very slow, (B) a fast and (C) an extremely fast chemical reaction.

$$k_i \propto D_i/x_i \tag{14.43}$$

Since $k_G >> k_L$, only the influence of $k_L$ is taken into account in the following.

If the mass transfer of a gaseous reaction partner into the liquid is accompanied by a chemical reaction, the following case can occur depending on the reaction rate and the mobility of the reaction partners: The concentration of A is not only reduced to zero in the solution; in addition, the reaction front shifts from the liquid bulk to the liquid-side boundary layer. As a result, the liquid-side boundary is apparently reduced and finally eliminated in a chemical way ("chemisorption"), see Fig. 86. This process increases the mass transfer coefficient by the "e*nhancement factor* **E**" as compared to its numerical value for purely physical absorption.

The target quantity E will depend on the parameters of mass transfer $\{k_L, D_A, D_B\}$ and reaction kinetics $\{k_2, c_A^*, c_B\}$, whereby $k_2$ stands for the rate constant of a 2nd order reaction:

$$\{E; k_L, D_A, D_B; k_2, c_A^*, c_B) \tag{14.44}$$

Apart from the trivial, obvious dimensionless numbers $\{E, D_A/D_B, c_A^*/c_B\}$, four parameters remain which form a single additional dimensionless number, namely the *Hatta* number Hat (for a 2nd order reaction):

$$Hat_2 \equiv \sqrt{D_A k_2 c_B}/k_L \tag{14.45}$$

If the numbers $D_A/D_B$ and $c_A^*/c_B$ are formulated as being a ratio of the diffusion currents

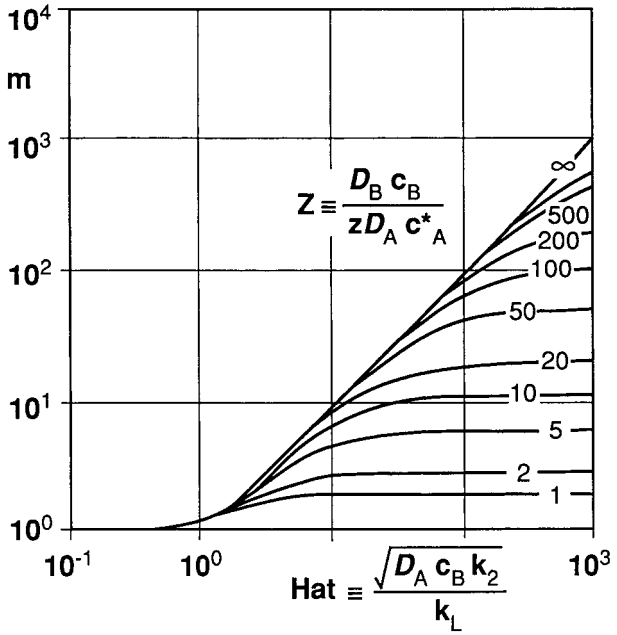


**Fig. 87** Enhancement factor E for gas absorption with subsequent chemical conversion as a function of the Hatta number, Hat, and the ratio of the diffusion currents, Z.

$$Z \equiv \frac{D_B c_B}{z D_a c_A^*} \tag{14.46}$$

the resulting functional relationship is:

$$E = f(Hat_2, Z). \tag{14.47}$$

This pi-relationship can be treated theoretically by assuming that the gradients of the diffusion rates of the two mass flows and the chemical reaction rate are equal (steady-state approximation):

$$D_A \frac{d^2 c_A^*}{dx^2} = D_B \frac{d^2 c_B}{dx^2} = k c_A^* c_B \tag{14.48}$$

This differential equation was numerically solved by *van Krevelen and Hoftijzer* [126] using the simplifying assumption of an idealized concentration profile and the results were graphically presented as a work sheet, **Fig. 87**. The following three ranges can be differentiated:

1. Hat < 0.5: m = 1. In this case, physical absorption governs the rate. This can be increased by more stirring more vigorously or with a better dispersion of the gas throughput.

2. Hat > 2; $c_{B >>} c_A^* \rightarrow Z \approx \infty B >> c_A^*$ we are dealing with a pseudo-1st order reaction: $k_2 c_B = k_1'$ and the Hatta number therefore reads:

$$Hat_1 \equiv \sqrt{D_A k_1'}/k_L \tag{14.49}$$

In this range, E increases directly proportionally to $Hat_1$. Since E was defined as the e*nhancement* or acceleration factor in relation to the respective value in pure physical absorption ($g^o \equiv G/A$ – mass flux density at physical absorption)

$$E \equiv \frac{g}{g^o} = \frac{g}{k_L c_A^*} \tag{14.50}$$

it follows from the here valid relationship $E = Hat_1$ that

$$\frac{g}{k_L c_A^*} = \frac{\sqrt{D_A k_1'}}{k_L} \quad \rightarrow \quad g = \sqrt{D_A k_1'}\ c_A^* \tag{14.51}$$

From this relationship it can be deduced that $k_L$ is replaced, in the case of chemisorption, by the kinetic expression $\sqrt{D_A k_1'}$, which in the given reaction system only depends on the temperature.

3. Hat > 2; Z << ∞: With increasing $k_2 c_B$ and, subsequently, increasing Hatta number, the molecular mobility of B and, consequently, Z become increasingly important. In this range, E is increasingly dependent on the mixing intensity in the reaction system which reduces diffusion resistances.

It should be pointed out that the relationship {E, $Hat_2$, Z} in Fig. 87, found by *van Krevelen* and *Hoftijzer* on the basis of theoretical reasoning, was convincingly confirmed by laboratory measurements; see works of *Nijsing* et al. [127], *Yoshida* and *Miura* [128], as well *Hofer* and *Mersmann* [129].

*Scale-up in Chemical Engineering.* Marko Zlokarnik


ISBNs: 3-527-30266-2 (Hardback); 3-527-60056-6 (Electronic)

# 15
# Selected Examples of the Dimensional-analytical Treatment of Processes in the Realms of the Living World

**Introductory remark**

The results of evolution – the so-called living world: fauna and flora – cannot be lumped together by means of dimensional analysis, because each group, as such, does not consists of geometrically similar species and is not adapted to the same living conditions (animals, birds, fishes). The biological treatises, which refer to the "Size and Shape in Biology" [130] or to the "Size and Scaling in Human Evolution" [131], only mean that in the living world, inspite of strong deviations from the geometric similarity (differently shaped bodies), astounding relationships exist, which exert a "similar" influence of the relevant physical parameters upon the size and shape of the species.

In contrast, correlations between egg mass of any bird species and the physical parameters influencing it, can be quite easily represented in a dimensional-analytical manner because here practically geometrically similar objects are concerned.

On the other hand, it is beyond question that creatures are subjected to the same physical regularities and frame conditions on Earth as the inanimate nature. These are therefore describable by the same dimensionless numbers as in inanimate nature and in technology.

For instance, the processes of motion in the living world are perfectly describable by dimensional analysis and from these correlations valuable information is obtained about a similar process concerning another, larger or older species. The scale-invariance of dimensionless representation is an advantage for the living world, which should not be underestimated: The relevant dimensions of length span here over a whole of eight decades.

To illustrate this, some examples will be given in this chapter.

**Example 46**: The consideration of rowing from the viewpoint of dimensional analysis

Why should larger boats containing many oarsman go faster than smaller ones containing fewer oarsmen? *Th. A. McMachon* [133] pursued this question and his approach deserves to be represented here.

Before examining his reasoning, we should remind ourselves of the Example 9 in which the drag resistance, F, of a ship's hull was treated. It has been pointed out that its dependence on the geometric, material and process related parameters can be represented by

$$\mathrm{Ne} = f(\mathrm{Re}, \mathrm{Fr}) \tag{15.1}$$

The symbols correspond to

$$\mathrm{Ne} \equiv \frac{F}{\rho v^2 l^2}, \quad \mathrm{Re} \equiv \frac{vl\rho}{\mu} \quad \text{und} \quad \mathrm{Fr} \equiv \frac{v^2 l}{g}.$$

In principle, the relationship (15.1) is, with respect to $f$ (Re), similar to that of the drag coefficient on a sphere. In the range of Re = $10^3$–$10^5$, the drag coefficient is approximately independent on Re.

The dependence Ne = $f$ (Fr) describes bow wave development and bow wave resistance in ships. Of course, it it not existing in submarines. At moderate speeds and large ratios of boat length to boat width it is practically negligible. Only the friction loss of the ship's hull has to be overcome. Under these frame conditions (Re and Fr irrelevant),

$$\mathrm{Ne} = \mathrm{const} \rightarrow F \propto v^2 l^2 \tag{15.2}$$

This means that at a given speed (v = const) and considering geometrically similar ship bodies, due to the proportionality between the wetted surface of the ship's hull and the displacement volume of the ship's body ($V \propto l^3$), the relationship

$$F/V \propto l^{-1} \qquad (v = \mathrm{const}) \tag{15.3}$$

exists. This motivated the construction of larger and larger ships of iron in the 19th century.

*McMachon* [133] comparatively evaluated the results obtained from four Championships in rowing (Olympics 1964 Tokyo and 1968 Mexico City; World rowing championship 1970 Ontario, International Championship 1970 Lucerne). Firstly, he ascertained that all competitive shells (single scull, pair-oared, four-oared without cox, eight-oared heavy weight) were geometrically similar. The slenderness ratio l/b is reasonably invariant of boat length. In addition, reasonably invariant is the boat weight per oarsmean. Furthermore, full-scale towing tank tests have shown that the resistance due to leeway and wave-making together constitute only 8% of the total drag at 20 km/h, the Olympic target speed, for an eight-oared shell. The assumption can be summarized as follows:

1 Geometrical similarity between boats exists and the displaced water volumes, V, of the boats are similar to each other.
2 The boat weight per oarsman (number z), $W_0$, is a constant.
3 Each oarsman contributes the same power, P, and weight, W.
4 Skin friction drag is the only hindering force.

From the relationship

$$V \propto z\,W_0 + z\,W = z\,(W_0 + W) \propto z \rightarrow z \propto l^3 \tag{15.4}$$

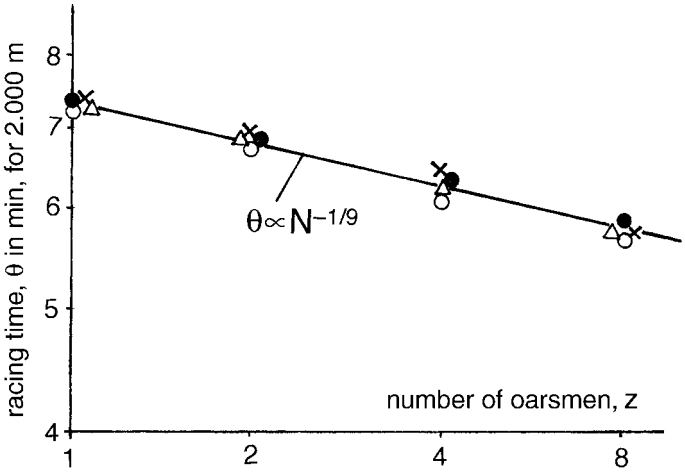


**Fig. 88** Correspondence between racing time θ [min] for 2.000 m in calm or near calm conditions and the number of oarsmen, z. Legend: Δ Tokyo 1964; • Mexico 1968; x Ontario 1970; o Luzern 1973; from [133].

it follows that the displaced volume per oarsman ($V \propto l^3$) remains constant.

The total power, P, required to move the boat at velocity, v, is proportional to the product of the drag resistance and velocity:

$$z\,P \propto v\,F$$

If F is taken into consideration according to (15.2), it follows that:

$$z\,P \propto v^3\,l^2$$

Because P has been assumed to be constant (assumption 3), it follows from eq. (15.4) that:

$$z \propto l^3 \rightarrow l^2 \propto z^{2/3}$$

This gives the relationship between z and v to be

$$v^3 \propto \frac{z}{l^2} \propto \frac{z}{z^{2/3}} \propto z^{1/3} \rightarrow v \propto z^{1/9} \tag{15.5}$$

This relationship is shown in **Fig. 88** for four boat types and four Championships and proves an excellent agreement between the prediction given by dimensional analysis and the measured data.

**Example 47**: Why most animals swim beneath the water surface

In dealing with this question, we should first look at the flow conditions at the liquid surface. It is well known that longer waves move faster than shorter ones and that large ships can travel faster than small ones. Both things have to do with the wave formation at the liquid surface, for which the gravitational acceleration, g, is also characteristic of. Therefore, the motion of a body at the liquid surface is dependent on the Froude number, Fr. From the structure of this pi-number

$$\mathrm{Fr} \equiv \frac{v^2}{gl} \tag{15.6}$$

it can be seen that at given flow conditions $v^2 \propto l$ applies.

As the characteristic wave dimension, l, the wave crest or the distance between two crests can be taken. A doubling of this length leads to the fourfold travelling or spreading velocity of the waves.

Due to water displacement, a ship produces waves at travelling. A bow wave, a few waves along the ship's hull and a stern wave are created. At full speed, the so-called "hull speed", it is left with a bow wave and a stern wave, the two separated by the length of the ship's hull. The critical value of the Froude number at this state is $\mathrm{Fr} \approx 0.16$. Going faster than this requires that the ship leave its beneficial stern wave astern and try to cut through or climb up its bow wave. Both would result in a dramatic rise in power demand.

The consequence is that a ship with a length of 100 m can easily travel at $v \approx 13$ m/s (25 sea miles per hour), whereas a ship of 10 m length achieves only $v \approx 4$ m/s (8 sea miles per hour). This facts also speak in favor of long ship bodies.

*S. Vogel* [134] reports on findings in the living world regarding this matter. A duck, with a hull length of about one third of a meter, hits hull speed at 0.7 m/s. Fully submersed, it can swim several times as fast. A mink, towed along the surface above hull speed, had up to ten times as much drag as it had when fully submerged.

The critical value of the Froude number shows why decent surface speeds are off-limits for the sizes of most of Nature's "vessels" and why even air breathers mostly swim submerged. An occasional animal porpoises up and down through the interface or planes on the surface, but only a large whale could consider migrating as a surface ship.

Snorkeling is rare, perhaps because swimming deep enough to keep wave drag low requires breathing against to much hydrostatic pressure.

**Example 48**: Transition from walking to running – a function of the Froude number

*R. McNeill Alexander* (quoted in [134]) pointed to another, more general and "closer to home" application of the Froude number. He noted that in a walking gait, an animal uses gravitational energy storage in pendulum fashion to reduce the work of repeatedly accelerating inertial legs. Therefore, animals of all sizes should walk in a dynamically similar manner at a given Froude number, when the characteristic length is given by the hip-to-ground distance.

To keep storing energy as they walk faster, animals increase amplitude, or stride length, rather than frequency. Dynamic similarity implies that all will reach the practical amplitude maximum at about the same Froude number, Fr = 0.5–0.6. At that point, animals ranging from small insects to large mammals shift to a trot or some other gait that uses elastic energy storage (mainly in tendons) instead of gravitational storage.

The transition point is size dependent. For a typical adult, the gait transition happens at about the expected 8 km/h (5 mph)

*Alexander* also noted that the trot-to-gallop transition for quadrupeds occurs at Fr = 2–4. This is a fairly specific transition point considering the size range involved.

However, it must be considered that an animal is in free fall for a time within each stride, therefore it would be reasonable to think that gravity retains its importance. If the period of falling is a fixed fraction of stride duration and if running speed at transition varies with leg length multiplied by the stride frequency – which is supported by observation – then the respective transition point has to be set by by a fixed Froude number.

**Example 49**: Walking and springing on water

The high surface tension of water is an important physical property in the living world. It allows the tiniest creature (insects, spiders) to walk and even to jump on the water surface. The question arises about which frame conditions have to be fulfilled for this.

We should first ask what could be the maximum size which limits this process. As a characteristic length, l, the perimeter of the wetted surface of the legs is taken. Because here the surface tension, σ, counteracts the gravitation, g, the Bond number will describe the process:

$$\mathrm{Bd} \equiv \frac{\rho g l^2}{\sigma} \triangleq \frac{mg}{\sigma l} < 1 \tag{15.7}$$

Its numerical value has to be < 1, if surface tension has to overcome the gravitational force. The left hand expression confirms that only very tiny creatures will manage this, because the length enters this fraction with the square (leg surface).

The equivalent expression on the right hand is formed by the mass, $m \propto \rho\, l^3$. An insect of m = 0.1 g will need l = 1.3 mm. This perimeter of the wetted leg surface can easily be provided by the four legs displaying a fringe of hydrophobic foot hairs. They are needed, if the insect is bound to jump vertically from the water surface. In this case, surface support has to be an order of magnitude greater.

In the determination of the lower limit of this process, it is not the support but the locomotion we are interested in. The water's surface tension will pull against an animal whichever way it tries to move. Can it get enough inertial force to offset the force of surface tension? These frame conditions are determined by the Weber number:

$$\mathrm{We} \equiv \frac{\rho\, l\, v^2}{\sigma} \tag{15.8}$$

So the animal has to be sufficiently large and fast, because size and speed act in the same way. Therefore, really tiny creatures have problems. *D'Arcy Thompson* (quoted in [134]) has put it in this way:

*"A water beetle finds the surface of a pool a matter of life and death, a perilous entanglement or an indispensable support."*

**Example 50**: What makes sap drift up a tree?

Could capillary rise account for the ascent of sap? This question can be easily answered by formulating the Bond number as a fraction of the weight force of the lifted water column, to the force exerted by the surface tension:

$$\mathrm{Bd} \equiv \frac{\rho\, g\, h\, r}{2\sigma} \tag{15.9}$$

(h – capillary rise height, r – capillary radius)

For the Bond number not to exceed one with a typical conduit radius of r = 0.05 mm, the rise height must remain h < 3 m. This wouldn't be much of a tree; therefore capillary rise cannot be responsible for it [134].

It is a generally accepted opinion, that columns of sap are maintained by the considerable internal cohesion of water, in essence hanging from the tops of trees and drawn up by evaporative water loss from the leaves. How can the water columns remain open to the air at the top? If the water vapor quite clearly leaves the trees, why air doesn't enter? The answer is that the relevant capillary radius of the cell walls is much smaller, $r \approx 10^{-4}$ mm. With this radius, the Bond number won't rise above one and air won't be pulled in by gravity until a tree exceeds 1.500 m in height – over an order of magnitude higher than any tree ever known.

*Scale-up in Chemical Engineering*. Marko Zlokarnik


ISBNs: 3-527-30266-2 (Hardback); 3-527-60056-6 (Electronic)

## List of important, named pi-numbers

| *name* | *symbol* | *pi-number* | *remarks* |
|---|---|---|---|
| ***A Mechanical process engineering*** | | | |
| Archimedes | Ar | $\frac{g\Delta\rho l^3}{\rho\nu^2}$ | $\equiv (\Delta\rho/\rho)$ Ga |
| Bond | Bd | $\frac{\rho\, g\, l^2}{\sigma}$ | $\equiv$ We/Fr |
| Brinkman | Br | $\frac{v^2\mu}{(J\, k\Delta T)}$ | **J** – Joule's heat equivalent |
| Deborah | De | $\lambda\, n$ | $\lambda$ – relaxation time |
| Euler | Eu | $\frac{\Delta\rho}{\rho v^2}$ | |
| Froude | Fr | $\frac{v^2}{lg}$ | |
| Froude, extend. | Fr* | $\frac{v^2\rho}{l\, g\, \Delta\rho}$ | $\equiv$ Fr $(\rho/\Delta\rho)$ |
| Galilei | Ga | $\frac{gl^3}{\nu^2}$ | $\equiv Re^2/Fr$ |
| Laplace | La | $\frac{\Delta p d}{\sigma}$ | $\equiv$ Eu We |
| Mach | Ma | $v/v_s$ | $v_s$ – velocity of sound |
| Newton | Ne | $\frac{F}{\rho v^2 l^2}$ | F – force |
| | – " – | $\frac{P}{\rho v^3 l^2}$ | P – power |
| Ohnesorge | Oh | $\frac{\mu}{(\rho\sigma l)^{1/2}}$ | $\equiv We^{1/2}/Re$ |

| *name* | *symbol* | *pi-number* | *remarks* |
|---|---|---|---|
| Reynolds | Re | $\frac{v\,l}{\nu}$ | $\nu \equiv \mu/\rho$ |
| Stokes | Sto | $\frac{\rho_p d_p^2 v}{l\mu}$ | $\equiv Re_p\,(d_p/l)$ |
| Strouhal | Sr | $l\,f/v$ | $f$ – frequency |
| Viscosity ratio | Vis | $\mu_w/\mu$ | w – wall |
| Weber | We | $\frac{\rho v^2 l}{\sigma}$ | |
| Weissenberg | Wi | $N_1/\tau$ | $N_1$ – 1. normal sress |
| ***B Thermal process engineering (heat transfer)*** | | | |
| Fourier | Fo | $a\,t/l^2$ | $a$ – thermal diffusivity |
| Grashof | Gr | $\frac{\beta \Delta T g l^3}{\nu^2}$ | $\equiv \beta \Delta T$ Ga |
| Nusselt | Nu | h l/k | h – heat transfer coefficient<br>k – heat conductivity |
| Péclet | Pe | $v\,l/a$ | $\equiv$ Re Pr |
| Prandtl | Pr | $\nu/a$ | $a \equiv k/(\rho\, c_p)$ |
| Rayleigh | Ra | $\frac{\beta \Delta T g l^3}{a\nu}$ | $\equiv$ Gr Pr |
| Stanton | St | $\frac{h}{v\rho C_p}$ | $\equiv \frac{Nu}{RePr}$ |
| ***C Thermal process engineering (mass transfer)*** | | | |
| Bodenstein | Bo | $v\,l/D_{ax}$ | $D_{ax}$ – dispersion coefficient |
| Lewis | Le | $a/D$ | $\equiv$ Sc/Pr |
| Schmidt | Sc | $\nu/D$ | $D$ – mass diffusivity |
| Sherwood | Sh | $k\,l/D$ | k – mass transfer coefficient |
| Stanton | St | k/v | $\equiv \frac{Sh}{ReSc}$ |

| *name* | *symbol* | *pi-number* | *remarks* |
|---|---|---|---|
| ***D Chemical reaction engineering*** | | | |
| Arrhenius | Arr | $\frac{E}{RT}$ | E – energy of activation |
| Damköhler | Da | $\frac{c\Delta H_R}{\rho C_p T_0}$ | eq. (14.7) |
| | $Da_I$ | $k_1 \tau$ | $k_1$ – reaction rate constant<br>$\tau$ – mean residence time |
| | $Da_{II}$ | $k_1 L^2/D$ | $\equiv Da_I$ Bo |
| | $Da_{III}$ | $k_1 \tau \left(\frac{c\Delta H_R}{\rho C_p T_0}\right)$ | $\equiv Da_I$ Da |
| | $Da_{IV}$ | $\frac{k_1 c\Delta H_R l^2}{kT_0}$ | $\equiv Da_I$ Pe Da |
| Hatta | $Hat_1$ | $(k_1 D)^{1/2}/k_L$ | 1st order reaction |
| | $Hat_2$ | $(k_2 c_2 D)^{1/2}/k_L$ | 2nd order reaction |
| Prater | $\beta$ | eq. (14.29) | $\equiv$ Da $Le^{-(1+n)}$ |
| Thiele modulus | $\Phi$ | $L\sqrt{k_1/D}$ | $\equiv {Da_{II}}^{1/2}$ |
| Weisz modulus | $\Psi'$ | eq. (14.44) | $\equiv \eta_K \Phi^2 = \eta_K Da_{II}$ |

## Literature

**1** Bridgman, P. W., *Dimensional analysis* Yale University Press, New Haven 1922, 1931, 1951 Reprint from AMS Press, New York 1978.

**2** Walzel, P., Spraying and Atomizing of Liquids Chapter 6-1/14 in Volume B2 of Ullmann's Encyclopedia of Industrial Chemistry, VCH 1988

**3** West, G. B., Los Alamos Science 1984, No. 11, 2–20: Scale and Dimension – From Animals to Quarks

**4** Rayleigh, Lord, Nature 95 (1915) No 2368 (March 18), 66–68: The principle of similitude

**5** Pawlowski, J., *Die Ähnlichkeitstheorie in der physikalisch-technischen Forschung – Grundlagen und Anwendungen* Springer-Verlag Berlin-Heidelberg-New York 1971

**6** Görtler, H., *Dimensionsanalyse – Theorie der physikalischen Dimensionen mit Anwendungen* Springer Verlag Berlin-Heidelberg-New York 1975

**7** Stanton, T. E., J. R. Pannell, Phil. Trans. Roy. Soc. London 214 (1914), 199–225: Similarity of Motion in Relation to the Surface Friction of Fluids

**8** Eck, B., *Technische Strömungslehre*, S. 123 Springer-Verlag Berlin-Göttingen-Heidelberg 1961

**9** Nikuradze, J.,VDI-Forschungsheft 361, Ausgabe B, Band 4, Juli/August 1933, 2–22: Strömungsgesetze in rauhen Rohren

**10** Dağ söz, A. K., Chem.-Ing. -Tech. 60 (1988) 6, 479–481: Eine neue Gleichung für den Übergangsbereich der Rauhigkeitsfunktion für die Nikuradze-Sandrauhigkeit

**11** Langhaar, H. L., *Dimensional Analysis and Theory of Models John Wiley & Sons Inc., New York 1951 Reprint from R. E. Krieger Publ. Co. Inc., Huntington,N.Y. 1980*

**12** Hilpert, R., Forschung Ing.Wesen 4 (1933) 5, 215–224: Wärmeabgabe von geheizten Drähten und Rohren im Luftstrom

**13** Eckert, E.R.G., E. Soehngen, Trans. Amer. Soc. Mech. Engrs. 74 (1952), 343–347: Distribution of heat transfer coefficients around circular cylindres in crossflow at Reynolds numbers from 20 to 500.

**14** Gröber-Erk-Grigull: *Wärmeübertragung* ; Springer-Verlag Berlin-Göttingen-Heidelberg, 3. edition 1963

**15** Zlokarnik, M., Chem.-Ing.-Tech. 42 (1970) 15, 1009–1011: Einfluß der Dichte- und Zähigkeitsunterschiede auf die Mischzeit beim Homogenisieren von Flüssigkeitsgemischen

**16** Zlokarnik, M., Korresp. Abwasser 32 (1985) 7, 598–603: Neue Flotationstechniken zur Abtrennung und Eindickung von Klärschlamm bei der biologischen Abwasserreinigung; Teil 2: Entgasungsflotation

**17** Zlokarnik, M., Ger. Chem. Eng. 9 (1986), 314-320: Design and Scale-up of Mechanical Foam Breakers

**18** Merrifield, C. W., Trans. Inst. Naval Arch. (London) 11 (1870), 80–93: The experiments recently proposed on the resistance of ships

**19** Froude, W., Trans. Inst. Naval Arch. (London) 15 (1874), 36–73: On experiments with H.M.S. "Greyhound"

**20** Weber, M., Jahrbuch Schiffsbautech. Ges. 20 (1919), 355–477: Die Grundlagen der Ähnlichkeitsmechanik und ihre Verwertung bei Modellversuchen

**21** Pawlowski, J., Seminar on The Theory of Similarity, given at Bayer AG, D – Leverkusen, 1967

**22** Zlokarnik, M.: *Stirring - Theory and Practice* WILEY-VCH 2001, ISBN 3-527-29996-3

**23** ibid., Chapter 5: Suspension of Solids in Liquids (S/L system ), p. 206 +

**24** ibid., Chapter 4: Gas-liquid contacting, p. 126 +

**25** Zlokarnik, M., Chem.- Ing.- Tech. 40 (1968) 15, 765–768: Homogenisieren von Flüssigkeiten durch aufsteigende Gasblasen

**26** Pawlowski, J. , GVC-Kolloquium "Ähnlichkeitstheoretische Methoden und ihr verstärkter Einsatz in der Praxis", Mainz 1984

**27** Pawlowski, J.: *Veränderliche Stoffgrößen in der Ähnlichkeitstheorie* Salle+Sauerländer 1991

**28** Meier, E., Chem.- Ing.- Tech. 41 (1969) 7, 472–478: Einfluß konzentrations- und temperaturabhängiger Diffusionskoeffizienten auf die Trocknung hygroskopischer Kunststoffe

**29** Sieder, E.N., G.E. Tate, Ind. Engng. Chem. 28 (1936) 12, 1429–1435: Heat Transfer and Pressure Drop of Liquids in Tubes

**30** Hruby, M., Int. Chem. Engng. 7 (1967) 1, 86–90: Relationship between the dissipation of mechanical energy and heat transfer in agitated vessels

**31** Hackl, A., W. Wittmer, Chem.-Ing.-Tech. 39 (1967) 13, 789–791: Zum Wärmeübergang in innenbeheizten Rührgefäßen

**32** Hackl, A., W. Gröll, Verfahrenstechnik 3 (1969) 4, 141–145: Zum Wärmeübergangsverhalten zähflüssiger Öle

**33** Zlokarnik, M., Chem.- Ing.- Tech. 41 (1969) 22, 1995–1202: Wärmeübergang an der Wand eines Rührbehälters beim Kühlen und Heizen im Bereich $10^0 < Re < 10^5$

**34** Dunlap Jr., I.R., J.H. Rushton, Chem. Engng. Progr. Symp. Series 49 (1953) 5, 137–151: Heat-transfer coefficients in liquid mixing using vertical-tube baffles

**35** Pawlowski, J., Verfahrenstechnik 8 (1974) 9, 269–272: Modellversuche an Newtonschen Flüssigkeiten mit temperaturabhängiger Viskosität

**36** Pawlowski, J., Rheologica Acta 6 (1967) 1, 54–61; abbreviated version in AIChE J. 15 (1969) 2, 303–305: Relationship Between Process Equations for Processes in Connection With Newtonian and Non-Newtonian Substances

**37** Henzler, H.-J., E.E. Schäfer, Chem.- Ing.- Tech. 59 (1987) 12, 940–944: Viskose und elastische Eigenschaften von Fermentationslösungen

**38** Werner, F., A. Mersmann, Chem.- Ing.- Tech. 70 (1998) 7, 890–894 und 8, 1027 - 1030: Zur Rheologie von Polymerlösungen, Teil 1 und 2

**39** Metzner, A.B., R.E. Otto, AIChE J. 3 (1957)1, 3–10: Agitation of Non-Newtonian Fluids

**40** Henzler, H.-J., Chem.- Ing.- Tech. 60 (1988) 1, 1–8: Rheologische Stoffeigenschaften – Erklärung, Messung, Erfassung und Bedeutung

**41** Ford, D.E., J. Ulbrecht, AIChE J. 21 (1975) 6, 1230–1233: Blending of polymer solutions with different rheological properties

**42** Opara, M., Verfahrenstechnik 9 (1975) 9, 446–449: Homogenisieren von nicht-Newtonschen Flüssigkeiten im Rührgefäß

**43** Müller, W. (TU Dortmund), VDI-Forschungsberichte, Reihe 3 (1985), Nr. 103: Untersuchung von Homogenisiervorgängen in nicht-Newtonschen Flüssigkeiten mit einem neuen bildanalytischen Verfahren

**44** Pörtner, R., U. Werner, Chem.- Ing.- Tech. 61 (1989) 3, 250–251: Betrachtungen zur Effektivität von Rührern bei Homogenisierprozessen in strukturviskosen und viskoelastischen Flüssigkeiten

**45** Pörtner, R., G. Langer, U. Werner, Chem.- Ing.- Tech. 63 (1991) 2, 172–173: Zur dimensionsanalytischen Beschreibung von Mischprozessen in gerührten Newtonschen, strukturviskosen und viskoelastischen Flüssigkeiten

**46** Riabouchinsky, D., Nature 95 (1915), 591: Letter to the Editor

**47** Rayleigh, Lord, Nature 95 (1915), 644: Letter to the Editor

**48** Sedov, L.I., *Similarity and Dimensional Methods in Mechanics* (Translation of the 4. Russian edition) Infosearch Ltd. London 1959

**49** Zlokarnik, M., Chem. Eng. Sci. 53 (1998) 17, 3023–3030: Problems in the application of dimensional analysis and scale-up of mixing operations

**50** Zlokarnik, M., Korresp. Abw. 27 (1980) 11, 728–734: Koaleszenzphänomene im System gasförmig/flüssig und deren Einfluß auf den $O_2$-Eintrag bei der bilogischen Abwasserreinigung

**51** Kipke, K.D., Chem.-Ing.-Tech. 54 (1982) 5, 416–425: Offene Probleme in der Rührtechnik

**52** Weber, M., Chem.-Ing. Tech. 67 (1995) 3, 330–333: Unterschiede zwischen bewehrten und unbewehrten Rührbehältern im turbulenten Strömungsbereich im Hinblick auf die Maßstabsübertragung

**53** Judat, H., Ger. Chem. Eng. 5 (1982), 357 – 363: Gas/Liquid Mass Transfer in Stirred Vessels – A Critical Revue

**54** Zlokarnik, M., Adv. Biochem. Eng. 11 (1979), 158–180: Scale-up of Surface Aerators for Waste Water Treatment

**55** Schmidtke, N.W., J. Horváth, Progr. Wat. Tech. 9 (1977) 2, 477 – 493: Scale-up methodology for surface aerated reactors

**56** Pawlowski, J., Seminar on "Theory of Similarity in Process Engineering" Bayer AG, Leverkusen, 1989

**57** Zlokarnik, M., Chem.-Ing.-Tech. 39 (1967) 9/10, 539–548: Eignung von Rührern zum Homogenisieren von Flüssigkeitsgemischen

**58** Zlokarnik, M., Chem.-Ing.-Tech. 38 (1966) 3, 357 – 366 und 7, 717–723: Auslegung von Hohlrührern zur Flüssigkeitsbegasung Teil 1: Bestimmung des Durchsatzes und der Wellenleistung Teil 2: Ermittlung des erreichbaren Stoff- und Wärmeaustausches

**59** Pawlowski, J. und M. Zlokarnik, Chem.-Ing.-Tech. 44 (1972) 16, 982–986: Optimieren von Rührern für eine optimale Abfuhr der Reaktionswärme

**60** Zlokarnik, M., Chem.-Ing.-Tech.45 (1973) 10a, 689–692: Rührleistung in begaster Flüssigkeit

**61** Müller, W. und H. Rumpf, Chem.-Ing.-Tech.39 (1967) 5/6, 365–373: Das Mischen von Pulvern in Mischern mit axialer Mischbewegung

**62** Ullrich, M., Chem.-Ing.-Tech.41 (1969) 16, 903–907: Entmischungserscheinungen in Kugelschüttungen

**63** Entrop, W., International Symposium on Mixing, B – Mons 1978, paper D1: Scaling-up solid-solid mixers

**64** Müller, W., Chem.-Ing.-Tech.53 (1981) 11, 831–844: Methoden und derzeitiger Kenntnisstand für Auslegungen beim Mischen von Feststoffen

**65** *Pawlowski, J.: Transportvorgänge in Einwellen-Schnecken Verlag Salle+Sauerländer 1990*

**66** Bauckhage, K., Chem.-Ing.-Tech. 62 (1990) 8, 613–625: Das Zerstäuben als Grundverfahren

**67** Sauter, J., Forschungsarbeiten, Heft 279 (1926): Die Größenbestimmung von Brennstoffteilchen

**68** Dahl, H. D., E. Muschelknautz, Chem. Eng. Technol. 15 (1992) 224–231: Atomisation of Liquids and Suspensions with Hollow Cone Nozzles

**69** Wallis, G.B., S. Makkenchery, ASME Journal of Fluid Eng. 96 (1974), 298: The Hanging Film Phenomenon in Vertikal Annular Two-Phase Flow

**70** Pushkina, O.L., J.L. Sorokin, Heat Transfer – Soviet Research 1 (1969), 56: Breakdown of Liquid Film Motion in Vertical Tubes

**71** Eichhorn, R., ASME Journal of Fluid Eng. 102 (1980) 9, 372–375: Dimensionless Correlation of the Hanging Film Phenomenon

**72** Schneider, H., T. Roth, Hochschulkurs Emulgiertechnik, Universität Karlsruhe 1996, XIII-1/18: Emulgierverfahren in der Lebensmittelindustrie

**73** Karbstein, H. , Ph-Thesis Universität Karlsruhe 1994: Untersuchungen zum Herstellen und Stabilisieren von Öl-in-Wasser-Emulsionen

**74** Karbstein, H., H. Schubert, Chem.- Ing.-Tech. 67 (1995) 5, 616–619: Einflußparameter auf die Auswahl einer Maschine zum Erzeugen feindisperser O/W-Emulsionen

**75** Klinksiek, B., Hochschulkurs Emulgiertechnik, Universität Karlsruhe 1996, XIV-1/42: Emulsionsherstellung mit dem Strahldispergator

**76** van Lent, B., B. Klinksiek, Chem.- Ing.- Tech. 69 (1997) 6, 793–698: Korrelation physikalischer mit anwendungstechnischen Größen bei Dispersionen

**77** Karbstein, H., F. Müller, R. Polke, Aufbereitungstechnik 37 (1996) 10, 469–479: Scale-up for Grinding in Stirred Ball Mills

**78** Kwade, A., H.-H. Stender, Aufbereitungstechnik 39 (1998) 8, 373–382: Constant Grinding Result at Scale-Up of Stirred Media Mills

**79** Koglin, B., J. Pawlowski, H. Schnöring, Chem.-Ing.-Techn. 53 (1981) 8, 641–647: Kontinuierliches Emulgieren mit Rotor/Stator-Maschinen: Einfluß der volumen- bezogenen Dispergierleistung und der Verweilzeit auf die Emulsionsfeinheit

**80** Zlokarnik, M., Ger. Chem. Eng. 5 (1982) 2, 109–115: New Approaches in Flotation Processing and Waste Water Treatment in the Chemical Industry

**81** Zlokarnik, M., J. Susa, Chem.-Ing.-Techn. 68 (1996) 12, 1572–1574: Selbstansaugende und radialstrahlende Trichterdüse

**82** Zlokarnik, M., Int. Application Number: PTC/EP98/00375, 23 January 1998 Apparatus and Method for Induced Air flotation

**83** Scherzinger, B., Fortschritts-Berichte VDI, Reihe 15 Umwelttechnik, Nr. 214, 1999: Entwicklung der Begasungsflotation in der Umwelttechnik

**84** Zlokarnik, M., Water Research 32 (1998) 4, 1095–1102: Separation of activated sludge from purified waste water by Induced Air Flotation (IAF)

**85** Zlokarnik, M., Kem. Ind. (YU-Zagreb) 34 (1985) 1, 1–6: Anwendung der Flotation bei der Reinigung der Prozessabwässer der chemischen Industrie sowie bei der Klärschlammabtrennung nach biologischer Abwasserreinigung

**86** Zlokarnik, M., Ger. Chem. Eng. 7 (1984), 150–159: Scale-Up in Process Engineering

**87** Bender, W., Dissertation TU Karlsruhe 1971: Zur Berechnung des Durchsatzes von Schälschleudern

**88** Bürkholz, A., Int. Chem. Eng. 29 (1989) 1, 26 – 37: Description of particle *collection by inertial forces using a group derived by dimensional analysis*

**89** Zlokarnik, M., Chem.-Ing.-Tech. 43 (1971) 6, 329–335: Eignung von Einlochböden als Gasverteiler in Blasensäulen

**90** Kast, W., Chem.-Ing.-Tech. 35 (1963) 11, 785–788: Untersuchungen zum Wärmeübergang in Blasensäulen

**91** Kölbel, H. et al., Chem.-Ing.-Tech. 30 (1958) , 400–404, 729 – 734 and 32 (1960), 84 – 88: Wärmeübergang an Blasensäulen I, II, III

**92** Zlokarnik, M., Adv. Biochem. Eng. 8 (1978), 133–151: Sorption Characteristics for Gas-Liquid Contacting in Mixing Vessels

**93** Zlokarnik, M., Chem. Eng. Sci. 34 (1979) 10, 1265–1271: Sorption characteristics of slot injectors and their dependency on the coalescence behaviour of the system

**94** *Scale-up of Dryers, Drying Tech., 12 (1994) 1&2, 1–443*

**95** Kerkhof, Piet J.A.M., in [94], 1–46: The Role of Theoretical and Mathematical Modelling in Scale-up

**96** Genskow, Lary R., in [94], 47–58: Dryer Scale-up Methodology for Process Industries

**97** Toei, R., M. Okazaki, H. Tamon, in [94], 99–149: Coventional Basic Design for Convection and Conduction Dryers

**98** Oakley, D.E, in [94], 217–233: Scale-up of Spray Dryers with the Aid of Computational Fluid Dynamics

**99** Masters, K., in [94], 235–257: Scale-up of Spray Dryers

**100** Bahu, R.E., in [94], 329–339: Fluidized Bed Dryer Scale-up

**101** Szentmarjay, T., A. Szalay, E. Pallay, in [94], 341–350: Scale-up of the Mechanically Spouted Bed Dryer with Inert Particles

**102** Passos, M.L., A.S. Mujumdar, G. Massarani, in [94], 351–391: Scale-up of Spouted Bed Dryers: Criteria and Applications

**103** Papadakis, S.E., T.A.G. Langrish, I.C. Kemp, R.E.Bahu, in [94], 259–277: Scale-up of Cascading Rotary Dryers

**104** Kemp, I.C., in [94], 279–297: Scale-up of Pneumatic Conveying Dryers

**105** Ohmori, T., M. Miyahara, M. Okazaki, R. Toei, in [94], 299–328: Heat Transfer in a Conductive-Heating Agitated Dryer

**106** Moyers,C.G., in [94], 393–3416: Scale-up of Layer Dryers: A Unified Approach

**107** Sano, Y., Drying Tech. 10 (1992) 3, 591–622: Drying of polymer solution

**108** Hall, C.W., Drying Tech. 10 (1992) 4, 1081–1095: Dimensionless numbers and groups for drying

**109** Jordan, H., Diploma thesis University Köln 1994, executed at BAYER AG, D – Leverkusen: Selektive Trocknung von mit einem Lösungsmittelgemisch beladenen Polymerfilmen bei festoffseitiger Stoffübergangshemmung.

**110** Rutte, R., SWISS CHEM 11 (1989) 10, 33–37: Kontinuierliche trägerfreie Elektrophorese

**111** *"Biostream separator" of CJB Developmens Limited*

**112** Tarnopolsky, Y., M. Roman, P.R. Brown, Sep. Sci. Tech. 28 (1-3) (1993), 719–731: A new approach to scaling up electrophoresis

**113** Damköhler, G., Z. f. Elektrochemie 42 (1936), 846–862: Einflüsse der Strömung, Diffusion und des Wärmeüberganges auf die Leistung von Reaktionsöfen

**114** Thiele, E.W., Ind. Engng. Chem. 31 (1939) 7, 916–920: Relation between Catalytic Activity and Size of Particles

**115** Aris, R., Chem. Eng. Sci. 6 (1957), 262–268: On shape factors for irregular particles – I

**116** Prater, C.D., Chem. Eng. Sci. 8 (1958), 284–286: The temperature produced by heat of reaction in the interior of porous particles

**117** Weisz, P.B., J.S. Hicks, Chem. Eng. Sci. 17 (1962), 265–275: The behaviour of porous cat-

alyst particles in view of internal mass and heat diffusion effects

**118** Bischoff, K.B., Chem. Eng. Sci. 22 (1967), 525–530: An extension of the general criterion for importance of pore diffusion with chemical reactions

**119** Levenspiel, O.: *Chemical Reaction Engineering John Wiley & Sons, Inc., New York 1962 und 1972*

**120** Froment, F.G., K.B. Bischoff: *Chemical Reactor Analysis and Design Willey Series in Chemical Engineering John Wiley & Sons, New York 1979, 1990*

**121** Westerterp, K.R., W.P.M. van Swaaij, A..C.M. Beenackers: *Chemical Reactor Design and Operation John Wiley & Sons, Chichester 1987, 1990*

**122** Trambouze, P., Chem. Eng. Progress, Feb. 1990, 23–31: Reactor Scaleup Methodology

**123** Euzen, J-P., P. Trambouze, J-P Wauquier: *Scale-up Methodology for chemical Processes Gulf Publishing Company, Houston/Texas, 1993*

**124** Baldyga, J. und Bourne, J. R.: *Principles of Micromixing, in Encyclopedia of Fluid Mechanics (Ed.: Cheremisinoff ) Vol.1, Chapter 6, S.148/195 Gulf Publ. Company, Houston 1985*

**125** Korischem, B., Diploma thesis University Dortmund 1987, executed at BAYER AG, D – Leverkusen: Homogenisieren von Flüssigkeiten mit Düsen

**126** Krevelen, van D.W., P.J. Hoftyzer, Chem. Eng. Sci. 2 (1953) 4, 145–156: Graphical design of gas-liquid reactors

**127** Nijsing, R.A.T.O., R.H. Hendriksz, H. Kramers, Chem. Eng. Sci. 10 (1959), 88–104: Absorption of $CO_2$ in jets and falling films of electrolyte solutions, with and without chemical reaction

**128** Yoshida, F. und Miura, Y., I & EC Process Des. Dev. 2 (1963) 4, 263–268: Gas Absorption in Agitated Gas-Liquid Contactors

**129** Hofer, H., A. Mersmann, Chem.-Ing.-Tech. 52 (1980) 4, 362–363: Zur Problematik der physikalisch und chemisch bestimmten Phasengrenzfläche in Gas/Flüssigkeits-Kontaktapparaten

**130** Mc Machon, Th. A., Science 179 (1973), 1201–1204: Size and Shape in Biology

**131** Pilbeam, D., St. J. Gould, Science 186 (1974), 892–901: Size and Scaling in Human Evolution

**132** Rahn, H., A. Ar, Ch.V. Paganelli, Scientific American 240 (Febr. 1979), 46–55: How Birds Eggs Breathe

**133** Mc Machon, Th. A., Science 173 (1971), 349–351: Rowing: A Similarity Analysis

**134** Vogel, S., Physics Today 51 (1998) 11, 22–27: Exposing life's limits with dimensionless numbers

**135** Vogel, S.: *Life's devices: The physical World of Animals and Plants Princeton University Press, Princeton, N.J. (1988)*

**136** Levin, M. and M. Zlokarnik: Dimensional Analysis of Tableting Process, in *Pharmaceutical Process Scale-Up*, Marcel Dekker, Inc. New York, Basel 2002

**137** Walzel, P., F. Schmelz, S. Schneider, Chem.-Ing.-Tech. 73 (2001) 12, 1599–1602: Herstellen monodisperser Tropfen mit pneumatischen Ziehdüsen

**138** Stender, H.-H., A. Kwade, J. Schwedes, 3rd ECCE Nuremberg, 26–28 June 2001, Paper 376: Constant grinding conditions at scale-up of stirred media mills

**139** Poggel, M., Th. Melin, Chem.-Ing.-Tech. 73 (2001) 12, 1635–1638: Freiflusselektrophorese in einem technischen Maßstab

*Scale-up in Chemical Engineering*. Marko Zlokarnik


ISBNs: 3-527-30266-2 (Hardback); 3-527-60056-6 (Electronic)

# Index